TOLL-7 AND TOLL-6:
CENTRAL NERVOUS SYSTEM FUNCTIONS AS *DROSOPHILA* NEUROTROPHIN RECEPTORS

By

GRAHAM MCILROY

A thesis submitted to

The University of Birmingham

for the degree of

DOCTOR OF PHILOSOPHY

School of Biosciences

College of Life and Environmental Sciences

University of Birmingham

September 2011

Abstract

The *Drosophila* Toll receptor is crucial for dorsoventral patterning in embryos, and also for the fly's innate immune response. Toll also functions during central nervous system development, and promotes the survival and targeting of neurons. There are nine Toll paralogues in *Drosophila*, and it is unknown whether any of these also function in the CNS. Toll's ligand, Spz, has an NGF domain. NGF is a vertebrate neurotrophin - a growth factor that regulates the development and function of the nervous system. *Drosophila Neurotrophin 1* (*DNT1*), identified by homology to the vertebrate neurotrophin BDNF, and *DNT2* are paralogues of *spz*. The three DNTs – *DNT1, DNT2* and *spz* – are structural and functional homologues of vertebrate neurotrophins, and they promote neuronal survival, targeting and synaptogenesis in *Drosophila*. However, the receptors for DNT1 and DNT2 are unknown.

Here, using a combination of *in situ* hybridisations and reporters that drive GFP expression, I show that *Toll-7* and *Toll-6* are expressed in CNS neurons, in all stages. By generating null mutant flies and gain-of-function transgenic flies, I show that *Toll-7* and *Toll-6* genetically interact with *DNT1* and *DNT2*, resulting in a synergistic and specific decrease in viability of the DNT-Toll double mutants at 18°C compared to the single mutants. Loss of function *Toll-7* and *Toll-6* mutants display abnormal adult locomotion behaviour, and increased apoptosis and motor axon targeting defects in embryos. Expressing activated forms of *Toll-7* and *Toll-6* in neurons rescues naturally occurring cell death in the embryonic central nervous system, and rescues the semi-lethality of *Toll-7Toll-6* double mutants. Remarkably, expressing activated receptors in neurons rescues the *DNT1DNT2* double mutant semi-lethality at 18°C, and rescues the excess CNS cell death of *DNT1* and *DNT2* mutant embryos. Using signalling in S2 cell culture as a readout for ligand binding, I demonstrate that recombinant DNT1 can activate NFκB signalling through Toll-7, and DNT2 through Toll-7 and Toll-6.

Altogether, my data show that Toll-7 and Toll-6 function in the *Drosophila* CNS as DNT receptors. This evidence of a link between the Toll and Neurotrophin families provides novel insights into CNS development, and into the evolution of the nervous and immune systems.

For Mum and Dad

Rich and Alex

and Adnan

Acknowledgements

The most important person to thank is my PhD supervisor, Dr Alicia Hidalgo. This project would not have been possible without your patience, encouragement, enthusiasm, knowledge, skill, and insight. Thank you for your excellent supervision, for helping me develop as a scientist, and for the tapas.

I would like to thank all members of the Hidalgo lab. Thanks to Bangfu, Kentaro, Manuel, Ben, Simon, Samaher, Ann, and Martin for the help, advice and friendship over the years. Thanks to Janine and Sarah, for the generation of the mutants.

I would also like to thank Prof Nick Gay, for welcoming me into his lab to carry out the protein work, and for very useful discussions. Thanks to Jukka for all the technical help and for helping to make sense of the data. And thanks to other members of the Gay lab for advice and support, especially Chris, Miranda and Monique.

Thanks also to past and present members of the Soller and Brogna labs, for making the lab such a fun place to work. Thanks to the team of technicians for keeping the lab running. Thanks to the MRC for funding my studentship, and to the School of Biosciences and the British Society Developmental Biology for funding attendances at conferences.

Table of Contents

List of figures

List of tables

List of abbreviations

18w	18 Wheeler
5-HT	5-Hydroxytryptamine
BDNF	Brain-Derived Neurotrophic Factor
CK	Cystine knot
CNS	Central nervous system
CRC	Cysteine-rich cluster
CTD	C-terminal domain
DAG	Diacylglycerol
DM	Dorsal median
DNT	*Drosophila* Neurotrophin
Dpp	Decapentaplegic
EGF	Epidermal Growth Factor
ERK	Extracellular-Signal-Regulated Kinase
FasII	Fasciclin II
FasIII	Fasciclin III
Gd	Gastrulation Defective
GDNF	Glial Cell-Derived Neurotrophic Factor
GFP	Green Fluorescent Protein
GNBP	Gram Negative Binding Protein
HMGB1	High-Mobility Group Protein B1
HRP	Horse Radish Peroxidase
Ig	Immunoglobulin
IMD	Immune Deficiency
IP_3	Inositol Trisphosphate
ISN	Intersegmental nerve
JNK	c-Jun N-terminal Kinase
LIG	Leucine-rich repeat and Immunoglobulin domain
LPS	Lipopolysaccharide
LRR	Leucine-rich repeat
LTP	Long-term potentiation
MAP	Mitogen-Activated Protein
MMP	Matrix Metalloprotease
NGF	Nerve Growth Factor
NMJ	Neuromuscular junction
NPC	Neuronal progenitor cell
NT-3	Neurotrophin-3
NT-4/5	Neurotrophin-4/5
PAMP	Pathogen-associated molecular pattern
PBS	Phosphate-buffered saline
PBTw	Phosphate-buffered saline, 0.1% Tween-20
PBTx	Phosphate-buffered saline, 0.1% Triton-X-100
PCR	Polymerase chain reaction

PDGF	Platelet-Derived Growth Factor
PGRP	Peptidoglycan Recognition Protein
PI3K	Phosphatidylinositol 3-Kinases
PLC	Phospholipase C
PNS	Peripheral nervous system
PRR	Pathogen recognition receptor
PtdIns	Phosphatidylinositol
Rel	Relish
Rho	Rhomboid
rpm	Revolutions per minute
SI	Survival index
Sim	Single-Minded
SN	Segmental nerve
Sog	Short Gastrulation
SP	Signal peptide
SPE	Spätzle Processing Enzyme
Spz	Spätzle
TEV	Tobacco etch virus
TGF	Transforming Growth Factor
TIR	Toll/Interleukin-1 Receptor
TLR	Toll-Like Receptor
TNF	Tumour Necrosis Factor
TNFRSF	Tumour Necrosis Factor Receptor superfamily
tPA	Tissue Plasminogen Activator
TRAF	Tumour Necrosis Factor Receptor-Associated Factor
TRPV	Transient Receptor Potential Vanilloid
VNC	Ventral nerve cord
Zen	Zerknüllt

CHAPTER 1
INTRODUCTION

One of the fundamental questions in neurobiology is how is the brain built. This question encompasses two different concepts. Firstly, in an individual, what controls the development of a brain, from a fertilised egg to a behaving adult? And secondly, over evolution, how has the complex brain evolved from a simpler ancestral nervous system? It is the emergence and elaboration of signalling mechanisms over evolution, and the expression of genes during neural development, that underlie the complexity and diversity of animal nervous systems. Therefore, by investigating the evolution of the complex brain, we can better understand the mechanisms by which it develops.

Vertebrate neurotrophins are key signalling molecules that control the development and function of the nervous system. They are target-derived trophic factors that promote the targeting and survival of neurons, matching innervation to the organs' requirements (Levi-Montalcini, 1987). And by modulating neuronal morphology and excitability, they influence the functioning of the nervous system throughout life (Huang and Reichardt, 2001). Consistent with their central roles in brain development and functioning, dysfunction in neurotrophin signalling is responsible for a wide range of neurological and psychiatric illnesses, including Alzheimer's disease, anxiety and depression (Chao et al., 2006). It was initially thought the neurotrophins were a vertebrate innovation, and that they were responsible for increased complexity seen in vertebrate nervous systems (Jaaro et al., 2001, Barde, 1994). However, there is now abundant evidence that members of the neurotrophin

family and their receptors are present throughout the invertebrates (DeLotto and DeLotto, 1998, Mizuguchi et al., 1998, van Kesteren et al., 1998, Ormond et al., 2004, Benito-Gutiérrez et al., 2006, Bothwell, 2006, Hallböök et al., 2006, Zhu et al., 2008). In *Drosophila*, functional homology between the *Drosophila* neurotrophins (DNTs) and their vertebrate counterparts has been demonstrated. DNTs promote neuronal survival and targeting, as well as influencing synaptic structural plasticity and adult behaviour (Zhu et al., 2008, Sutcliffe et al., Submitted). Therefore, neurotrophin signalling is a conserved mechanism for nervous system development, from flies to humans.

To better understand how *Drosophila* neurotrophins regulate nervous system development and function, it is essential that their receptors are identified. Of the DNTs, only the receptor for Spätzle is known: Toll (Weber et al., 2003). And Toll promotes neuronal survival and targeting in the central nervous system (CNS) (Zhu et al., 2008, Halfon et al., 1995, Rose et al., 1997). The receptors for DNT1 and DNT2 remain to be identified. In this thesis, I present evidence that *Toll* paralogues, *Toll-7* and *Toll-6*, are expressed in the *Drosophila* nervous system, and promote neuronal survival and targeting. Furthermore, I show that *Toll-7* and *Toll-6* mutants genetically interact with *DNT1* and *DNT2* mutants, and that expressing constitutively active receptors in neurons can rescue *DNT* mutant phenotypes. Finally, evidence is provided that shows DNTs can activate cell signalling through Toll-7 and Toll-6. It is hoped that this work will contribute to a deeper understanding of how the nervous system develops. And the characterisation of Tolls – homologues of vertebrate innate immune receptors – as neurotrophin receptors raises intriguing questions about the relationship between the immune and nervous systems.

1.1 *Drosophila* Toll

Toll is a type I transmembrane protein, with an extracellular N-terminus, a transmembrane domain, and the C-terminus intracellular. The ectodomain is made up of leucine-rich repeats (LRRs), which are divided into two blocks. The first block contains 15 LRRs, and is capped at the C-terminal end by a cysteine-rich cluster (CRC); the second block contains 3 LRRs, and is capped by N-terminal and C-terminal CRCs (protein architecture obtained from the UniProt database, accession number P08953) (Fig 1.1). The intracellular region of Toll contains a Toll/Interleukin -1 Receptor (TIR) domain. TIR domains do not possess intrinsic catalytic activity, but can initiate intracellular signalling through the recruitment of adapter proteins.

Toll is maternally expressed in early embryos, and also zygotically expressed later in embryogenesis. At the syncytial blastoderm stage, maternal Toll is uniformly distributed at the plasma membrane, and expression diminishes during cellularisation (Gerttula et al., 1988, Hashimoto et al., 1991). Zygotic *Toll* is expressed in the gut, salivary glands and epidermis (Gerttula et al., 1988). *Toll* is expressed in migrating cells, and Toll protein localises to the sites of contact between cells, including the fused epidermal layers at the dorsal midline and at segment borders (Hashimoto et al., 1991). Toll is also expressed in embryonic muscle, where it localises to the points of contact between adjacent muscles (Halfon et al., 1995). Finally, *Toll* is expressed in embryonic neurons, and *Toll-Gal4>UAS-GAP-GFP* labels neurons in the larval and adult CNS (Zhu et al., 2008, Sutcliffe, 2010).

1.1.1 Toll in dorsoventral patterning

The Toll gene was first identified as a key component of the dorsoventral patterning pathway in *Drosophila* early embryos (Anderson and Nüsslein-Volhard, 1984). *Toll* is a member of the 'dorsal-group' of maternal effect genes, and acts downstream of *nudel*, *pipe*, *gastrulation defective* (*gd*), *snake*, *easter*, and *spätzle* (*spz*) and upstream of *dorsal* (Anderson et al., 1985). The Toll signalling pathway in dorsoventral patterning is well understood, and results in a gradient of activated Dorsal, a *Drosophila* NFκB homologue (Moussian and Roth, 2005) (Fig 1.1).

Dorsoventral patterning starts in the maternal egg chamber, where the somatic expression of Nudel, Pipe and Windbeutel initiate the establishment of ventral cell fates (Stein et al., 1991). Pipe has sulfotransferase activity, although its substrate remains unknown, and is expressed on the ventral side of the follicular epithelium, (Zhu et al., 2005, Nilson and Schüpbach, 1998, Stein et al., 2008). Nudel, a multi-domain protein with proteolytic activity, is uniformly expressed (LeMosy et al., 1998). Downstream of Pipe and Nudel, in the perivitelline space, a proteolytic cascade sequentially activates Gd, Snake and Easter (Dissing et al., 2001). Nudel initiates the cascade, and Pipe restricts Snake activity to the ventral side of the embryo (Dissing et al., 2001, Han et al., 2000, LeMosy et al., 2001, Cho et al., 2010).

The final proteolytic step is the generation of mature Spz from its inactive pro-peptide form by Easter, after which it binds Toll (DeLotto and DeLotto, 1998, Stein et al., 1991, Schneider et al., 1994, Weber et al., 2003). Cleaved Spz is a dimer, and binding of one Spz dimer to Toll induces receptor dimerization, resulting in a 2:2 signalling complex (Gangloff et al., 2008). Downstream signalling follows the endocytosis of this complex (Huang et al., 2010).

Toll has an intracellular TIR domain, which recruits adapter proteins to the bound receptor to activate Dorsal (Fig 1.1). These adapters all contain a Death-Domain, a domain involved in protein-protein interactions, and comprise MyD88, Tube and Pelle (Kambris et al., 2003, Hecht and Anderson, 1993). MyD88 and Tube are bound via their death domains, and localise to the plasma membrane (Sun et al., 2004). The death domain of Pelle then binds that of Tube, though it is unclear whether the formation of the MyD88/Tube/Pelle trimer requires Toll (Sun et al., 2004, Moncrieffe et al., 2008). Upon binding of Spz, Toll's TIR domain forms a homotypic interaction with the TIR domain of MyD88, resulting in the recruitment and activation of the adapter multimer (Sun et al., 2002). Pelle also carries a kinase domain and triggers the activation of Dorsal, possibly through interaction with dTRAF2 (Shen et al., 2001). dTRAF2 is required for Toll signalling in immunity, though the survival of *dTRAF2* null mutant flies to adulthood indicates it is not essential for embryogenesis (Cha et al., 2003).

In the absence of signalling, Dorsal is found in the cytoplasm in a complex with the IκB homologue Cactus (Whalen and Steward, 1993). Ventrally-restricted Toll signalling leads to the degradation of Cactus and the nuclear localisation of Dorsal to direct gene expression (Bergmann et al., 1996, Reach et al., 1996). The phosphorylation of both Dorsal and Cactus is required for the nuclear localisation of Dorsal (Gillespie and Wasserman, 1994, Drier et al., 1999), while further modifications are likely to target Cactus for proteasome-mediated degradation (Fernandez et al., 2001).

In the nucleus, Dorsal functions as a transcription factor to promote or repress gene expression. At high concentrations (ventrally) it activates the transcription of *twist* and *snail*, which specify the mesoderm; at low concentrations (laterally) it activates *sim* to specify the mesectoderm, and *rho* and *sog* transcription to specify the neuroectoderm; and throughout all ventral and lateral regions, it represses *zen*, which specifies the dorsal ectoderm (Moussian

and Roth, 2005, Stathopoulos and Levine, 2002, Huang et al., 1997). Thus, the gradient of nuclear Dorsal, triggered by ventrally restricted Toll signalling, establishes the dorsoventral axis in *Drosophila* embryogenesis.

1.1.2 Toll in immunity

Spz also activates Toll in the innate immune response (Lemaitre et al., 1996). In this context, Toll signalling is activated in response to invasion by Gram-positive bacteria and fungi (Valanne et al., 2011) (Fig 1.1). Pathogens are recognised by two families of pathogen recognition receptors (PRR): Peptidoglycan recognition proteins (PGRP) and Gram-negative binding proteins (GNBP), which can be membrane-associated or circulating in the haemolymph (Ferrandon et al., 2007). Different members of these families can detect Gram-positive or -negative bacteria, or fungi. Binding of one of these proteins to the pathogen triggers a proteolytic cascade that results in the activation of Spz and its binding to Toll. However, the proteases involved in this pathway are not the same as those used in dorsoventral patterning.

The first serine protease in the immune cascade is ModSP, and responds to PRR binding to both bacterial and fungal pathogens (Buchon et al., 2009). ModSP functions upstream of Grass, the next protease in the cascade, but may not activate it directly (Buchon et al., 2009). Parallel to ModSP and Grass are the protease Persephone and its serpin inhibitor Necrotic, and Persephone is also able to activate Toll signalling (Levashina et al., 1999, Ligoxygakis et al., 2002b). Persephone responds to 'danger signals' associated with infection, and activates Toll independently of PRRs and Grass (Gottar et al., 2006, El Chamy et al., 2008). Grass and Persephone pathways next converge on Spheroide, Sphinx1/2 and Spirit: four proteins with sequence similarity to serine proteases of which only one, Spirit, is thought to be catalytically

active (Kambris et al., 2006). Downstream of Spheroide, Sphinx1/2 and Spirit is Spätzle Processing Enzyme (SPE); and SPE directly cleaves Spz, releasing the Cys-knot to bind to Toll (Jang et al., 2006).

The intracellular signalling cascade activated by Toll during dorsoventral patterning, is also activated in the innate immune response (Gay and Gangloff, 2007). However, in immunity, Dif is activated, another *Drosophila* NFκB (Manfruelli et al., 1999, Meng et al., 1999). In the larva, Dif and Dorsal show redundancy, but in the adult, Dif is required for an immune response (Rutschmann et al., 2000). The target genes of the NFκB signalling pathway on immune challenge include those encoding anti-microbial peptides, such as Drosomycin, an anti-fungal peptide (Lemaitre et al., 1996).

The immune response to Gram-negative bacteria in *Drosophila* uses a different signalling pathway. Different PRRs signal via IMD to activate Relish (Rel), a third NFκB homologue (Ferrandon et al., 2007). However, there is evidence for cross-talk between these two signalling pathways. Activating upstream components of the Toll and IMD pathways together produces a synergistic effect on antimicrobial peptide expression (Tanji et al., 2007). Moreover, the NFκB paralogues can form heterodimers; the Dif-Rel heterodimer is a much more potent activator of Drosomycin expression than the Dif homodimer (Han and Ip, 1999, Tanji et al., 2010).

1.1.3 Toll in the nervous system

In addition to its well-defined roles in dorsoventral patterning and immunity, Toll is also involved in the development of the epidermis, muscle and nervous system. Loss of *Toll* expression in the epidermis results in disrupted muscle development; similar muscle phenotypes are seen in *spz*, *tube* and *pelle* mutants (Halfon and Keshishian, 1998). And in

Toll mutant larvae, the muscle defects are associated with misrouting of motor axons, and loss of motor neurons (Halfon et al., 1995). Halfon and colleagues predicted that the non-cell-autonomous effect of *Toll* could be due to a secreted factor acting on neurons. *Toll* mutant embryos also show axon targeting defects. The expression of *Toll* in muscles 15, 16 and 17 prevents the inappropriate targeting of the RP3 motor axon (Rose et al., 1997). Targeting of RP3 to muscles 6 and 7 is promoted by *Fasciclin III* (*FasIII*), and the growth cone evaluates the relative amounts of Toll and FasIII it encounters before establishing a synapse (Rose and Chiba, 1999). In this context, muscle-expressed Toll inhibits the intimate membrane interactions between the growth cone and the muscle that are required for synapse formation (Suzuki et al., 2000). *Toll* is also required for cell survival in the embryonic CNS, as *Toll* mutant embryos have increased apoptosis in the developing ventral nerve cord (VNC) (Zhu et al., 2008). Therefore, *Toll* can have cell-autonomous functions in neurons, where it promotes neuronal survival and targeting. However, the upstream activating events and downstream signalling pathways of Toll have not been as well characterised in the nervous system as in dorsoventral patterning and innate immunity.

1.1.4 Other Toll functions

Toll has additional functions in *Drosophila* development, which have been less extensively explored. For example, *Toll* is required for the formation of the dorsal vessel, the *Drosophila* heart (Wang et al., 2005). Toll is expressed on the lateral surfaces of adjoining cardioblasts, and its effects were attributed to roles in cell adhesion (Wang et al., 2005, Keith and Gay, 1990). *Toll* also regulates haematopoiesis in the fly, and Spz was not shown to be involved in this process (Qiu et al., 1998).

Fig 1.1 - Toll signalling pathways

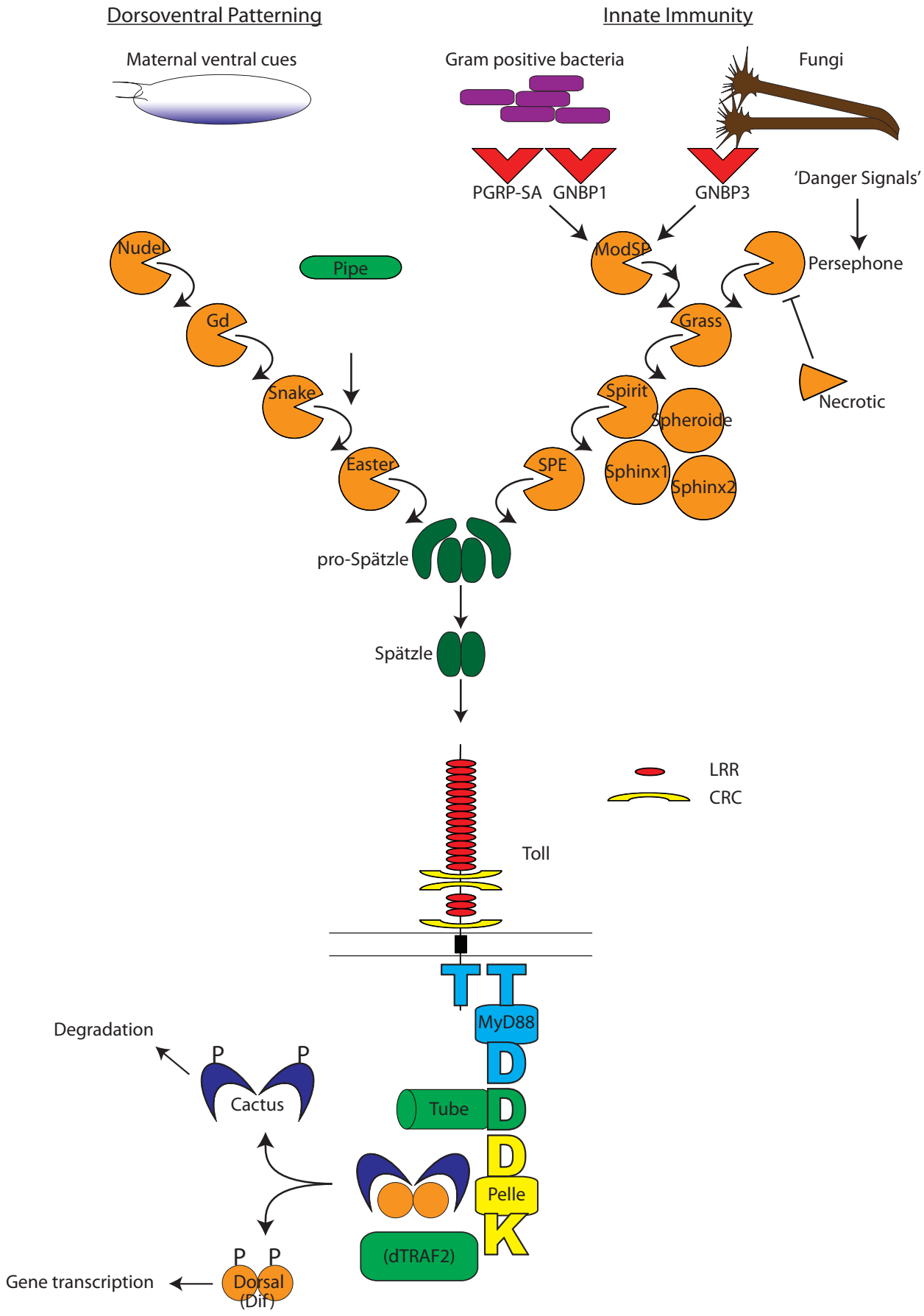

Fig 1.1 – Toll signalling pathways
During early embryogenesis, maternal cues trigger a protease cascade, resulting in the cleavage and activation of Spätzle. In the innate immune response, the sensing of invading pathogens activates a different set of proteases, which also cleaves pro-Spätzle. Inside the cell, a series of adapter proteins are recruited through interactions between their TIR (T) and Death (D) domains. The kinase (K) Pelle causes the degradation of Cactus and the activation of Dorsal. In innate immunity, dTRAF2 and Dif are also required. Extracellular protein domains of Toll are indicated. For references, see main text.

1.1.5 Other *Drosophila* Tolls

Drosophila Toll belongs to a family of nine paralogues. These are *Toll*, *18 wheeler* (*18w*), *Toll-3* (also called *MstProx*), *Toll-4*, *Toll-5* (also called *Tehao*), *Toll-6*, *Toll-7*, *Toll-8* (also called *Tollo*), and *Toll-9*. Nearly all of the *Drosophila* paralogues share the same protein architecture, with two extracellular blocks of LRRs and an intracellular TIR domain (Tauszig et al., 2000, Imler and Hoffmann, 2001). The main difference between the *Toll* paralogues is in the number of LRRs. The exception is *Toll-9*, which has a single block of LRRs in the ectodomain, compared to the two blocks seen in the other Tolls (Imler and Hoffmann, 2001). *Toll-9* is more closely related to the vertebrate Toll-like receptors (TLRs) than other *Drosophila* Tolls.

Of the *Toll* paralogues in the fly, *18w* has been the most studied. It is expressed in stripes in the early embryo, and is found in multiple organs as the embryo develops (Eldon et al., 1994). Loss of function results in semi-lethality, and adult escapers have deformed legs, wings and antennae (Eldon et al., 1994). 18w is involved in cell migration in the ovary and the salivary gland, and can interact with Rho-GTPase signalling (Kleve et al., 2006, Kolesnikov and Beckendorf, 2007). Like *Toll*, *18w* can influence the innate immune response, though this is primarily due to its role in the development of the fat body, which produces anti-microbial peptides (Williams et al., 1997, Ligoxygakis et al., 2002a). Toll-5 (Tehao) can interact with Toll, synergistically activating Dorsal in S2 cells, though its *in vivo* functions remain to be determined (Luo et al., 2001). *Toll-8* is expressed in the wing imaginal disc, where it antagonises Dpp signalling (Kim et al., 2006). In the imaginal disc epithelium, Toll-8 interacts with Rel during sensory organ development, and is involved in neuronal specification (Ayyar et al., 2007). *Toll-8* has also been shown to induce expression of the

neuronal Horse Radish Peroxidase (HRP) epitope, however a normal HRP labelling pattern in *Toll-8* mutant embryos indicates that additional factors are involved (Seppo et al., 2003, Yagi et al., 2010). Expression of *Toll-9* in cultured cells and in larval fat bodies results in the constitutive expression of anti-microbial peptides (Ooi et al., 2002, Bettencourt et al., 2004). This effect is attributed to a tyrosine residue that recapitulates the activating mutation in the $Toll^{10b}$ allele. However, the lack of a phenotype in *Toll-9* mutant flies calls into question the *in vivo* function of *Toll-9* (Narbonne-Reveau et al., 2011). Finally, over-expressing or mutating *18w, Toll-6, Toll-7* and *Toll-8* can lead to morphological defects in tissues derived from various imaginal discs, including leg and wing defects, extra bristles, and rough eye phenotypes (Yagi et al., 2010).

Of the *Toll* paralogues, *Toll-7* and *Toll-6* are also expressed in the embryonic CNS (Kambris et al., 2002). However, nothing is known about their function in the nervous system. Moreover, the ligands for the *Toll* paralogues have not been identified, and little is known about the intracellular pathways they activate. Since Toll promotes neuronal development, it is compelling to test whether *Toll-7* and *Toll-6* also carry out neuronal functions, and to investigate the ligands of these *Toll* paralogues.

1.2 Human Toll-Like Receptors

A search for human homologues of *Drosophila Toll* led to the discovery of *hToll*, which was found to signal through NFκB to induce the expression of inflammatory cytokines (Medzhitov et al., 1997). An earlier screen of cDNA clones also identified *rsc786* as a *Toll* homologue (Nomura et al., 1994, Mitcham et al., 1996). rsc786 (renamed TLR1), hToll (TLR4), were the first members of an emerging family of TLRs (Rock et al., 1998). The human TLR family is now made up of 10 members, and represents a key pathogen-sensing system for both innate

and adaptive immune responses (Takeda et al., 2003). The protein structure of TLRs is homologous to that of *Drosophila* Toll-9, with a single block of extracellular LRRs and a single juxtamembrane CRC, and an intracellular TIR domain.

TLR4 is activated in response to lipopolysaccharide (LPS), a marker of Gram-negative bacteria, which requires the co-receptors CD14 and MD2 (Miyake, 2003). *TLR4* mutant alleles are associated with a reduced responsiveness to LPS and increased risk of infection in mice and humans (Poltorak et al., 1998, Qureshi et al., 1999, Arbour et al., 2000). Unlike *Drosophila* Toll, vertebrate TLRs are directly activated by pathogen-associated molecular patterns (PAMPs), including those associated with Gram-positive and -negative bacteria, fungi and viruses (Gay and Gangloff, 2007). However, once TLRs are activated, the intracellular signalling molecules are homologous to those activated by *Drosophila* Toll, culminating in the activation of NFκB and the expression of inflammatory cytokines (Gay and Gangloff, 2007). In addition, a TLR-3, -7, -8 and -9 form signalling endosomes, and through IRF transcription factors induce the expression of type I interferons (Kumar et al., 2009). As well as directly detecting PAMPs, TLRs are activated by an array of endogenous ligands, some of which are normally intracellular and are released during necrosis (Sloane et al., 2010). These 'damage-associated molecular patterns' (DAMPs) induce an inflammatory response through TLRs with the aim of repairing tissue damage, although prolonged activation is associated with inflammatory disease and cancer (Chen and Nuñez, 2010).

As well as mediating the release of pro-inflammatory cytokines as part of the innate immune response, TLRs represent the link between the innate and adaptive immune system in vertebrates. It has long been known that an adaptive immune response (through the recruitment of T- and B-cells) can only occur if the innate immune system has been engaged. This was proposed as a mechanism to ensure the adaptive immune system only responds to

pathogens, and not to 'self' antigens (Janeway, 1989). It is now know that TLRs play a central role in the activation of the adaptive immune response. TLRs induce the expression of co-stimulatory molecules on antigen-presenting cells, which are required for the activation of T-cells (Iwasaki and Medzhitov, 2004). In this way, only cells that have recognised a pathogen (through TLR binding of PAMPs) are able to activate T-cells and initiate an adaptive immune response. In addition, a number of the cytokines released following TLR activation are responsible for the recruitment and differentiation of a wide range of immune cells.

1.2.1 TLRs in the nervous system

TLRs have been primarily studied in the context of the immune system, and outside the brain. However, the CNS is not completely isolated from the immune system, and TLRs play a key role in the regulation of innate immunity in neural tissue (Rivest, 2009). TLRs are widely expressed in CNS glia, in particular the resident innate immune cells – microglia (Jack et al., 2005). TLR signalling in microglia represents a major mechanism of pathogen-recognition and engagement of the innate immune response in the CNS (Kong and Le, 2011, Lehnardt, 2010). TLRs are also activated in CNS injury and disease, including Alzheimer's disease (Downes and Crack, 2010, Salminen et al., 2009). TLRs mediate neuroprotection following infection and injury; however the inflammatory response mediated by TLRs can also be detrimental to the CNS, leading to neurodegeneration (Okun et al., 2009, Hanisch et al., 2008).

The expression and function of TLRs in neurons is less understood. Transcripts and protein for TLRs 1-9 have been detected in rodent neurons, (Mishra et al., 2006, Ma et al., 2006, Tang et al., 2008, Goethals et al., 2010). mRNA for all human ten TLRs has been detected in neurons (Zhou et al., 2009). Adding TLR-3 and -8 agonists to primary human neurons, and a

TLR-4 agonist to a neuronal cell line, induces the activation of a reporter plasmid, indicating the expression of functional TLR proteins (Zhou et al., 2009, Peltier et al., 2010). Moreover, TLR-3 has been detected by immunocytochemistry on a neuronal cell line, and TLR-3 and TLR-4 have been detected by immunohistochemistry on human neuronal explants (Préhaud et al., 2005, Jackson et al., 2006, Wadachi and Hargreaves, 2006). In most of these studies, neuronal TLRs were found to carry out immune functions, effecting inflammatory responses to infection or injury. This indicates that, to some extent, neurons are immunologically competent, and could contribute to the defence of the nervous system from pathogens.

Evidence is accumulating that neuronal TLRs carry out additional functions, separate from those relating to immunity, that relate more directly to neuronal development and physiology (Okun et al., 2011). During embryogenesis, neuronal progenitor cells (NPCs) express TLR-2 and TLR-3, both of which negatively regulate the proliferation of NPCs (Okun et al., 2010b, Lathia et al., 2008). Similarly, TLR-4 prevents proliferation in retinal progenitor cells (Shechter et al., 2008). In adult neurogenesis, the data are less clear. In one study, TLR-2 was found to promote neurogenesis, while TLR-4 continued to suppress the proliferation and differentiation of NPCs (Rolls et al., 2007). However, a second study did not record any effect on proliferation or differentiation of NPCs by TLR-2 or -4, although it noted that adult NPCs could respond to TLR agonists by releasing cytokines (Covacu et al., 2009). In all of these studies, the downstream signalling of TLRs was to NFκB.

There is also evidence that TLRs can function in neurons. Neuronal expression of TLR-3 is concentrated in the growth cone, and activation by a synthetic ligand polyinosinic:polycytidylic acid (poly I:C) results in growth cone collapse and inhibition of neurite extension (Cameron et al., 2007). Activation of TLR-3 *in vivo* was associated with decreased axon number and behavioural deficits (Cameron et al., 2007). TLR-8 is enriched in

axons, and activating it with resiquimod inhibits neurite growth, as well as inducing apoptosis (Ma et al., 2006). The inhibition of neuronal outgrowth and the induction of cell death occur independently following TLR-8 stimulation. Remarkably, the effects of activating axonal TLR-3 and -8 do not require the nuclear localisation of NFκB (Ma et al., 2006, Cameron et al., 2007). This raises intriguing the possibilities that NFκB could function at the membrane, or that TLRs can also activate additional signalling pathways.

Most research has focussed on activation of neuronal TLRs by pathogens, but less is known about the role of endogenous ligands. High-Mobility Group Protein B1 (HMGB1, also called HMG1 and amphoterin) is emerging as a candidate endogenous TLR ligand with neuronal functions. HMGB1 was discovered through its properties of promoting neurite outgrowth, which are mediated by the receptor RAGE (Rauvala and Pihlaskari, 1987, Hori et al., 1995). HMGB1 has also been shown to bind TLR2 and TLR4 to activate NFκB in macrophages, although this has not yet been demonstrated in neurons (Park et al., 2004, Park et al., 2006). In zebrafish, HMGB1 is required for the development of the forebrain, where it promotes cell survival, though the receptor it binds was not identified (Zhao et al., 2011). Interestingly, HMGB1 induces expression of AMIGO, a CNS receptor with extracellular homology to the vertebrate neurotrophin receptor, Trk (Kuja-Panula et al., 2003). Moreover, HMGB1 signalling through TLR4 induces Matrix Metalloproteinase 9 (MMP9) expression, and it potentiates the activity of Tissue Plasminogen Activator (tPA). These two extracellular proteases are involved in regulating neurotrophin processing (Qiu et al., 2010, Roussel et al., 2011, Bruno and Cuello, 2006). Therefore HMGB1 may link the TLR and neurotrophin signalling pathways.

TLRs also function in the adult nervous system. Loss of TLR-3-mediated neurogenesis in the adult hippocampus is associated with altered memory formation and anxiety behaviour in

mice (Okun et al., 2010a). In a model of stroke, TLR-2 and -4 promote cell death, and knock-out mice show improved functional recovery (Tang et al., 2007). TLR-4 is upregulated in response to Amyloid β aggregates and mediates JNK-dependent neuronal death, and patients with Alzheimer's disease show a reduction in TLR-4-positive neurons (Tang et al., 2008). And in a model of epilepsy, neuronal TLR-4 is upregulated after seizure induction, and TLR-4 antagonists show anticonvulsant activity (Maroso et al., 2010). Much more research needs to be carried out on TLRs in the nervous system, to establish their neuronal functions, and determine their roles in health and disease.

1.3 Neurotrophins

Drosophila Toll, and its ligand Spz, have well characterised functions in dorsoventral patterning and innate immunity (Valanne et al., 2011, Moussian and Roth, 2005). *Toll* also is expressed in neurons, and promotes neuronal survival and targeting (Zhu et al., 2008, Halfon et al., 1995, Rose et al., 1997). Spz is a *Drosophila* neurotrophin, and functions in the CNS to promote cell survival and targeting, to regulate synaptic structural plasticity in the larval NMJ, and to influence adult behaviour (Zhu et al., 2008, Sutcliffe et al., Submitted). It is therefore compelling to explore the link between the neurotrophin and Toll families of proteins.

1.3.1 *Drosophila* Neurotrophins

For a long time, the existence of Neurotrophins in *Drosophila* was questioned. When the *Drosophila* genome was published, no neurotrophin homologues were found (Adams et al., 2000). Although there is extensive apoptosis in the developing *Drosophila* nervous system, it was thought that cell survival was pre-determined, and not subject to non-cell-autonomous control (White et al., 1994, Truman, 1984). The small size of the fly's CNS, its 'hard-wired'

development, and the apparent lack of neurotrophins lead to the theory that invertebrate brains are not subject to the trophic controls that characterise the mammalian CNS (Barde, 1994, Jaaro et al., 2001). However, there is evidence that neuronal number is plastic in *Drosophila*. In a population of wild-type embryos, there is variability in neuron number, and also in the number of cells undergoing apoptosis (Bossing et al., 1996, Schmidt et al., 1997, Rogulja-Ortmann et al., 2007). In the developing eye, retinal photoreceptors require retrograde survival signals from the optic lobe, for which EGF receptors are necessary (Campos et al., 1992, Baker and Yu, 2001). Conversely, optic lobe neurons require retinal axon input and glial trophic support for survival (Fischbach and Technau, 1984, Dearborn and Kunes, 2004, Xiong and Montell, 1995). Interactions between neurons and glia influence many aspects of neuronal function, and in the VNC, glia maintain neuronal survival (Edenfeld et al., 2005, Booth et al., 2000). Apoptosis is a conserved aspect of neurodevelopment, and while there are examples of pre-determined cell death, neurotrophism is a mechanism shared by flies and mammals (Buss et al., 2006, Miguel-Aliaga and Thor, 2009, Hidalgo and ffrench-Constant, 2003, Hidalgo, 2002, Hidalgo et al., 2006).

The first clue to identifying a *Drosophila* neurotrophin homologue came from structural studies. The crystallisation of NGF revealed a cystine-knot structure with subunits dimerising in parallel along their flat surface (McDonald et al., 1991). The amino acid sequence of Spz closely resembles the signal peptide, pro-domain, Cys-knot architecture of NGF (Morisato and Anderson, 1994). Moreover, the cysteine residues within the Cys-knot are similarly positioned to those of NGF. In 1998, two groups showed that the predicted structure of Spz was homologous to that of NGF, and that it could form parallel dimers like the vertebrate neurotrophins (Mizuguchi et al., 1998, DeLotto and DeLotto, 1998). This was later confirmed by crystallography (Hoffmann et al., 2008). Spz was also found to be a structural homologue

of the horseshoe crab Coagulogen, although Coagulogen forms end-on-end polymeric fibres after proteolytic activation (Bergner et al., 1996). A family of *spz* paralogues was identified in the *Drosophila* genome, and were originally proposed to be more closely related to *coagulogen* than to the vertebrate neurotrophins (Parker et al., 2001). Spz and Coagulogen share a common mechanism of activation, by a cascade of homologous serine proteases, which was likened to the blood clotting cascade found in mammals (Osaki and Kawabata, 2004). Despite the divergent structures of the multimers, the homologous activation pathway in response to immune challenge caused attention to be directed to the similarities between Spz and Coagulogen.

The Hidalgo lab re-examined the question by performing an unbiased search of the fly genome using PSI-BLAST and TBLASTN to identify distantly-related homologues of all vertebrate neurotrophin Cys-knots (Zhu et al., 2008). Using carp BDNF as the query resulted in the identification of *DNT1*, which was found to be a member of the *spz* family (*spz2*). Using FUGUE, which aligns protein sequences according to structural conservation (Shi et al., 2001), three members of the Spz family were found to be significantly homologous to human neurotrophins (Zhu et al., 2008). The *Drosophila* neurotrophins (DNTs) comprise *DNT1* (*spz2*), *DNT2* (*spz5*), and *spz*; and the DNTs are more closely related to the vertebrate neurotrophins than to *coagulogen* (Zhu et al., 2008). As well as being structural homologues of the vertebrate neurotrophins, the DNTs also carry out the same functions associated with canonical neurotrophins. They promote neuronal survival and targeting during development, are involved in synaptic structural plasticity at the neuromuscular junction (NMJ), and are required for normal adult behaviour (Zhu et al., 2008, Sutcliffe et al., Submitted). Zhu et al. demonstrated that neurotrophins are expressed in neuronal target tissues, function as cleaved mature Cys-knot growth factors, and act in a non-cell-autonomous manner. Therefore, the

neurotrophins are a conserved family of signalling molecule that link the structure and function of the nervous system, and are conserved from flies to humans.

1.3.2 Vertebrate Neurotrophins

Neurotrophins are a key family of signalling molecules that regulate multiple aspects of nervous system development and function, including cell survival, axon targeting and synaptic plasticity (Huang and Reichardt, 2001). The first neurotrophin to be discovered was Nerve Growth Factor (NGF). NGF is target-derived, exhibits trophic and tropic influences on developing neurons, and maintains neuronal survival throughout life (Levi-Montalcini, 1987). Brain-Derived Neurotrophic Factor (BDNF) is a second neurotrophic factor with structural and functional homology to NGF (Barde et al., 1982, Leibrock et al., 1989). And neurotrophin-3 (NT-3) and NT-4/5 complete the family of 4 proteins found in most vertebrates (Rosenthal et al., 1990, Maisonpierre et al., 1990b, Ernfors et al., 1990, Hohn et al., 1990, Hallböök et al., 1991, Berkemeier et al., 1991). The neurotrophins are found in all vertebrates, though NT-4/5 is absent from birds, and bony fishes possess an additional NT-6/7, reflecting gene losses and duplications in those lineages (Hallböök et al., 2006).

Neurotrophins belong to a large superfamily of proteins containing cystine-knots, which also include TGFβ, PDGF and hormone glycoproteins (Sun and Davies, 1995). However, position of the cysteine residues and the protein structure of the neurotrophins is different from other members of the superfamily. An important characteristic of the neurotrophins is the 'head-to-head' orientation of the dimers, aligned along their long axis (Sun and Davies, 1995, McDonald et al., 1991). All neurotrophins form homodimers that are structurally very similar; and a number of heterodimers can form *in vitro*, though the biological significance of this is unknown (Wiesmann and de Vos, 2001).

Neurotrophins are translated as pre-pro-proteins, possessing a signal peptide, an N-terminal pro-domain, and a C-terminal Cys-knot (Bibel and Barde, 2000). Cleavage of the pro-domain releases the mature Cys-knot protein. All neurotrophins can be cleaved by furin and members of the PC family of serine proteases, and NGF can be cleaved by the kallikrein-family protease, γNGF (Seidah et al., 1996b, Seidah et al., 1996a, Edwards et al., 1988). NGF and BDNF are processed differently: NGF processing is directed towards constitutive secretion, while BDNF is also sorted into the regulated secretion pathway that is controlled by neuronal activity (Mowla et al., 1999). The pro-domains are required for neurotrophin processing, and are responsible for the differences in cleavage and sorting between NGF and BDNF (Suter et al., 1991, Nomoto et al., 2007). The processing and sorting of neurotrophins *in vivo* depends on the cell type and its endogenous proteases, and relates to the type of signalling required by the tissue (Lessmann et al., 2003). In addition, pro-neurotrophins can be released from cells, without cleavage of the pro-domain (Mowla et al., 1999). Extracellular pro-neurotrophins can be cleaved by Matrix Metalloproteases (MMPs) and plasmin (Lee et al., 2001). Tissue Plasminogen Activator (tPA) is a serine protease responsible for the generation of active plasmin from its precursor, and is secreted from neurons following electrical stimulation (Nagappan et al., 2009). Consequently, the cleavage of proBDNF by tPA/plasmin can also be regulated by neuronal activity, which can influence the establishment of long-term potentiation (LTP) – one of the functions of BDNF (Pang et al., 2004).

1.4 Vertebrate Neurotrophin receptors

1.4.1 p75^{NTR} and Trks

p75^{NTR} is a membrane protein of 70-80kDa, and binds all four cleaved neurotrophins with relatively low affinity (Bothwell, 1995). p75^{NTR} also binds pro-neurotrophins with high

affinity (Lee et al., 2001). The $p75^{NTR}$ protein contains four Cys-rich clusters in the ectodomain, and an intracellular death domain (Chao et al., 1986, Johnson et al., 1986, Radeke et al., 1987, Chapman, 1995) (Fig 1.2). $p75^{NTR}$ became the founding member of the TNF receptor superfamily (Smith et al., 1994).

A second class of neurotrophin receptors are the Tropomyosin-Receptor-Kinase (Trk) family: TrkA, TrkB and TrkC. In their extracellular domains, Trk receptors consists of an N-terminal block of three LRRs flanked by CRCs, followed by two immunoglobulin (Ig) C2 domains (Martin-Zanca et al., 1989, Shelton et al., 1995) (Fig 1.2). Trks possess an intracellular tyrosine kinase domain, which is phosphorylated following neurotrophin binding (Klein et al., 1991, Kaplan et al., 1991).

Trk receptors are relatively promiscuous in their binding to neurotrophins. NGF preferentially binds to TrkA, BDNF and NT-4 to TrkB, and NT-3 to TrkC; to a lesser extent, NT-3 also activates TrkA and TrkB (Reichardt, 2006). However alternative splicing of Trk receptors can modulate their neurotrophin-binding affinities. The inclusion of a short stretch of amino acids in the juxtamembrane ectodomain of TrkA makes the receptor responsive to NT-3, and the longer version of TrkB is more sensitive to NT-3 and NT-4 (Clary and Reichardt, 1994, Strohmaier et al., 1996). The promiscuity of neurotrophin/Trk binding is unusual, and contrasts with the relatively specific interactions of most ligand/receptor pairs.

1.4.2 Trk-$p75^{NTR}$ interactions and neurotrophin binding

When they are expressed separately, $p75^{NTR}$ and TrkA bind NGF with a similar, relatively low affinity, but when they are co-expressed, high affinity binding is reported with increased receptor internalisation (Hempstead et al., 1991, Mahadeo et al., 1994, Chao, 2003). The co-operation of $p75^{NTR}$ and TrkA in producing the high affinity binding has been mapped to the

transmembrane and intracellular domains of both proteins (Esposito et al., 2001). And the interaction of the TrkB intracellular domain with $p75^{NTR}$ is phosphorylation-dependent (Bibel et al., 1999). Moreover, the presence of $p75^{NTR}$ increases the specificity of neurotrophin binding to their preferred Trk receptor (Roux and Barker, 2002). However, other groups have shown that TrkA binds NGF with high-affinity independently of $p75^{NTR}$, and it is unclear whether Trks directly bind to $p75^{NTR}$ during signalling (Klein et al., 1991, Jing et al., 1992, Bothwell, 1995, Roux and Barker, 2002, Wehrman et al., 2007, Barker, 2007). Further structural studies are needed determine how Trks and $p75^{NTR}$ together form the high affinity binding site.

$p75^{NTR}$ directly binds to neurotrophin Cys-knot dimers. A systematic deletion analysis showed that all four cysteine-rich clusters of $p75^{NTR}$ are required for neurotrophin binding (Baldwin et al., 1992). This was confirmed by the crystal structure of the $p75^{NTR}$ ectodomain/NGF complex (He and Garcia, 2004). $p75^{NTR}$ binds the interface of neurotrophin dimers, and 2:2 binding depends on glycosylation of the receptor , (He and Garcia, 2004, Aurikko et al., 2005, Gong et al., 2008). Gong and colleagues showed that this disparity was due to structural differences in $p75^{NTR}$ resulting from glycosylation.

The binding of neurotrophins to Trks requires the receptors' second Ig domain, which also confers receptor-ligand specificity (Urfer et al., 1995). In agreement with this, a crystal structure shows the second Ig domain forms a complex with NGF, and there is symmetrical binding along the interface of the NGF dimer resulting in a 2:2 stoichiometry (Wiesmann et al., 1999). It is currently unclear how $p75^{NTR}$ and Trk receptors interact to form high-affinity neurotrophin binding sites (Aurikko et al., 2005, Wehrman et al., 2007, Zaccaro et al., 2001, Barker, 2007).

1.4.3 Sortilin

Sortilin represents a third class of neurotrophin receptor. Sortilin contains an extracellular VPS10 domain, forming a β-propeller, and a short intracellular domain involved in vesicle trafficking (Petersen et al., 1997, Quistgaard et al., 2009) (Fig 1.2). Sortilin directly binds pro-neurotrophins with higher affinity than the mature forms, and forms a signalling complex with $p75^{NTR}$ (Nykjaer et al., 2004, Teng et al., 2005, Yano et al., 2009, Feng et al., 2010). The precise mechanisms of neurotrophin binding and interactions with $p75^{NTR}$ and Trk receptors remain to be explored.

1.5 Neurotrophin signalling

1.5.1 $p75^{NTR}$ signalling pathways

Because it lacks intrinsic catalytic activity, $p75^{NTR}$ initiates intracellular signalling through a number of adapter proteins, which interact either in the juxtamembrane region or in its death domain (Roux and Barker, 2002) (Fig 1.3). The interacting proteins Tumour Necrosis Factor Receptor-Associated Factor 6 (TRAF6), Neurotrophin Receptor-Interacting Factor (NRIF) and Neurotrophin Receptor-Interacting MAGE homologue (NRAGE) have been shown to activate JNK, a pro-apoptotic MAP kinase (Gentry et al., 2004, Salehi et al., 2002). The interaction of $p75^{NTR}$ with Neurotrophin Receptor-Associated Cell Death Executer (NADE) activates an alternative pro-apoptotic pathway through a 14-3-3 protein, while engagement of Schwann Cell Factor 1 (SC1) repressed Cyclin E (Kimura et al., 2001, Chittka et al., 2004). $p75^{NTR}$-mediated activation of TRAF6 can also lead to the recruitment of Interleukin-1 Receptor-Associated Kinase (IRAK) and the adapter protein p62, which together activate NFκB, a pro-survival transcription factor (Khursigara et al., 1999, Mamidipudi et al., 2002).

Fig 1.2 – Protein domains of vertebrate neurotrophin receptors and *Drosophila* Toll

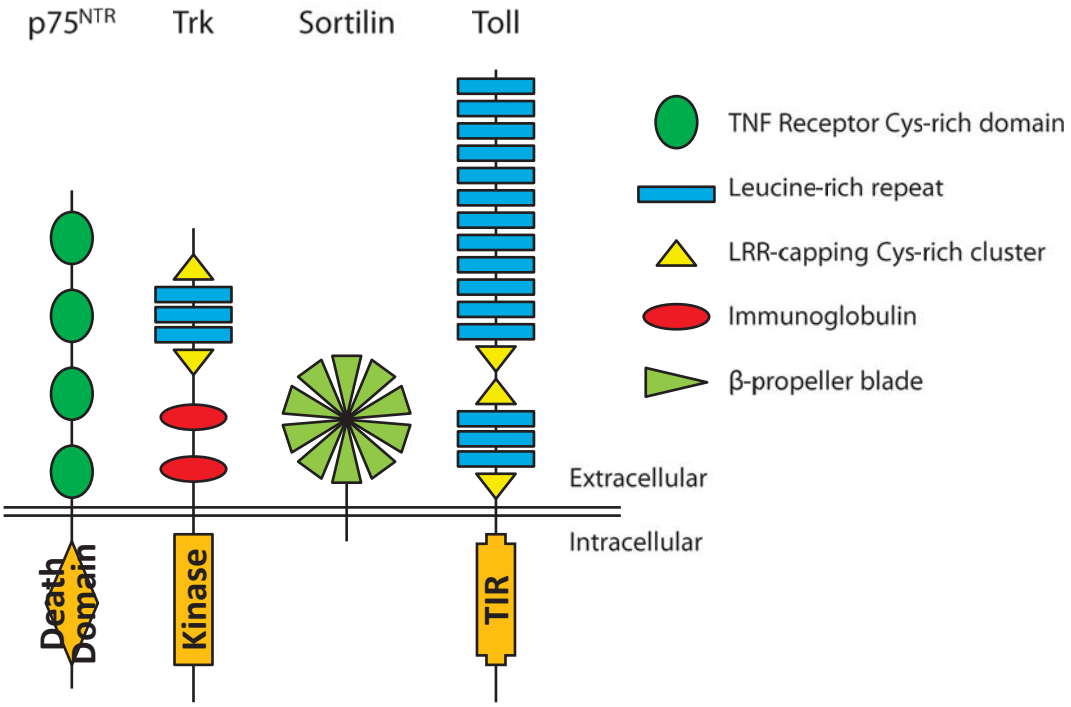

Vertebrate neurotrophin receptors are modular proteins made up of a number of discreet domains. The *Drosophila* Toll receptor is also shown for comparison.

Signalling TRAF and IRAK proteins to activate NFκB is reminiscent of the Toll signalling pathway.

Unbound $p75^{NTR}$ activates RhoA, resulting in reorganisation of the actin cytoskeleton (Yamashita et al., 1999). Neurotrophin binding to $p75^{NTR}$ blocks this pathway, therefore neurotrophin/$p75^{NTR}$ signalling negatively regulates RhoA. $p75^{NTR}$ has been shown to activate Ras, a small G-protein upstream of the pro-survival MAP kinase ERK (Blöchl et al., 2004). A further $p75^{NTR}$-activated pathway involves sphingolipid metabolism, and the release of Ceramide. Ceramide can then interact with a broad range of signalling molecules, including NFκB, JNK, ERK and PI3K (Dobrowsky and Carter, 1998, Blöchl and Blöchl, 2007).

1.5.2 Trk Receptor signalling pathways

Ligand binding results in Trk receptor dimerisation, leading to the autophosphorylation of several tyrosine residues in its intracellular domain (Huang and Reichardt, 2003) (Fig 1.4). Two phospho-tyrosine residues are principally responsible for the engagement of Trk-interacting proteins, and the activation of cell signalling cascades: Y490, which is close to the membrane and N-terminal to the kinase domain, and Y785, which lies outside the kinase domain at the C-terminal end of the receptor (residues numbered according to their positions in TrkA, and are conserved across all Trks).

Neurotrophin binding of Trks activates PLCγ (Vetter et al., 1991). PLCγ is phosphorylated following neurotrophin binding, and induces the breakdown of PtdIns(4,5)P_2 to IP_3 and DAG, which are second messengers that can carry out a range of functions (see below) (Reichardt, 2006). Y785, at the C-terminal of Trk receptors, serves as the docking point for PLCγ, and phosphorylation of this residue activates PLCγ (Obermeier et al., 1993, Loeb et al., 1994).

The juxtamembrane Y450 recruits Shc and Frs2, which activate signalling by two distinct pro-survival molecules (Stephens et al., 1994, Meakin et al., 1999). Activated Trk receptors signal through ERK, a member of the MAP kinase family. Recruitment of Shc activates the signalling pathway involving Grb2, SOS and Ras, which leads to the activation of Raf-1, MEK and ERK (English et al., 1999). The activation of ERK by Ras is relatively short-lived, however Trk receptors can initiate prolonged ERK signalling, through an alternative activation pathways (Huang and Reichardt, 2003). By signalling through Crk, C3G and Rap1, activation of MEK and ERK is via B-Raf (York et al., 1998). The longer-lasting activation of ERK has been shown to be initiated by FRS2, which can bind Y450 instead of Shc (Kao et al., 2001). Alternatively, Trk signalling via an ankyrin-rich membrane-spanning protein (ARMS) can activate Crk, and has been shown to function independently of Y450 (Arévalo et al., 2004).

Three mechanisms activate pro-survival PI3K/Akt signalling through Trks. As well as signalling through ERK, Ras can activate PI3K; NGF-TrkA signalling and electrical activity synergistically interact in neurons to evoke Ras-mediated Akt signalling (Rodriguez-Viciana et al., 1994, Vaillant et al., 1999). The second mechanism of Akt activation is through the binding of Gab1 to PI3K, which occurs downstream of Shc and Grb at Y450 (Holgado-Madruga et al., 1997). And third, IRS-1, already known as an activator of PI3K signalling in response to insulin, is also phosphorylated by Trks (Backer et al., 1992, Yamada et al., 1997).

1.5.3 Neurotrophins and cell survival

Neurotrophins maintain the survival of neurons, and this is seen predominantly in vertebrate sensory and sympathetic neurons (Huang and Reichardt, 2001). The pro-survival effect is primarily mediated by mature neurotrophins binding Trk receptors, and activating pro-

Fig 1.3 – p75^{NTR} signalling pathways

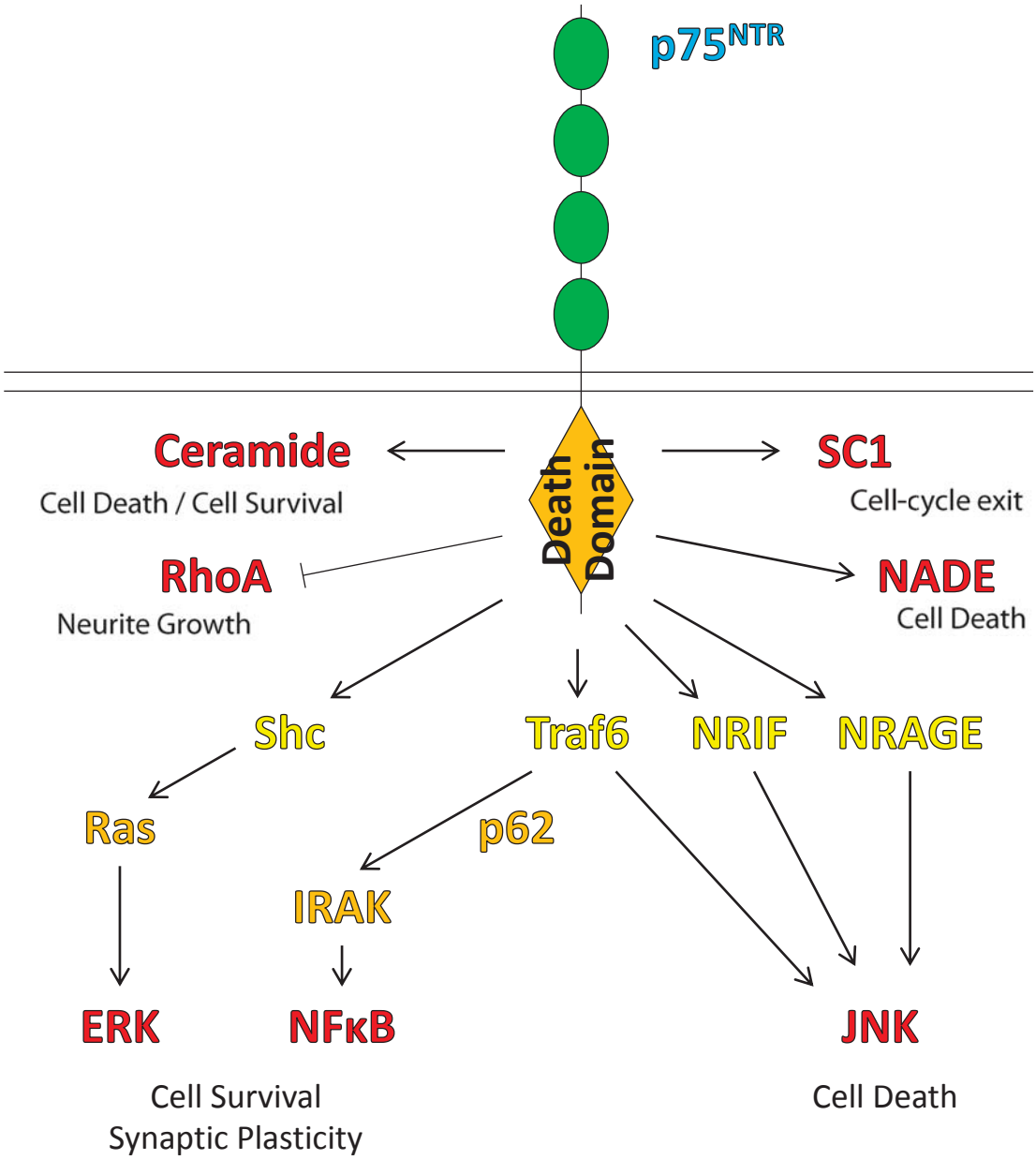

Ligand binding to p75^{NTR} activates a wide range of cell signalling pathways. Pro-growth and survival effects are mediated by RhoA, ERK and NFκB, while pro-apoptotic signals are primarily mediated by JNK, as well as NADE and SC1. Ceramide generation can have pro-survival and pro-apoptotic effects on cells. For references, see main text.

Fig 1.4– Trk signalling pathways

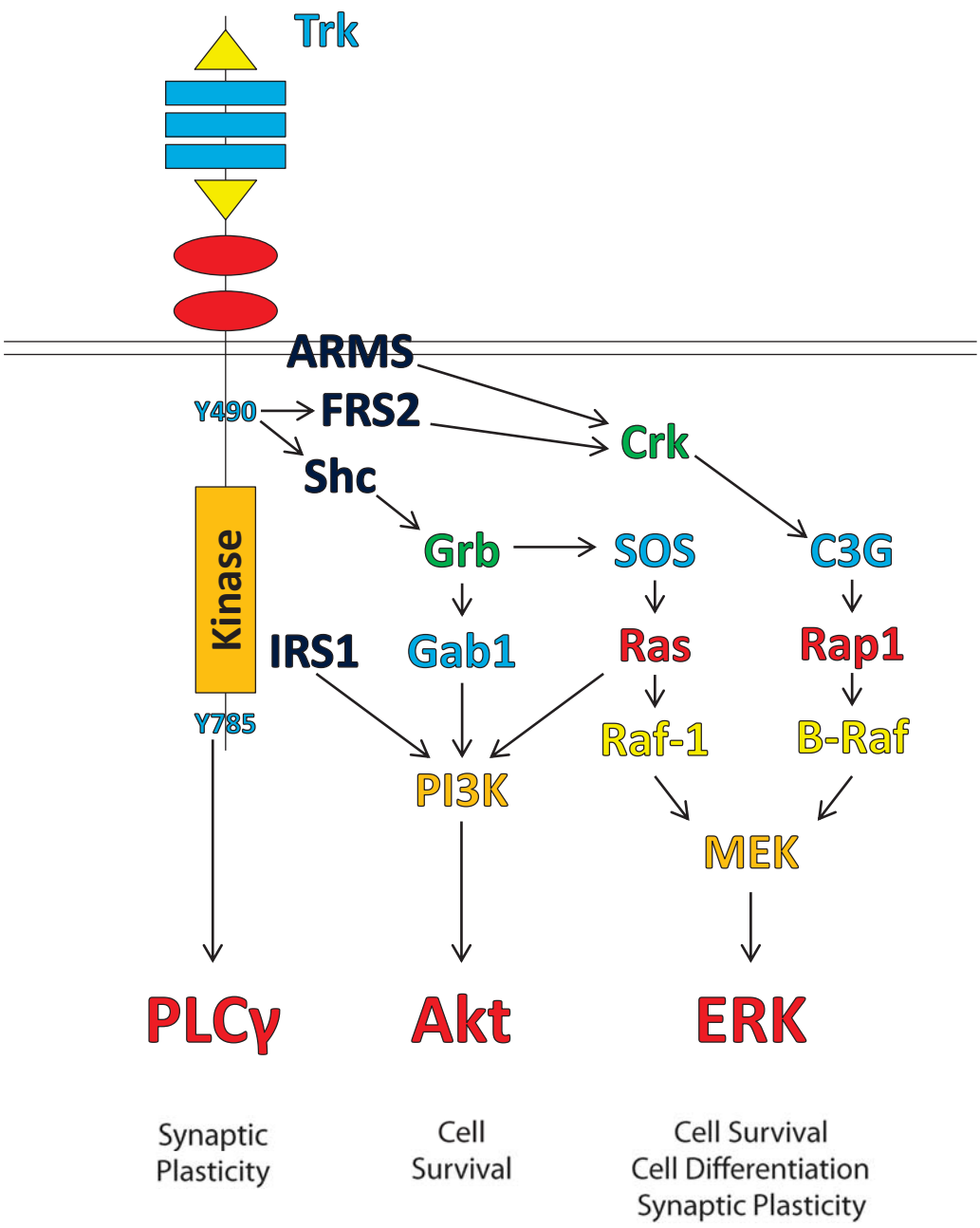

Ligand binding to Trk receptors results in the activation of a number of cell signalling pathways. The principal effectors of Trk signalling are PLCγ, Akt and ERK. The phosphotyrosine residues involved in signal transduction are shown – their positions in TrkA are given. For references, see main text.

survival signalling pathways. Signalling through Akt mediates the pro-survival activity of neurotrophins, and this is achieved through transcriptional regulation as well as direct inhibition of pro-apoptotic molecules (Crowder and Freeman, 1998, Kaplan and Miller, 2000). Akt activates NFκB to promote neuronal survival and differentiation, and inhibits Bad and Bax to block apoptosis. The activation of ERK in neurons is also pro-survival, although ERK is also involved in promoting neuronal differentiation (Creedon et al., 1996, Meakin et al., 1999). Consistent with their pro-survival functions, knock-out mice lacking any of the neurotrophins or Trks show a reduction in the number of neurons (Huang and Reichardt, 2001).

Pro-neurotrophins, signalling through $p75^{NTR}$ and Sortilin, induce apoptosis by activating JNK signalling (Lee et al., 2001, Nykjaer et al., 2004, Yano et al., 2009). And at high concentrations, in the absence of a Trk, mature neurotrophins can also signal through $p75^{NTR}$ to cause cell death (Bamji et al., 1998). A $p75^{NTR}$-hypomorphic mouse has been shown to possess increased numbers of spinal cord neurons, consistent with a function in inducing cell death (Frade et al., 1996). However, the role of $p75^{NTR}$ in increasing neurotrophin affinity at Trk receptors (and therefore pro-survival signalling) complicates matters, and a different $p75^{NTR}$-null mouse has a dramatically reduced neuronal cell number (von Schack et al., 2001). The opposite functions of mature neurotrophins promoting cell survival through Trks, and pro-neurotrophins promoting apoptosis through $p75^{NTR}$, were consolidated into a 'Yin and Yang' model of neurotrophin action (Lu et al., 2005). However, it is unlikely that the situation is so straight-forward, since $p75^{NTR}$ is able to activate multiple pro-survival pathways

In addition to its pro-apoptotic functions, $p75^{NTR}$ signals through NFκB to promote cell survival (Maggirwar et al., 1998, Hamanoue et al., 1999). When Trks and $p75^{NTR}$ are co-expressed, the pro-survival signalling pathways activated by Trk block the $p75^{NTR}$-mediated

apoptotic signals, while NFκB continues to signal (Yoon et al., 1998, Davey and Davies, 1998). Thus, Trk signalling appears to trump $p75^{NTR}$ signalling in the control of cell survival. Activation of $p75^{NTR}$, in the absence of Trk signalling, can prevent apoptosis through NFκB, regardless of any concomitant JNK signalling; ceramide generation can activate PI3K, and prevent apoptosis through Akt; and tyrosine residues present on the $p75^{NTR}$ death domain can become phosphorylated, bind Ras, and signal via the Shc/Grb2/SOS pathway to activate ERK (Hughes et al., 2001, Song and Posse de Chaves, 2003, Blöchl et al., 2004). *In vivo*, it is most likely that the true signalling pathways activated will depend on the cell context, the repertoire of receptors and signalling molecules present, and the balance of mature versus pro-neurotrophins.

1.5.4 Neurotrophins and cell shape

Neurotrophins induce the neuronal differentiation of a phaeochromocytoma cell line (PC12), and promote neurite outgrowth from sensory neurons (Levi-Montalcini, 1987). Neuronal differentiation is often measured by the extent of neurite outgrowth from PC12 cells or cultured neurons, and can be uncoupled from pro-survival signalling pathways (Meakin and MacDonald, 1998). One model to explain this is the dual activation of ERK signalling. Short-lived ERK activation through Ras promotes survival, whereas prolonged ERK activation through FRS2 and ARMS results in enhanced neurite outgrowth, and therefore differentiation (Meakin et al., 1999, Arévalo et al., 2004). NFκB is also involved in promoting neurite extension in response to neurotrophins (Gutierrez and Davies, 2011). Signalling through $p75^{NTR}$, NFκB increases the length of dendrites, involving cross-talk with the Notch pathway; and activation of NFκB via Trk and Src promotes the growth of neuronal processes (Salama-Cohen et al., 2005, Gavaldà et al., 2009). *In vivo*, systemic administration of NGF in mice

increases the size and complexity of sensory neurons, and BDNF injected into the optic tectum of tadpoles increases the axonal complexity of retinal ganglion cells (Ruit et al., 1990, Cohen-Cory and Fraser, 1995).

In addition to promoting the formation and outgrowth of neurites, neurotrophins promote axon targeting, and can signal as chemoattractants (Campenot, 1977, Gundersen and Barrett, 1979). Interestingly, the effects of the different neurotrophins are not equal: NGF- and BDNF-mediated attraction is dependent on cAMP, while NT-3-mediated attraction is blocked on cGMP inhibition (Song and Poo, 1999). Intracellular activation of PI3K and PLCγ by Trk has been shown mediate the chemoattractive effects of NGF on the growth cone (Ming et al., 1999). $p75^{NTR}$ can signal independently of Trks to promote axon extension. In the absence of neurotrophins, $p75^{NTR}$ activates RhoA, a small GTPase that promotes growth cone collapse; binding of neurotrophin reduced RhoA activity, and therefore increases neurite elongation (Yamashita et al., 1999, Gehler et al., 2004). However, the role of $p75^{NTR}$ in axon guidance is complicated by its interaction with the Nogo receptor (NgR) and LINGO. $p75^{NTR}$ acts as a co-receptor with NgR and LINGO, and inhibits the growth of axons through myelin-rich environments (Wang et al., 2002, Mi et al., 2004). In this context, interaction of myelin components with $p75^{NTR}$ and NgR activates RhoA, therefore preventing axon growth (Yamashita and Tohyama, 2003). The regulation of neuronal differentiation and targeting by neurotrophins involves Trks and $p75^{NTR}$, multiple intracellular signalling pathways, and can be influenced by additional extra- and intracellular factors.

1.5.5 Neurotrophins and neural function

Neurotrophins regulate multiple aspects of neural function, for example the influence of NGF on pain sensation. Firstly, NGF is preferentially required for the survival of nociceptive

neurons, and NGF and TrkA mutant mice exhibit severe sensory phenotypes, while the control of movement is less affected (Silos-Santiago et al., 1995, Smeyne et al., 1994, Crowley et al., 1994). Secondly, NGF/TrkA signalling induces the structural differentiation of pain-sensing neurons: TrkA is required for innervation of the skin, independently of its roles in cell survival (Patel et al., 2000). Thirdly, NGF induces the expression of calcitonin gene-related peptide (CGRP) and substance P, markers of pain receptor differentiation and peptide neurotransmitters of nociceptive signals (Patel et al., 2000). And fourthly, TrkA signalling increases the sensitivity of the TRPV1 nociceptor to painful stimuli, through a PLCγ-mediated depletion of inhibitory PtdIns(4,5)P_2 (Chuang et al., 2001). Similarly to their effects on sensory neurons, neurotrophins are involved in many aspects of autonomic nervous system function, from the survival and phenotypic specification of neurons to the control of neurotransmitter production and conductivity (Ernsberger, 2009).

In the CNS, BDNF regulates synaptic transmission, where it promotes the induction of long-term potentiation (LTP) in hippocampal neurons, and LTP is impaired in BDNF-mutant mice (Figurov et al., 1996, Korte et al., 1995, Patterson et al., 1996). LTP is a long-lasting sensitisation of a synapse by high-frequency stimulation, and results in enhanced synaptic transmission that lasts for days (Malenka and Nicoll, 1999). BDNF signalling through TrkB has been found to regulate a number of aspects of LTP (Minichiello, 2009). BDNF and TrkB expression are upregulated in hippocampal glutamatergic neurons after LTP induction (Patterson et al., 1992). Acting pre-synaptically, BDNF/Trk signalling can enhance glutamate release (Li et al., 1998, Xu et al., 2000). In the post-synaptic neuron, BDNF potentiates NMDA- and AMPA-type glutamate receptor activity, and can induce the transcription and translation of AMPA receptors (Levine et al., 1998, Caldeira et al., 2007). And BDNF is also required for the changes in dendritic spine morphology that characterise late stages of LTP

(Tanaka et al., 2008). PLCγ mediates the effects of TrkB activation, and is required both pre- and post-synaptically to enhance LTP (Minichiello et al., 2002, Gärtner et al., 2006). While it was not been shown to affect LTP, $p75^{NTR}$ can modulate dendritic morphology, AMPA receptor expression, and long-term depression (LTD – a reduction in synaptic excitability following low-frequency stimulation) (Zagrebelsky et al., 2005, Rösch et al., 2005). And pro-BDNF, signalling through $p75^{NTR}$, enhances LTD (Woo et al., 2005). Similarly to cell survival, mature and pro-neurotrophins are thought to evoke opposite responses by signalling through Trk or $p75^{NTR}$: the Yin-Yang model neurotrophin function (Lu et al., 2005).

Defects in neurotrophin signalling can lead to neurological and psychiatric illness. NGF/TrkA signalling is essential for the development of the sensory and sympathetic nervous systems (Huang and Reichardt, 2001). Disruption of peripheral TrkA signalling in humans leads to Congenital Insensitivity to Pain with Anhidrosis (CIPA), a genetic disorder mapped to the TrkA gene (Indo et al., 1996). In the CNS, NGF is required for the survival and targeting of cholinergic neurons to the cortex, and exogenous NGF prevents age-associated degeneration of these neurons (Chen et al., 1997, Fischer et al., 1987). These studies also showed an association between NGF-mediated cholinergic neuron survival and improved memory function in rodents, consistent with the cholinergic model of Alzheimer's disease (Bartus et al., 1982). Again, the opposing roles of pro- and mature NGF, and the balance between them, are thought to contribute cholinergic cell survival and to the pathology of Alzheimer's disease, and the therapeutic delivery of NGF is being actively pursued as a potential treatment of the illness (Cuello et al., 2010, Covaceuszach et al., 2009).

A polymorphism of BDNF is known in humans, and is associated with memory impairments (Egan et al., 2003). Mice heterozygous for BDNF, which is normally highly expressed in the hippocampus, also show learning deficits (Linnarsson et al., 1997). This mutation is a single

residue substitution in the BDNF pro-domain: the valine at position 66 is mutated to methionine. The result of this mutation is a reduced activity-dependent BDNF secretion through the regulated pathway, emphasising the importance of the pro-domain for neurotrophin processing (Egan et al., 2003, Suter et al., 1991). Knock-in mice with the equivalent mutation have reduced hippocampal volume, reduced dendritic complexity, and show increased anxiety-related behaviours (Chen et al., 2006). Similarly, human carriers of the Val66Met allele show reduced brain volume, memory impairments, and increased anxiety (Chen et al., 2008).

1.5.6 Non-neuronal functions of Neurotrophins

Neurotrophins play a role in early development, and have functions before the specification of neurons. In the chicken, the expression of TrkC is seen from the neural plate stage and TrkB from the neural tube stage, and both can influence cell proliferation and differentiation (Bernd, 2008). In chick and quail embryos, neurotrophins and their receptors are expressed during gastrulation and neurulation (Baig and Khan, 1996, Zhang et al., 1996). In the early quail embryo, TrkC is most prominently expressed; similarly, in rats, the TrkC ligand NT-3 is expressed early in embryogenesis (Zhang et al., 1996, Maisonpierre et al., 1990a). And even earlier in mouse development, shortly after fertilisation, BDNF/TrkB signalling has a role in the maturation of oocytes to pre-implantation embryos, and the development of the blastocyst (Kawamura et al., 2005, Kawamura et al., 2007).

Vertebrate neurotrophins play roles in the development and function of other tissues. $p75^{NTR}$ and Trk receptors are expressed in the gut, skeletal muscle, heart, kidney and epidermis (Thomson et al., 1988, Tessarollo et al., 1993, Shelton et al., 1995). Pancreatic β-cells respond to neurotrophin signalling, and $p75^{NTR}$ is required for kidney development (Polak et al., 1993,

Sariola et al., 1991). In the skin, neurotrophins have pro-survival effects on melanocytes, and induce proliferation of keratinocytes (Yaar et al., 1994, Pincelli et al., 1994). Within the vasculature, neurotrophin signalling induces proliferation of endothelial cells and is angiogenic, and promotes the proliferation and migration of smooth muscle cells (Cantarella et al., 2002, Donovan et al., 1995). Neurotrophins and their receptors are up-regulated in vascular injury and disease, and it has been proposed that they play a role in a wide range of tissue repair paradigms (Donovan et al., 1995, Micera et al., 2007).

Neurotrophins have effects on the immune system. NGF induces the proliferation and differentiation of mast cells (Aloe and Levi-Montalcini, 1977, Matsuda et al., 1991). This indicates that NGF can behave like a conventional immune cytokine, and that it may play an important role in the innate and adaptive immune systems (Levi-Montalcini et al., 1996). As well as responding to exogenous NGF, they also synthesise and release their own NGF, and that NGF induces mast cell degranulation (Leon et al., 1994, Mazurek et al., 1986). ProNGF has been shown to induce Natural Killer cell death, signalling through $p75^{NTR}$ and Sortilin (Rogers et al., 2010). The expression of neurotrophins and their receptors is now known across a wide range of immune cell types, and in almost all immunologically important tissues and organs (Vega et al., 2003); NGF has been associated with allergic and autoimmune disorders (Nockher and Renz, 2006a, Nockher and Renz, 2006b, Seidel et al., 2010).

Neurotrophins represent a possible mechanism for communication between the immune and nervous systems. Lymphoid tissues are extensively innervated by sympathetic neurons, and the spleen is a rich source of neurotrophins to support this innervation (Felten et al., 1985, Maisonpierre et al., 1990a). This represents a nervous-to-immune direction of communication, and could allow sympathetic modulation of an immune response.

Communication from immune-to-neural cells is well established, particularly in the context of pain (Moalem and Tracey, 2006). Here, peripheral immune cells degranulate in response to injury or infection, and the released peptides and neurotransmitters directly and indirectly activate afferent pain fibres. Moreover, mast cells are found in the brain, where they may influence neuronal activity or local immune responses, and have been implicated in multiple sclerosis pathogenesis (Silver et al., 1996).

The complexity in neurotrophin processing and binding is reflected by their diverse – and often contradictory – effects on cell signalling. In many contexts, the 'yin and yang' model describes well the effects of pro- and mature neurotrophins in cell survival and synaptic signalling. However there are multiple instances when Trks and $p75^{NTR}$ carry out similar functions. Experiments on neurotrophin function are carried out *in vitro*, in cultured cell lines, in primary cell cultures, in tissue explants, and *in vivo*. This wide range of experimental paradigms generates a wealth of results that are frequently not comparable. Ultimately, cell context is likely to determine the true, *in vivo* functions of the neurotrophins. Using model organisms is a preferred method to investigate neurotrophin function. However, in the use of knock-out mice, it is often difficult to distinguish developmental from adult phenotypes. And neuronal phenotypes could be influenced by loss of neurotrophin signalling in other tissues, such as the immune system. Moreover, experiments in vertebrate models are expensive, can take a relatively long time to complete, and must satisfy strict ethical rules. The use of *Drosophila* lends itself to the investigation of neurotrophin function, since this family of growth factors is conserved. There are well-established techniques for gene knock-out or knock-in, which can be carried out relatively quickly, without ethical objection. To use *Drosophila* in neurotrophin research, it is essential that the DNT receptors are identified.

1.6 Invertebrate Neurotrophin receptors

The identification of neurotrophins in *Drosophila* indicated that these molecules are part of a conserved mechanism for regulating neuronal structure and function. However, it is less clear whether neurotrophin receptors are similarly conserved between vertebrates and flies. Homologues of mammalian Trks and $p75^{NTR}$ are found across vertebrate and invertebrate deuterostome species, including the lancelet, acorn worm and sea urchin (Bothwell, 2006, Hallböök et al., 2006, Benito-Gutiérrez et al., 2006).

1.6.1 Invertebrate Trk homologues

Evidence of Trk homologues in protostomes includes cross-reactivity of neural tissue with anti-Trk antibodies. In the squid giant synapse, a protein that is labelled with anti-TrkA is phosphorylated on NGF application (Moreno et al., 1998). And the earthworm shows immunoreactivity to Trk and $p75^{NTR}$ in neurons and non-neuronal tissues (Lucini et al., 1999, Davoli et al., 2002). However, these sorts of cross-reactivity studies should be taken with caution, since antibodies have been found to bind non-specifically to an invertebrate plasma protein (Hahn et al., 1996).

A significant advance in understanding the evolutionary origin of the Trk family came with the identification of a Trk homologue in the snail *Lymnaea*. Ltrk has an intracellular kinase domain that retains many of the residues unique to the Trk family of receptors, and has an extracellular domain that is very closely related to the Trks (van Kesteren et al., 1998, Beck et al., 2004). One difference is that the two extracellular IgC2 domains of vertebrate Trks are replaced with a single IgC1 domain in Ltrk. Ltrk is expressed extensively in juvenile and adult CNS neurons, and is required for neuronal survival and neurite outgrowth, indicating

that Trk functions have also been conserved (Bulloch et al., 2005, van Kesteren et al., 1998). In another snail, *Aplysia*, a receptor tyrosine kinase was found whose intracellular domain was most closely related to that of the Trks (Ormond et al., 2004). Because the EGF domain-containing extracellular region shares no homology to the Trks, it was named ApTrkL (Aplysia Trk-Like). Like vertebrate Trks, it has functions in synaptic long-term facilitation through activation of ERK, though this is in response to 5-HT signalling (Ormond et al., 2004). It is interesting to note that, although absent in the primitive deuterostome *Amphioxus*, and the protostome *Aplysia*, the C-terminal tyrosine responsible for PLCγ activation in vertebrate Trks is conserved in *Lymnaea* (van Kesteren et al., 1998).

Trk homologues have been identified in the genome of the waterflea, *Daphnia pulex* (Wilson, 2009). The water flea is a crustacean, and therefore an arthropod like *Drosophila*. Remarkably, *Daphnia* Trk is highly homologous to vertebrate Trks, sharing the same extracellular domains (including two IgC2 domains), a Trk-specific tyrosine kinase domain, and a C-terminal 'PLCγ-docking' tyrosine residue (Wilson, 2009). This study also found a *Daphnia* homologue to ApTrkL, sharing a common extracellular EGF domain, a Trk-like kinase domain, and C-terminal extension also seen in the *Aplysia* receptor. Wilson found Trk homologues in an additional snail (*Lottia*) and an annelid (*Capitella*), and TrkL homologues in *Lottia* and insects, including the honeybee, *Apis* (Wilson, 2009). This suggests that a Trk was present in the bilateral ancestor of protostomes and deuterostomes, and that a TrkL gene likely emerged in the protostomes. These data suggest that Trk was lost before the emergence of the insects, and that TrkL was lost in *Drosophila*. The true evolutionary origin of the Trks is likely to become clearer as more genomes are sequenced, and as their annotation improves. The *in vivo* functions of most invertebrate Trk homologues also remain to be demonstrated.

In flies, a receptor with an homologous kinase domain to Trk was sought, resulting in the identification of Dtrk (Pulido et al., 1992). However, it was noted at the time that the extracellular domain was not conserved with vertebrate Trks, and that there were some differences in the kinase domain. In fact, Dtrk lacks the juxtamembrane NPXY phosphotyrosine binding domain found in all vertebrate Trks (incorporating the Y450 of TrkA). Functional characterisation of Dtrk showed it to be involved in Semaphorin/Plexin signalling during axon guidance, and it was re-named Off-track (Winberg et al., 2001). In the meantime, two further neuronal receptor tyrosine kinases were identified in flies, with intracellular homology to vertebrate Trks: Dror and Dnrk (Wilson et al., 1993, Oishi et al., 1997). The vertebrate Trk receptors belong to a superfamily sharing a homologous kinase domain, with divergent extracellular domains (Sossin, 2006). This group comprises the Rors (including Dror), the Musks (including Dnrk), the Discoidin receptors (including *Drosophila* Ddr), and the Trks. To date, no bona fide Trk homologue has been identified in flies.

There are proteins that share a similar extracellular domain organisation with vertebrate Trks, possessing LRR domains flanked by CRCs, followed by Ig domains. These LIG proteins belong to a number of families, and are found in vertebrates, flies and nematodes (Vogel et al., 2003, Dolan et al., 2007). A family of vertebrate LIGs, the AMIGOS, promote neurite outgrowth and neuronal survival, and an unrelated LIG, Linx, positively regulates GDNF and NGF signalling in the developing nervous system (Kuja-Panula et al., 2003, Ono et al., 2003, Mandai et al., 2009). In flies, LIGs include the Kekkons (Keks), Lambik, and CG16974. Kek1 and Kek2 are expressed in the CNS (Musacchio and Perrimon, 1996). Kek1 negatively regulates EGF signalling, while Kek5 negatively regulates BMP signalling (Ghiglione et al., 1999, Alvarado et al., 2004, Evans et al., 2009). However, the CNS functions of these receptors have not been explored. Interestingly, the Keks are phylogenetically more related to

vertebrate Trks than to Lambik (Mandai et al., 2009). This suggests that the combination of LRR and Ig domains arose early in evolution, although relatively little is known about *Drosophila* LIG receptor signalling mechanisms.

Trk receptors are modular, comprising distinct extracellular and intracellular catalytic domains. Over the course of evolution, these motifs may have been swapped, shared, and rearranged, and are now found in a vast array of different protein families. This 'bricolage' theory has been used to explain the building of the Trk receptor, and also the evolution of the superfamily of receptor tyrosine kinases (Benito-Gutiérrez et al., 2006, Sossin, 2006). As more invertebrate genomes are sequenced, and more functional studies are carried out, a clearer picture should emerge of when LRR, Ig and tyrosine kinases first came together, and how this receptor came to shape the development and function of the nervous system.

1.6.2 Invertebrate p75^{NTR} homologues

p75^{NTR} homologues have also been identified in invertebrates. There is one known TNFRSF member in *Drosophila*, called Wengen (Kanda et al., 2002). Wengen lacks a death domain, and it was suggested that the death domain-containing TNFR was a vertebrate innovation (Bridgham et al., 2003). Interestingly, Bridgham and colleagues proposed that the TNFRs in vertebrates could have recruited death-domain signalling from the Toll-like receptors in order to activate apoptotic pathways. Toll and its homologues are also well known to activate NFκB signalling, a potent pro-survival molecule. And Wengen can signal through Dorsal, an NFκB homologue (Kato et al., 2011). Wengen has also been found to be more similar to p75^{NTR} than any other of the vertebrate TNFRSF members (Bothwell, 2006). Similarly to the Trks, the newly available sequences of a number of invertebrate species reveal a more ancient origin of p75^{NTR}. TNFRSF members with death domains are found across all animals (Wiens and

Glenney, 2011). In the scallop (a mollusc), a TNFRSF member with a death domain has been cloned, and is involved in the immune response (Li et al., 2009). This receptor is similar to $p75^{NTR}$, though is more closely related to other known invertebrate TNFRSF members. Other invertebrate $p75^{NTR}$ homologues have been identified from sequenced genomes, but lack functional characterisation. These include $p75^{NTR}$ homologues in the invertebrate deuterostomes, the lancelet, the acorn worm and the sea urchin (Bothwell, 2006, Robertson et al., 2006). $p75^{NTR}$ homologues are also found in protostome genomes, including another mollusc (*Lottia*), an annelid (*Capitella*) and the arthropod, *Daphnia* (Wilson, 2009). A TNFRSF member with homology to $p75^{NTR}$, incorporating in intracellular death domain, has even been found in the cnidarian, *Nematostella* (Robertson et al., 2006). This suggests that $p75^{NTR}$ descends from an ancient receptor, originating before the emergence of bilateral animals, and that it is more ancient than the Trks.

1.7 *Drosophila* as a model organism

The *Drosophila* nervous system is a model to investigate many aspects of neuronal function, from neurogenesis to behaviour. The embryonic CNS consists of an anterior central brain, and a ventral nerve cord (VNC) that runs along the ventral midline of the embryo. The embryonic stem cells that give rise to the nervous system – the neuroblasts – first appear in stage 8, and delaminate from the ectoderm at stage 9 (stages according to Campos-Ortega and Hartenstein, 1985). Neuroblasts undergo asymmetrical division to yield another neuroblast and a ganglion mother cell (GMC); the GMC divides to produce two neurons or glia, which begin to differentiate at stage 12 (Goodman and Doe, 1993). From stage 14 to 17, the VNC condenses, becoming shorter and thicker (Fig 1.5A, B). As neurons arise and differentiate, commissural pioneer axons cross the midline to create the commissures, and the longitudinal connective

tracts are pioneered anteriorly and posteriorly to connect each segment (Hidalgo and Brand, 1997). There are two commissures (anterior and posterior) per segment that connect the longitudinal connectives, giving the embryonic neuropile a ladder-like appearance, and the neuropile occupies a dorsal position within the cell bodies of the VNC (Goodman and Doe, 1993) (Fig 1.5C, D). Clusters of peripheral nervous system (PNS) cells arise from the ectoderm, and form the sensory organs (Jan and Jan, 1993). The sensory neurons differentiate from stage 13, and their axons project towards the CNS in anterior and posterior fascicles in each hemisegment (Fig 1.5D). At the same time, motor neurons project out of the CNS to the muscle along two fascicles per hemisegment (Goodman and Doe, 1993) (Fig 1.5D). The sensory and motor axons meet halfway, and their combined tracts form the segmental and intersegmental nerves.

In the larva, the CNS continues to grow, particularly in the thoracic VNC and the optic lobes (Fig 1.5E). Neuroblasts that arose in the embryo undergo a second wave of division, and generate large numbers of immature, post-mitotic neurons (Prokop and Technau, 1991). During metamorphosis, a number of changes occur to produce the adult CNS. Many of the larval interneurons undergo re-modelling, and extend their axons and dendrites; immature neurons arising during post-embryonic neurogenesis differentiate, and send out axons to their targets; and cells that are no longer required are removed by apoptosis, particularly in the abdominal VNC (Truman, 1990). Also during metamorphosis, new sensory neurons enter the CNS from the periphery. The adult CNS is made up of a number of ganglia (Fig 1.5F). The larval VNC gives rise to the adult VNC and also the sub-oesophageal ganglion of the central brain. The larval brain hemispheres develop into the large optic lobes of the adult, and the supra-oesophageal ganglion of the central brain, which contains the central complex and the mushroom bodies (Hartenstein, 1993).

Fig 1.5 - The Drosophila nervous system.

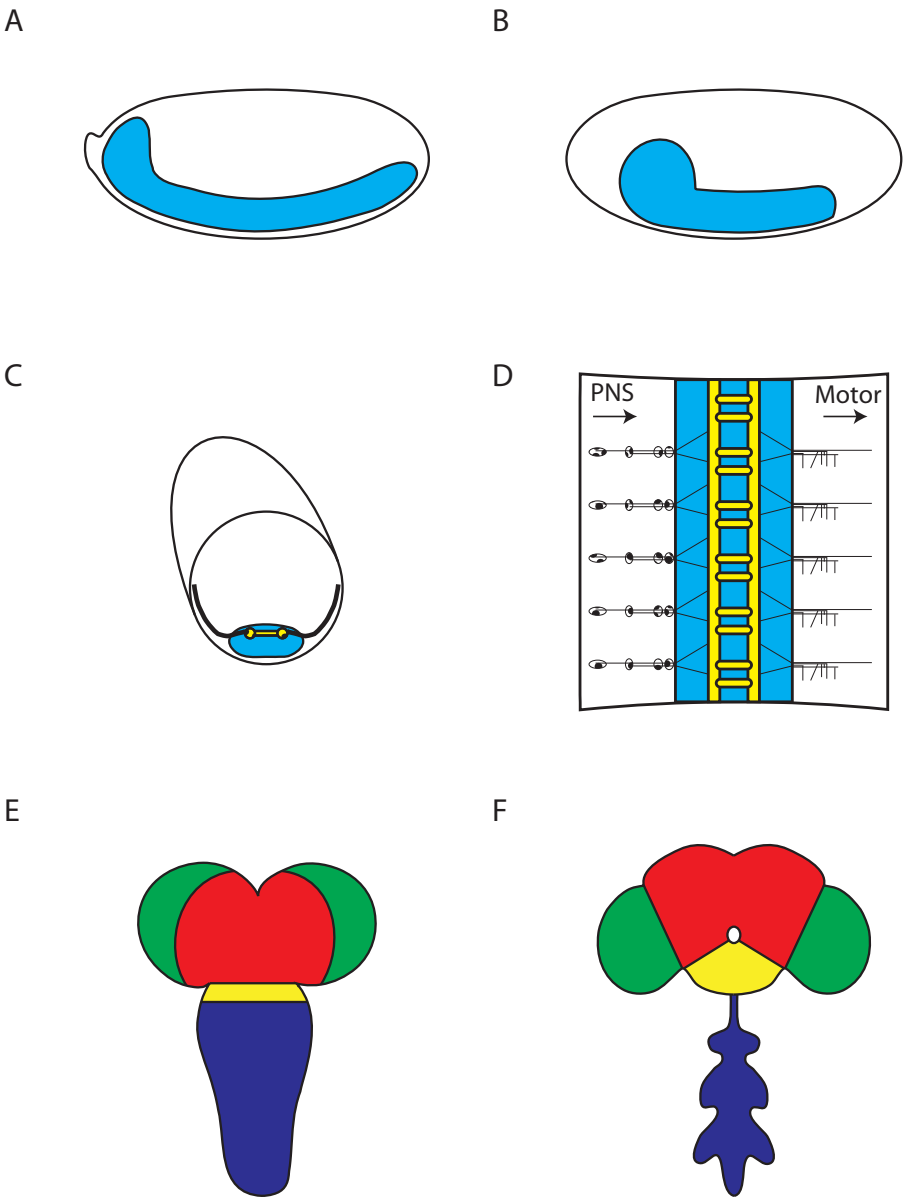

(A) In stage 13 embryos, the CNS (blue) occupies the entire length of dorsal midline. (B) By the end of embryogenesis at stage 17, the CNS has condensed. (C) The neuropile (yellow) is located dorsally within the VNC, and nerves project to the periphery. (D) Cartoon of a dissected embryo. The sensory neurons of the PNS project into the CNS (left), and motor neurons project to the muscle (right), along two nerve roots. (E) The larval CNS develops into (F) the adult CNS during metamorphosis. The larval origins of the adult ventral nerve cord (dark blue), sub-oesophageal ganglion (yellow), supra-oesophageal ganglion (red) and optic lobes (green) are indicated in (E).

1.8 Aims

Toll-7 and *Toll-6*, paralogues of *Toll*, are expressed in the CNS, but their functions are unknown (Kambris et al., 2002). *Toll* is expressed in the *Drosophila* CNS, where it promotes cell survival and axon targeting (Zhu et al., 2008, Halfon et al., 1995). The ligand for Toll, Spz, functions as a *Drosophila* neurotrophin, a ligand family that also includes DNT1 and DNT2 (Zhu et al., 2008). However, the receptors for DNT1 and DNT2 are unknown, and Toll-7 and Toll-6 are appealing candidates.

The aims of my thesis are to investigate the functions of Toll-7 and Toll-6 in the *Drosophila* nervous system, and to test whether they can serve as DNT receptors. To characterise Toll-7 and Toll-6, my aims are: (1) To determine the expression patterns of *Toll-7* and *Toll-6* in embryos, and in the larval and adult CNS. (2) To generate *Toll-7* and *Toll-6* null alleles as tools to characterise their function. (3) To test the genetic interaction of mutant and gain-of-function receptors with DNT mutants, using a lethality assay. This will show whether the *Toll-7* and *Toll-6* share common signalling pathways with the DNTs, and whether activated receptors can rescue a *DNT* mutant phenotype. (4) To investigate the functions of *Toll-7* and *Toll-6* in the nervous system, by examining their effects on adult locomotion, axon targeting and cell survival. This will show whether *Toll-7* and *Toll-6* are required for nervous system development and function, and indicate whether that have roles in common with the DNTs. (5) To generate recombinant DNT protein, and test in cell culture whether DNTs can activate signalling through Toll-7 and Toll-6. In this thesis, I aim to explore the intriguing connections between the neurotrophin and Toll families.

CHAPTER 2
METHODS

2.1 Genetics

2.1.1 Fly strains

Drosophila melanogaster were cultured on standard cornmeal agar medium, supplemented with dried yeast. Unless indicated, experiments were carried out at 25°C, in a 12 hour light/dark period. Stocks were maintained at 18°C, and transferred every 28 days. The stocks used and generated are given in Table 2.1.

2.1.2 Genetic protocols

Conventional genetic techniques were used to balance mutant alleles, Gal4 drivers and UAS transgenes on the 2nd and 3rd chromosomes (Protocols A-C, Fig 2.1). Alleles were combined by recombination on the 2nd chromosome following Protocol D (Fig 2.2) and on the 3rd chromosome following Protocol E (Fig 2.3). Double mutants on the 2nd and 3rd chromosomes were made following Protocol F (Fig 2.4). P-element transformant flies were mapped following Protocol G (Fig 2.5). P-element mobilisation for imprecise excision mutagenesis of *Toll-7* followed Protocol H (Fig 2.6), and of *Toll-6* followed Protocol I (Fig 2.7). Mutagenesis of *Toll-7* was carried out by the Hidalgo lab technician, Janine Fenton, before I arrived in the lab. *Toll-6* Mutagenesis was carried out with Janine Fenton and BSc student Sarah Quail.

Transgenes were expressed in flies using the UAS/Gal4 system (Brand and Perrimon, 1993). To express genes in the CNS, *elavGal4* and *ChaGal4* lines were used, which drive expression

Table 2.1 – Fly Stocks

No.	Genotype	Source	Protocol
1	*yw*	Hidalgo lab collection	
2	*IF / CyOlacZ*	Hidalgo lab collection	
3	*MKRS / TM6BlacZ*	Hidalgo lab collection	
4	*IF / CyO ; MKRS / TM2*	Hidalgo lab collection	
5	*IF / CyOlacZ ; MKRS / TM6BlacZ*	Hidalgo lab collection	
6	*en ; + / SM6aTM6B*	Hidalgo lab collection	
7	*φC31;;ZH-attP-86Fa (J35)*	Bloomington	
8	*yw ; ; Δ2-3Sb / TM6*	Hidalgo lab collection	
9	*GE17034 (Toll-7 P-element)*	A gift from JL Imler	
10	*GE26951 (Toll-6 P-element)*	A gift from JL Imler	
11	*UAS GAP GFP*	A gift from A Chiba	
12	*UAS mCD8 GFP*	Hidalgo lab collection	
13	*UAS Histone GFP*	Hidalgo lab collection	
Driver lines			
14	*elav Gal4*	Hidalgo lab collection	
15	*Cha Gal4*	A gift from R Baines	
16	*D42 (Toll-6) Gal4 / TM3*	A gift from S Sanyal	
17	*Toll-7 Gal4 / CyO*	G McIlroy, this work	Transgenesis by BestGene Inc
DNT mutants			
18	*DNT1[41] / DNT1[41]*	Hidalgo lab collection	
19	*Df4342 / TM6BlacZ*	Hidalgo lab collection	
20	*DNT2[e03444] / DNT2[e03444]*	Hidalgo lab collection	
21	*Df6092 / TM6BlacZ*	Hidalgo lab collection	
22	*spz[2] / TM6BlacZ*	Bloomington	
23	*DNT1[41]DNT2[e03444] / TM6BlacZ*	Hidalgo lab collection	
24	*DNT1[41]spz[2] / TM6BlacZ*	Hidalgo lab collection	
25	*DNT2[e03444]spz[2] / TM6BlacZ*	Hidalgo lab collection	
Toll-7 single mutants			
26	*Toll-7[P8] / CyOlacZ*	J Fenton	Hop-out line 9
27	*Toll-7[P8] ; + / SM6aTM6B*	G McIlroy, this work	C using lines 6 and 26
28	*Toll-7[P114] / CyOlacZ*	J Fenton	Hop-out line 9
29	*Toll-7[P114] ; + / SM6aTM6B*	G McIlroy, this work	C using lines 6 and 28
30	*Df(2R)BSC22 / SM6a*	Bloomington	
31	*Df(2R)BSC22 / CyOlacZ*	G McIlroy, this work	A using lines 2 and 30

(continued…)

Table 2.1 – Fly Stocks (cont.)

No.	Genotype	Source	Protocol
Toll-6 single mutants			
32	*Toll-6[26] / TM6BlacZ*	G McIlroy, this work	Hop-out of line 10
33	*Toll-6[31] / TM6BlacZ*	G McIlroy, this work	Hop-out of line 10
34	*Df(3L)XG4 / TM3*	Bloomington	
35	*Df(3L)XG4 / TM6BlacZ*	G McIlroy, this work	B using lines 3 and 34
Toll-7 and *Toll-6* double mutants			
36	*Toll-7[P8] / CyOlacZ ; Toll-6[26] / TM6BlacZ*	G McIlroy, this work	F using lines 26 and 32
37	*Toll-7[P8] ; Toll-6[26] / SM6aTM6B*	G McIlroy, this work	C using lines 6 and 36
38	*Toll-7[P114] / CyOlacZ ; Toll-6[31] / TM6BlacZ*	G McIlroy, this work	F using lines 28 and 33
39	*Toll-7[P114] ; Toll-6[31] / SM6aTM6B*	G McIlroy, this work	C using lines 6 and 38
Toll-7, Toll-6, and *DNT* double mutants			
40	*Toll-7[P114] / CyOlacZ ; DNT1[41] / TM6BlacZ*	G McIlroy, this work	F using lines 18 and 28
41	*Toll-7[P114] ; DNT1[41] / SM6aTM6B*	G McIlroy, this work	C using lines 6 and 40
42	*Toll-7[P114] / CyOlacZ ; DNT2[e03444] / TM6BlacZ*	G McIlroy, this work	F using lines 20 and 28
43	*Toll-7[P114] ; DNT2[e03444] / SM6aTM6B*	G McIlroy, this work	C using lines 6 and 43
44	*Toll-7[P8] / CyOlacZ ; spz[2] / TM6BlacZ*	G McIlroy, this work	F using lines 22 and 26
45	*Toll-7[P8] ; spz[2] / SM6aTM6B*	G McIlroy, this work	C using lines 6 and 44
46	*DNT1[41]Toll-6[26] / TM6BlacZ*	G McIlroy, this work	E using lines 18 and 32
47	*DNT2[e03444]Toll-6[26] / TM6BlacZ*	G McIlroy, this work	E using lines 20 and 32
48	*Toll-6[26]spz[2] / TM6BlacZ*	G McIlroy, this work	E using lines 22 and 32
DNT and *elav Gal4* driver combined lines			
49	*DNT1[41]elav Gal4 / TM6BlacZ*	Hidalgo lab collection	
50	*DNT2[e03444]elav Gal4 / TM6BlacZ*	G McIlroy, this work	E using lines 14 and 20
51	*spz[2]elav Gal4 / TM6BlacZ*	B Sutcliffe, Hidalgo lab	
52	*DNT1[41]DNT2[e03444]elav Gal4 / TM6BlacZ*	B Sutcliffe, Hidalgo lab	
Toll-7, Toll-6, and *Cha Gal4* driver combined lines			
53	*Toll-7[P8]Cha Gal4 / CyOlacZ*	G McIlroy, this work	D using lines 15 and 26
54	*Toll-7[P8]Cha Gal4 / CyOlacZ ; Toll-6[26] / TM6BlacZ*	G McIlroy, this work	F using lines 32 and 53
55	*Toll-7[P8]Cha Gal4 ; Toll-6[26] / SM6aTM6B*	G McIlroy, this work	C using lines 6 and 54

(continued…)

Table 2.1 – Fly Stocks (cont.)

No.	Genotype	Source	Protocol
Activated receptor lines			
56	*UAS Toll[10b]*	A gift from YT Ip	
57	*UAS Toll-7[ΔLRR] / TM6BlacZ*	G McIlroy, this work	Transgenesis into line 7
58	*UAS Toll-7[Cys-Tyr] / CyO*	G McIlroy, this work	Transgenesis by BestGene Inc
59	*UAS Toll-6[ΔLRR] /TM6BlacZ*	G McIlroy, this work	Transgenesis into line 7
60	*UAS Toll-6[Cys-Tyr] / TM2*	G McIlroy, this work	Transgenesis by BestGene Inc
Activated receptor and *DNT* mutant lines			
61	*UAS Toll-7[Cys-Tyr] / CyOlacZ ; DNT1[41] / TM6B*	G McIlroy, this work	F using lines 18 and 58
62	*Df6092UAS Toll-6[Cys-Tyr] / TM6BlacZ*	G McIlroy, this work	E using lines 21 and 60
63	*spz[2]UAS Toll-7[ΔLRR] / TM6BlacZ*	G McIlroy, this work	E using lines 22 and 57
64	*spz[2]UAS Toll-6[ΔLRR] / TM6BlacZ*	G McIlroy, this work	E using lines 22 and 59
Activated receptor and *DNT* double mutant lines			
65	*UAS Toll[10b] / CyOlacZ ; DNT1[41]DNT2[e03444] / TM6BlacZ*	G McIlroy, this work	F using lines 23 and 56
66	*DNT1[41]DNT2[e03444]UAS Toll-7[ΔLRR] / TM6BlacZ*	G McIlroy, this work	E using lines 23 and 57
67	*UAS Toll-7[Cys-Tyr] / CyOlacZ ; DNT1[41]DNT2[e03444] / TM6BlacZ*	G McIlroy, this work	F using lines 23 and 58
68	*DNT1[41]DNT2[e03444]UAS Toll-6[ΔLRR] / TM6BlacZ*	G McIlroy, this work	E using lines 23 and 59
69	*DNT1[41]DNT2[e03444]UAS Toll-6[Cys-Try] / TM6BlacZ*	G McIlroy, this work	E using lines 23 and 60
Activated receptor, and Toll-7 or Toll-6 mutant lines			
70	*Toll-6[26]UAS Toll-7[ΔLRR] / TM6BlacZ*	G McIlroy, this work	E using lines 32 and 57
71	*Toll-7[P8]UAS Toll-7[Cys-Tyr] / CyOlacZ*	G McIlroy, this work	D using lines 26 and 58
72	*Toll-6[26]UAS Toll-6[ΔLRR] / TM6BlacZ*	G McIlroy, this work	E using lines 32 and 59
Activated receptor, and *Toll-7* and *Toll-6* double mutant lines			
73	*Toll-7[P8] / CyOlacZ ; Toll-6[26]UAS Toll-7[ΔLRR] / TM6BlacZ*	G McIlroy, this work	F using lines 26 and 70
74	*Toll-7[P8] ; Toll-6[26]UAS Toll-7[ΔLRR] / SM6aTM6B*	G McIlroy, this work	C using lines 6 and 73
75	*Toll-7[P8]UAS Toll-7[Cys-Tyr] / CyolacZ ; Toll-6[31] / TM6BlacZ*	G McIlroy, this work	F using lines 33 and 71
76	*Toll-7[P8]UAS Toll-7[Cys-Tyr] ; Toll-6[31] / SM6aTM6B*	G McIlroy, this work	C using lines 6 and 75
77	*Toll-7[P8] / CyOlacZ ; Toll-6[26]UAS Toll-6[ΔLRR] / TM6BlacZ*	G McIlroy, this work	F using lines 26 and 72
78	*Toll-7[P8] ; Toll-6[26]UAS Toll-6[ΔLRR] / SM6aTM6B*	G McIlroy, this work	C using lines 6 and 77

Fig 2.1 – Changing of balancers for the 2nd and 3rd chromosomes

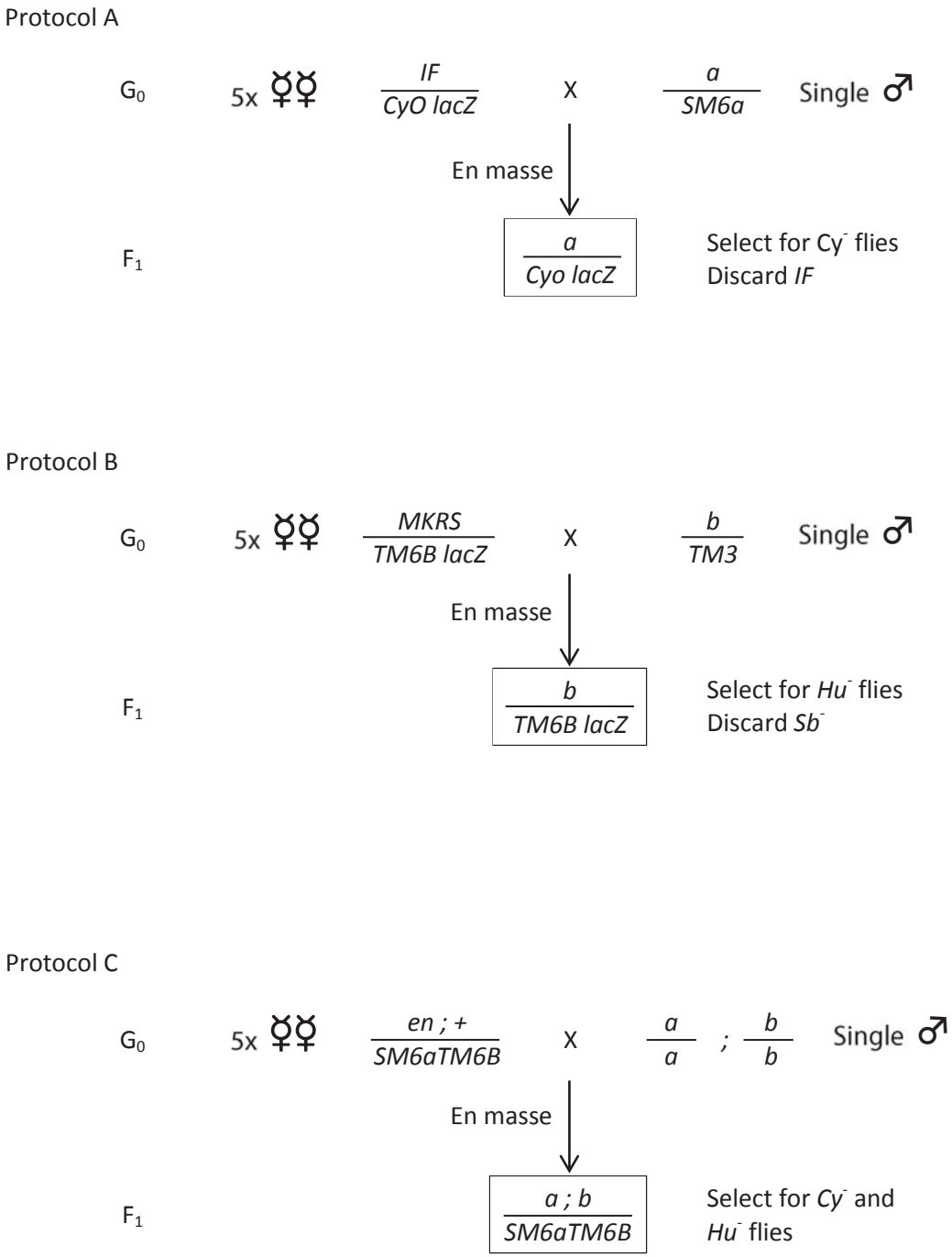

Balancer chromosomes were changed to generate fly lines indicated in Table 1. Protocols A and B were used to identify and exclude heterozygous embryos from experiments, by staining with anti-β-gal. Protocols B and C were used to identify heterozygous pupae for alleles on the 3rd, or second and third chromosomes, respectively, by identifying TM6B pupae marked with Tb-.

Fig 2.2 – Recombination on the 2nd chromosome

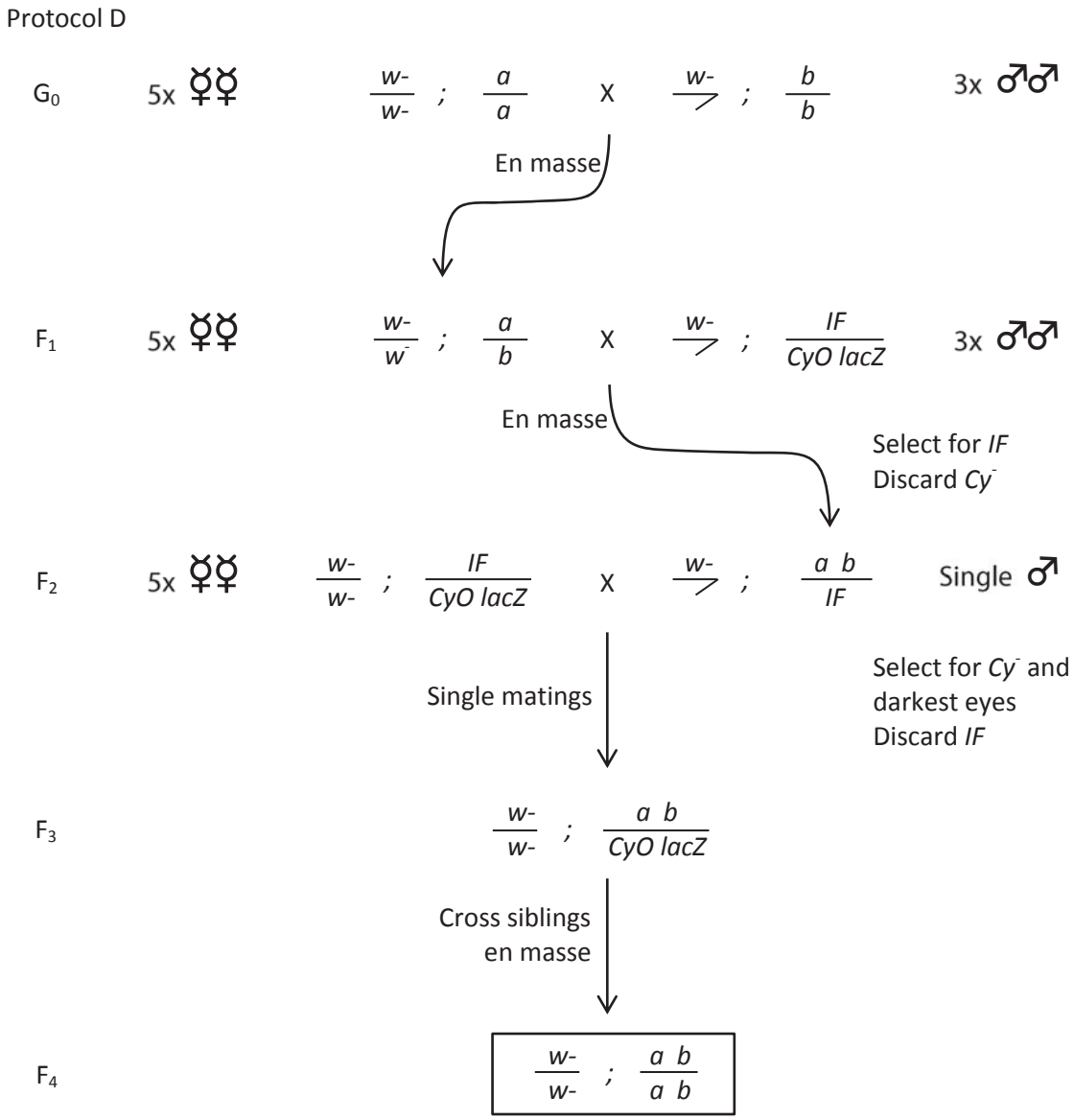

Protocol D was used combine alleles, transgenes and drivers on the 2nd chromosome, using recombination. 20-50 single males were crossed in the F_2 to generate unique recombinant lines. The presence of hop-out alleles was tested by genomic PCR, Gal4 by crossing the line to UAS GFP and examining larvae with epifluorescence, and UAS lines by eye colour and genomic PCR. Non-recombinant lines were discarded.

Fig 2.3 – Recombination on the 3nd chromosome

Protocol E

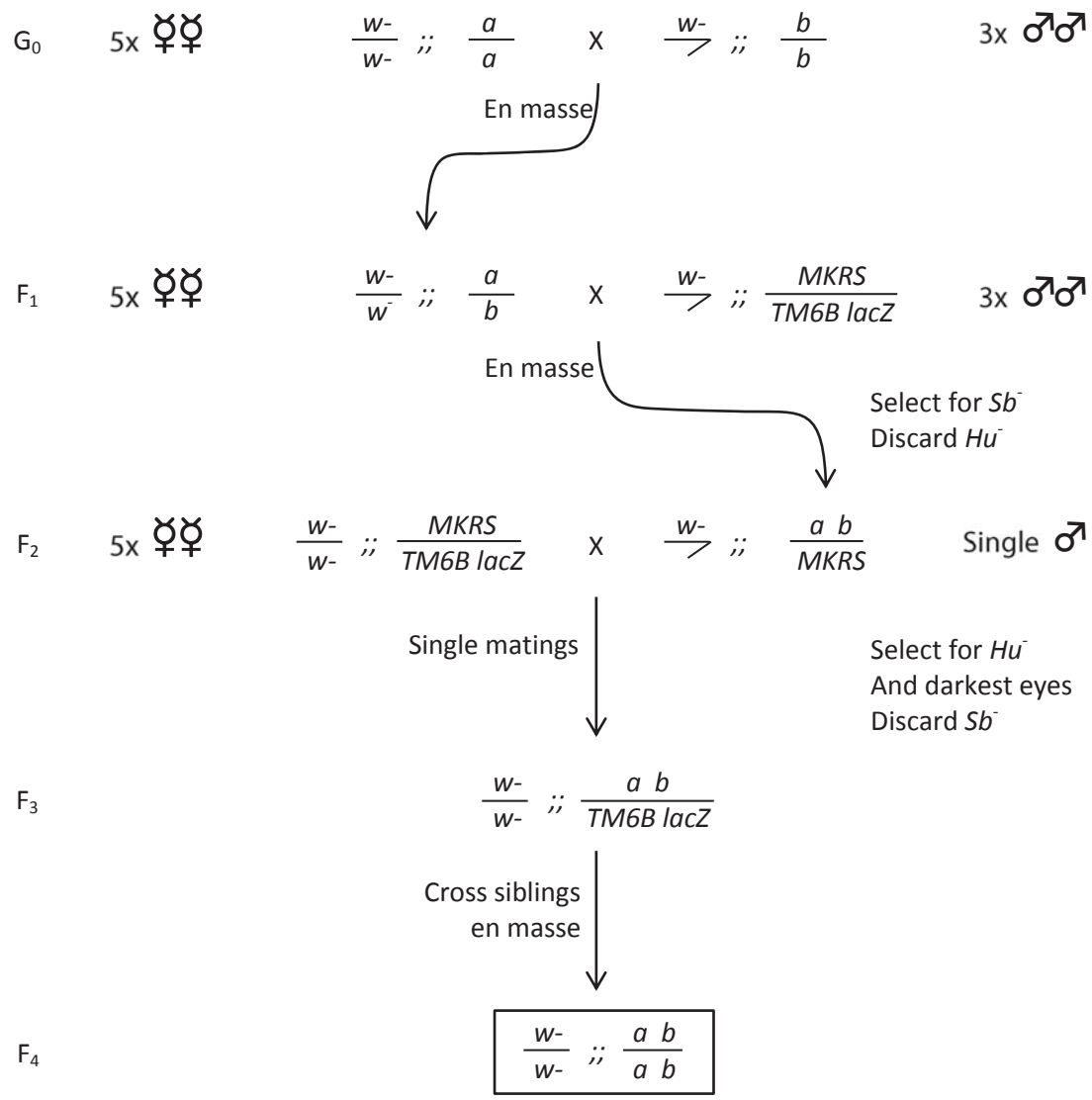

Protocol E was used combine alleles, transgenes and drivers on the 3rd chromosome, using recombination. 10-100 single males were crossed in the F_2 to generate unique recombinant lines. The presence of hop-out alleles was tested by genomic PCR, Gal4 by crossing the line to UAS GFP and examining larvae with epifluorescence, and UAS lines by eye colour and genomic PCR. The presence of spz^2 was tested by lethality following back-cross to the parental spz^2/TM6B line. Non-recombinant lines were discarded.

Fig 2.4 – Double mutants for 2nd and 3nd chromosomes

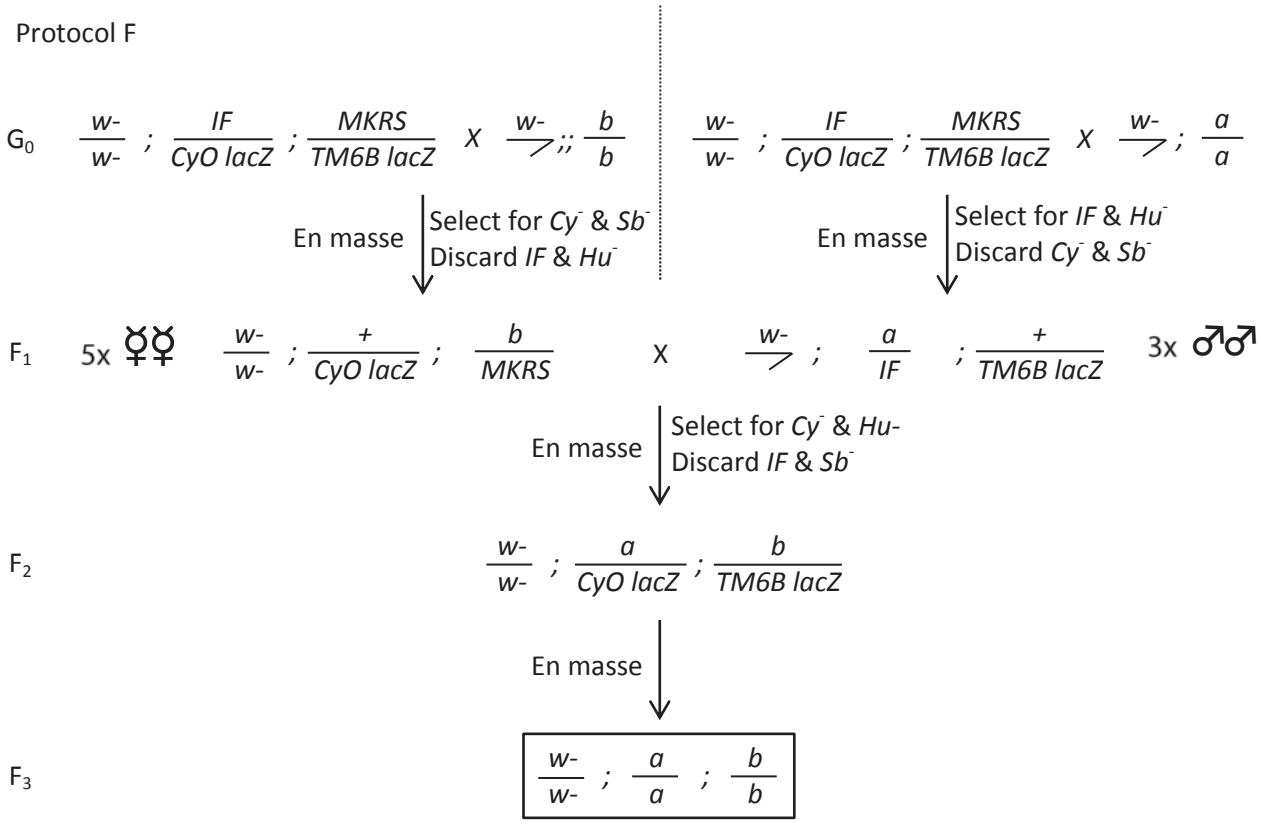

Protocol F was used to combine alleles on the 2nd and 3rd chromosomes. At least 8 copies of the F_1 cross were set up, to ensure the correct F_2 flies were among the progeny

Fig 2.5 – Mapping P-element transgenes

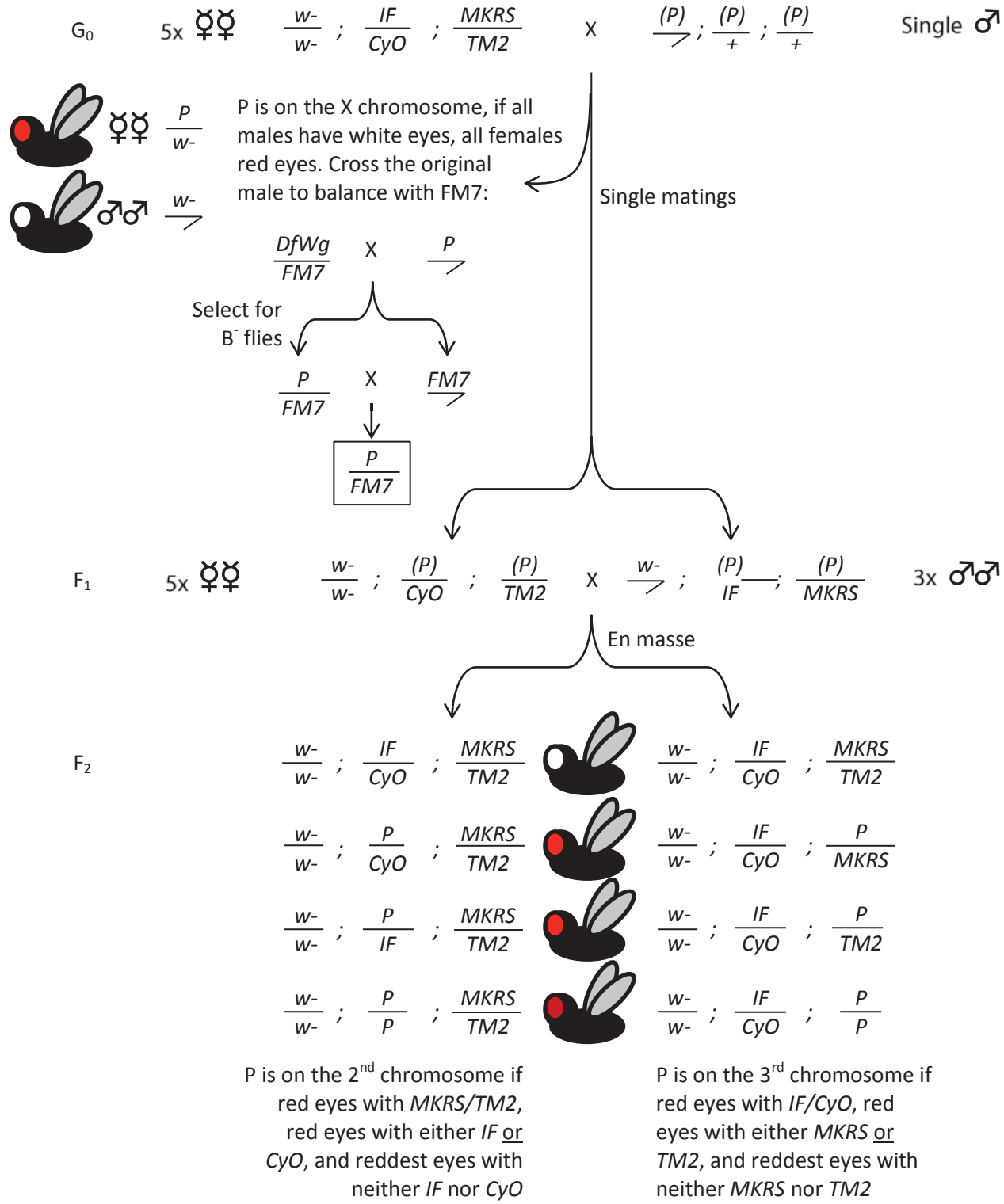

Protocol G was used to map transgenes that had been inserted into the genome on a P-element transposon. The P-element was marked with *mini-white*, giving the flies red eyes. The P-element (P) could have landed on the X, 2nd, 3rd or 4th chromosome. If the segregation did not match this protocol, the P-element could have landed on the 4th chromosome, or on more than one chromosome.

Fig 2.6 – P-element mobilisation: imprecise excision of Toll-7

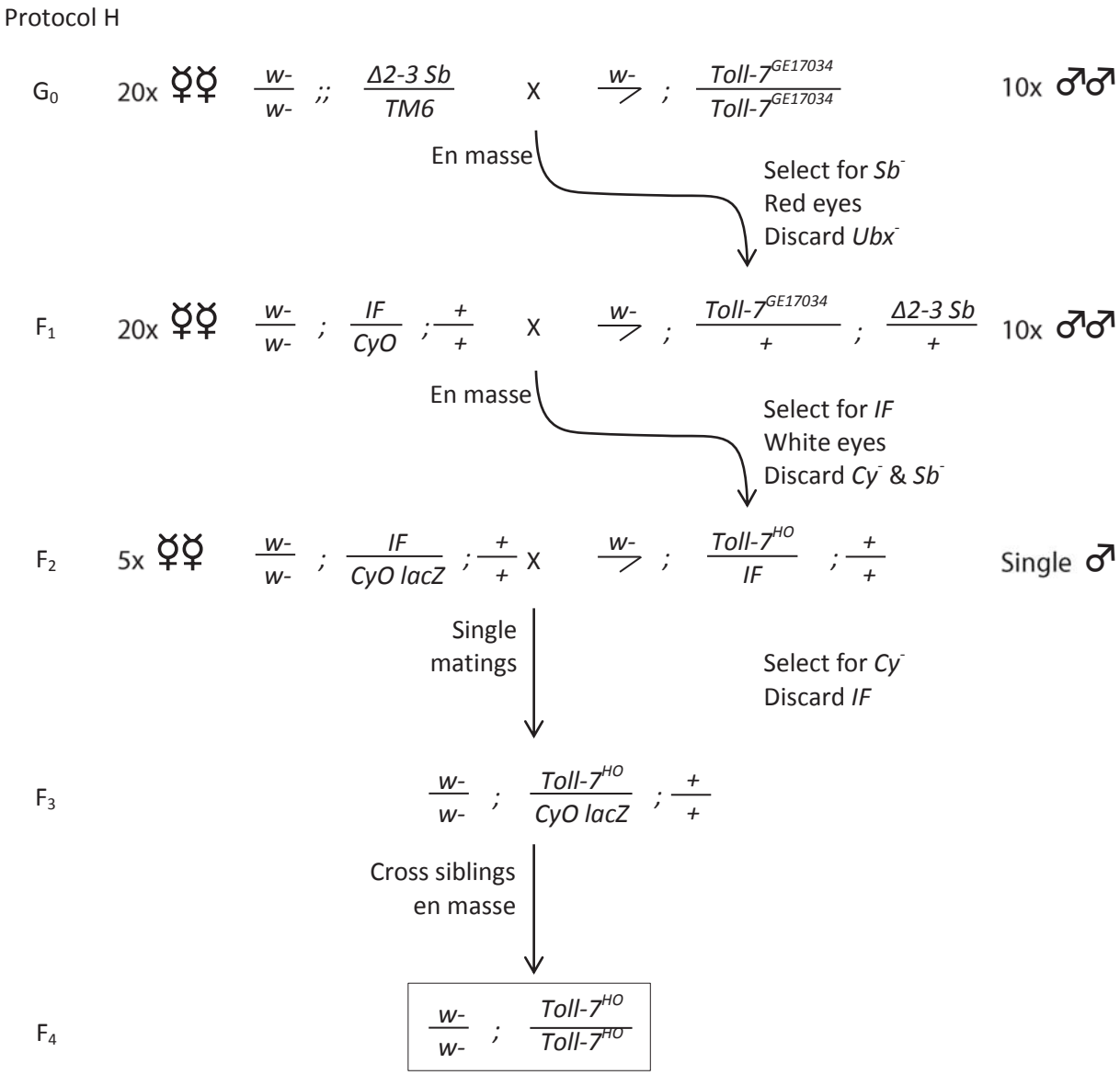

Protocol H was used in the P-element imprecise excision mutagenesis of *Toll-7*. The GE17034 P-element is marked with *mini-white*, which gives the flies red eyes. The putative mutants in the F_4 were screened by PCR and genomic sequencing. Null alleles were kept, other lines were discarded. This was carried out by Janine Fenton.

Fig 2.7 – P-element mobilisation: imprecise excision of *Toll-6*

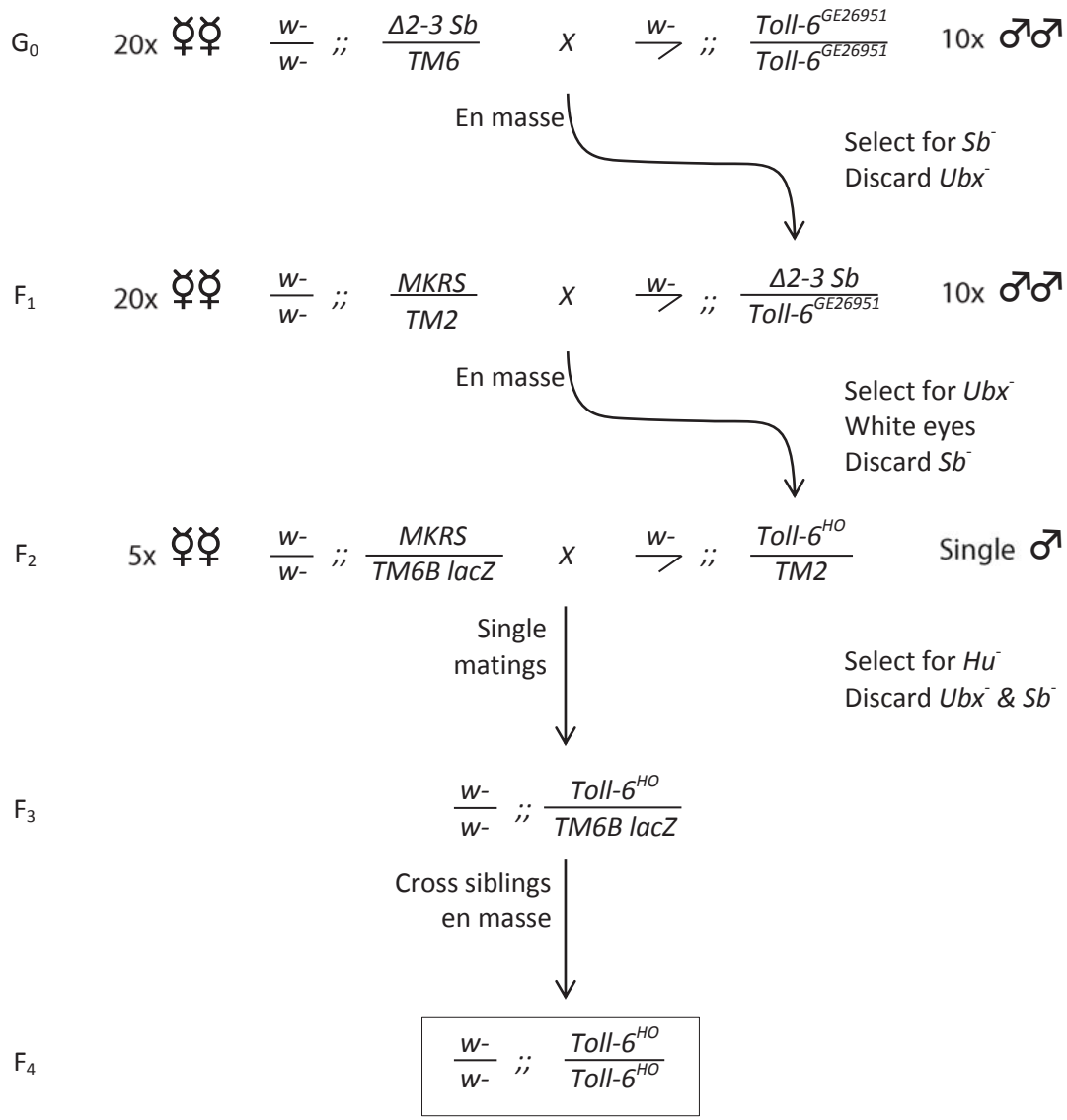

Protocol I was used in the P-element imprecise excision mutagenesis of *Toll-6*. The GE26951 P-element is marked with *mini-white*, and gives the flies red eyes. The putative mutants in the F_4 were screened by PCR and genomic sequencing. Null alleles were kept, other lines were discarded. This was carried out with Janine Fenton and Sarah Quail.

in all neurons and in cholinergic neurons, respectively. Expression constructs were cloned downstream of UAS and transformed into flies. When the Gal4 fly line and the UAS line were crossed, neuronally expressed Gal4 bound to the UAS elements to drive the expression of the transgene. Similarly, *Toll-7* and *Toll-6* Gal4 lines were used to drive expression of membrane-bound GFP, to reveal the morphology of those cells.

2.1.3 Transgenesis

To prepare transformation constructs containing ΔLRR activated receptors, 10µg plasmid DNA was precipitated by adding a 10% volume of 3M sodium acetate pH5.2 and 2x volume ethanol, chilling for 10 minutes at -20°C, and centrifuging for 10 minutes at 13000rpm. The pellet was washed in 70% ethanol, and air dried. The DNA was dissolved in 20µl injection buffer (0.1mM NaH_2PO_4, 5mM KCl, filtered to 0.2µm (Pall Acrodisc)) to give a final concentration of 0.5µg/µl. For microinjection, glass micropipettes (outer diameter 1mm, inner diameter 0.78mm, Clark) were pulled using a PC-10 Micropipette Puller (Narishige), and were loaded with the DNA solution. Flies carrying an attP site at cytogenetic location 86F (line J35, genotype: *φC31;;ZH-attP-86Fa*) were bred in a large cage with a grape-juice agar base to collect the embryos, which was changed every 45 minutes to synchronise egg laying. Embryos were collected before the cellular blastoderm stage, were briefly dechorionated in a 10% sodium hypochlorite (VWR) solution, and washed thoroughly with water. Embryos were aligned, and attached to a glass coverslip (VWR) with heptane glue (Scotch tape adhesive dissolved in heptane). Embryos were desiccated in air for 10 minutes before injection. DNA was injected into the posterior end of the embryos, prior to pole cell formation, using an MN-153 micro-manipulator (Narishige) an IM-30 microinjector (Narishige) and JunAir 3-4 air compressor. The embryos were then covered by a layer of halocarbon oil 700 (Sigma), and

kept in a humid large petri dish until hatching. First instar larvae were collected, and transferred to fly food supplemented with wet yeast paste (Red Star). All steps from egg laying to collection of eclosing adults took place at 18°C. Adult flies eclosing from injected embryos (G_0) were crossed to *yw* flies, and transformants were identified in the F_1 progeny by their red eyes. Stocks were established using Protocol G (Fig 2.5). For *UAS-Toll-7*$^{\Delta LRR}$, 2080 embryos were injected, of which 146 hatched as larvae and 26 eclosed as adults. Of the adult flies obtained, 5 were identified as transformants by their red eyes. For *UAS-Toll-6*$^{\Delta LRR}$, 1230 embryos were injected, yielding 40 larvae and 13 adults. 2 transgenic fly lines were identified.

UAS-Toll-7$^{Cys\text{-}Tyr}$ and *UAS-Toll-6*$^{Cys\text{-}Tyr}$ constructs were transformed using P-element Transposase into *yw* flies by BestGene Inc. The transgenes in the fly lines received from the company were mapped using Protocol G (Fig 2.5, materials and methods). The *UAS-Toll-7*$^{Cys\text{-}Tyr}$ line used was mapped to the 2nd chromosome, *UAS-Toll-6*$^{Cys\text{-}Tyr}$ to the 3rd.

2.1.4 Survival Index

Lethality was assessed at 18°C, in the progeny of heterozygous flies balanced with *TM6B* for mutant alleles on the 3rd chromosome, or *SM6aTM6B* for alleles on the 2nd chromosome. These balancer chromosomes are marked with *Tb*$^{-}$, which means heterozygous pupae are identifiable from their shape (Fig 2.8A). As the progeny receive one copy of the chromosome from each parent, and *TM6B/TM6B* is embryonic lethal, the Mendelian expectation is that 1/3 of the progeny will be homozygous and 2/3 heterozygous over *TM6B* (Fig 2.8B, C). The survival index (SI) is a measure of how mutant alleles affect viability:

$$SI = 2 \times \frac{Number\ of\ Homozygotes}{Number\ of\ Heterozygotes}$$

For wild-type alleles:

$$SI = 2 \times \frac{(1/3)}{(2/3)} = 1$$

When the SI is below 1, there are fewer homozygotes than would be expected for wild-type, indicating that the mutant allele being tested reduces viability. If an allele is lethal, there are no homozygotes, and the SI is 0.

2.2 Molecular biology

The plasmids used during the course of the project are given in Table 2.2. The cloning of full-length, wild-type *Toll-7* and *Toll-6*, as well as *pPTGAL-Toll-7 5kb upstream* (used to generate the *Toll-7-Gal4* fly line) are described in Chapter 3. The cloning of constitutively active receptors and *DNT* constructs for protein expression are described below. All primers used are referred to by number, and the sequences are given in Tables 2.3-2.7.

2.2.1 Genomic DNA extraction

15 adult flies were anaesthetised and kept chilled in an eppendorf tube. The genomic DNA was isolated using a Gentra Puregene Tissue Kit (Qiagen), according to the supplied instructions, and was stored at -20°C. To screen mutant fly lines, Single-Fly DNA preparations were made (Gloor et al., 1993). A single anaesthetised fly was placed in an eppendorf, squashed, incubated for 30 minutes at 37°C in squishing buffer (25mM NaCl, 10mM Tris pH8, 1mM EDTA, 200µg/ml Proteinase K (Invitrogen), in water), followed by heat inactivation at 95°C for 2 minutes.

Fig 2.8 - Mendelian segregation can be observed in pupae

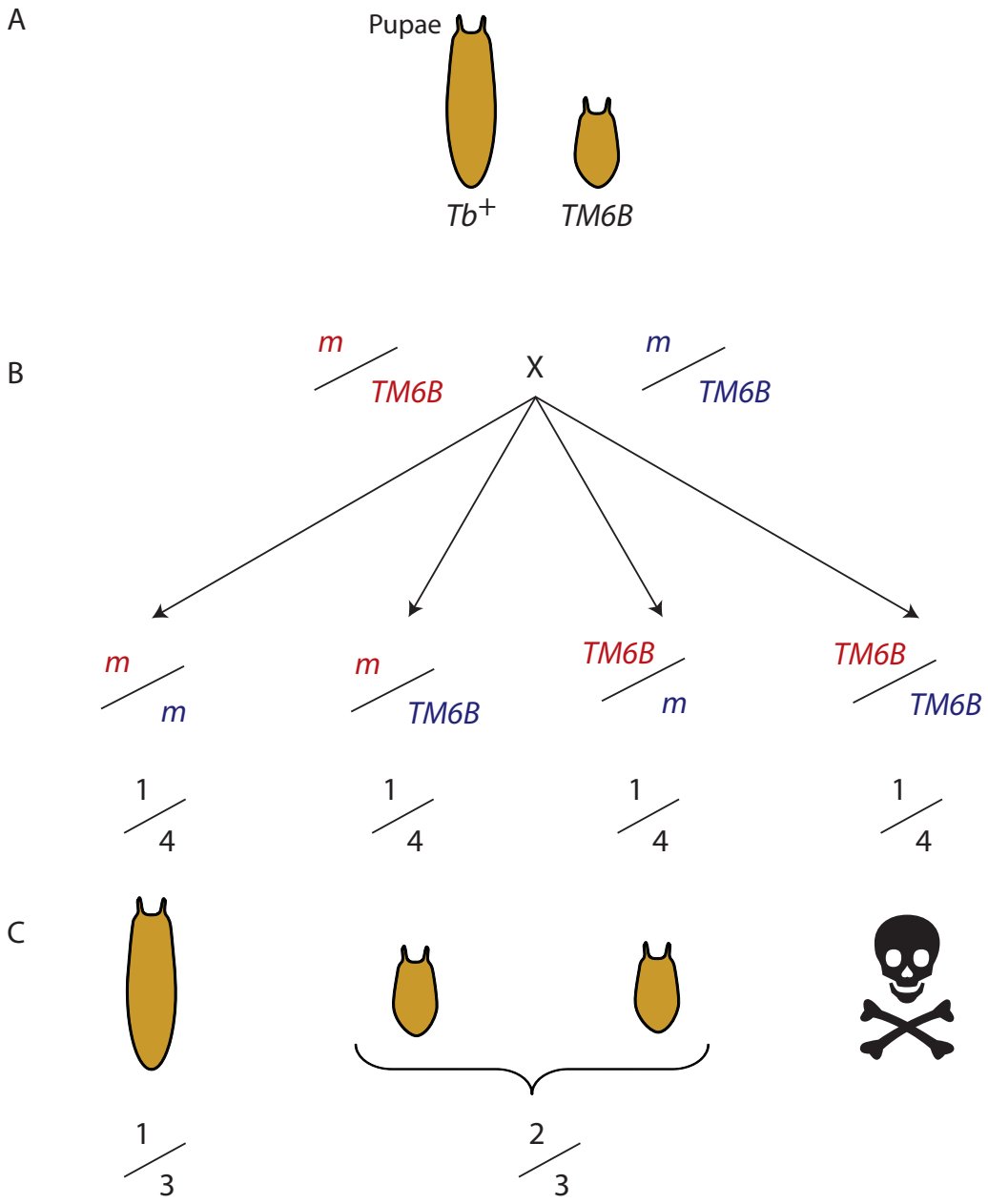

(A) *TM6B* pupae can be distinguished from *Tb*⁺ pupae by their shorter shape. (B) Following a cross, progeny receive one copy of each chromosome from each parent (red and blue). (C) When heterozygous flies are crossed, and the progeny pupae counted, 1/3 of the are homozygous for chromosome *m*, while 2/3 of the progeny are heterozygous according to Mendelian segregation. *TM6B/TM6B* homozygotes die during embryogenesis, and therefore never pupate.

2.2.2 Polymerase Chain Reaction (PCR)

DNA was amplified by PCR from genomic DNA and cDNA plasmids. When high-fidelity was not required, BioTaq (Bioline) DNA polymerase was used. 50µl reaction volumes included 5µl 10x NH_4 Buffer, 1.5µl 50mM $MgCl_2$ solution, 1µl 10mM dNTP mix (Roche), 5µl 3µM each primer, 1-3µl DNA template, 0.6µl BioTaq in water. A PTC-200 thermal cycler (MJ Research) was used to run the PCR, and temperature Program 1 was used when amplifying with BioTaq (Table 2.8). For high-fidelity cloning, Phusion (NEB) was used. Each 50µl reaction contained 10µl 5x Buffer HF, 1µl 10mM dNTP mix, 5µl 3µM each primer, 1-3µl DNA template, 0.5µl Phusion in water. When amplifying with Phusion, PCR Program 2 was used (Table 2.9).

Overlapping PCR was used to join two fragments of DNA that had been amplified separately, and had >40bp identical sequence at the point of overlap. 50µl reactions contained 0.5µl Phusion, 10µ 5x Buffer HF, 1µl 10mM dNTP mix, 5µl 3µM each primer directed at the 3' and 5' ends of the final product, and the rest of the mix was made up of equimolar amounts of each fragment to be joined. Since Phusion DNA polymerase was used, PCR was run with Program 2 (Table 2.9).

To confirm the presence of *Toll-7* mutant alleles in putative recombinants, primers 7.2 and 7.4 were used (Table 2.3), which flanked original P-element insertion site and the resulting genomic deletion. Similarly, to confirm the presence of *Toll-6* mutant alleles in putative recombinants, primers 6.2 and 6.8 were used (Table 2.4). To confirm the presence of the $DNT1^{41}$ mutant allele in putative recombinants, primers 1.1 and 1.2 were used (Table 2.5), which identify the *white* gene in the *DNT1* locus. And to confirm the presence of the

DNT2^{e03444} mutant allele, primers 2.1 and 2.2 were used (Table 2.6), which identify the P-element in the *DNT2* locus.

2.2.3 Agarose gel electrophoresis and DNA purification

To check the size of DNA fragments, and to purify amplified DNA for cloning, PCR products were run on 0.8%-1% agarose (Bioline) gels in TAE buffer + ethidium bromide (Sigma). DNA was mixed with 17% volume of 6x DNA loading buffer (0.25% bromophenol blue, 0.25% xylene cyanol FF, 30% glycerol (Sigma) in water). Gels were run at 65V until the dye-front had travelled to the end of the gel. 0.5μg of a 1kb ladder (NEB) was used as a molecular weight marker. DNA was visualised under UV light using a Gel Doc 2000 (BioRad). To extract the DNA, bands were cut from the gel using a razor blade, and DNA was purified using the QIAquick Gel Extraction kit (Qiagen) according to the kit instructions. DNA was eluted into 50μl 10mM Tris pH8.

2.2.4 Gateway cloning

A number of constructs were generated using Gateway cloning (Invitrogen). Gateway technology is based on the recombination of DNA across specific 'att' sites; the process of cloning a DNA fragment into an expression clone is summarised in (Fig 2.9). For expression in S2 cells, a destination vector with an Actin promoter and a C-terminal HA tag was used. For expression in flies following P-element transformation, the destination vector contained a UAS promoter, a C-terminal HA tag, P-element sequences, and the *mini-white* gene. For expression in flies following φC31 transformation, the destination vector contained a UAS promoter, a C-terminal FLAG tag, an attB site for transformation, and the *mini-white* gene.

When Gateway cloning was used (see Table 2.2), amplified DNA fragments included at the 5' end an attB1 sequence, and at the 3' end an attB2 sequence. 50fmol of purified PCR product was added to 50fmol (150ng) of the pDONR^{221} donor vector, and mixed with 2µl BP Clonase II enzyme (Invitrogen), to a total volume of 10µl in TE. The Clonase II enzyme reagent includes a 5x buffer. The reaction was incubated at 25°C overnight. Reactions were stopped by adding 1µg Proteinase K and incubating for 10 minutes at 37°C. This was then used to transform E.coli. For LR reactions, 150ng each of entry clone and destination vector were mixed in 8µl TE, and 2µl LR Clonase II enzyme (Invitrogen) was added. Reactions were incubated overnight at 25°C, and stopped with 1µg Proteinase K treatment for 10 minutes at 37°C. This was then used to transform E. coli.

2.2.5 Conventional restriction enzyme cloning

Conventional cloning using restriction enzymes was also carried out to generate constructs (see Table 2.2). DNA fragments were amplified by PCR using primers containing restriction enzyme sites, and subsequently digested with the appropriate enzyme. Plasmids were digested with the same enzymes as the inserts. Digestion reactions were carried out in 15µl volumes, including 100-500ng DNA, 1.5µl of 10x buffer, and 0.5µl each enzyme (Roche), incubated at 37°C for 3 hours, and inactivated by incubating at 65°C for 10 minutes. Cut fragments and vectors were purified from the reaction mix using the QIAquick PCR Purification kit (Qiagen) according to the instructions. DNA was eluted in 30µl 10mM Tris pH8.

The DNA insert was ligated into the vector. A 3-fold molar excess of insert was mixed with the vector to a final DNA amount of 200-400ng, into 17µl water, to which 2µl 10x T4 buffer and 1µl T4 Ligase (NEB) were added. Ligation reactions were incubated overnight at 18°C, and inactivated at 65°C for 10 minutes. This was then used to transform E. coli.

Fig 2.9 - Gateway Cloning

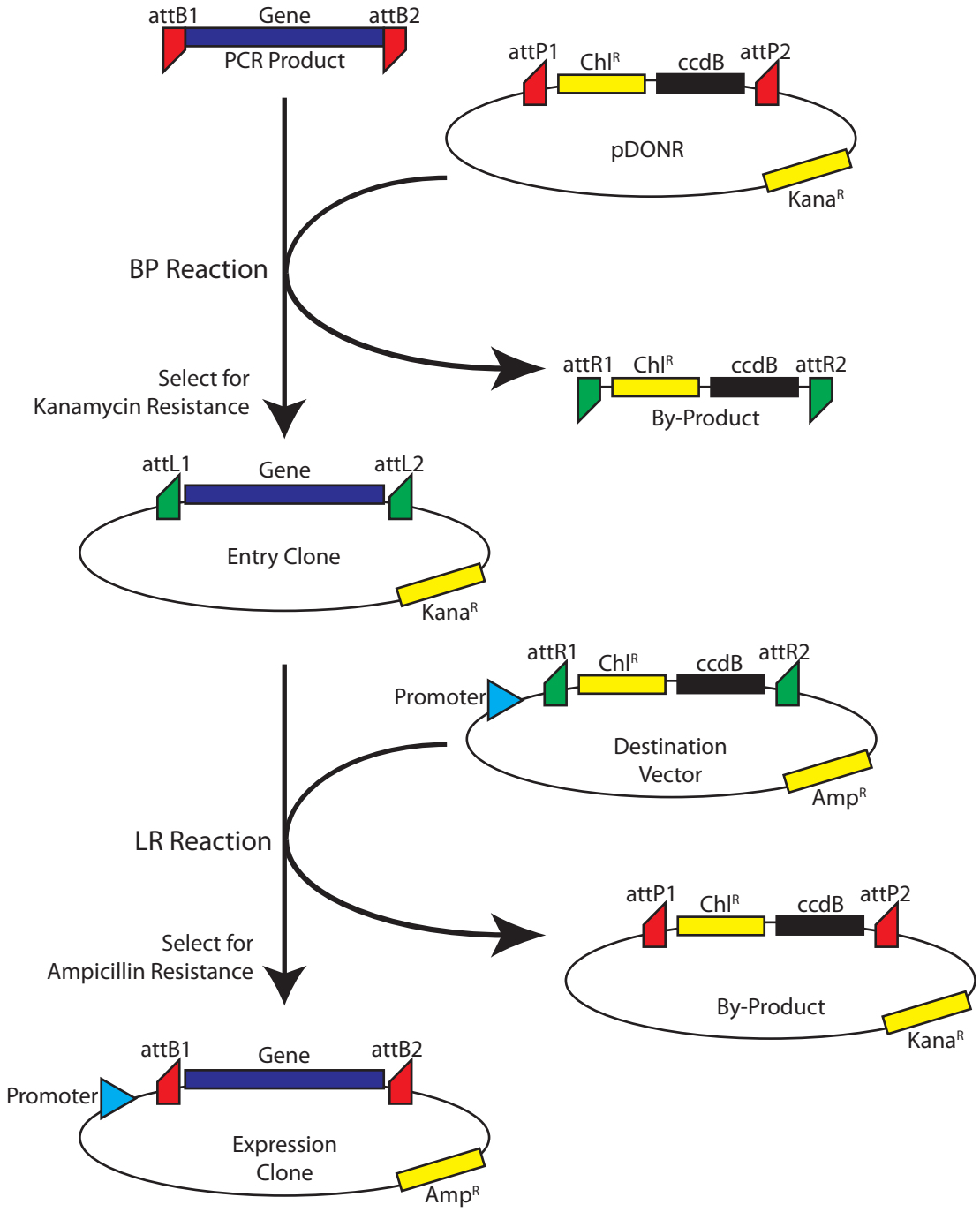

During a BP reaction, recombination between attB sites in a PCR product and attP sites in pDONR creates an entry clone. Entry clones are selected for with Kanamycin. The toxic *ccdB* gene kills bacteria containing the empty pDONR. During an LR reaction, recombination between attL and attR sites places the DNA fragment into an expression clone. The expression clone is slelcted for with Ampicillin, non-recombined destination vectors kill bacteria with the *ccdB* gene.

2.2.6 Transformation of E. coli

DNA clones were transformed into DH5α (Invitrogen) chemically competent E. coli cells. Large plasmids were transformed into One Shot OmniMAX cells (Invitrogen). 25µl of cells was thawed on ice, and 1µl plasmid DNA was added. The cells were incubated for 30 minutes on ice, heat-shocked for 30 seconds at 42°C, and returned to ice for 2 minutes. 500µl SOC medium was added, and E. coli were grown for 1 hour shaking at 225rpm at 37°C. 20µl and 200µl of the culture were spread onto LB + agar plates, containing the relevant antibiotic for colony selection (50µg/ml ampicillin, 50µg/ml kanamycin, or 100µg/ml chloramphenicol, Sigma). Plates were incubated overnight at 37°C.

To recombine pFastBac constructs into Bacmid DNA for protein expression with Baculovirus, DH10Bac (Invitrogen) E. coli were used, according to the manufacturer's instructions. The transformed cells were spread on LB + agar plates containing 50µg/ml kanamycin, 7µg/ml gentamycin and 10µg/ml tetracycline for bacterial selection, and 100µg/ml Bluo-gal and 40µg/ml IPTG for blue-white selection (Sigma).

2.2.7 Amplification of plasmid DNA

Single colonies were picked with a sterile pipette tip and inoculated into 2ml of LB medium containing the relevant antibiotic (see above), and miniprep cultures were grown overnight shaking at 225rpm, 37°C. 1.5ml of each culture was transferred to an eppendorf, the cells were pelleted by centrifuging at 13000rpm for 30 seconds, and the supernatant was discarded. Cells were re-suspended in 350µl STET (0.1M NaCl, 10mM Tris pH8, 1mM EDTA pH8, 5% Triton-X-100 (Sigma)) plus 30µl 5mg/ml Lysozyme (Sigma) solution. Samples were boiled at 100°C for 1 minute, incubated on ice for 2 minutes, then centrifuged at 13000rpm for 20

minutes. The resulting pellet was removed, and DNA was precipitated with 200µl 5M ammonium acetate and 800µl isopropanol, and chilled at -20°C for 10 minutes. DNA was pelleted at 13000rpm for 15 minutes, washed with 80% ethanol in water, air dried, and dissolved in 50µl 10mM Tris pH8.

Resultant clones were scrutinised with diagnostic restriction enzyme digests. Once a correct clone had been identified, 100µl from the miniprep LB culture was used to inoculate 50-100ml of LB medium containing the relevant antibiotic (maxiprep). This was grown overnight shaking at 225rpm, 37°C. DNA was isolated from the cultures using a QIAfilter Plasmid Maxi kit (Qiagen), according to the kit instructions.

2.2.8 DNA sequencing

All constructs identified by diagnostic digests were sequenced. When using Gateway cloning, the 'Entry' clone was sequenced before transfers into destination vectors. In each sequencing reaction, 500ng plasmid DNA and 3pmol primer were made up to 10µl in water, and sent to the Genomics Facility, School of Biosciences, University of Birmingham for sequencing. The coding region and integration sites of each construct were sequenced. *Toll-7* constructs were sequenced using primers 7.16-7.25 (Table 2.3); *Toll-6* constructs were sequenced using primers 6.17-6.27 (Table 2.4); *DNT1* constructs were sequenced with primers 1.16-1.22 (Table 2.5); *DNT2* constructs were sequenced with primers 2.10-2.12 (Table 2.6). To sequence the insertion site in plasmids, primers V.1 and V.2 were used in pDONR entry clones, and V.3 and V.4 were used in Baculovirus clones (Table 2.7). At least two overlapping sequences were obtained for every base, which were compared to the sequence predicted sequence from FlyBase, using the Kalign tool through the European Bioinformatics Institute website (www.ebi.ac.uk).

Table 2.2 – Plasmid vectors and constructs

Name	Description	Source	Cloning method
Gateway Vectors			
pDONR[221]	Gateway donor vector	Invitrogen	
pUAS-gw-HA-attB	Destination vector for Phi C31 transgenics with C-terminal 3xHA tag	T Murphy	
pUAS-gw-FLAG	Destination vector for transposase transgenics, with C-terminal 3xFLAG tag	T Murphy	
pAct5C-gw-HA	Destination vector for cell expression, C-terminal 3xHA tag	T Murphy	
pAct5C-gw	Destination vector for cell expression, no tags	T Murphy	
Baculovirus Vectors			
pFastBac1	For Baculovirus, no tags	Invitrogen	
pK503-9	For Baculovirus, pFastBac1 with N-terminal EGT signal peptide and FLAG tag	A gift from N Gay	
Plasmids for cell culture			
pPsnail-Luc	Firefly Luciferase downstream of snail promoter - Dorsal reporter	A gift from AJ Courey	
pRenillaLuc	Renilla Luciferase downstream of actin promoter - Luciferase control	A gift from S Brogna	
pPac-FLAG-Dorsal	Dorsal cDNA downstream of actin promoter	A gift from AJ Courey	
pMT-Gal4	Gal4 under metallothionine promoter, copper-inducible	Drosophila Genomics Resource Centre	
Toll-7 constructs			
pDONR-Toll-7	Full length Toll-7, no stop codon, Gateway entry clone	G McIlroy, this work, see Chapter 3	Gateway cloning
pAct5C-Toll-7-3HA	Full length Toll-7 with C-terminal 3xHA, for S2 cell expression	G McIlroy, this work, see Chapter 3	Gateway cloning
pDONR-Toll-7[ΔLRR]	Activated Toll-7[ΔLRR], no stop codon, Gateway entry clone	G McIlroy, this work, see section 2.2.9	Gateway cloning
pUAS-Toll-7[ΔLRR]-3HA-attB	Activated Toll-7[ΔLRR] with C-terminal 3xHA, for ϕC31 transgenesis	G McIlroy, this work, see section 2.2.9	Gateway cloning
pDONR-Toll-7[Cys-Tyr]	Activated Toll-7[Cys-Tyr], no stop codon, Gateway entry clone	G McIlroy, this work, see section 2.2.9	Gateway cloning
pUAS-Toll-7[Cys-Tyr]-3FLAG	Activated Toll-7[Cys-Tyr] with C-terminal 3xFLAG, for P-element transgenesis and S2 cell expression	G McIlroy, this work, see section 2.2.9	Gateway cloning
pPTGAL-Toll-7 5kb upstream	5kb of Toll-7 regulatory region, upstream of Gal4, for P-element transgenesis	G McIlroy, this work, see Chapter 3	Enzymatic cloning
Toll-6 constructs			
pDONR-Toll-6	Full length Toll-6, no stop codon, Gateway entry clone	G McIlroy, this work, see Chapter 3	Gateway cloning
pAct5C-Toll-6-3HA	Full length Toll-6 with C-terminal 3xHA, for S2 cell expression	G McIlroy, this work, see Chapter 3	Gateway cloning
pDONR-Toll-6[ΔLRR]	Activated Toll-6[ΔLRR], no stop codon, Gateway entry clone	G McIlroy, this work, see section 2.2.9	Gateway cloning
pUAS-Toll-6[ΔLRR]-3HA-attB	Activated Toll-6[ΔLRR] with C-terminal 3xHA, for ϕC31 transgenesis	G McIlroy, this work, see section 2.2.9	Gateway cloning
pDONR-Toll-6[Cys-Tyr]	Activated Toll-6[Cys-Tyr], no stop codon, Gateway entry clone	G McIlroy, this work, see section 2.2.9	Gateway cloning
pUAS-Toll-6[Cys-Tyr]-3FLAG	Activated Toll-6[Cys-Tyr] with C-terminal 3xFLAG, for P-element transgenesis and S2 cell expression	G McIlroy, this work, see section 2.2.9	Gateway cloning

(Continued…)

Table 2.2 – Plasmids (continued)

Name	Description	Source	Cloning method
DNT1 protein expression constructs			
pK503-9-DNT1 CK	DNT1 CK with N-terminal EGT signal peptide, FLAG tag, 6His and Thrombin site, for Baculovirus expression	G McIlroy, this work, see section 2.2.11	Enzymatic cloning
pK503-9-DNT1 CK + CTD	DNT1 CK + CTD with N-terminal EGT signal peptide, FLAG tag, 6His and Thrombin site, for Baculovirus expression	G McIlroy, this work, see section 2.2.11	Enzymatic cloning
pFastBac1-DNT1 Pro + CK	DNT1 Pro-domain + CK with C-terminal TEV site and 6His, for Baculovirus expression	G McIlroy, this work, see section 2.2.11	Enzymatic cloning
pFastBac1-Spz Pro-6HisTEV-DNT1 CK + CTD	Spz pro-domain, 6His tag, TEV cleavage site, DNT1 CK + CTD, for Baculovirus expression	G McIlroy, this work, see section 2.2.11	Enzymatic cloning
pDONR-DNT1 Pro-TEV6HisV5-DNT1 CK + CTD	Full length DNT1 with internal TEV site, and 6His and V5 tags, Gateway entry clone	G McIlroy, this work, see section 2.2.11	Gateway cloning
pAct5C-DNT1 Pro-TEV6HisV5-DNT1 CK + CTD	Full length DNT1 with internal TEV site, and 6His and V5 tags, for S2 cell expression	G McIlroy, this work, see section 2.2.11	Gateway cloning
DNT2 protein expression constructs			
pFastBac-DNT2 FL	DNT2 full-length with C-terminal TEV site and 6His, for Baculovirus expression	G McIlroy, this work, see section 2.2.12	Enzymatic cloning
pK503-9-DNT2 CK	DNT2 CK with N-terminal EGT signal peptide, FLAG tag, 6His and Thrombin site, for Baculovirus expression	G McIlroy, this work, see section 2.2.12	Enzymatic cloning
pDONR-DNT2 Pro-TEV6HisV5-DNT2 CK	Full length DNT2 with internal TEV site, and 6His and V5 tags, Gateway entry clone	G McIlroy, this work, see section 2.2.12	Gateway cloning
pAct5C-DNT2 Pro-TEV6HisV5-DNT2 CK	Full length DNT2 with internal TEV site, and 6His and V5 tags, for S2 cell expression	G McIlroy, this work, see section 2.2.12	Gateway cloning

Table 2.3 – Toll-7 Primers

Number	Original Name	Sequence	Description
7.1	start-forw	ACCATGGCGGCAATCCTGCT	5' of Toll-7 just before ATG, Forward
7.2	1kbup-forw	GCAAGATACGCATACGGAGA	1kb upstream of Toll-7 ATG, Forward
7.3	3kbupforw	GAGCCGGCGTCTGATAATAG	3kb upstream of Toll-7 ATG, Forward
7.4	1kbreverse	GGAACAGTCCTTTGGGAAGC	1kb downstream of Toll-7 ATG, Reverse
7.5	3kbreverse	CCAGTGCAGCACTGCCAGT	3kb downstream of Toll-7 ATG, Reverse
7.6	1.6kbreverse	TCCCCGCTCTATGCTCTGGAT	1.6kb downstream of Toll-7 ATG, Reverse
7.7	2.1kbreverse	TTACCACCCAGGTAAAATTCT	2.1kb downstream of Toll-6 ATG, Reverse
7.8	Tl7attB1FwdTag	GGGGACAAGTTTGTACAAAAAAGCAGGCT TCATGGCGGCAATCCTGCTGC	5' of Toll-7 just before ATG, with attB1 site, Forward
7.9	Tl7attB2RevTag	GGGGACCACTTTGTACAAGAAAGCTGGGT CCACCAGATACGCCTGAACAT	End of Toll-7 coding region, with attB2 site, Reverse
7.10	Tl7 SP-MluI Rev	TC**ACGCGT**TAACATGGCGCTGGCACTCGA	End of Toll-7 Signal Peptide, with **MluI** site, Reverse
7.11	Tl7MluII-TM+ICFwd	TA**ACGCGT**GAATCGTATATTCCCTTGCTG	Start of Toll-7 TM and Intracelluar domain, with **MluI** site, Forward
7.12	Tl7 C-Y Rev	CTGCCAGTTCCCGAACTTGCGGCCAT*GTA* GTAGATATCCTGGGCATCCTG	Mutated *Cys to Tyr*, Reverse
7.13	Tl7 C-Y Fwd	TTGTCCAGGATGCCCAGGATATCTAC*TAC* ATGGCCGCAAGTTCGGGAACT	Mutated *Cys to Tyr*, Forward
7.14	BamHITl7UpCRev	ATCGAT**GGATCC**GGTTTTGGGTGTTGTGC TTGGGGGGCCA	Start of Toll-7, with **BamHI** site, Reverse
7.15	NotITl7Up5Fwd	ATATAT**GCGGCCGC**AAGCTTGTGCTGATT TTTCGAAACTT	5kb upstream of Toll-7, with **NotI** site, Forward
7.16	Toll7 0.4kbFwd	TGCGTCTCATTGAGCGACAGC	For sequencing of plasmids, 0.4kb into Toll-7, Forward
7.17	Toll7 0.8kbFwd	ATTCGCACTGCCGAGCAGATG	For sequencing of plasmids, 0.8kb into Toll-7, Forward
7.18	Toll7 1.2kbFwd	ACTTCCAACCACGTGGATAAC	For sequencing of plasmids, 1.2kb into Toll-7, Forward
7.19	Toll7 1.6kbFwd	CATGTTGCGCACTCTTGACCT	For sequencing of plasmids, 1.6kb into Toll-7, Forward
7.20	Toll7 2.0kbFwd	TAAGCTTCAGGAGGAGATTCG	For sequencing of plasmids, 2.0kb into Toll-7, Forward
7.21	Toll7 2.4kbFwd	TGGTGCTGCAGTGCGTCCTTT	For sequencing of plasmids, 2.4kb into Toll-7, Forward
7.22	Toll7 2.8kbFwd	AATTGCGCACCCTTCATGGCT	For sequencing of plasmids, 2.8kb into Toll-7, Forward
7.23	Toll7 3.2kbFwd	GACTTTAACGCCACAGGTGCT	For sequencing of plasmids, 3.2kb into Toll-7, Forward
7.24	Toll7 3.4kbFwd	GAGAAGCTCTACGATGCCGTG	For sequencing of plasmids, 3.4kb into Toll-7, Forward
7.25	Toll7 3.8kbFwd	AAATTGCGCTACGCACTGCCC	For sequencing of plasmids, 3.8kb into Toll-7, Forward

Restriction enzyme sites in bold, Gateway sequences underlined, *Cys-Tyr mutated codons in italics*

Table 2.4 – Toll-6 Primers

Number	Original Name	Sequence	Description
6.1	UpReg5kb-For	GTAAACACTTGCGGATGCTCA	5kb upstream of Toll-6 ATG, Forward
6.2	UpReg2kb-For	CCTTCTTGGTTGCATGTGCCA	2kb upstream of Toll-6 ATG, Forward
6.3	UpReg1kb-For	GATACCAGGACTACTTTAGGT	1kb upstream of Toll-6 ATG, Forward
6.4	Start Fwd	CGCAAACCCATTTTCCGGTG	5' of Toll-6 just before ATG, Forward
6.5	Mid-Rev	GGAACTGGGTCCAATGCGCT	2kb downstream of Toll-6 ATG, Reverse
6.6	Mid-Fwd	GGATCTGGGCGAGAACATGA	2kb downstream of Toll-6 ATG, Forward
6.7	End-Rev	CACTGGTTGCGCAGTTTGTC	End of Toll-6 coding region, Reverse
6.8	Mid-Rev2	GGAGCTCAGGTTCAGGATCT	1.9kb downstream of Toll-6 ATG, Reverse
6.9	UpReg1.5kb-For	GGAGGCGTTCTGTTGGCTGA	1.5kb upstream of Toll-6 ATG, Forward
6.10	UpReg3.5kb-For	GCTGTCAGCTACACCATGCT	3.5kb upstream of Toll-6 ATG, Forward
6.11	Tl6attB1FwdTag	GGGGACAAGTTTGTACAAAAAAGCAGGCT TCATGATCTACTATATGCTAC	5' of Toll-6 just before ATG, with attB1 site, Forward
6.12	Tl6attB2RevTag	GGGGACCACTTTGTACAAGAAAGCTGGGT CCGCCCACAGGTTCTTCTGCT	End of Toll-6 coding region, with attB2 site, Reverse
6.13	Tl6SP-MluIRev	AT**ACGCGT**GTGGTGCTTGGTGGACAGCGA	End of Toll-6 Signal Peptide, with **MluI** site, Reverse
6.14	Tl6MluI-TM+ICFwd	AC**ACGCGT**ATCGAGGGACTGCTGCCCCTG	Start of Toll-6 TM and Intracelluar domain, with **MluI** site, Forward
6.15	Toll6 C-Y Rev	AGAACACTCGTAGCATTGTTGTAGAT*GTA*G CTCACCCTGGAGGCATCTAT	Mutated *Cys to Tyr*, Reverse
6.16	Toll6 C-Y Fwd	AGATCATAGATGCCTCCAGGGTGAGC*TAC*A TCTACAACAATGCTACGAGT	Mutated *Cys to Tyr*, Forward
6.17	Toll6 0.4kbFwd	CTGGATCAGCCGGAAATAGCC	For sequencing of plasmids, 0.4kb into Toll-6, Forward
6.18	Toll6 0.8kbFwd	TGCACCCTGTCCGAGTTGTCT	For sequencing of plasmids, 0.8kb into Toll-6, Forward
6.19	Toll6 1.2kbFwd	GAGGTGTACCTGCAGAATAAT	For sequencing of plasmids, 1.2kb into Toll-6, Forward
6.20	Toll6 1.6kbFwd	ATCCGGATGCCTTCCGGAACT	For sequencing of plasmids, 1.6kb into Toll-6, Forward
6.21	Toll6 2.0kbFwd	CCGATAATCGTTTGGAATCCT	For sequencing of plasmids, 2.0kb into Toll-6, Forward
6.22	Toll6 2.4kbFwd	TTGGCTGCAGAAGATTAACCA	For sequencing of plasmids, 2.4kb into Toll-6, Forward
6.23	Toll6 2.8kbFwd	TATGCGAACAACTCGAACGTG	For sequencing of plasmids, 2.8kb into Toll-6, Forward
6.24	Toll6 3.2kbFwd	TCTACAACAATGCTACGAGTG	For sequencing of plasmids, 3.2kb into Toll-6, Forward
6.25	Toll6 3.4kbFwd	TCCACCAACTGTCTAATGAAC	For sequencing of plasmids, 3.4kb into Toll-6, Forward
6.26	Toll6 3.8kbFwd	ATCTGCGTACCAGCACCTGCA	For sequencing of plasmids, 3.8kb into Toll-6, Forward
6.27	Toll6 4.2kbFwd	GGAGCATCAGCACCACCACAA	For sequencing of plasmids, 4.2kb into Toll-6, Forward

Restriction enzyme sites in bold, Gateway sequences underlined, *Cys-Tyr mutated codons in italics*

Table 2.5 – DNT1 Primers

Number	Original name	Sequence	Description
1.1	White-Start-For	TCAAATACCCTTGGATCGAAGT	Start of Mini-White gene, in DNT locus, Forward
1.2	cDNAEnd-2_Rev	TTGCTAGAACTCTCGTGACA	30bp upstream of 3' UTR End of DNT1, Reverse
1.3	SphIHTbDNT1CKFwd	ACTACT**GCATGC**TCACCATCACCATCACCATCTGGTTCC GCGTGGATCTAAAAAGAGGCGTGAAGACGAAGGCAGC	**SphI**-6His-Thrombin, start of DNT1 Cys knot, Forward
1.4	HindIII DNT1 CK Rev	GCCC**AAGCTT**TTAGCGATAACCATCCACTTGGCAGGAG	End of DNT1 Cys knot, with **HindIII** site, Reverse
1.5	HindIII DNT1 End Rev	GCCC**AAGCTT**TTACTGGATAGACTGCCGGCGGTTGTGG	End of DNT1 CTD, with **HindIII** site, Reverse
1.6	SpeI DNT1 St Fwd	GTACGT**ACTAGT**ATGAAAGCTGGCCGCGCCTTC	Start of DNT1, with **SpeI** site Forward
1.7	XhoI HT DNT1CK R	AATTGG**CTCGAG**TTAATGATGATGATGATGATGGCCCTG AAAATACAGGTTTTCGCGATAACCATCCACTTGGCA	**XhoI**-6His-TEV, at end of DNT1 Cys knot, Reverse
1.8	SpzPro EcoRI St F	GCATACTC**GAATTC**ATGATGACGCCCATGTGGATA	Start of Spz, with **EcoRI** site, Forward
1.9	3His TEV R	GCCCTGAAAATACAGGTTTTCGTGATGGTG	3His-TEV, Reverse
1.10	TEV DNT1CK F	GAAAACCTGTATTTTCAGGGCGAAGACGAAGGCAGCGC AGGTGGG	TEV, start of DNT1 Cys knot, Forward
1.11	DNT1 3' XhoI End R	GCATACTC**CTCGAG**TCACTGGATAGACTGCCGGCG	End of DNT1, with **XhoI** site, Reverse
1.12	attB1DNT1StF	GGGGACAAGTTTGTACAAAAAAGCAGGCTTCATGAAAG CTGGCCGCGCCT	Start of DNT1, with attB1 site, Forward
1.13	V56HTEVDNT1ProR	AGGAGAGGGTTAGGGATAGGCTTACCATGGTGATGGTG ATGGTGGCCCTGAAAATACAGGTTTTCCCTCTTTTTGCTC AGGCTGAAGTCA	End of DNT1 ProDomain, TEV-6His-V5, Reverse
1.14	6HV5DNT1CKF	AGGGCCACCATCACCATCACCATGGTAAGCCTATCCCTA ACCCTCTCCTCGGTCTCGATTCTACGCGTGAAGACGAAG GCAGCGCAGGTG	Start of DNT1 Cys knot, TEV-6His-V5, Forward
1.15	attB2DNT1EndR	GGGGACCACTTTGTACAAGAAAGCTGGGTTCACTGGAT AGACTGCCGGCG	End of DNT1, with attB2 site, Reverse
1.16	DNT1 0.5kb Fwd	GCTGCTTTTGCCCATAGTGTT	For sequencing of plasmids, 0.5kb into DNT1, Forward
1.17	DNT1 0.5 Rev	TTGCGGGTAGAGCTCTTTATG	For sequencing of plasmids,0.5kb into DNT1, Reverse
1.18	DNT1 1kb Fwd	TAGCCAGGAGGAGGAGAAGAT	For sequencing of plasmids, 1kb into DNT1, Forward
1.19	DNT1 1kb Rev	CCTCCACCTCAGAGTATGACT	For sequencing of plasmids, 1kb into DNT1, Reverse
1.20	DNT1 1.5kb Rev	TTCGTCTTCACGCCTCTTTTT	For sequencing of plasmids, 1.5kb into DNT1, Reverse
1.21	DNT1 2.1kb Fwd	GATGATGACGAAGATCGCTAT	For sequencing of plasmids, 2.1kb into DNT1, Forward
1.22	DNT1 2.1kb Rev	TACTTCTTGGAACTGGAACTG	For sequencing of plasmids, 2.1 into DNT1, Reverse

Restriction enzyme sites in bold, Gateway sequences underlined, 6His tags in blue, V5 tags in green, TEV and Thrombin protease sequences in red

Table 2.6 – DNT2 Primers

Number	Original name	Sequence	Description
2.1	White-End-Rev	ATGGTGGGCATAATAGTGTTGT	End of Mini-White gene, in e03444 P-element, Reverse
2.2	Spz5-EcoRI-Start For	CG**GAATTC**ATGCAAATCGACGGCGAATGA	5' of DNT2 just before ATG, with **EcoRI** site, Forward
2.3	NotI HT DNT2EndR	ACAAAT**GCGGCCGC**TTAATGATGATGATGATGATGGCCC TGAAAATACAGGTTTTCATTGGCGGCTATCGTGCAGACA	**NotI**-6His-TEV at end of DNT2 Cys knot, Reverse
2.4	SphIHTbDNT2CKFwd	ACTACT**GCATGC**TCACCATCACCATCACCATCTGGTTCCG CGTGGATCTAGGACAAAGCGCCAAAGTCCGGGGCGC	**SphI**-6His-Thrombin upstream of DNT2 Cys knot, Forward
2.5	HindIII DNT2 End Rev	GCCC**AAGCTT**TTAATTGGCGGCTATCGTGCAGACA	End of DNT2 Cys knot, with **HindIII** site, Reverse
2.6	attB1DNT2StF	GGGGACAAGTTTGTACAAAAAAGCAGGCTTCATGACAAA AAGTATTAAAC	Start of DNT2, with attB1 site, Forward
2.7	V56HTEVDNT2ProR	AGGAGAGGGTTAGGGATAGGCTTACCATGGTGATGGTGATGGTGGCCCTG AAAATACAGGTTTTCTTGGCGCTTTGTCCTCGAACGCTTC	End of DNT2 pro-domain, TEV-6His-V5, Reverse
2.8	6HV5DNT2CKF	AGGGCCACCATCACCATCACCATGGTAAGCCTATCCCTAACCCTCTCCTCGG TCTCGATTCTACGAGTCCGGGGCGCTCCACCCTCTGCC	Start of DNT2 Cys knot, TEV-6His-V5, Forward
2.9	attB2DNT2CKR	GGGGACCACTTTGTACAAGAAAGCTGGGTTTAATTGGCG GCTATCGTGCA	End of DNT2, with attB2 site, Reverse
2.10	DNT2 0.5kb Fwd	TGGAAACCCGCTCTTTGTCAG	For sequencing of plasmids, 0.5kb into DNT2, Forward
2.11	DNT2 0.5kb Rev	AGAAGATACGTGGGTGCTTCC	For sequencing of plasmids, 0.5kb into DNT2, Reverse
2.12	DNT2 0.9kb Rev	TGATGAACTGCGATGTCGTCT	For sequencing of plasmids, 0.9kb into DNT2, Reverse

Restriction enzyme sites in bold, Gateway sequences underlined, 6His tags in blue, V5 tags in green, TEV and Thrombin protease sequences in red

Table 2.7 – Vector primers

Number	Original name	Sequence	Description
V.1	M13_Forward	GTAAAACGACGGCCAGT	M13 sequencing primer, Forward
V.2	M13_Reverse	GGAAACAGCTATGACCA	M13 sequencing primer, Reverse
V.3	pFstBc B4MCSFwd	TTCCGGATTATTCATACCGTC	Just before Multi-cloning site of pFastBac1 vector, Forward
V.4	SV40 Rev	GTGTGGGAGGTTTTTTAAAGC	Just after Multi-cloning site of various vectors within SV40 polyA, Reverse

Table 2.8 – PCR program used when amplifying with BioTaq DNA polymerase

Program 1 – For BioTaq		
Temperature	Time	
98°C	2 minutes	
98°C	30 seconds	
Tm-4°C	30 seconds	x10
68°C	(1 minute / kb) + 1 minute	
98°C	30 seconds	
Tm-3°C	30 seconds	x25
68°C	(1 minute / kb)	
72°C	15 minutes	
4°C	Forever	

Tm is the lowest melting temperature of the primers used

Table 2.9 – PCR program used when amplifying with Phusion DNA polymerase

Program 2 – for Phusion		
Temperature	Time	
98°C	2 minutes	
98°C	30 seconds	
Tm-3°C	30 seconds	x35
72°C	(30 seconds / kb)	
72°C	15 minutes	
4°C	Forever	

2.2.9 Generation of a constitutively active *Toll*-7 and *Toll-6* constructs

To over-express constitutively active forms of *Toll-7* and *Toll-6*, I generated constructs bearing activated receptors downstream of UAS in transformation vectors, following two different strategies. The first strategy followed the example of $Toll^{\Delta LRR}$: the endogenous signal peptide of each receptor was fused to the transmembrane domain, thereby removing the entire extracellular domain (Fig 2.10). For both receptors, the signal peptide was amplified from genomic DNA, incorporating a 5' attB1 site and a 3' MluI site (Toll-7: primers 7.8 and 7.10; Toll-6: primers 6.11 and 6.13). The transmembrane + intracellular domains were separately amplified, incorporating a 5' MluI site and a 3' attB2 site (Toll-7: primers 7.9 and 7.11; Toll-6: primers 6.12 and 6.14). Fragments were digested with MluI, and signal peptides were ligated to their respective transmembrane + intracellular fragments with T4 ligase. The constructs were then cloned into pDONR using Gateway BP Clonase. The correct clones were identified with restriction digests. Toll-$7^{\Delta LRR}$ was digested with PstI and PvuI, and MluI (Fig 2.11A); Toll-$6^{\Delta LRR}$ was digested with HpaI and MluI (Fig 2.12A). Both clones were sequenced: neither the $Toll\text{-}7^{\Delta LRR}$ nor $Toll\text{-}6^{\Delta LRR}$ coding regions carried any additional mutations, and the sequence confirmed the signal peptide was correctly ligated in frame with the transmembrane + intracellular domains (Figs 2.11B and 2.12B). Gateway LR reactions between the pDONR-ΔLRR entry clones and the pUAS-gw-HA-attB destination vector were carried out to produce pUAS-Toll-$7^{\Delta LRR}$-HA-attB and pUAS-Toll-$6^{\Delta LRR}$-HA-attB, expression clones suitable for *Drosophila* transgenesis using the φC31 system.

The second strategy taken followed the example of $Toll^{10b}$: the cysteine that is mutated to tyrosine in $Toll^{10b}$ is conserved in *Toll-7* and *Toll-6*, and equivalent amino acid substitutions were made (Fig 2.13). In *Toll-7*, the cysteine at position 993 was mutated to tyrosine, in *Toll-6*,

the cysteine was in position 1020. For both receptors, the signal peptide and extracellular domain up to the target cysteine were amplified from genomic DNA. An attB1 site was incorporated at the 5' end, and the 3' primer encoded the cysteine to tyrosine mutation (Toll-7: primers 7.8 and 7.12; Toll-6: primers 6.11 and 6.15). Separately, the C-terminal half of the receptors were amplified, from the target cysteine until the end. The mutation was encoded in the 5' primer, and an attB2 site was incorporated at the 3' end (Toll-7: primers 7.9 and 7.13; Toll-6: primers 6.12 and 6.16). The two halves of each construct were connected in an overlapping PCR (Toll-7: primers 7.8 and 7.9; Toll-6: primers 6.11 and 6.12), and the resulting product was cloned into pDONR with BP Gateway cloning. The correct clones were identified with restriction digests. Toll-$7^{Cys\text{-}Tyr}$ was digested with ApaI and EcoRV (Fig 2.14A); Toll-$6^{Cys\text{-}Tyr}$ was digested with BglII and XhoI (Fig 2.15A). Both clones were sequenced. The sequence of *Toll-*$7^{Cys\text{-}Tyr}$ confirmed that the targeted cysteine had been mutated to tyrosine (Fig 2.14B, C). Two additional point mutations were found: proline to leucine at position 58, and valine to isoleucine at position 251 (Fig 14C). Val251Ile is a conservative, hydrophobic mutation falling in the extracellular domain; Pro58Leu is a less conservative change, and lies at the N-terminal of the extracellular domain. Also, there was a loss of a glutamine residue at the C-terminal end of the protein, reducing a poly-glutamine tract from 13 to 12 residues (Fig 2.14C). There are no mutations in the TIR domain, and it is not anticipated that the mutations will impede the constitutive activation of *Toll-*$7^{Cys\text{-}Tyr}$. The sequence of *Toll-*$6^{Cys\text{-}Tyr}$ confirmed that the targeted cysteine had been mutated to tyrosine (Fig 2.15B, C). In addition, two further point mutations were: threonine to alanine at position 252, and serine to threonine at position 862 (Fig 2.15C). These are all small amino acid residues, serine and threonine are both polar, and the mutations fall in the extracellular domain. They do not fall within the signalling TIR domain, so are unlikely to interfere with

the constitutive activation of *Toll-6*$^{Cys\text{-}Tyr}$. Gateway LR reactions between the pDONR-Cys-Tyr entry clones and the pUAS-gw-FLAG destination vector were carried out to produce pUAS-Toll-7$^{Cys\text{-}Tyr}$-FLAG and pUAS-Toll-6$^{Cys\text{-}Tyr}$-FLAG, subsequently used for *Drosophila* transgenesis.

2.2.10 Generation of clones for recombinant protein expression

DNT1 and *DNT2* constructs were made for protein expression with the Baculovirus system or in S2 cells. For Baculovirus, constructs containing an endogenous signal peptide from *DNT1* or *DNT2* were cloned into pFastBac1 (Invitrogen), which contains the polyhedron promoter for high levels of expression, and Tn7 transposon sequenced for shuttling into the bacmid during DH10Bac cell transformation (Luckow et al., 1993). For Cys-knot (CK) versions, lacking the endogenous signal peptide, constructs were cloned into pK503-9 (Laukkanen et al., 1996). This is a modified pFastBac1, introducing an exogenous signal peptide and FLAG tag at the N-terminal of the protein. For expression in S2 cells, coding sequences were cloned downstream of an Actin promoter. Constructs contained a 6His tag, for NiNTA-affinity purification and identification by western blot; certain constructs contained additional epitope tags for identification, and TEV or Thrombin recognition sequences to allow subsequent proteolytic cleavage of the pro-domain or tags. The template for PCR of DNT1 fragments was cDNA3 (Zhu et al., 2008). The template for PCR of DNT2 fragments was the LD26258 EST, a full-length cDNA clone for DNT2 (Berkeley *Drosophila* Genome Project).

2.2.11 Generation of DNT1 expression clones

The DNT1 CK coding sequence was amplified from DNT1 cDNA by PCR. The forward primer 1.3 included a 5’ SphI enzyme site, a 6His epitope tag, and a Thrombin protease

Fig 2.10 - Cloning of ΔLRR constitutively active receptor constructs

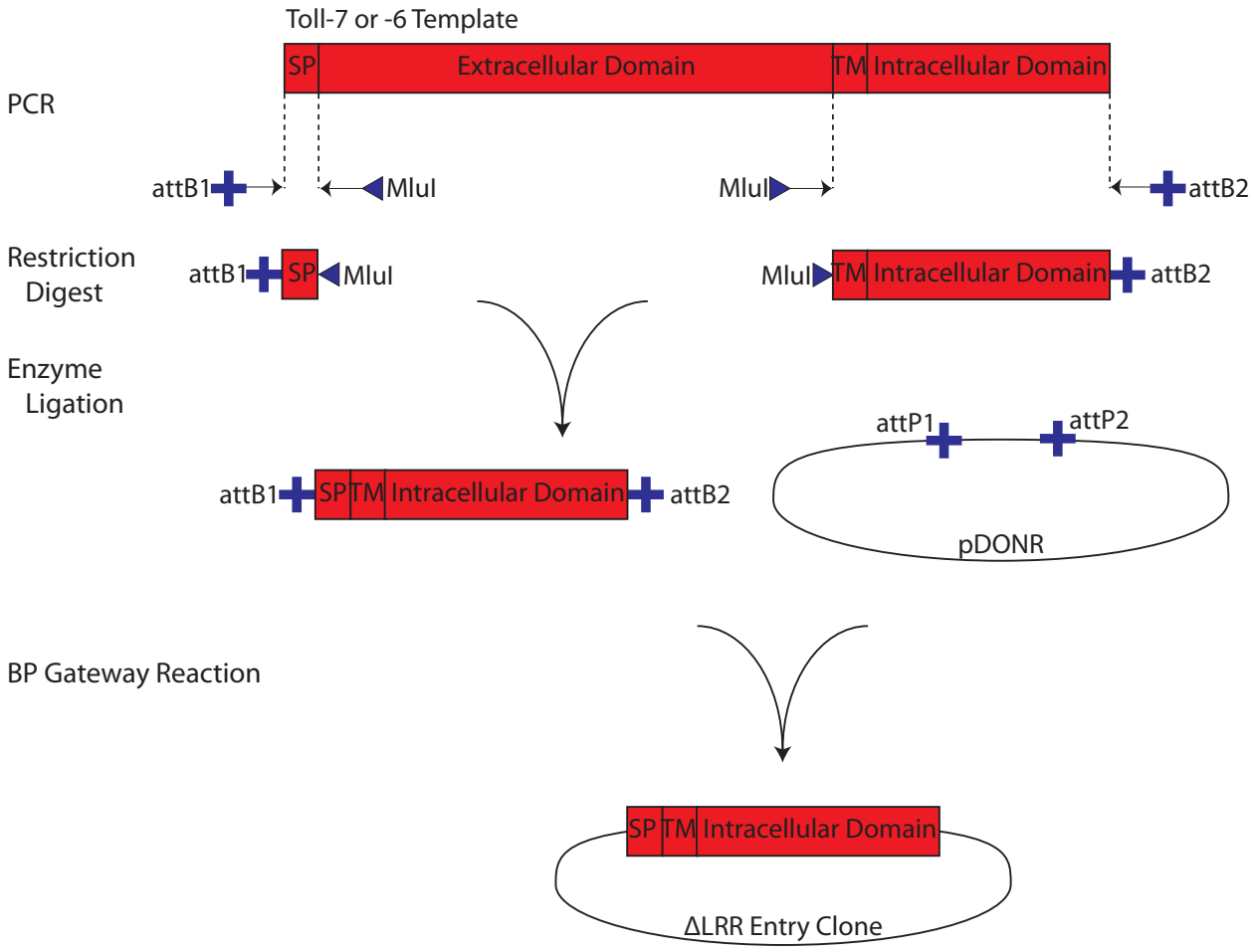

Cloning strategy for ΔLRR constructs. The signal peptide and transmembrane + intracellular domains were separately amplified by PCR, digested with MluI, and ligated with T4 Ligase. The resulting construct was cloned into pDONR by a Gateway BP reaction.

Fig 2.11 - Cloning of Toll-7$^{\Delta LRR}$

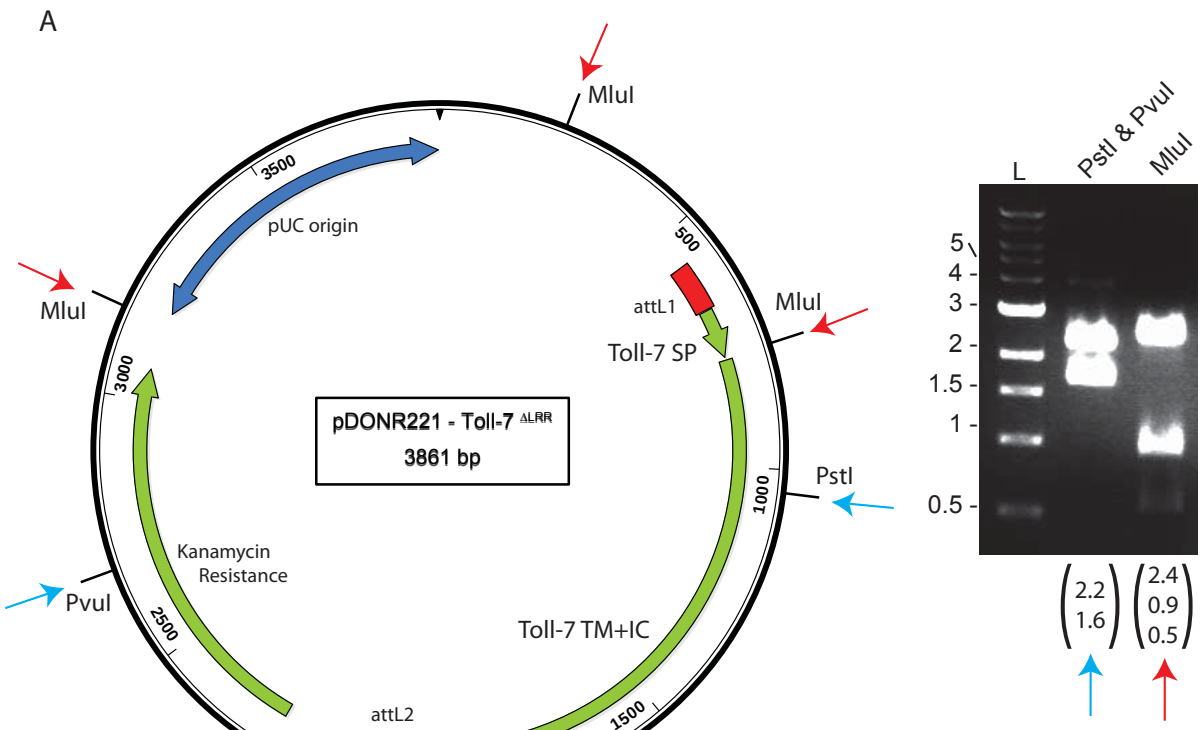

Toll-7$^{\Delta LRR}$ was cloned into pDONR. (A) Restriction digests were used to identify the correct clone. Enzyme sites are indicated on the map, and the DNA fragments are shown to the right. Predicted sizes given below each lane. (B, over) The sequenced gene region, compared to full-length *Toll-7*. Protein domains are shown, the deletion is indicated in red. CRC, cysteine-rich clusters lie C-terminal (CT) and N-terminal (NT) to leucine-rich domains.

Fig 2.11B – Sequence of cloned Toll-7$^{\Delta LRR}$


CRC-CT
Transmembrane
TIR
Tl7_Reference RNQWSCRCQFLQALTSYVADNALIVQDAQDIYCMAASSGTGSAALEDSSSNSGSLEKREL 1020
Tl7_DelLRR
Tl7_Reference DFNATGAACTDYYSGGSMLQHGIPESYIPLLAAALALLFLLVVIAMVFAFRESLRIWLFA 1080
Tl7_DelLRR TRESYIPLLAAALALLFLLVVIAMVFAFRESLRIWLFA 70
Tl7_Reference HYGVRVFGPRCEESEKLYDAVLLHSAKDSEFVCQHLAAQLETGRPPLRVCLQHRDLAHDA 1140
Tl7_DelLRR HYGVRVFGPRCEESEKLYDAVLLHSAKDSEFVCQHLAAQLETGRPPLRVCLQHRDLAHDA 130
Tl7_Reference THYQLLEATRVSRRVVILLTRNFLQTEWARCELRRSVHDALRGRPQKLVIIEEPEVAFEA 1200
Tl7_DelLRR THYQLLEATRVSRRVVILLTRNFLQTEWARCELRRSVHDALRGRPQKLVIIEEPEVAFEA 190
Tl7_Reference ESDIELLPYLKTSAVHRIRRSDRHFWEKLRYALPVDYPTFRGNNYTLELDHHNHERVKQP 1260
Tl7_DelLRR ESDIELLPYLKTSAVHRIRRSDRHFWEKLRYALPVDYPTFRGNNYTLELDHHNHERVKQP 250
Tl7_Reference ASPGLLYRQAPPPAYCGPADAVGIGAVPQVVPVNASVPAEQNYSTATTATPSPRPQRRGE 1320
Tl7_DelLRR ASPGLLYRQAPPPAYCGPADAVGIGAVPQVVPVNASVPAEQNYSTATTATPSPRPQRRGE 310
Tl7_Reference QPGSGSGGNHHLHAQYYQHHGMRPPSEHIYSSIDSDYSTLDNEQHMLMMPGAPGGLAMEA 1380
Tl7_DelLRR QPGSGSGGNHHLHAQYYQHHGMRPPSEHIYSSIDSDYSTLDNEQHMLMMPGAPGGLAMEA 370
Tl7_Reference AQRAQTWRPKREQLHLQQAQAGTLGSKASQAAHQQQQQQQQQQQQQPNPTAVSGQQQGPH 1440
Tl7_DelLRR AQRAQTWRPKREQLHLQQAQAGTLGSKASQAAHQQQQQQQQQQQQQPNPTAVSGQQQGPH 430
Tl7_Reference VQAYLV 1446
Tl7_DelLRR VQAYLV 436

Fig 2.12 - Cloning of Toll-6$^{\Delta LRR}$

A

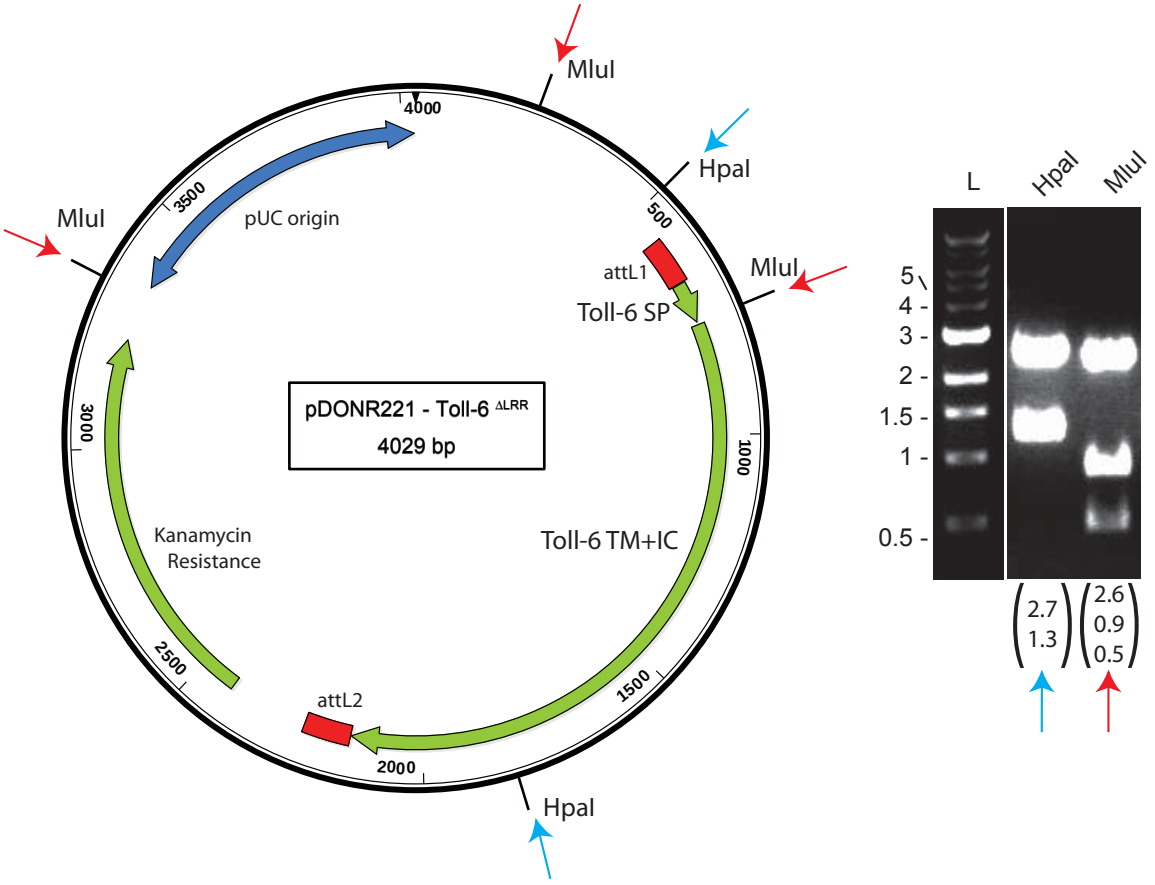

Toll-6$^{\Delta LRR}$ was cloned into pDONR. (A) Restriction digests were used to identify the correct clone. Enzyme sites are indicated on the map, and the DNA fragments are shown to the right. Predicted sizes given below each lane. (B, over) The sequenced gene region, compared to full-length *Toll-6*. Protein domains are given, and the deletion is indicated in red. CRC, cysteine-rich clusters lie C-terminal (CT) and N-terminal (NT) to leucine-rich domains.

Fig 2.12B – Sequence of cloned Toll-6$^{\Delta LRR}$


Transmembrane
TIR
Tl6_Reference IYNNATSVLREKNGTKCTLRDGVAHYMHTNEIEGLLPLLLVATCAFVAFFGLIFGLFCYR 1080
Tl6_DelLRR ----------TRIEGLLPLLLVATCAFVAFFGLIFGLFCYR 58
Tl6_Reference HELKIWAHSTNCLMNFCYKSPRFVDQLDKERPNDAYFAYSLQDEHFVNQILAQTLENDIG 1140
Tl6_DelLRR HELKIWAHSTNCLMNFCYKSPRFVDQLDKERPNDAYFAYSLQDEHFVNQILAQTLENDIG 118
Tl6_Reference YRLCLHYRDVNINAYITDALIEAAESAKQFVLVLSKNFLYNEWSRFEYKSALHELVKRRK 1200
Tl6_DelLRR YRLCLHYRDVNINAYITDALIEAAESAKQFVLVLSKNFLYNEWSRFEYKSALHELVKRRK 178
Tl6_Reference RVVFILYGDLPQRDIDMDMRHYLRTSTCIEWDDKKFWQKLRLALPLPNGRGNNNKRVVSG 1260
Tl6_DelLRR RVVFILYGDLPQRDIDMDMRHYLRTSTCIEWDDKKFWQKLRLALPLPNGRGNNNKRVVSG 238
Tl6_Reference CLSGRTPSVNMYATSHEYQAGNGGVIPPPSARYADCGSNNYATINECAAAGGGRGYKPIP 1320
Tl6_DelLRR CLSGRTPSVNMYATSHEYQAGNGGVIPPPSARYADCGSNNYATINECAAAGGGRGYKPIP 298
Tl6_Reference TSASAAAAACKFNTMNQLSKKQQRDLSVAGMAKTLEHQHHHNHQANRRSQHEYAVPSYLP 1380
Tl6_DelLRR TSASAAAAACKFNTMNQLSKKQQRDLSVAGMAKTLEHQHHHNHQANRRSQHEYAVPSYLP 358
Tl6_Reference SAAPAYDSVDYAKQQIRNNANCECVNLGTAKRAAGKNPASGLPSSFSSNFVPPGGASYNC 1440
Tl6_DelLRR SAAPAYDSVDYAKQQIRNNANCECVNLGTAKRAAGKNPASGLPSSFSSNFVPPGGASYNC 418
Tl6_Reference KKSCSCIGDDELLCSCGGGGGIGVNLLESGTQSSVTMSSSSNNSRQPELTHYESNLSLND 1500
Tl6_DelLRR KKSCSCIGDDELLCSCGGGGGIGVNLLESGTQSSVTMSSSSNNSRQPELTHYESNLSLND 478
Tl6_Reference DEDEDHDQQKNLWA 1514
Tl6_DelLRR DEDEDHDQQKNLWA 492

Fig 2.13 - Cloning of Cys-Tyr constitutively active receptor constructs

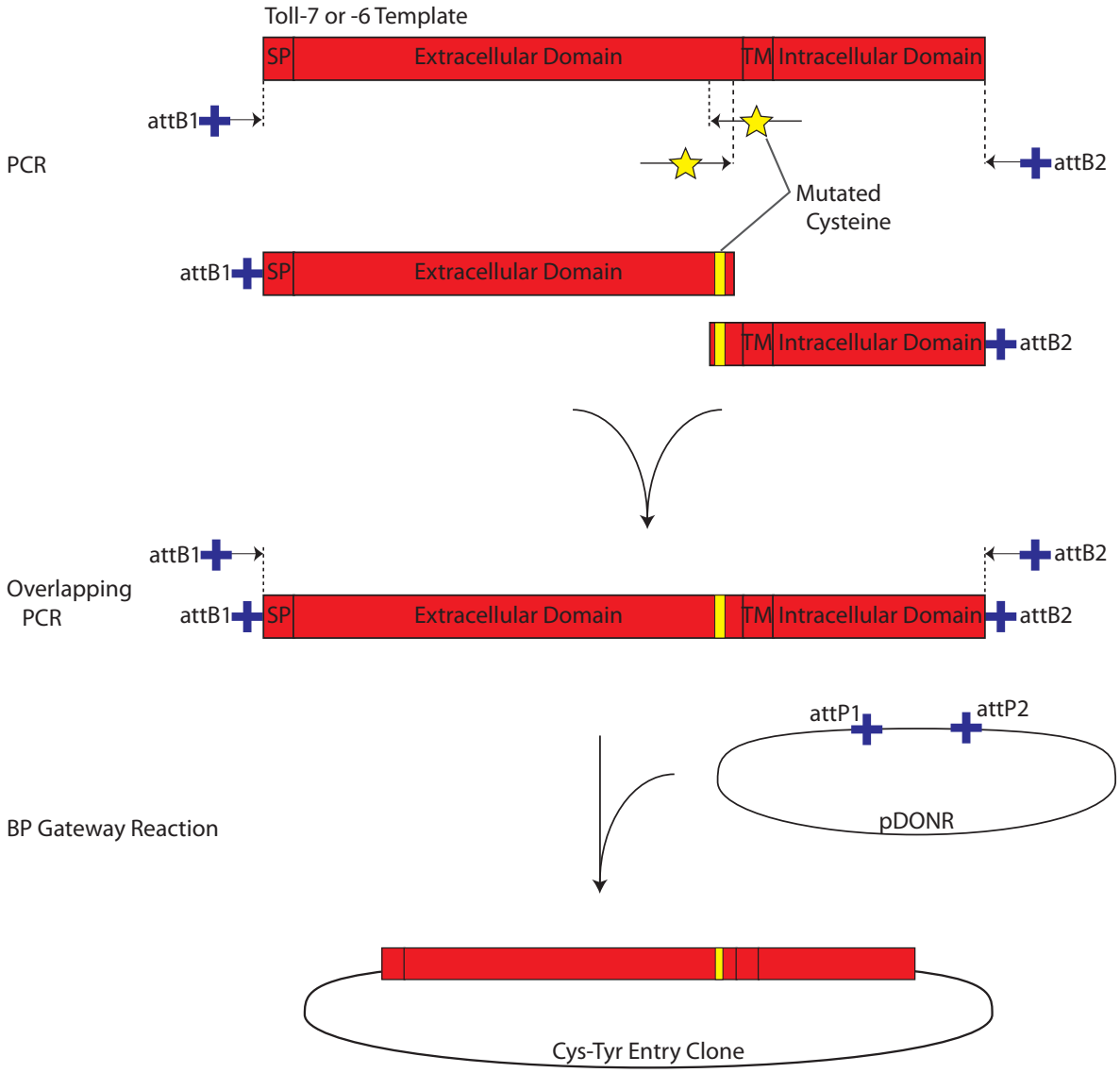

Cloning strategy for Cys-Tyr constructs. The N- and C-terminal halves of the receptors were amplified separately, introducing the Cys-Tyr mutation in the primers. The fragments were joined by overlapping PCR, and cloned into pDONR with a Gateway BP reaction.

Fig 2.14 - Cloning of Toll-7$^{Cys-Tyr}$

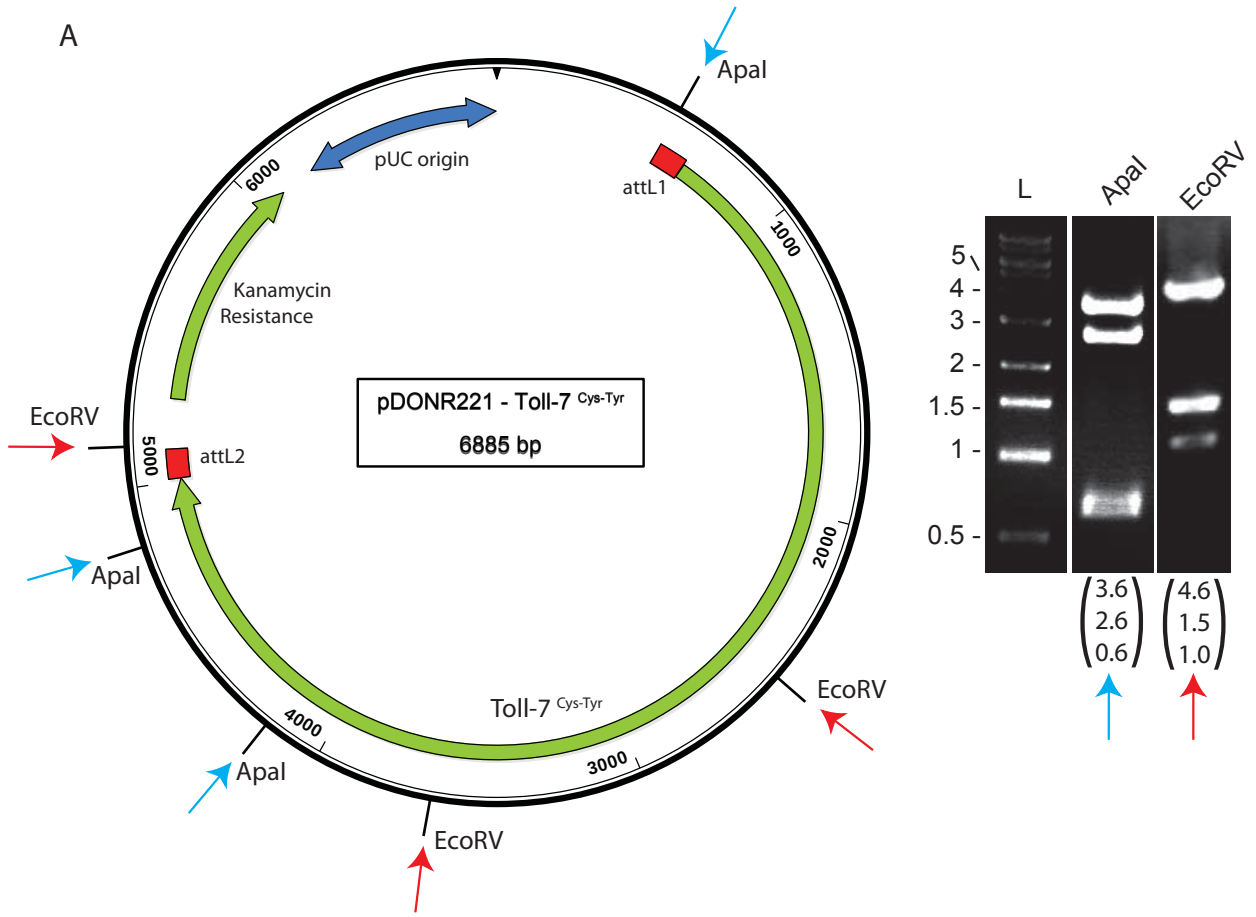

B

```
Toll-7          ALELIRIDGNRLVTLPIWQMHATHFGTRLKSISLGRNQWSCRCQFLQALTSYVADNALIV 985
Toll            NLTHLDISWNHLQMLNATVLGFLNRTMKWRSVKLSGNPWMCDCTAKP-LLLFTQDNFERI 773

Toll-7          QDAQDIYYMAASSGTGSAALEDSSSNSGSLEKRELDFNATGAACTDYYSGGSMLQHGIPE 1045
Toll            GDRNEMMCVNAEMP--TRMVELSTNDICPAEKG-------------------------V 805

Toll-7          SYIPLLAAALALLFLLVVIAMVFAFRESLRIWLFAHYGVRVFGPRCE------ESEKLYD 1099
Toll            FIALAVVIALTGLLAGFTAALYYKFQTEIKIWLYAHNLLLWFVTEED-----LDKDKKFD 860
```

Toll-7^{CysTyr} was cloned into pDONR. (A) Restriction digests were used to identify the correct clone. Enzyme sites are indicated on the map, DNA fragments are shown to the right. The predicted fragment sizes are given below each lane. (B) An alignment of Toll and Toll-7 juxtamembrane regions, showing conservation of cysteine residues. The mutated cysteine is highlighted in red, others in yellow. The transmembrane domain is underlined. (C, over) The sequenced gene region, compared to the predicted Toll-7 sequence. Mutated residues highlighted in red, including the targeted cysteine. Protein domains are given: CRC, cysteine-rich clusters lie C-terminal (CT) and N-terminal (NT) to leucine-rich domains.

Fig 2.14C – Sequence of cloned Toll-7$^{Cys\text{-}Tyr}$

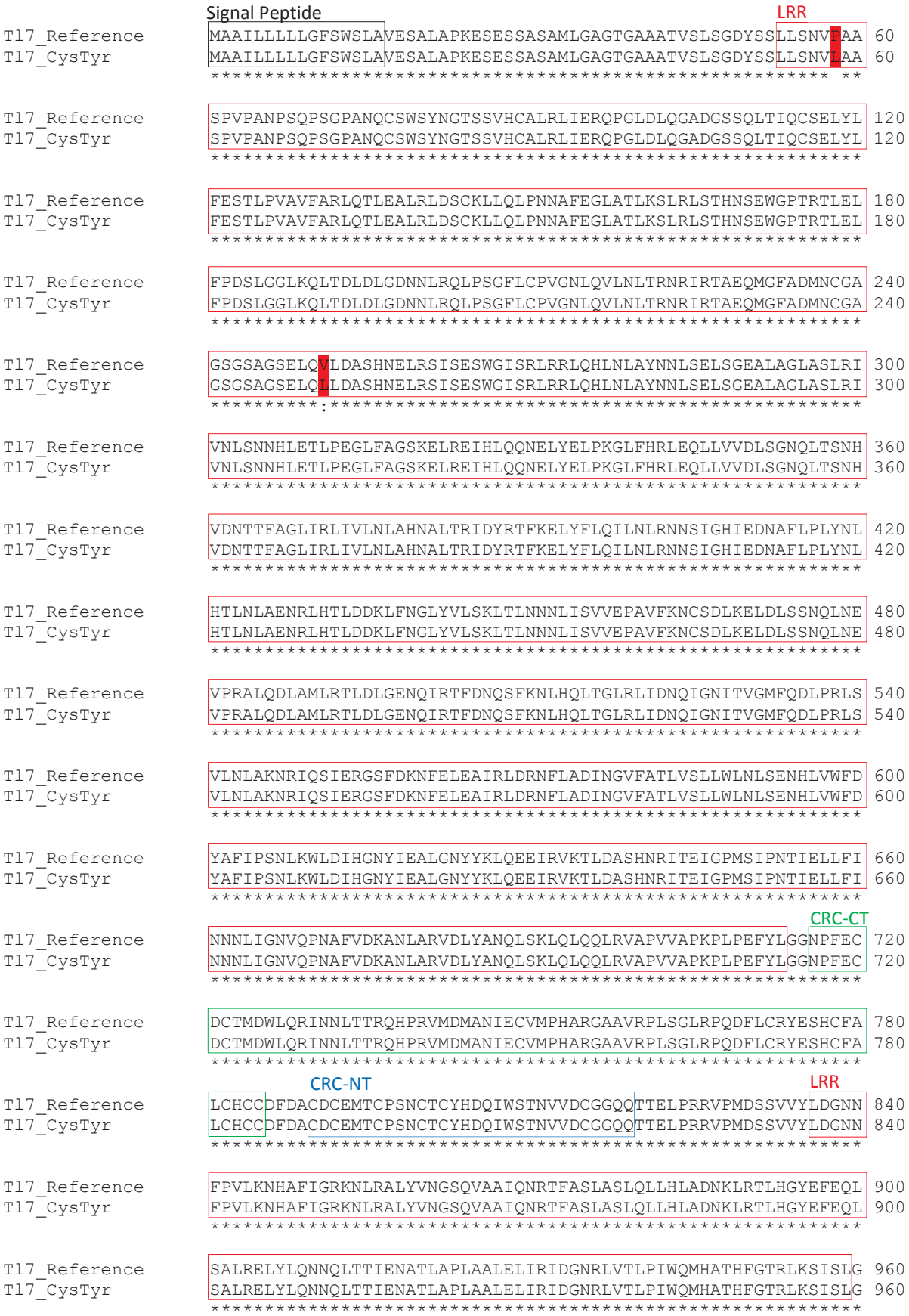


CRC-CT
Tl7_Reference RNQWSCRCQFLQALTSYVADNALIVQDAQDIYCMAASSGTGSAALEDSSSNSGSLEKREL 1020
Tl7_CysTyr RNQWSCRCQFLQALTSYVADNALIVQDAQDIYYMAASSGTGSAALEDSSSNSGSLEKREL 1020
Transmembrane
Tl7_Reference DFNATGAACTDYYSGGSMLQHGIPESYIPLLAAALALLFLLVVIAMVFAFRESLRIWLFA 1080
Tl7_CysTyr DFNATGAACTDYYSGGSMLQHGIPESYIPLLAAALALLFLLVVIAMVFAFRESLRIWLFA 1080
TIR
Tl7_Reference HYGVRVFGPRCEESEKLYDAVLLHSAKDSEFVCQHLAAQLETGRPPLRVCLQHRDLAHDA 1140
Tl7_CysTyr HYGVRVFGPRCEESEKLYDAVLLHSAKDSEFVCQHLAAQLETGRPPLRVCLQHRDLAHDA 1140
Tl7_Reference THYQLLEATRVSRRVVILLTRNFLQTEWARCELRRSVHDALRGRPQKLVIIEEPEVAFEA 1200
Tl7_CysTyr THYQLLEATRVSRRVVILLTRNFLQTEWARCELRRSVHDALRGRPQKLVIIEEPEVAFEA 1200
Tl7_Reference ESDIELLPYLKTSAVHRIRRSDRHFWEKLRYALPVDYPTFRGNNYTLELDHHNHERVKQP 1260
Tl7_CysTyr ESDIELLPYLKTSAVHRIRRSDRHFWEKLRYALPVDYPTFRGNNYTLELDHHNHERVKQP 1260
Tl7_Reference ASPGLLYRQAPPPAYCGPADAVGIGAVPQVVPVNASVPAEQNYSTATTATPSPRPQRRGE 1320
Tl7_CysTyr ASPGLLYRQAPPPAYCGPADAVGIGAVPQVVPVNASVPAEQNYSTATTATPSPRPQRRGE 1320
Tl7_Reference QPGSGSGGNHHLHAQYYQHHGMRPPSEHIYSSIDSDYSTLDNEQHMLMMPGAPGGLAMEA 1380
Tl7_CysTyr QPGSGSGGNHHLHAQYYQHHGMRPPSEHIYSSIDSDYSTLDNEQHMLMMPGAPGGLAMEA 1380
Tl7_Reference AQRAQTWRPKREQLHLQQAQAGTLGSKASQAAHQQQQQQQQQQQQQPNPTAVSGQQQGPH 1440
Tl7_CysTyr AQRAQTWRPKREQLHLQQAQAGTLGSKASQAAHQQQQQQQQQQQQ-PNPTAVSGQQQGPH 1439
Tl7_Reference VQAYLV 1446
Tl7_CysTyr VQAYLV 1445

Fig 2.15 - Cloning of Toll-6$^{Cys-Tyr}$

A

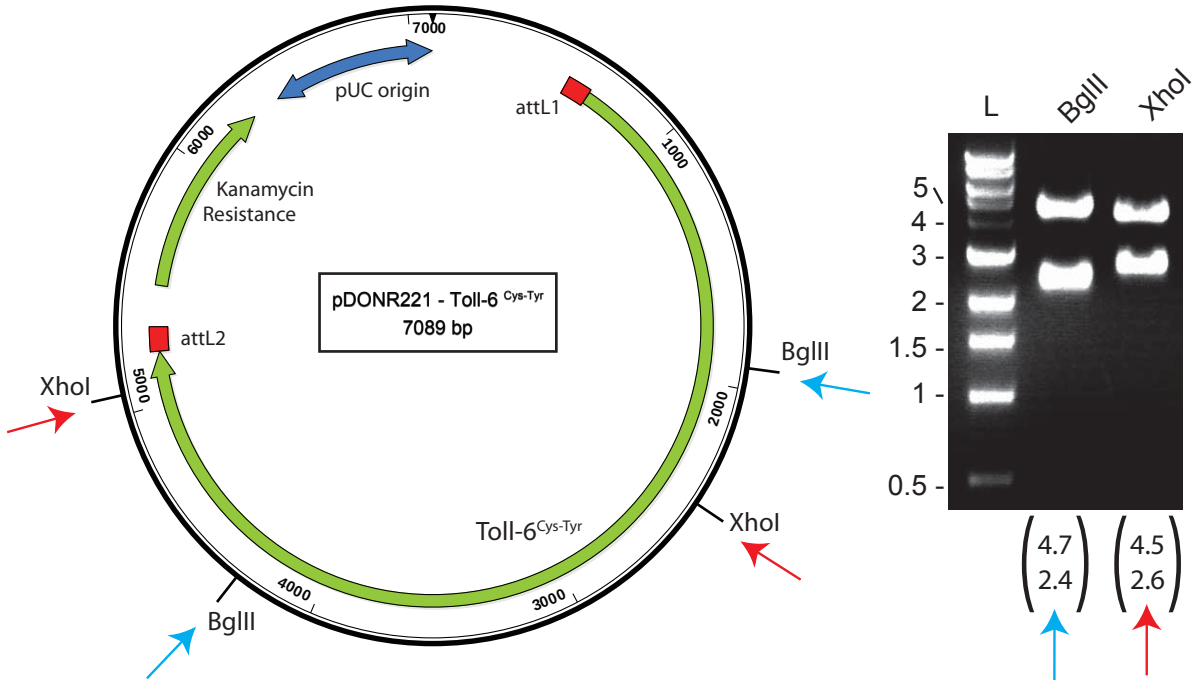

B

```
Toll-6          KLEVLRLDGNRLMHFEVWQLSANPY---LVEISLADNQWSCECGYLARFRNYLGQSSEKI 1012
Toll            NLTHLDISWNHLQMLNATVLGFLNRTMKWRSVKLSGNPWMCDCTAKP-LLLFTQDNFERI 773

Toll-6          IDASRVSYIYNN---ATSVLREKNGTKCTLRDGVAHY---------------MHTNEIEG 1054
Toll            GDRNEMMCVNAEMP--TRMVELSTNDICPAEKG-------------------------V 805

Toll-6          LLPLLLVATCAFVAFFGLIFGLFCYRHELKIWAHSTNCLMNFCYKSPRFVDQLDKERPND 1114
Toll            FIALAVVIALTGLLAGFTAALYYKFQTEIKIWLYAHNLLLWFVTEED-----LDKDKKFD 860
```

Toll-6^{CysTyr} was cloned into pDONR. (A) Restriction digests were used to identify the correct clone. Enzyme sites are indicated on the map, DNA fragments are shown to the right. The predicted fragment sizes are given below each lane. (B) An alignment of Toll and Toll-6 juxtamembrane regions, showing conservation of cysteine residues. The mutated cysteine is highlighted in red, others in yellow. The transmembrane domain is underlined. (C, over) The sequenced gene region, compared to the predicted *Toll-6* sequence. Mutated residues highlighted in red, including the targeted cysteine. Protein domains are given: CRC, cysteine-rich clusters lie C-terminal (CT) and N-terminal (NT) to leucine-rich domains.

Fig 2.15C – Sequence of cloned Toll-6$^{Cys\text{-}Tyr}$

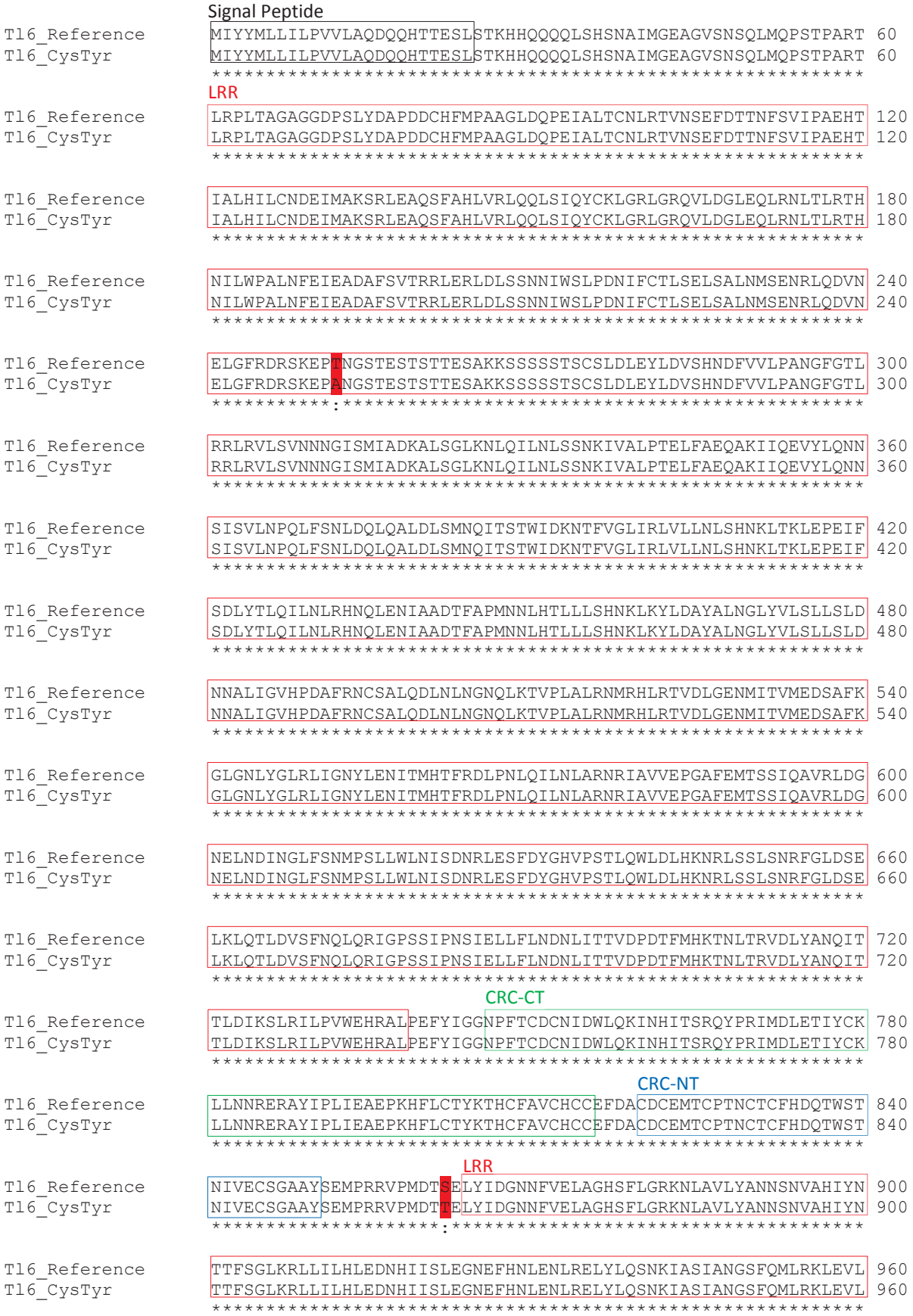


```
                    Signal Peptide
Tl6_Reference       MIYYMLLILPVVLAQDQQHTTESLSTKHHQQQQLSHSNAIMGEAGVSNSQLMQPSTPART 60
Tl6_CysTyr          MIYYMLLILPVVLAQDQQHTTESLSTKHHQQQQLSHSNAIMGEAGVSNSQLMQPSTPART 60
                    ************************************************************
                    LRR
Tl6_Reference       LRPLTAGAGGDPSLYDAPDDCHFMPAAGLDQPEIALTCNLRTVNSEFDTTNFSVIPAEHT 120
Tl6_CysTyr          LRPLTAGAGGDPSLYDAPDDCHFMPAAGLDQPEIALTCNLRTVNSEFDTTNFSVIPAEHT 120
                    ************************************************************

Tl6_Reference       IALHILCNDEIMAKSRLEAQSFAHLVRLQQLSIQYCKLGRLGRQVLDGLEQLRNLTLRTH 180
Tl6_CysTyr          IALHILCNDEIMAKSRLEAQSFAHLVRLQQLSIQYCKLGRLGRQVLDGLEQLRNLTLRTH 180
                    ************************************************************

Tl6_Reference       NILWPALNFEIEADAFSVTRRLERLDLSSNNIWSLPDNIFCTLSELSALNMSENRLQDVN 240
Tl6_CysTyr          NILWPALNFEIEADAFSVTRRLERLDLSSNNIWSLPDNIFCTLSELSALNMSENRLQDVN 240
                    ************************************************************

Tl6_Reference       ELGFRDRSKEPTNGSTESTSTTESAKKSSSSSTSCSLDLEYLDVSHNDFVVLPANGFGTL 300
Tl6_CysTyr          ELGFRDRSKEPANGSTESTSTTESAKKSSSSSTSCSLDLEYLDVSHNDFVVLPANGFGTL 300
                    ***********:************************************************

Tl6_Reference       RRLRVLSVNNNGISMIADKALSGLKNLQILNLSSNKIVALPTELFAEQAKIIQEVYLQNN 360
Tl6_CysTyr          RRLRVLSVNNNGISMIADKALSGLKNLQILNLSSNKIVALPTELFAEQAKIIQEVYLQNN 360
                    ************************************************************

Tl6_Reference       SISVLNPQLFSNLDQLQALDLSMNQITSTWIDKNTFVGLIRLVLLNLSHNKLTKLEPEIF 420
Tl6_CysTyr          SISVLNPQLFSNLDQLQALDLSMNQITSTWIDKNTFVGLIRLVLLNLSHNKLTKLEPEIF 420
                    ************************************************************

Tl6_Reference       SDLYTLQILNLRHNQLENIAADTFAPMNNLHTLLLSHNKLKYLDAYALNGLYVLSLLSLD 480
Tl6_CysTyr          SDLYTLQILNLRHNQLENIAADTFAPMNNLHTLLLSHNKLKYLDAYALNGLYVLSLLSLD 480
                    ************************************************************

Tl6_Reference       NNALIGVHPDAFRNCSALQDLNLNGNQLKTVPLALRNMRHLRTVDLGENMITVMEDSAFK 540
Tl6_CysTyr          NNALIGVHPDAFRNCSALQDLNLNGNQLKTVPLALRNMRHLRTVDLGENMITVMEDSAFK 540
                    ************************************************************

Tl6_Reference       GLGNLYGLRLIGNYLENITMHTFRDLPNLQILNLARNRIAVVEPGAFEMTSSIQAVRLDG 600
Tl6_CysTyr          GLGNLYGLRLIGNYLENITMHTFRDLPNLQILNLARNRIAVVEPGAFEMTSSIQAVRLDG 600
                    ************************************************************

Tl6_Reference       NELNDINGLFSNMPSLLWLNISDNRLESFDYGHVPSTLQWLDLHKNRLSSLSNRFGLDSE 660
Tl6_CysTyr          NELNDINGLFSNMPSLLWLNISDNRLESFDYGHVPSTLQWLDLHKNRLSSLSNRFGLDSE 660
                    ************************************************************

Tl6_Reference       LKLQTLDVSFNQLQRIGPSSIPNSIELLFLNDNLITTVDPDTFMHKTNLTRVDLYANQIT 720
Tl6_CysTyr          LKLQTLDVSFNQLQRIGPSSIPNSIELLFLNDNLITTVDPDTFMHKTNLTRVDLYANQIT 720
                    ************************************************************
                                                CRC-CT
Tl6_Reference       TLDIKSLRILPVWEHRALPEFYIGGNPFTCDCNIDWLQKINHITSRQYPRIMDLETIYCK 780
Tl6_CysTyr          TLDIKSLRILPVWEHRALPEFYIGGNPFTCDCNIDWLQKINHITSRQYPRIMDLETIYCK 780
                    ************************************************************
                                                                CRC-NT
Tl6_Reference       LLNNRERAYIPLIEAEPKHFLCTYKTHCFAVCHCCEFDACDCEMTCPTNCTCFHDQTWST 840
Tl6_CysTyr          LLNNRERAYIPLIEAEPKHFLCTYKTHCFAVCHCCEFDACDCEMTCPTNCTCFHDQTWST 840
                    ************************************************************
                                                LRR
Tl6_Reference       NIVECSGAAYSEMPRRVPMDTSELYIDGNNFVELAGHSFLGRKNLAVLYANNSNVAHIYN 900
Tl6_CysTyr          NIVECSGAAYSEMPRRVPMDTTELYIDGNNFVELAGHSFLGRKNLAVLYANNSNVAHIYN 900
                    ********************:***************************************

Tl6_Reference       TTFSGLKRLLILHLEDNHIISLEGNEFHNLENLRELYLQSNKIASIANGSFQMLRKLEVL 960
Tl6_CysTyr          TTFSGLKRLLILHLEDNHIISLEGNEFHNLENLRELYLQSNKIASIANGSFQMLRKLEVL 960
                    ************************************************************
```

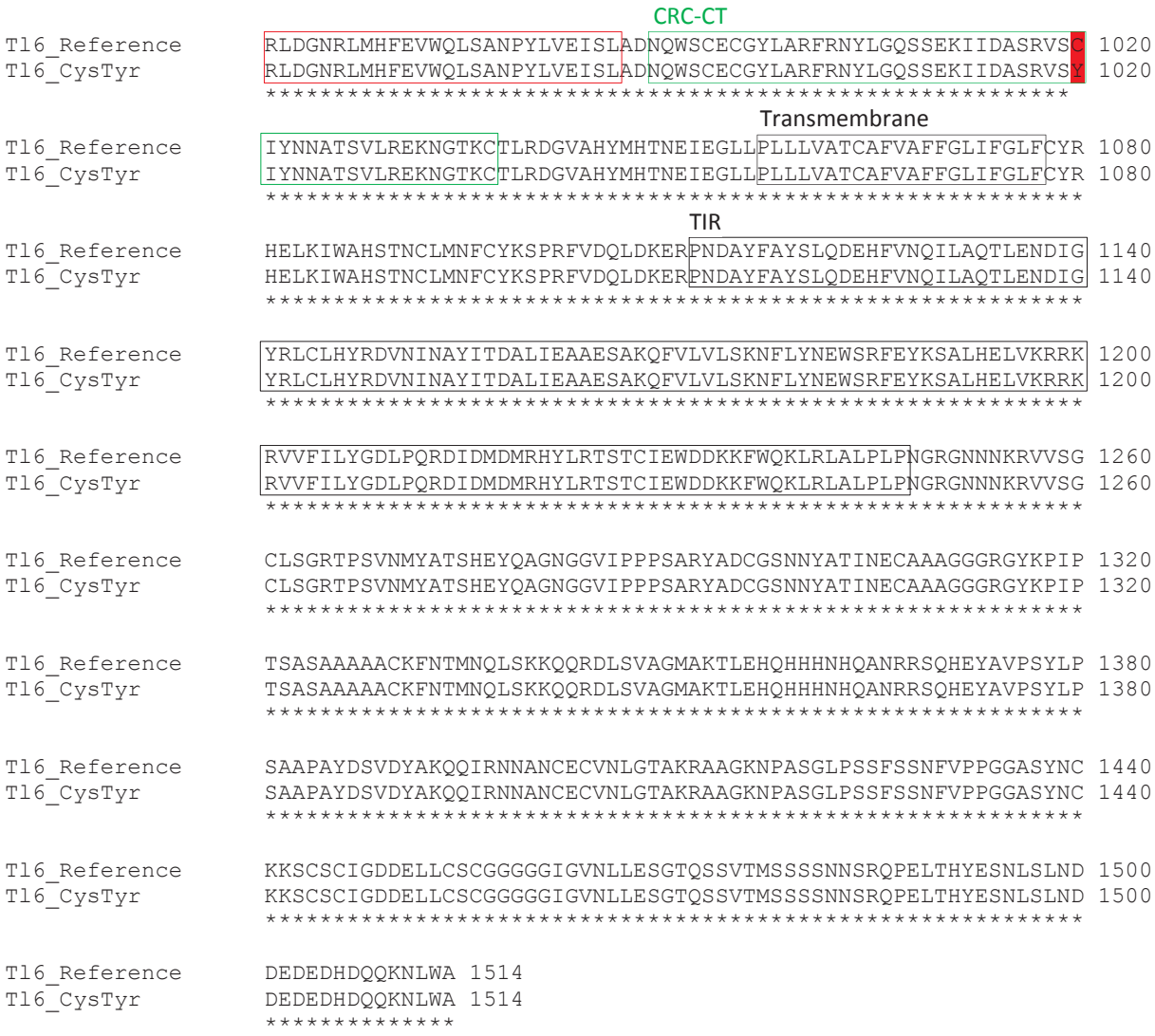
CRC-CT
Transmembrane
TIR
Tl6_Reference RLDGNRLMHFEVWQLSANPYLVEISLADNQWSCECGYLARFRNYLGQSSEKIIDASRVSC 1020
Tl6_CysTyr RLDGNRLMHFEVWQLSANPYLVEISLADNQWSCECGYLARFRNYLGQSSEKIIDASRVSY 1020
Tl6_Reference IYNNATSVLREKNGTKCTLRDGVAHYMHTNEIEGLLPLLLVATCAFVAFFGLIFGLFCYR 1080
Tl6_CysTyr IYNNATSVLREKNGTKCTLRDGVAHYMHTNEIEGLLPLLLVATCAFVAFFGLIFGLFCYR 1080
Tl6_Reference HELKIWAHSTNCLMNFCYKSPRFVDQLDKERPNDAYFAYSLQDEHFVNQILAQTLENDIG 1140
Tl6_CysTyr HELKIWAHSTNCLMNFCYKSPRFVDQLDKERPNDAYFAYSLQDEHFVNQILAQTLENDIG 1140
Tl6_Reference YRLCLHYRDVNINAYITDALIEAAESAKQFVLVLSKNFLYNEWSRFEYKSALHELVKRRK 1200
Tl6_CysTyr YRLCLHYRDVNINAYITDALIEAAESAKQFVLVLSKNFLYNEWSRFEYKSALHELVKRRK 1200
Tl6_Reference RVVFILYGDLPQRDIDMDMRHYLRTSTCIEWDDKKFWQKLRLALPLPNGRGNNNKRVVSG 1260
Tl6_CysTyr RVVFILYGDLPQRDIDMDMRHYLRTSTCIEWDDKKFWQKLRLALPLPNGRGNNNKRVVSG 1260
Tl6_Reference CLSGRTPSVNMYATSHEYQAGNGGVIPPPSARYADCGSNNYATINECAAAGGGRGYKPIP 1320
Tl6_CysTyr CLSGRTPSVNMYATSHEYQAGNGGVIPPPSARYADCGSNNYATINECAAAGGGRGYKPIP 1320
Tl6_Reference TSASAAAAACKFNTMNQLSKKQQRDLSVAGMAKTLEHQHHHNHQANRRSQHEYAVPSYLP 1380
Tl6_CysTyr TSASAAAAACKFNTMNQLSKKQQRDLSVAGMAKTLEHQHHHNHQANRRSQHEYAVPSYLP 1380
Tl6_Reference SAAPAYDSVDYAKQQIRNNANCECVNLGTAKRAAGKNPASGLPSSFSSNFVPPGGASYNC 1440
Tl6_CysTyr SAAPAYDSVDYAKQQIRNNANCECVNLGTAKRAAGKNPASGLPSSFSSNFVPPGGASYNC 1440
Tl6_Reference KKSCSCIGDDELLCSCGGGGGIGVNLLESGTQSSVTMSSSSNNSRQPELTHYESNLSLND 1500
Tl6_CysTyr KKSCSCIGDDELLCSCGGGGGIGVNLLESGTQSSVTMSSSSNNSRQPELTHYESNLSLND 1500
Tl6_Reference DEDEDHDQQKNLWA 1514
Tl6_CysTyr DEDEDHDQQKNLWA 1514

recognition sequence. The reverse primer 1.4 included a 3' HindIII restriction site. The amplified fragment and the pK502-9 vector were digested with SphI and HindIII, and they were ligated with T4 ligase (Fig 2.16). To identify the correct clone, restriction digests were carried out with SphI and HindIII, and ScaI (Fig 2.17A). To confirm the clone, the entire coding region was sequenced, which revealed no mutations (Fig 2.17B).

The DNA sequence encoding the DNT1 CK + C-terminal domain (CTD) was amplified from cDNA by PCR. Again, the forward primer 1.3 included a 5' SphI site, 6His and Thrombin sequences, and the reverse primer 1.5 contained the 3' HindIII site. The pK503-9 vector and the PCR product were digested with SphI and HindIII; the insert and vector were ligated using T4 Ligase (Fig 2.18). To identify the correct clone, restriction digests were carried out with EcoRV, and SphI and HindIII (Fig 2.19A). To confirm the clone, the coding region was sent for sequencing, which revealed no mutations (Fig 2.19B).

DNT1 CK with its endogenous signal peptide and pro-domain, but lacking the CTD, was amplified from cDNA by PCR. The forward primer 1.6 contained a 5' SpeI restriction site; the reverse primer 1.7 included the Tobacco etch virus (TEV) protease cleavage sequence, a 6His tag, and a 3' XhoI site. The PCR product and pFastBac1 vector were digested with SpeI and XhoI, ligated with T4 ligase (Fig 2.20). To identify the correct clone, restriction digests were carried out with XbaI and EcoRV, and XhoI and SpeI (Fig 2.21A). To confirm the clone, the coding region was sequenced, which revealed no mutations (Fig 2.21B).

The DNT1 CK+CTD was also cloned downstream of the Spz signal peptide and pro-domain. The Spz signal peptide + pro-domain sequences were amplified from pFastBac-SpzSP+Pro-6HisTEV-SpzCK (a gift from Dr Monique Gangloff, University of Cambridge), by PCR. The forward primer 1.8 included a 5' EcoRI enzyme site; the reverse primer 1.9 contained a His

tag and the TEV cleavage site. The DNT1 CK+CTD sequence was separately amplified by PCR from cDNA. The forward primer 1.10 incorporated 6His and Thrombin sequences complementary to the Spz pro-domain; the reverse primer 1.11 contained a 3' XhoI site. The two fragments were joined by overlapping PCR. The final fragment and the pFastBac vector were digested with EcoRI and XhoI, and were ligated with T4 ligase (Fig 2.22). To identify the correct clone, restriction digests were carried out with EcoRV, and BamHI (Fig 2.23A). To confirm the clone, the entire coding region was sequenced, which revealed no mutations (Fig 2.23B).

To express DNT1 in S2 cells, the entire DNT1 coding sequence was cloned downstream of an actin promoter, incorporating a TEV cleavage sequence, and 6His and V5 tags between the pro-domain and the CK. The DNT1 signal peptide and pro-domain were amplified from cDNA by PCR. The forward primer 1.12 included a 5' attB1 gateway cloning sequence; the reverse primer 1.13 included the TEV, 6His and V5 sequences. The DNT1 CK + CTD were separately amplified from cDNA by PCR. The forward primer 1.14 contained TEV, 6His and V5 sequences complementary to the pro-domain reverse primer; the reverse primer 1.15 contained a 3' attB2 Gateway cloning sequence. The two fragments were joined by overlapping PCR, and the insert was integrated into the pDONR plasmid using Gateway BP cloning (Fig 2.24). To identify the correct entry clone, restriction digests were carried out with XbaI and NotI, and EcoRV (Fig 2.25A). To confirm the clone, the entire coding region was sequenced, which revealed no mutations (Fig 2.25B). The resulting construct (DNT1 Pro-domain – TEV-6His-V5 – CK+CTD) was then transferred to pActin-gw by Gateway LR cloning.

Fig 2.16 - Cloning Strategy for DNT1 CK

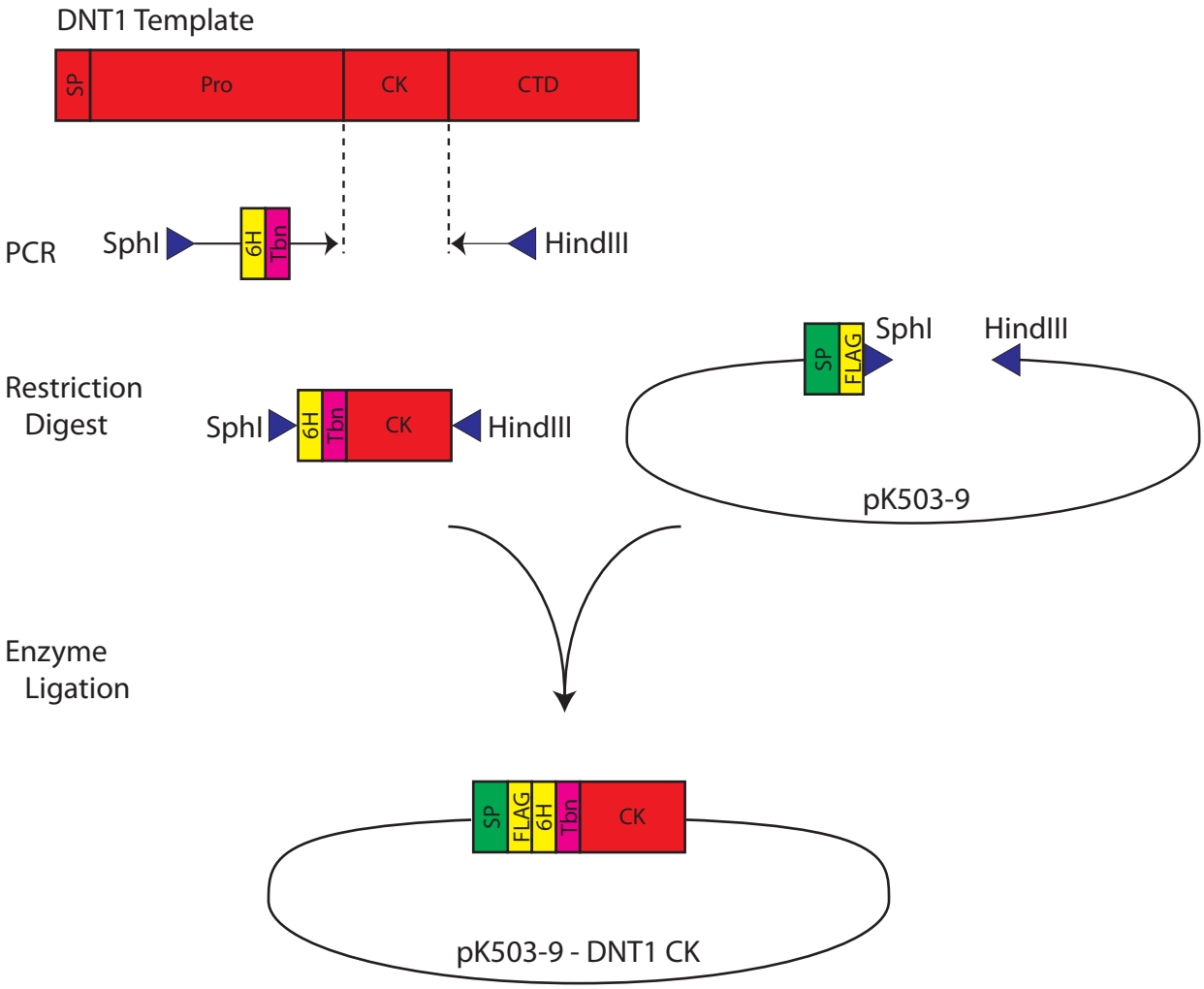

DNT1 CK was amplified by PCR from a cDNA template, with 6His, Thrombin (Tbn) and restriction enzyme sequences included in the primers. The insert and the vector were cut by restriction digest, and the insert was ligated in with T4 Ligase. Triangles indicate restriction enzyme sites.

Fig 2.17 - Identification of DNT1 CK clone

A

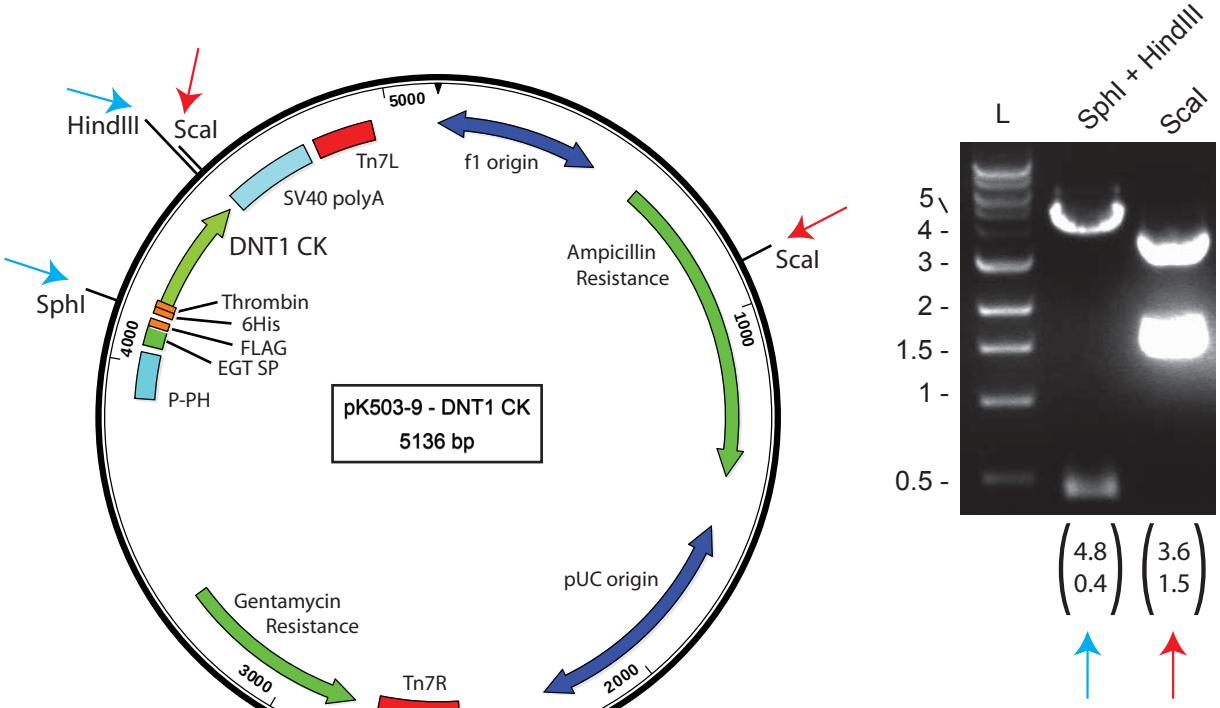

(A) Restricition digests were used to identify the correct clone. Enzyme sites are shown on the map, DNA fragments are shown on the right. Predicted sizes are given below each lane. (B, opposite) The sequenced gene region, compared to predicted sequence. Protein domains, epitope tags and protease recognition sequences are indicated.

Fig 2.17B – Sequence of cloned DNT1 CK

Fig 2.18 - Cloning Strategy for DNT1 CK + CTD

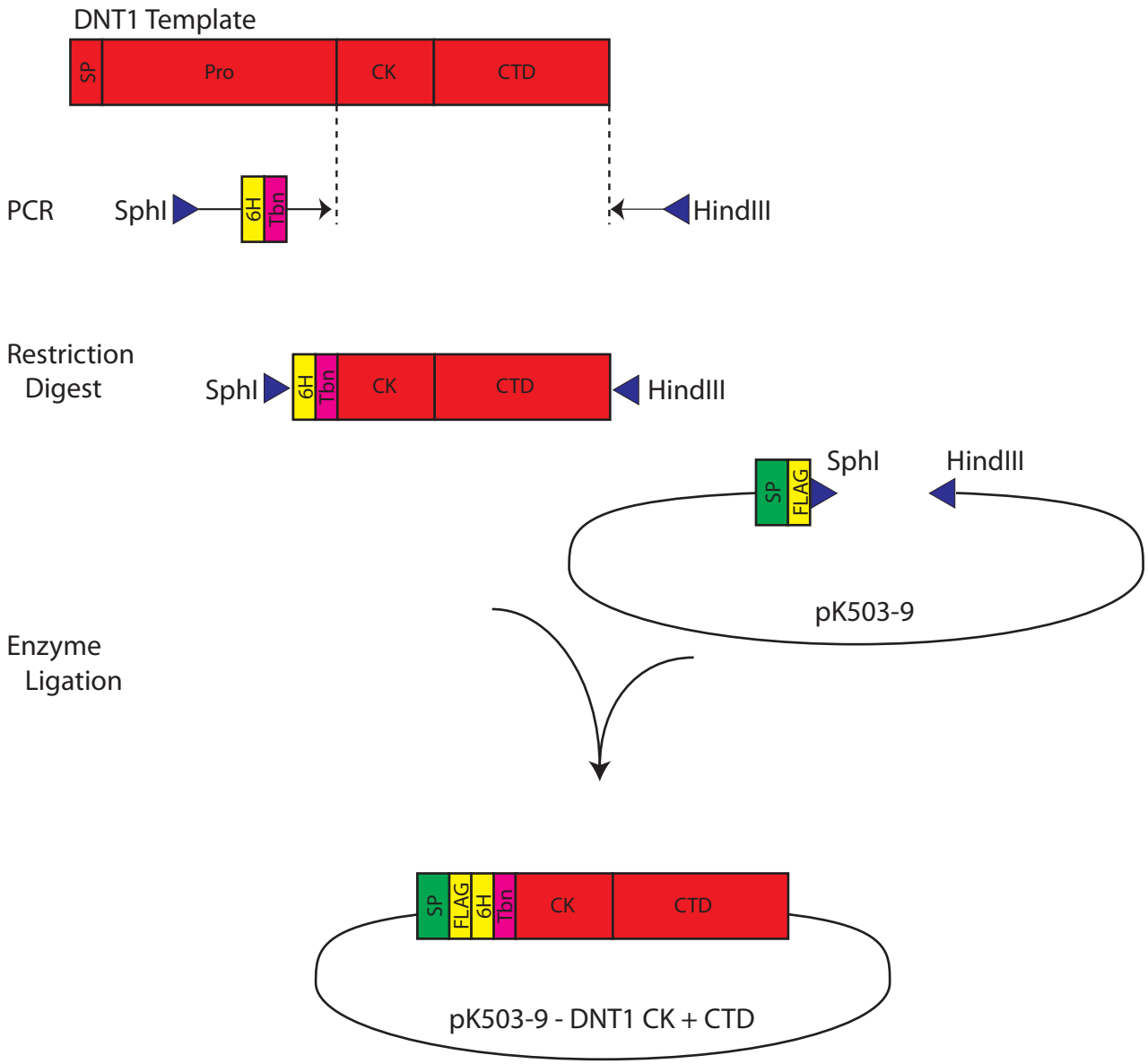

DNT1 CK + CTD was amplified by PCR from a cDNA template, with 6His, Thrombin (Tbn) and restriction enzyme sequences included in the primers. The insert and the vector were cut by restriction digest, and the insert was ligated in with T4 Ligase. Triangles indicate restriction enzyme sites.

Fig 2.19 - Identification of DNT1 CK + CTD clone

A

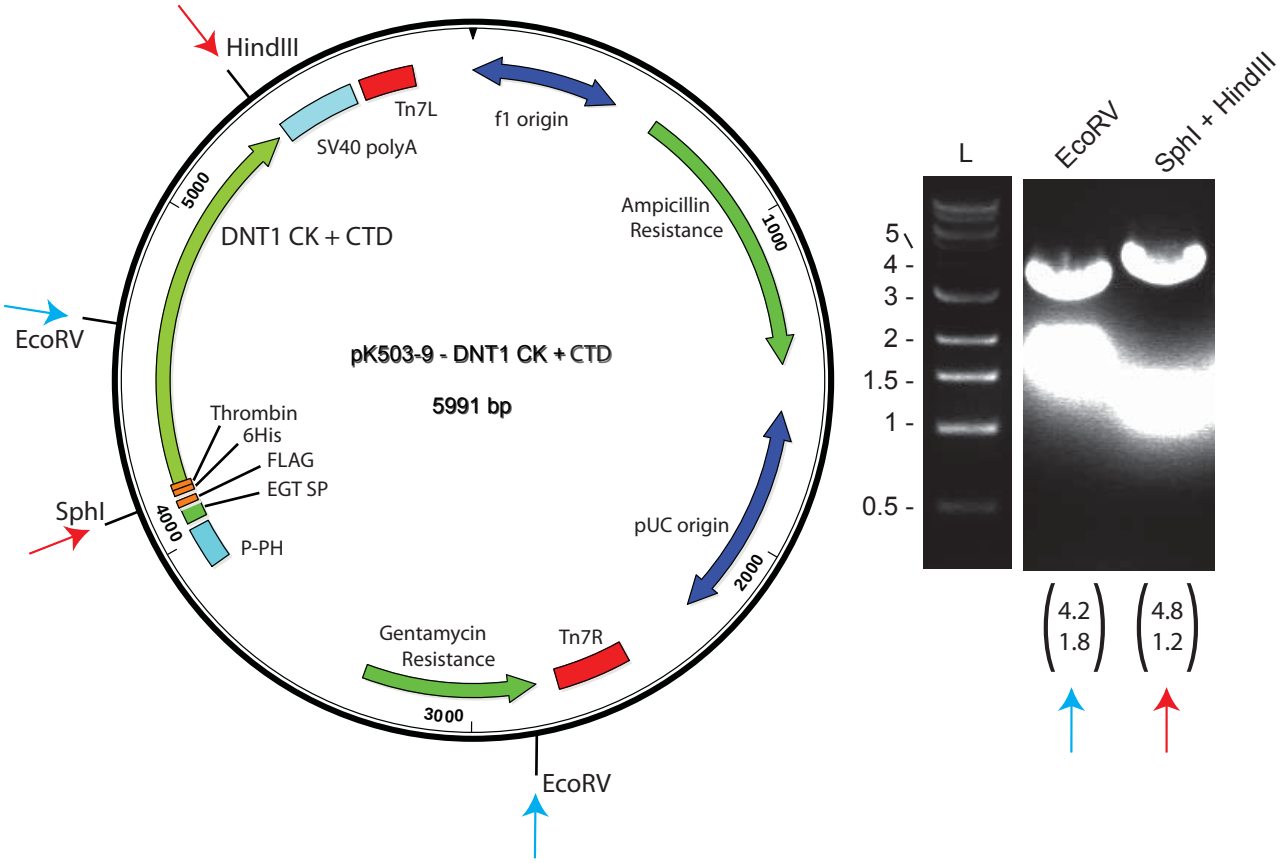

(A) Restriction digests were used to identify the correct clone. Enzyme sites are shown on the map, DNA fragments are shown to the right. Predicted sizes are given below each lane. (B, opposite) The sequenced gene region, compared to predicted sequence. Protein domains, epitope tags and protease recognition sequences are indicated.

Fig 2.19B – Sequence of cloned DNT1 CK+CTD

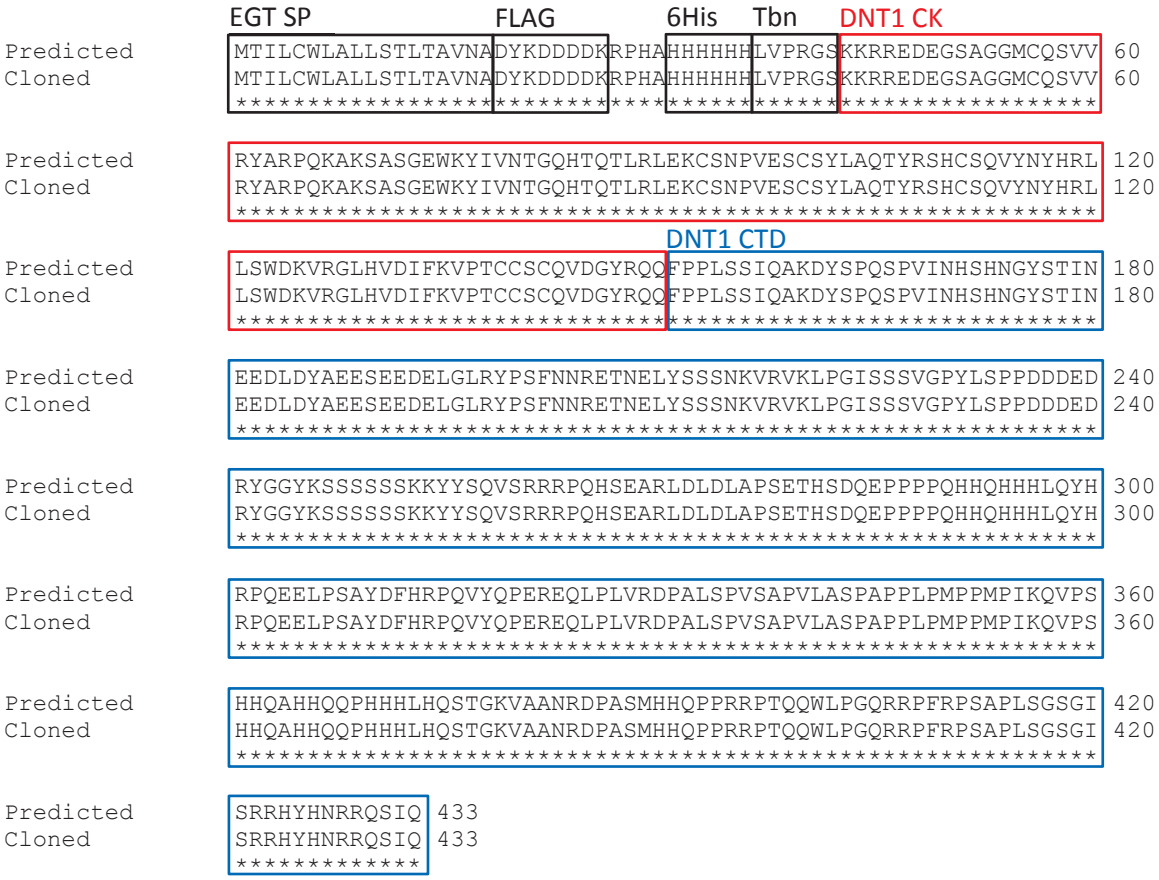

Fig 2.20 - Cloning strategy for DNT1 Pro-domain + CK

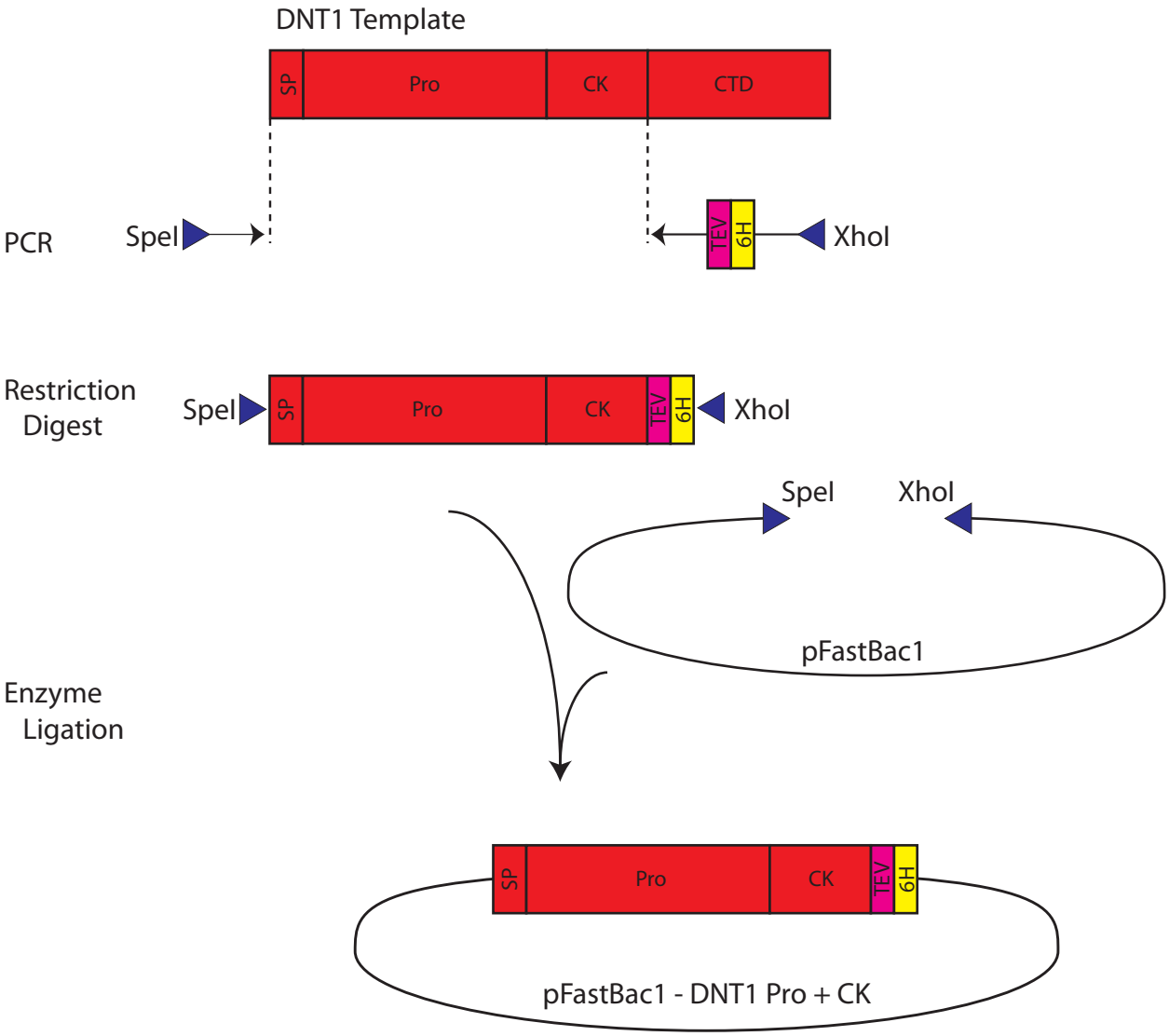

DNT1 Pro-domain + CK was amplified by PCR from a cDNA template, with 6His, TEV and restriction enzyme sequences included in the primers. The insert and the vector were cut by restriction digest, and the insert was ligated in with T4 Ligase. Triangles indicate restriction enzyme sites.

Fig 2.21 - Identification of DNT1 Pro-domain + CK clone

A

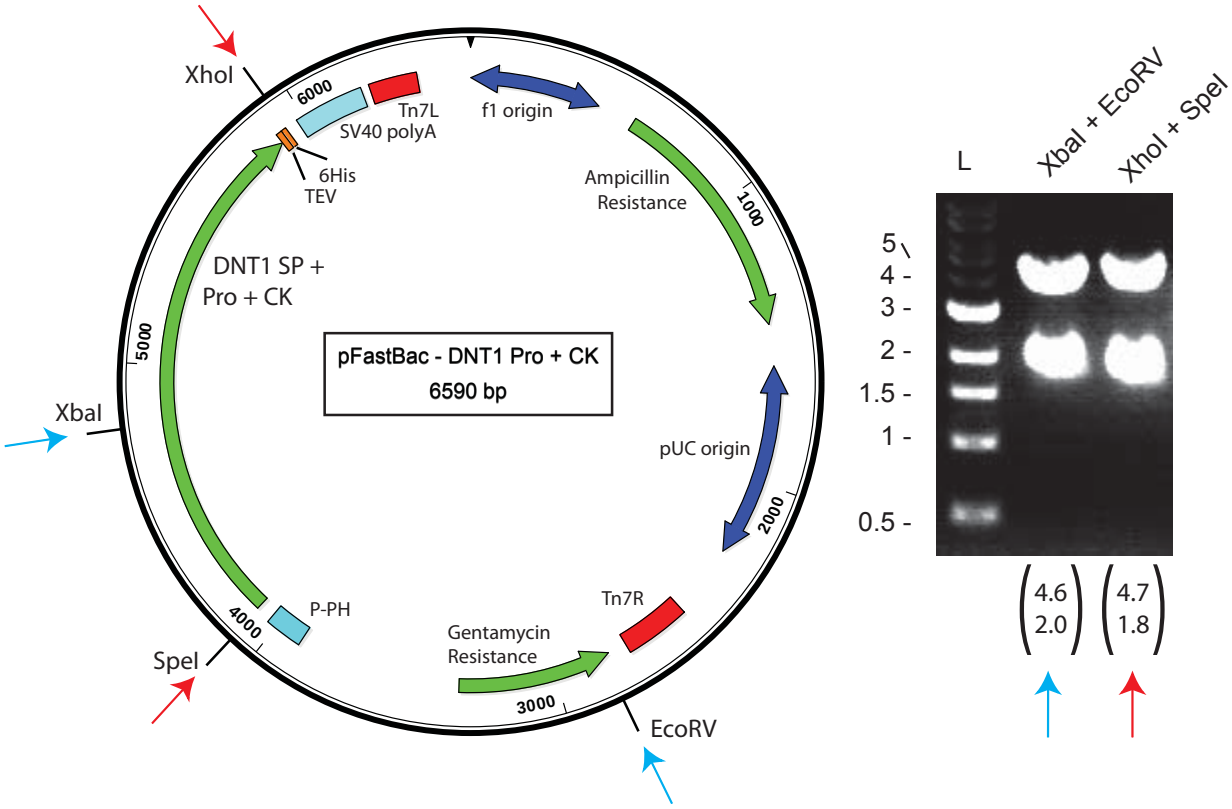

(A) Restriction digests were used to identify the correct clone. Enzyme sites are shown on the map, DNA fragments are shown to the right. Predicted sizes are given below each lane. (B, opposite) The sequenced gene region, compared to predicted sequence. Protein domains, epitope tags and protease recognition sequences are indicated.

Fig 2.21B – Sequence of cloned DNT1 Pro+CK

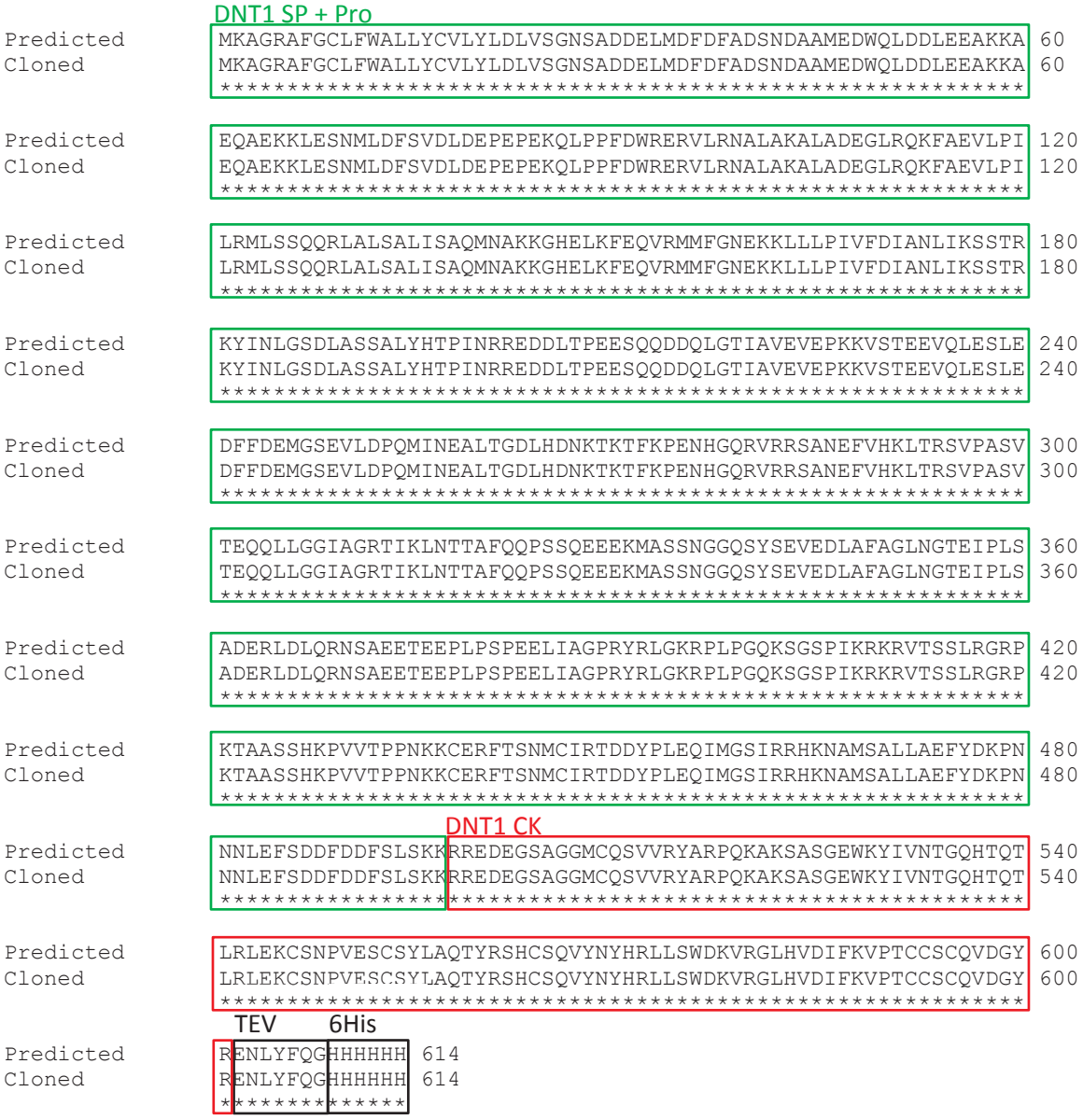

Fig 2.22 - Cloning strategy for Spz Pro-domain - DNT1 CK + CTD

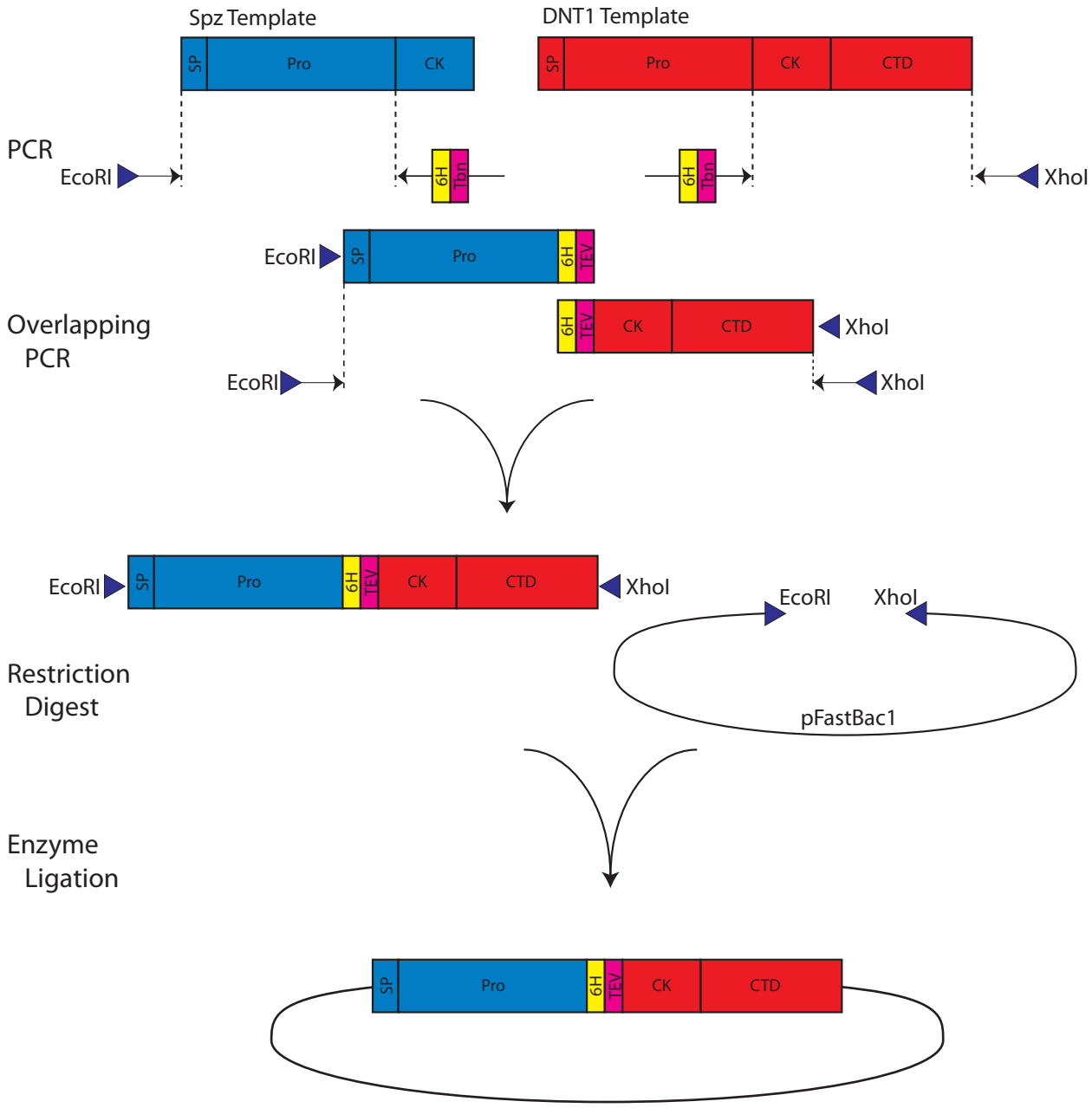

Spz signal peptide + pro-domain was amplified by PCR from cDNA, with restriction enzyme, 6His and TEV sequences included in the primers. DNT1 CK + CTD was similarly amplified by PCR. In third PCR reaction, the two fragments were joined and further amplified. The insert and the vector were cut by restriction digest, and the insert was ligated in with T4 Ligase. Triangles indicate restriction enzyme sites.

Fig 2.23 - Identification of Spz Pro - DNT1 CK + CTD clone

A

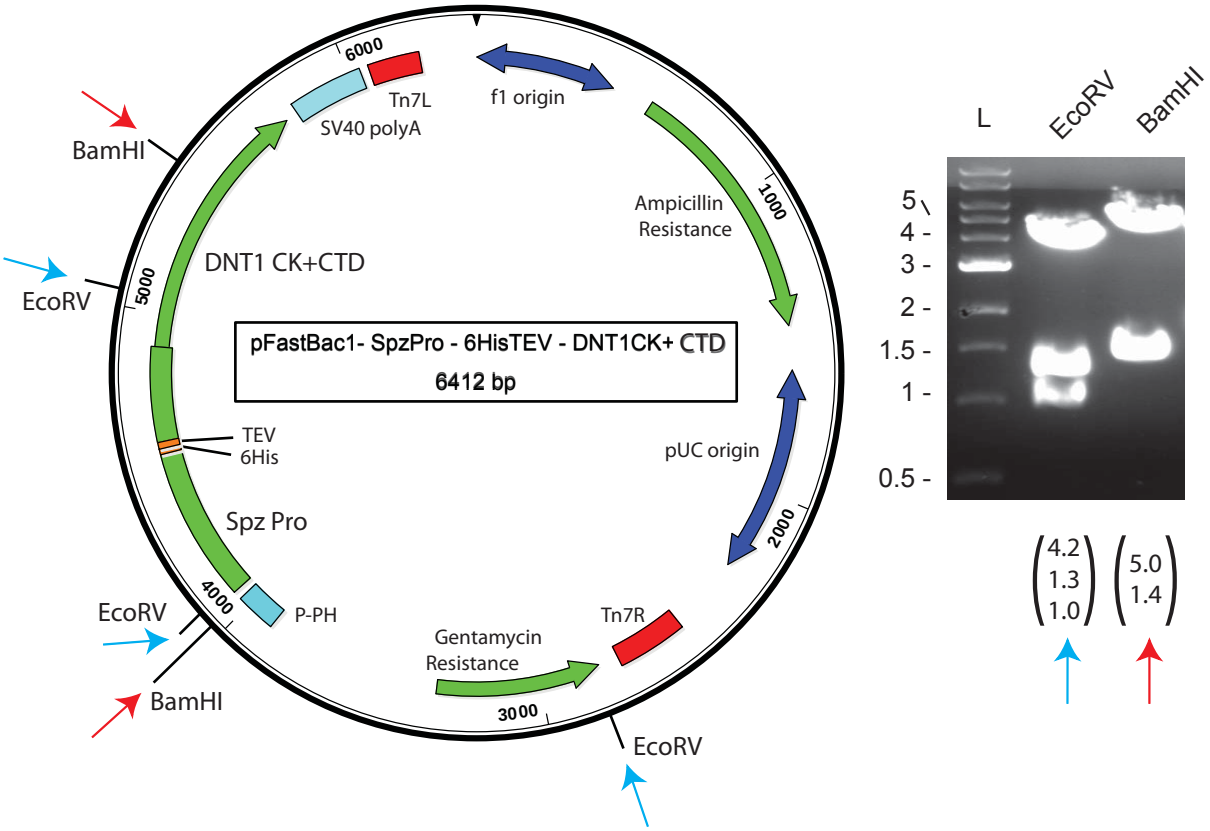

(A) Restricition digests were used to identify the correct clone. Enzyme sites are shown on the map, DNA fragments are shown on the right. Predicted sizes are given below each lane. (B, opposite) The sequenced gene region, compared to predicted sequence. Protein domains, epitope tags and protease recognition sequences are indicated.

Fig 2.23B – Sequence of cloned Spz Pro + DNT1 CK+CTD

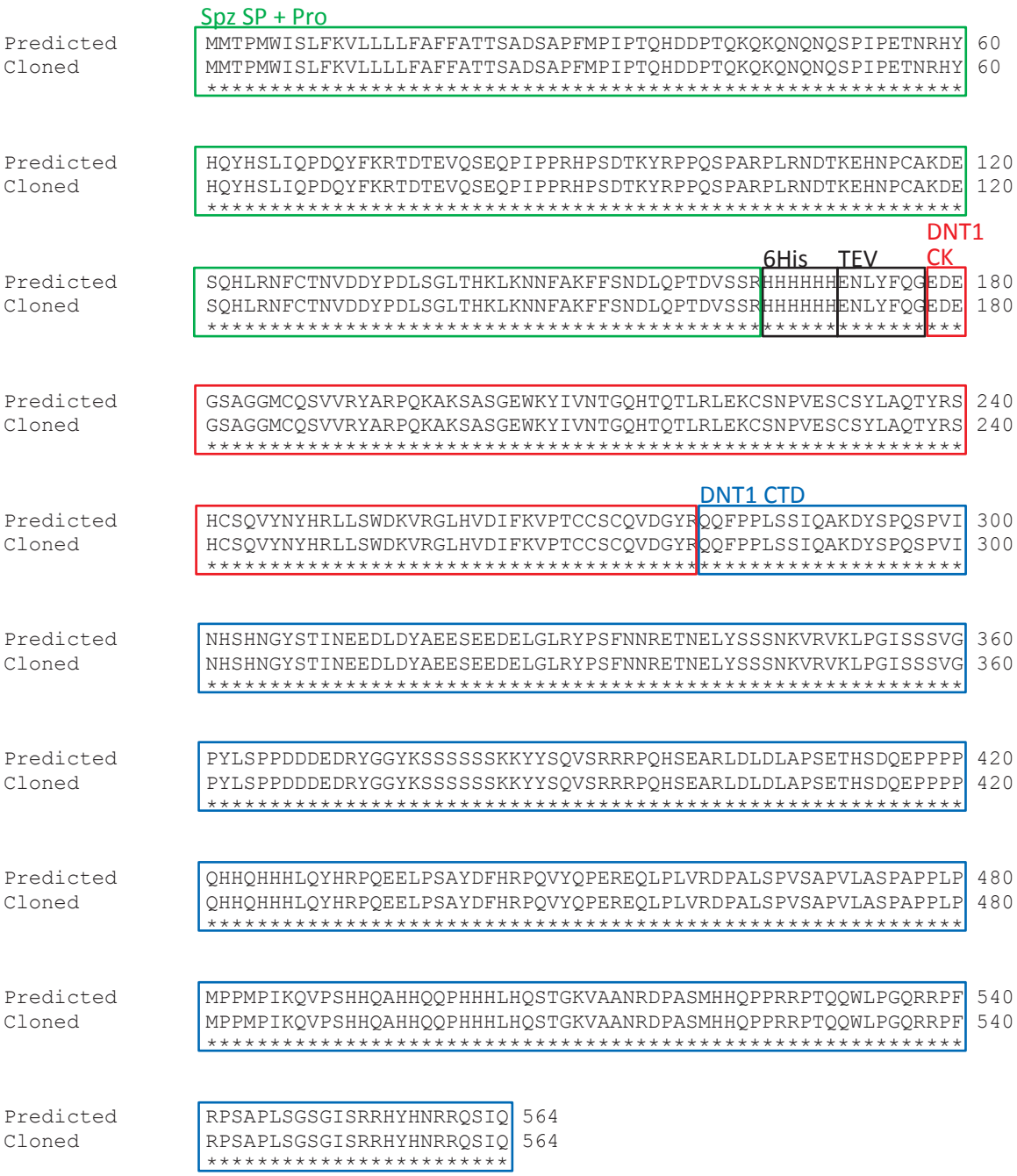

Fig 2.24 - Cloning strategy for DNT1 for S2 cell expression

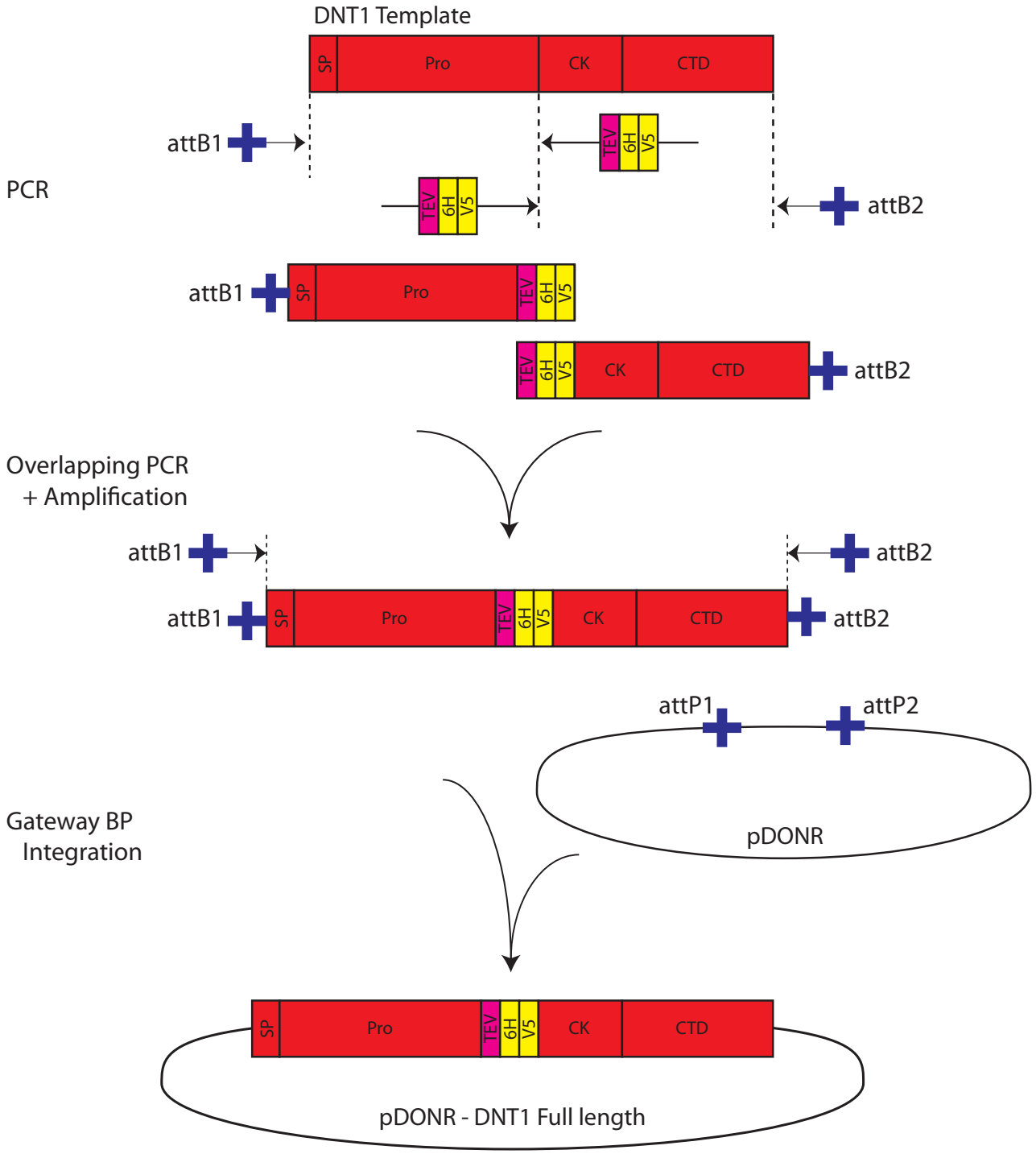

DNT1 signal peptide + pro-domain was amplified by PCR, as was the CK + CTD region, from cDNA. TEV cleavage, 6His, V5 and Gateway attB cloning sequences were included in the primers. The two fragments were joined by PCR, and amplified as a whole. The complete insert was then cloned into DONR using the Gateway system. Crosses indicate Gateway cloning sequences.

Fig 2.25 - Identification of DNT1 clone for expression in S2 cells

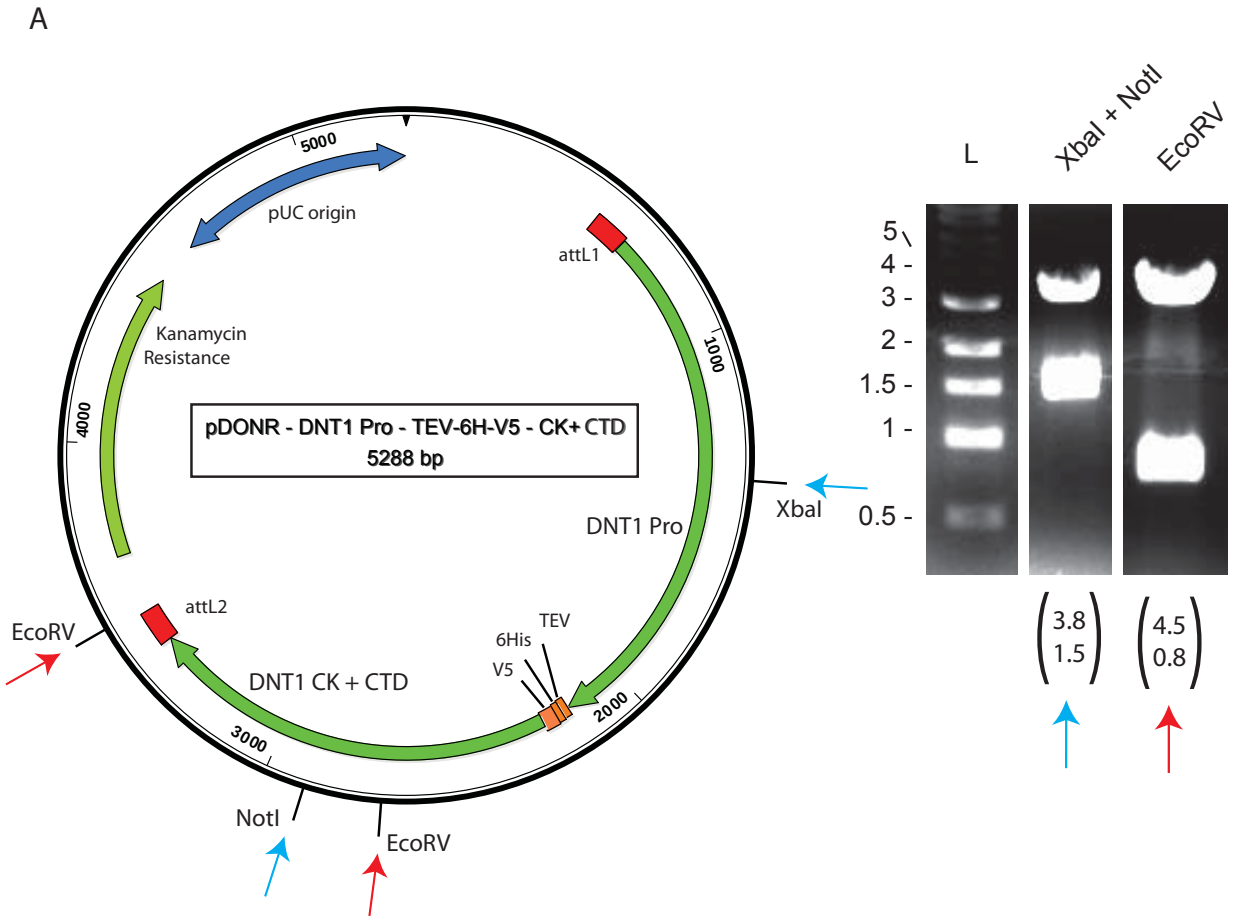

(A) Restricition digests were used to identify the correct clone. Enzyme sites are shown on the map, DNA fragments are shown on the right. Predicted sizes are given below each lane. (B, opposite) The sequenced gene region, compared to predicted sequence. Protein domains, epitope tags and protease recognition sequences are indicated.

Fig 2.25B – Sequence of DNT1 for S2 cell expression

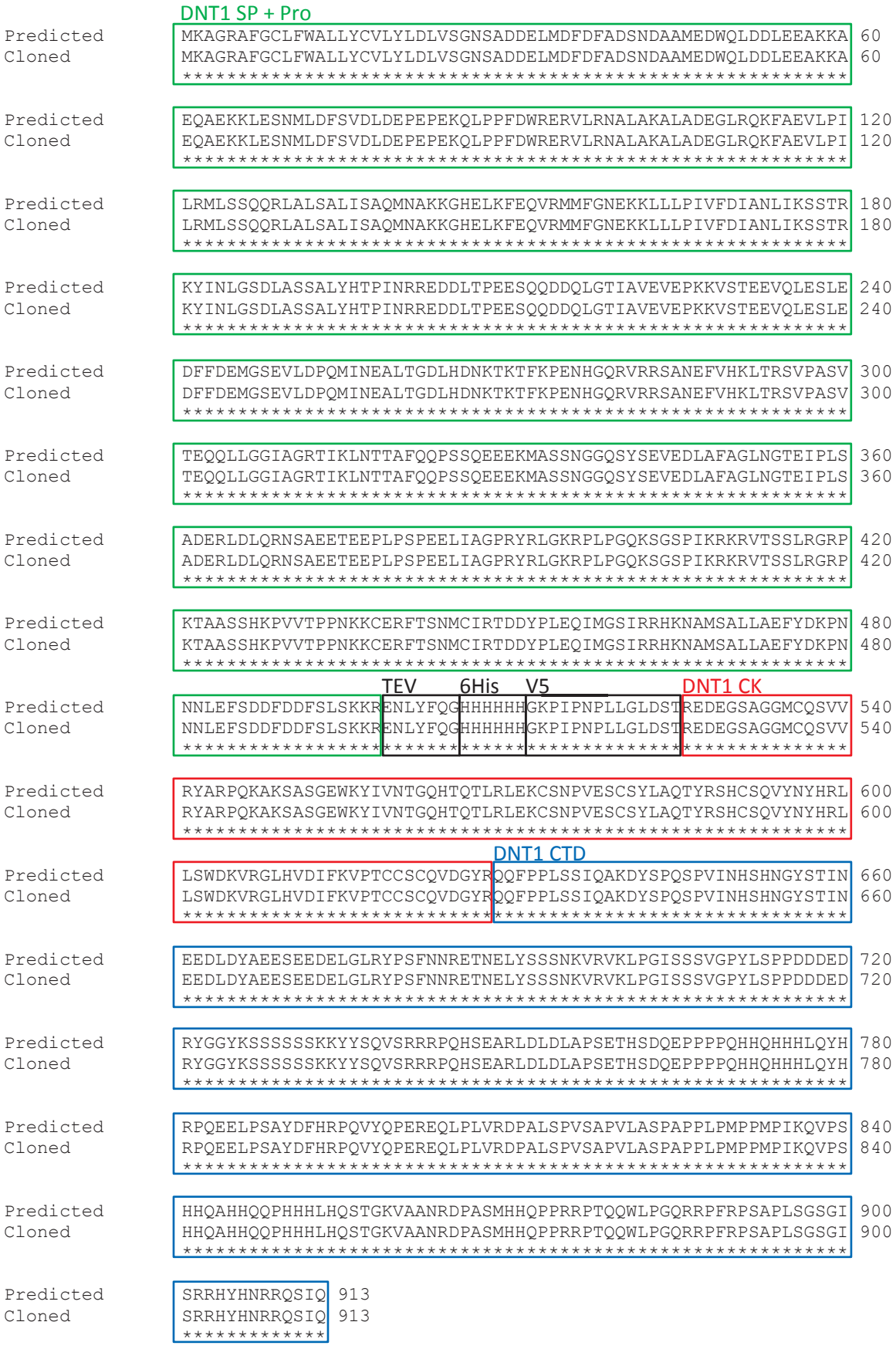

2.2.12 Generation of DNT2 expression clones

The DNT2 CK was amplified from cDNA by PCR. The forward primer 2.4 incorporated a 5' SphI site, and sequences for a 6His tag and Thrombin protease cleavage; the reverse primer 2.5 contained a 3' HindIII site. The insert and the pK503-9 vector were digested with SphI and HindIII, and ligated using T4 Ligase (Fig 2.26). To identify the correct clone, restriction digests were carried out with EcoRV and XhoI, and KspI (Fig 2.27A). To confirm the clone, the entire coding region was sequence, which revealed no mutations (Fig 2.27B).

The DNT2 CK, with its endogenous signal peptide and pro-domain, was amplified from cDNA by PCR. The forward primer 2.2 contained a 5' EcoRI restriction site; the reverse primer 2.3 included TEV, 6His and a 3' NotI sequence. The insert and the pFastBac1 vector were digested with EcoRI and NotI, and ligated with T4 Ligase (Fig 2.28). To identify the correct clone, restriction digests were carried out with KspI, and EcoRI and NotI (Fig 2.29A). To confirm the clone, the entire coding region was sequenced, which revealed no mutations (Fig 2.29B).

Finally, full-length DNT2 was cloned for expression in S2 cells, incorporating a TEV cleavage site and 6His and V5 epitope tags between the pro-domain and the CK. The DNT2 signal peptide and pro-domain were amplified from cDNA by PCR. The forward primer 2.6 contained a 5' attB1 Gateway cloning sequence; the reverse primer 2.7 included the TEV, 6His and V5 sequences. The CK was separately amplified with a forward primer 2.8 containing the TEV, 6His and V5 sequences complementary to the pro-domain reverse primer; the reverse primer 2.9 included a 3' attB2 sequence. The two fragments were joined by overlapping PCR, and the insert was incorporated into pDONR by gateway BP cloning (Fig 2.30). To identify the correct clone, restriction digests were carried out with XhoI and

BamHI, and EcoRV (Fig 2.31A). To confirm the clone, the entire coding region was sequenced, which revealed no mutations (Fig 2.31B). The resulting construct (DNT2 Pro-domain – TEV-6His-V5 – CK) was then transferred to pActin-gw by Gateway LR cloning.

2.3 Cell culture

2.3.1 S2 cell culture

Drosophila S2 cells (Invitrogen) were maintained in 25cm^2 flasks (BD), in Insect-Xpress medium (Lonza) supplemented with 1x penicillin/streptomycin/L-glutamine mix (Lonza) and 10% foetal calf serum (Lonza) (complete medium). Cells were grown at 27°C in air ($CO_2 \approx$ 0%). S2 cells stably transfected with a *Drosomycin-Luciferase* reporter of Dif activation (cell line 648-1B6, a gift from Prof Nick Gay, University of Cambridge, via Dr Lynne Prince, University of Sheffield) were maintained in complete medium supplemented with the selective antibiotic, 1µg/ml puromycin (Invitrogen) (Weber et al., 2003).

2.3.2 Transfection

Cells density was measured using a haemocytometer (Sigma), and cells were seeded at 3x10^6 per well of a 6-well plate in 2ml complete medium, and left to grow to confluence overnight. Cells were transfected with TranIT-2020 (Mirus), according to the manufacturer's instruction. The transfection mix contained 2-3µg of DNA, 250µl serum-free medium (SFM), and 3µl transfection reagent for each well. This was incubated in eppendorf tubes at room temperature for 30 minutes, after which 350µl SFM was added. Cells were washed with SFM, and the

Fig 2.26 - Cloning strategy for DNT2 CK

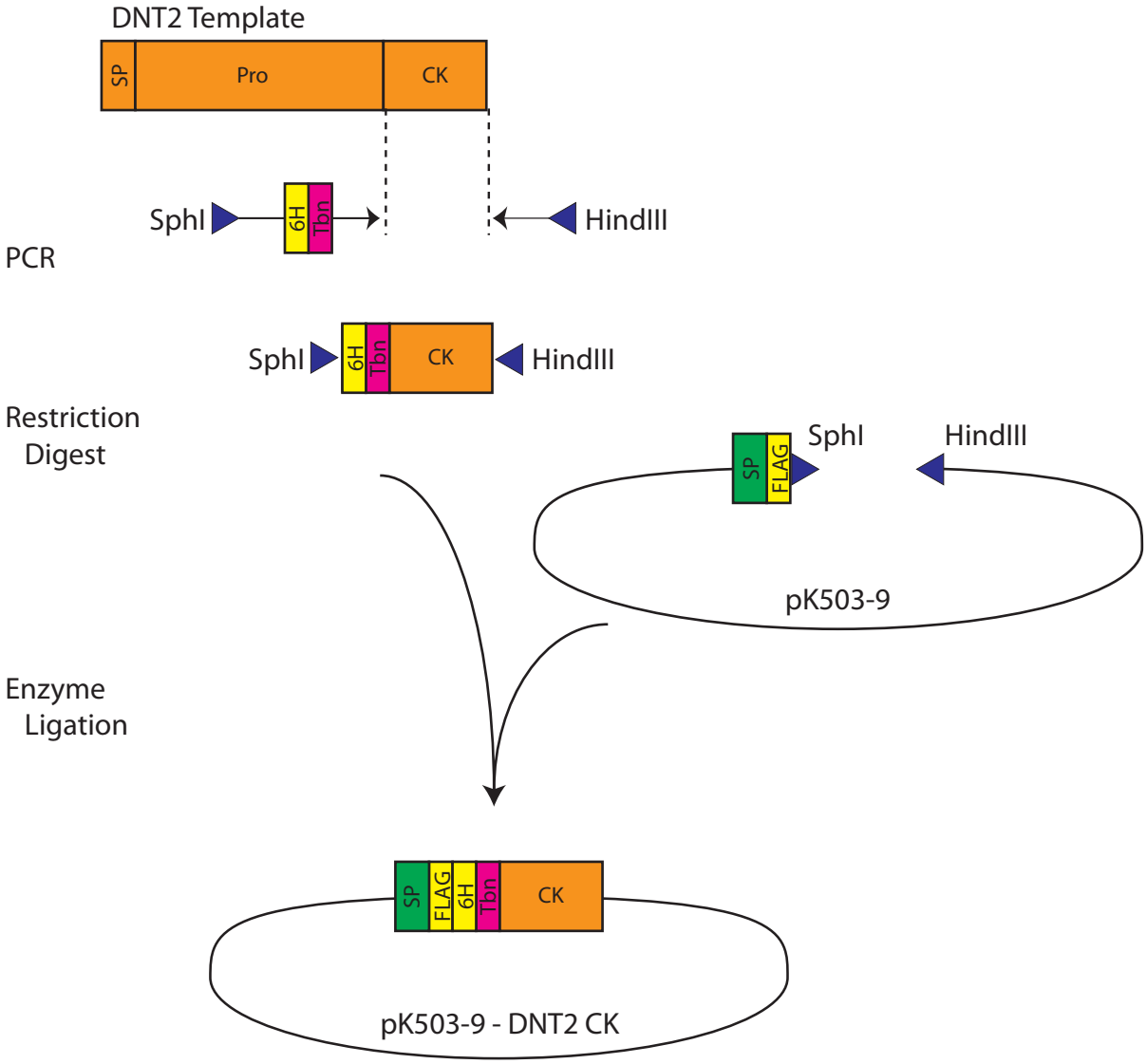

DNT2 CK was amplified by PCR from a cDNA template, with 6His, Thrombin (Tbn) and restriction enzyme sequences included in the primers. The insert and the vector were cut by restriction digest, and the insert was ligated in with T4 Ligase. Triangles indicate restriction enzyme sites.

Fig 2.27 - Identification of DNT2 CK clone

A

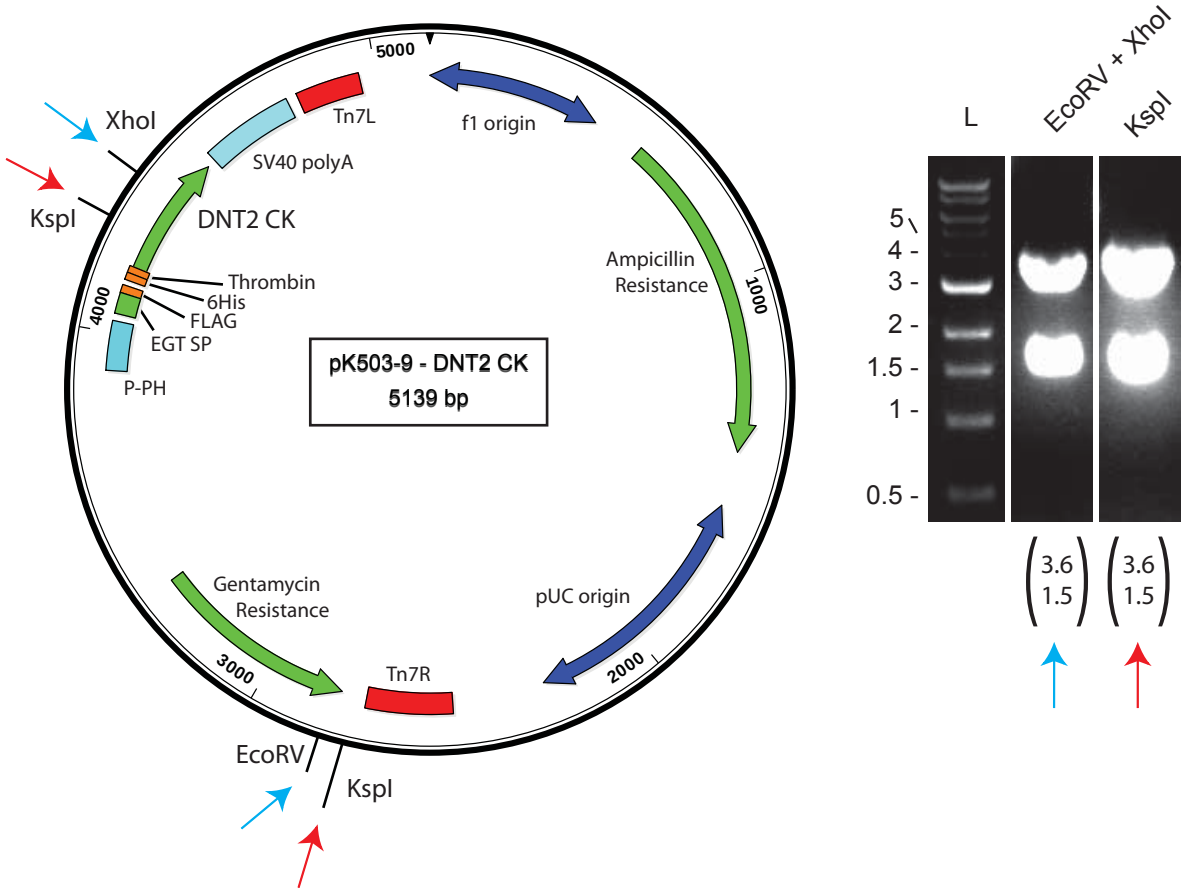

(A) Restricition digests were used to identify the correct clone. Enzyme sites are shown on the map, DNA fragments are shown on the right. Predicted sizes are given below each lane. (B, opposite) The sequenced gene region, compared to predicted sequence. Protein domains, epitope tags and protease recognition sequences are indicated.

Fig 2.27B – Sequence of cloned DNT2 CK

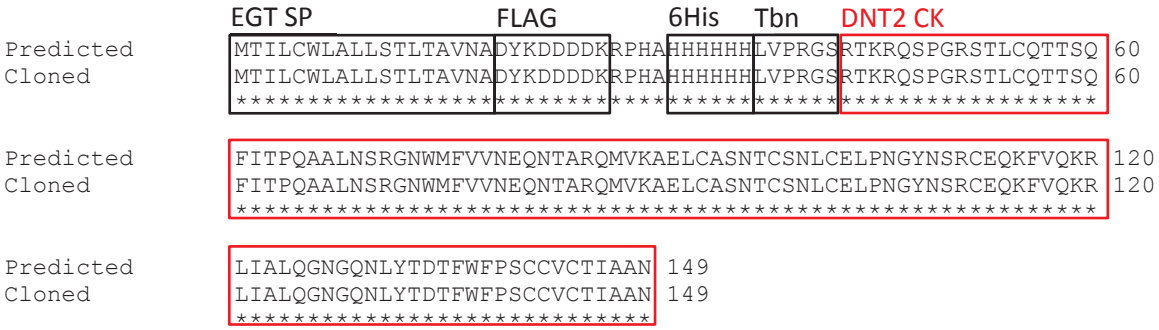

Fig 2.28 - Cloning strategy for full-length DNT2

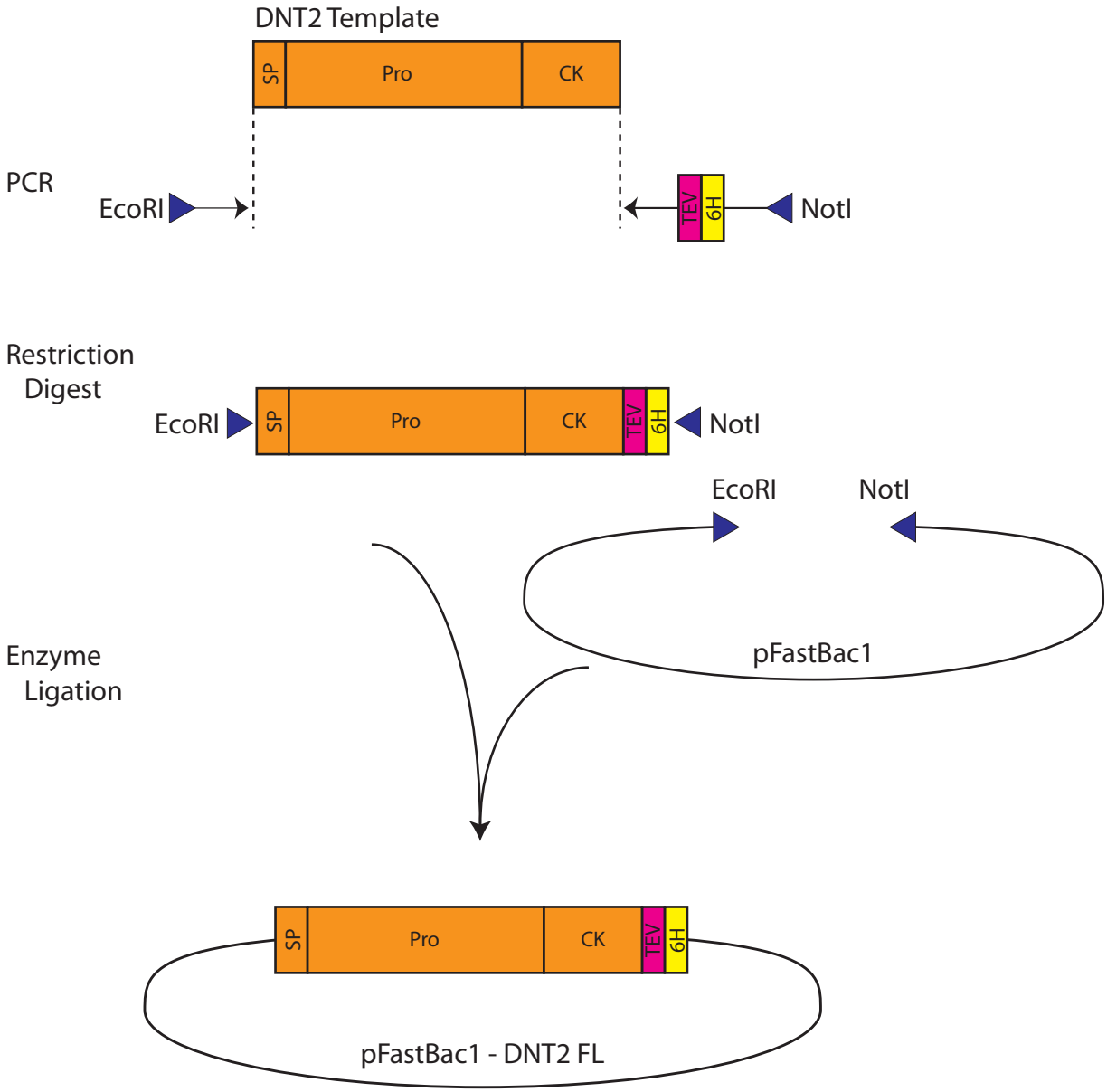

Full-length DNT2 was amplified by PCR from a cDNA template, with 6His, TEV and restriction enzyme sequences included in the primers. The insert and the vector were cut by restriction digest, and the insert was ligated in with T4 Ligase. Triangles indicate restriction enzyme sites.

Fig 2.29 - Identification of full-length DNT2 clone

A

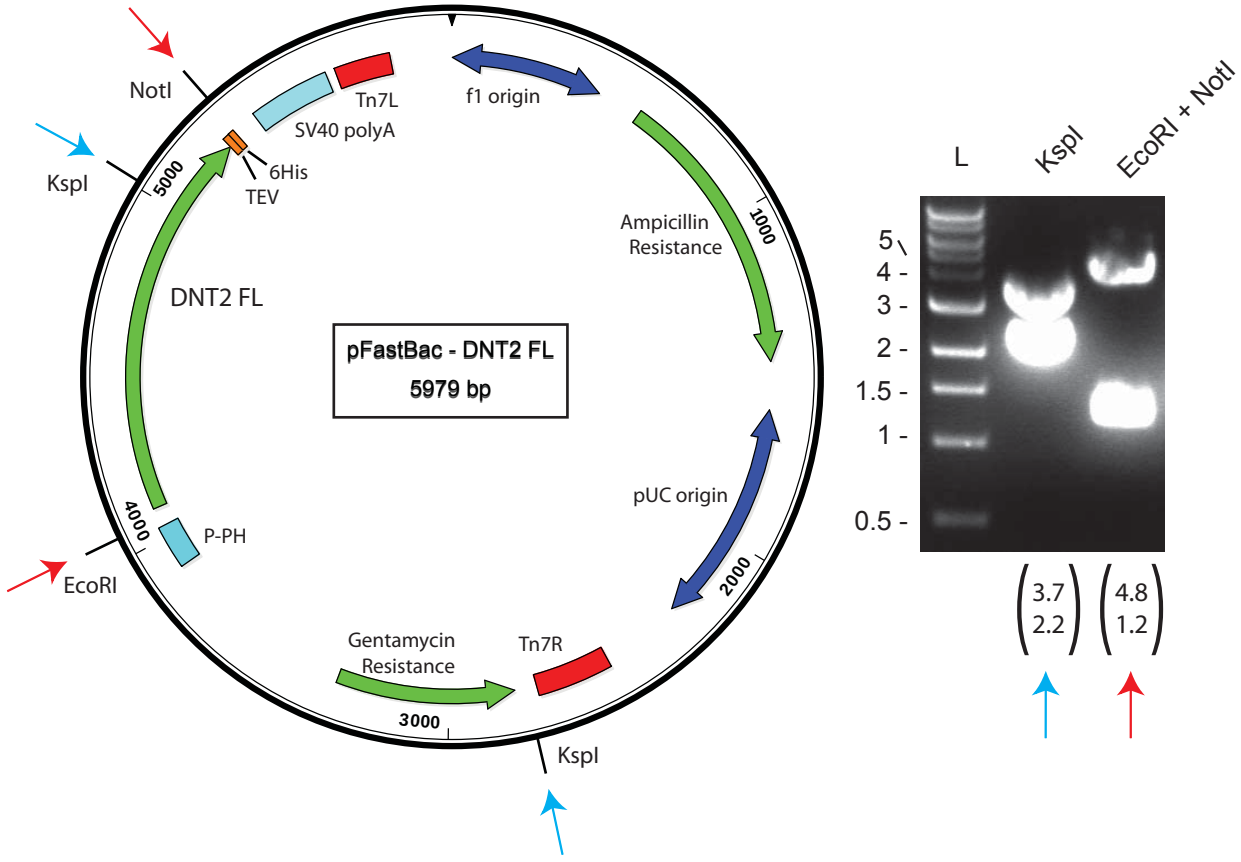

(A) Restricition digests were used to identify the correct clone. Enzyme sites are shown on the map, DNA fragments are shown on the right. Predicted sizes are given below each lane. (B, opposite) The sequenced gene region, compared to predicted sequence. Protein domains, epitope tags and protease recognition sequences are indicated.

Fig 2.29B – Sequence of cloned full-length DNT2

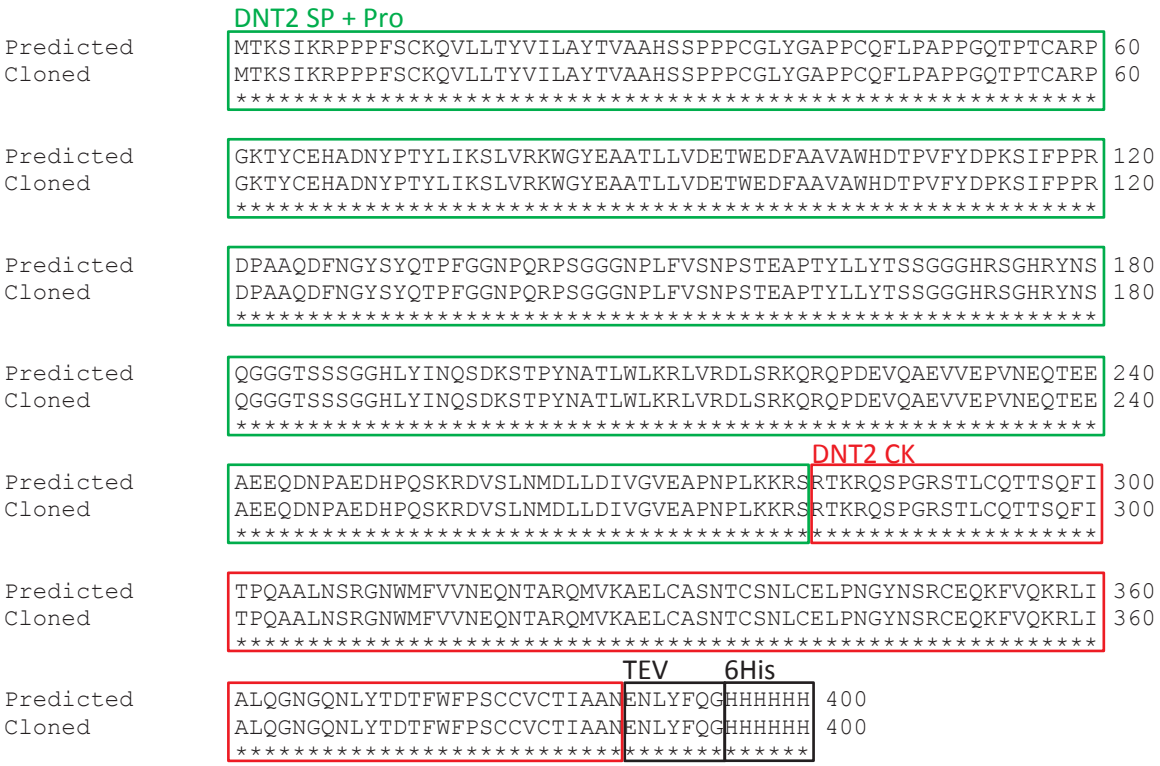

Fig 2.30 - Cloning strategy for DNT2 for S2 cell expression

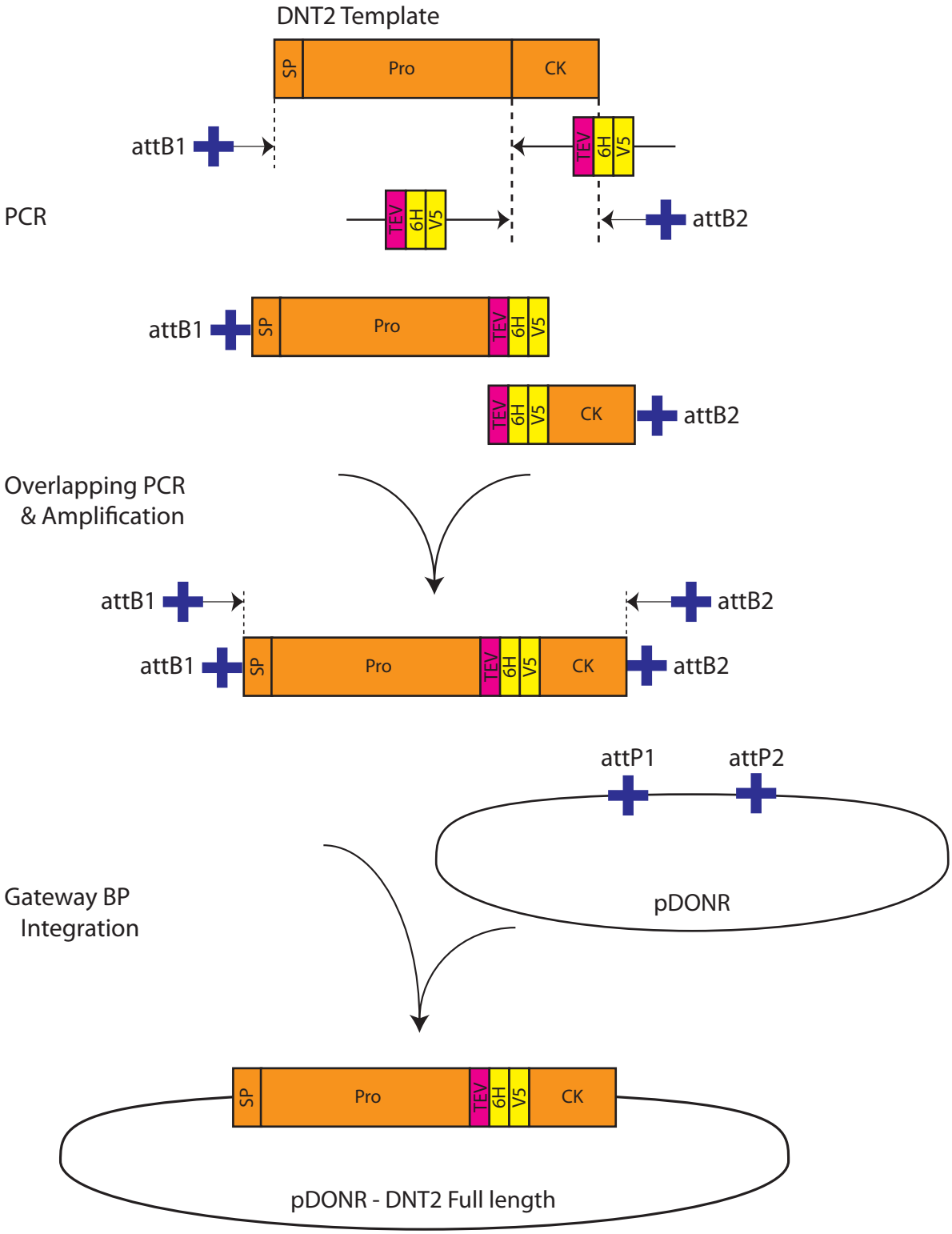

DNT2 signal peptide + pro-domain was amplified by PCR, as was the CK region, from cDNA. TEV cleavage, 6His, V5 and Gateway attB cloning sequences were included in the primers. The two fragments were ligated by PCR, and amplified as a whole. The complete insert was then cloned into DONR using the Gateway system. Crosses indicate Gateway cloning sequences.

Fig 2.31 - Identification of DNT2 clone for S2 expression

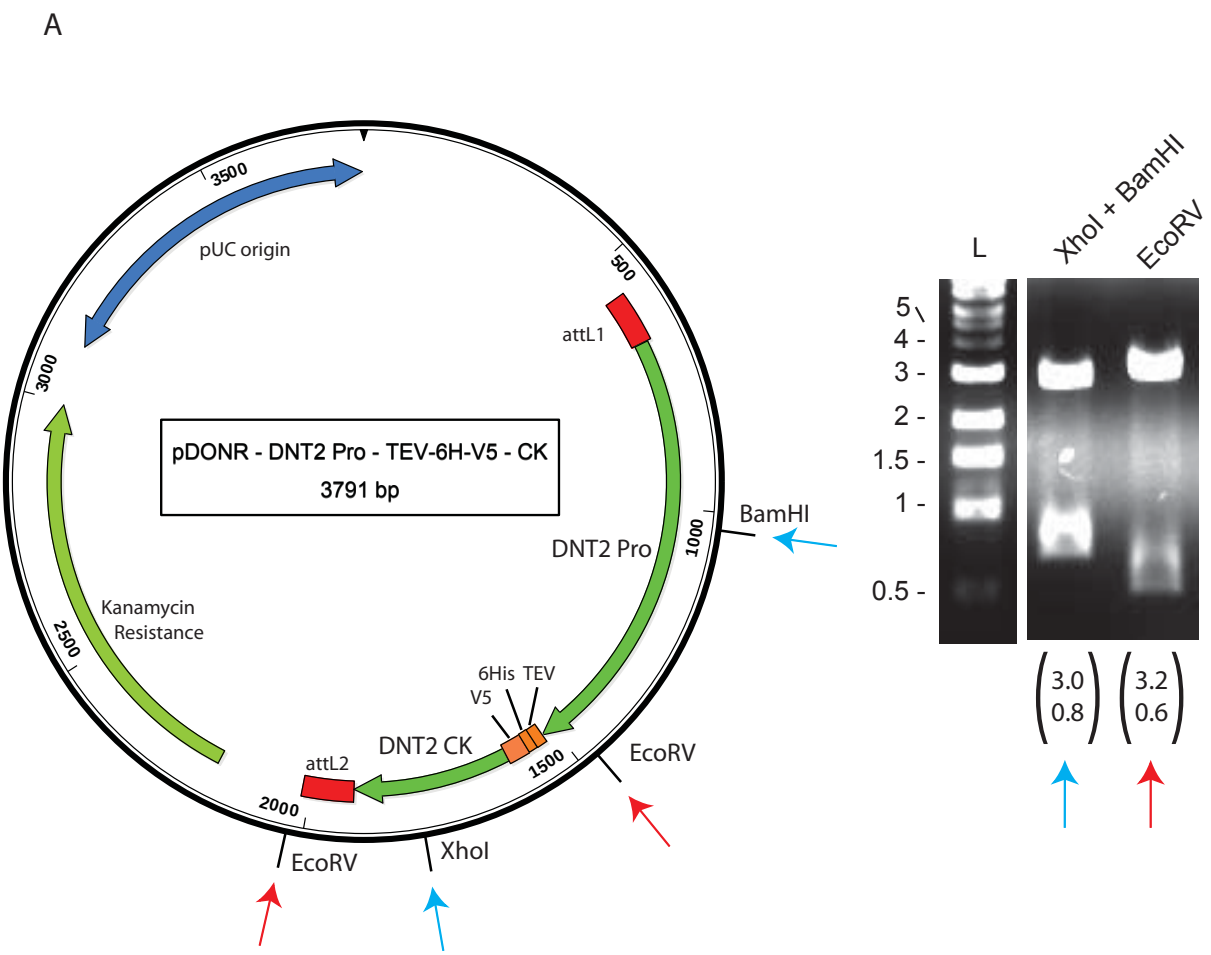

(A) Restricition digests were used to identify the correct clone. Enzyme sites are shown on the map, DNA fragments are shown on the right. Predicted sizes are given below each lane. (B, opposite) The sequenced gene region, compared to predicted sequence. Protein domains, epitope tags and protease recognition sequences are indicated.

Fig 2.31B – Sequence of cloned DNT2 for S2 cell expression

600µl transfection mix was gently added. The transfection was incubated at 27°C for 4 hours, after which the transfection mix was replaced with complete medium.

2.3.3 Luciferase reporter assay

Luciferase reporters were used to test the activation of *Drosophila* NFκB homologues, Dorsal and Dif. To test for Dorsal, a *snail-Luciferase* reporter construct was transiently transfected into S2 cells (a gift from Prof Albert Courey, UCLA) (Ratnaparkhi et al., 2008). Dorsal cDNA was also added to cells expressing the *snail-Luciferase* reporter to augment the signal (a gift from A Courey) (Chen et al., 1999, Ratnaparkhi et al., 2008). S2 cells stably transfected with *Drosomycin-Luciferase* were used to assay Dif activation. In all luciferase experiments, pAct-Renilla was co-transfected (a gift from Dr Saverio Brogna, University of Birmingham). This served as an internal control for cell number and transfection efficiency. Cells were transfected and treated according to the experimental conditions (see Chapter 6). Because they grew at a lower density than standard S2 cells, *Drosomycin-Luciferase* cells were pelleted from a 2ml culture and re-suspended in 400µl medium immediately before the Luciferase assay was performed. To determine the amount of Luciferase reporter present in the cells, and therefore the activity of NFκB, the Dual-Glo Luciferase Assay System (Promega) was used. 50µl of cell suspension was transferred in triplicate to an opaque 96-well plate. 40µl of the supplied Firefly Luciferase Substrate was added, incubated for 10 minutes at room temperature, and luminescence was measured using a SPECTRAFluro Plus (Tecan). 40µl Stop & Glo substrate was then added, which quenched the activity of Firefly Luciferase and served as the substrate for the control Renilla Luciferase. The plate was incubated at room temperature for 10 minutes before luminescence was measured. The relative Luciferase

activity was determined by dividing the Firefly measurement by the Renilla measurement for each well. All experiments were repeated at least three times in triplicate.

2.4 Protein biochemistry

2.4.1 Protein purification from Baculovirus

Protein purification from Baculovirus was carried out in collaboration with Dr Jukka Aurikko and Prof Nick Gay, Department of Biochemistry, University of Cambridge. Large-scale production of DNT protein was produced in insect cells using Baculovirus constructs described in Table 2.2, transferred to Bacmid DNA as described in Section 2.2.6. For each construct, 1l Sf9 insect cells (Invitrogen) were cultured in Sf900 II serum-free medium (Invitrogen), supplemented with 1x Penicillin/Streptomycin mix (Invitrogen) and 0.1% Pluronic F-68 (Invitrogen) to reduce shearing forces. Cells were cultured shaking at 120rpm, 28°C. Once the cells reached a density of $1x10^6$/ml, Baculovirus was added, and the cells were cultured further until the protein was ready to be harvested. The multiple of infection (MOI) and the length of culture time were according to the optimal conditions determined from samples obtained from the Baculovirus Facility, Department of Biochemistry, University of Cambridge (see Chapter 6). At the end of the culture period, cells were separated from the supernatant by centrifugation at 6000rpm, 4°C, for 15 minutes. The supernatant was then filtered to 0.2μm using a Sartobran P Capsule (Sartorius).

The filtered cell supernatant contained salts that would interfere with Ni-NTA affinity purification, so the solution was buffer-exchanged using a Centramate Tangential Flow Filtration System (Pall) into a final volume of 400ml PBS, 20mM imidazole (Sigma). The His-tagged DNT proteins were purified from the buffer-exchanged solution using 2ml

NiNTA-Agarose beads (Qiagen), incubating at room temperature, rolling for 1 hour. The beads were collected using the supplied column and washed twice with PBS, 350mM NaCl, 25mM imidazole. Protein was eluted in 2ml PBS, 500mM imidazole. To remove the imidazole, the protein was dialysed overnight at 4°C into PBS with a Spectra/Por MWCO 3500 (Spectrum) membrane. Protein concentration was measured using the Bradford assay: 10µl protein solution, 790µl water and 200µl BioRad Protein Assay Reagent were mixed, and absorbance at 595nm was recorded using a BioPhotometer (Eppendorf).

2.4.2 Protein purification from S2 cells

Small-scale quantities of DNT protein were produced using S2 cells cultured in 6-well plates, according to a protocol developed by Dr Chris Arnot and Prof Nick Gay, Department of Biochemistry, University of Cambridge. An entire 6-well plate was transfected with the relevant pActin-DNT plasmid (Table 2.2), and incubated for 36 hours following the addition of complete medium after transfection. The cell supernatant was separated from the cells by centrifugation at 5000rpm for 5 mins, was filtered to 0.2µm (Acrodisc, Pall), and was buffer-exchanged to PBS, 20mM imidazole using a Vivaspin6 5000MWCO Concentrator (Sartorius) at 4°C. His-tagged protein was purified from the solution using NiNTA spin columns (Qiagen). The columns were equilibrated to PBS, 10mM imidazole, and the protein was bound by centrifuging at 1000rpm. The column was washed twice in PBS, 20mM imidazole, 350mM NaCl, and the DNT protein was eluted into 600µl PBS, 500mM imidazole. Purified protein was buffer-exchanged to PBS using a Vivaspin6 5000MWCO concentrator.

2.4.3 SDS-PAGE

Protein samples were prepared by boiling at 100°C for 5 minutes in SDS loading buffer (100mM Tris pH 6.8, 4% SDS, 20% glycerol, 1 granule bromophenol blue (Sigma), 5% β-mercaptoethanol (Sigma), in water), chilling on ice for 2 minutes, then centrifuging for 3 minutes at 13000rpm. Samples were loaded into a 5% stacking gel (5% acrylamide (29:1) mix (National Diagnostics), 125mM Tris pH6.8, 0.1% SDS, 0.1% ammonium persulfate (National Diagnostics), 0.1% TEMED (Sigma)). Protein samples were run through a 12% resolving gel (12% acrylamide mix, 375mM Tris pH8.8, 0.1% SDS, 0.1% ammonium persulfate, 0.04% TEMED). The Prestained Protein Marker, Broad Range (NEB) or the Precision Plus Protein Prestained Standards (BioRad) were used as molecular weight markers on protein gels. Gels were run on at 100V, until the dye front reached the end of the gel. Gels were made and run using the mini-PROTEAN 3 system (BioRad). To identify protein bands, gels were stained with SimplyBlue SafeStain (Invitrogen) according to instructions.

2.4.4 Edman (N-terminal) sequencing

Edman degeneration was used to determine the N-terminal sequences of proteins. Proteins were blotted from unstained protein gels onto PVDF membranes (GE Healthcare) pre-soaked in methanol. Blotting took place in an Xcell SureLock Mini-Cell (Invitrogen) at 30V for 1 hour. The PVDF membrane was briefly stained with 0.1% Coomassie Blue R, 50% methanol in water, then destained in 10% acetic acid and 50% methanol. Stained membranes were given to the Protein and Nucleic Acid Chemistry (PNAC) facility at the Department of Biochemistry, University of Cambridge. The facility then returned the amino acid sequence found at the N-terminal of blotted proteins.

2.4.5 Western blot

Proteins were transferred from poly-acrylamide gels onto a nitrocellulose membrane using an Xcell SureLock Mini-Cell at 30V for 1 hour. Membranes were then blocked for 1 hour in blocking solution (5% non-fat milk powder, 0.05% Tween-20 (Sigma) in PBS) at room temperature. Primary antibodies (Table 2.10) were diluted in blocking solution, and incubated with the membrane overnight at 4°C. After washing 3x10 minutes in PBS, 0.05% Tween-20, HRP-conjugated secondary antibody was diluted in blocking solution and incubated for 2 hours at room temperature (Table 2.10). Secondary antibody then was washed 3 x 10 minutes with PBS + 0.05% Tween-20. Chemiluminescence was detected by mixing equal volumes of SuperSignal West Pico (Thermo) Substrate and Enhancer, and adding it to the membrane. After 5 minutes, luminescence was detected either using Amersham Hyperfilm ECL (GE Healthcare) autoradiography, or with the G:BOX Chemi (Syngene) and GeneSnap software.

2.4.6 Trypsin proteolysis

Trypsin proteolysis was done in collaboration with J Aurikko. Trypsin was used to cleave and degrade the DNT2 pro-domain, leaving the Cys-knot intact. The concentration of DNT2 was determined (see above), and a 1:100 dilution of Trypsin (Promega) was added to the protein solution. Proteolysis took place at 37°C for 30 minutes. DNT2 protein was re-purified from the proteolysis reaction using NiNTA-agarose (see above).

2.4.7 Fast Protein Liquid Chromatography (FPLC)

FPLC was carried out in collaboration with J Aurikko. DNT2 protein was purified using FPLC with size exclusion. The sample of DNT2 purified by NiNTA affinity was loaded onto a HighLoad 16/60 Superdex 200 column (GE Healthcare) after overnight equilibration with

Table 2.10 – Antibodies

Antibody	Donor	Dilution	Use	Source	Catalogue Number
Primary Antibodies					
anti-GFP	Rabbit	1:1000	Immunohistochemistry	Invitrogen	A11122
anti-FasII	Mouse	1:4	Immunohistochemistry	Developmental Studies Hybridoma Bank	1D4
anti-cleaved Caspase-3	Rabbit	1:50	Immunohistochemistry	Cell Signaling	#9661
anti-active Caspase-3	Rabbit	1:250	Immunohistochemistry	Abcam	Ab13847
anti-β-Gal	Mouse	1:750	Immunohistochemistry	Sigma	G4644
anti-His tag	Mouse	1:4000	Western Blot	BD Pharmingen	552565
anti-V5 tag	Mouse	1:5000	Western Blot	Invitrogen	46-0705
anti-HA tag	Mouse	1:100	Immunocytochemistry	Roche	12CA5
anti-Dorsal	Mouse	1:100	Immunocytochemistry	Developmental Studies Hybridoma Bank	7A4
anti-DIG AP-conjugated	Sheep	1:1000	In Situ Hybridisation	Roche	11093274910
Secondary Antibodies					
anti-Rabbit-Alexa488		1:250	Immunohistochemistry	Invitrogen	
anti-Mouse-Alexa488		1:250	Immunocytochemistry	Invitrogen	
anti-Mouse-Alexa546		1:250	Immunohistochemistry	Invitrogen	
anti-Mouse-Alexa647		1:250	Immunocytochemistry	Invitrogen	
anti-Mouse-Biotin		1:300	Immunohistochemistry	Vector Laboratories	
anti-Rabbit-Biotin		1:300	Immunohistochemistry	Vector Laboratories	
anti-Mouse-HRP		1:5000	Western Blot	Vector Laboratories	

PBS. Proteins were eluted according to size (largest proteins first) and detected by UV absorbance at 280nm using an Äkta FPLC (GE Healthcare), eluting with PBS at a flow rate of 1ml/min. 1ml fraction samples were analysed by SDS-PAGE and Coomassie staining.

2.5 Immunohistochemistry and immunocytochemistry

2.5.1 Fixation

Drosophila embryos, larval and adult brains, and S2 cells were fixed prior to immunostaining. To collect samples from all embryonic stages, embryos were collected on grape juice agar plates for 17 hours at 25°C. Embryos were rinsed in water, dechorionated in a 16% sodium hypochlorite solution, and washed thoroughly in water. Embryos were fixed in 3ml 4% formaldehyde (Sigma) in PBS, plus 3ml Heptane, for 20 minutes at room temperature. The formaldehyde was replaced with methanol, and the embryos were devitillinised by gently vortexing for 30 seconds. The fixed embryos were washed several times in methanol, and stored at -20°C.

Wandering larvae were collected, and anaesthetised in ice-cold PBS. Adult flies older than one day were collected under CO_2, briefly rinsed in ethanol, and transferred to ice-cold PBS. For 20 minutes, larval and adult brains were dissected in cold PBS and transferred immediately to 250µl 4% formaldehyde in PEM (0.1M PIPES, 2mM EGTA, 1mM $MgSO_4$ in water). After 20 minutes, the accumulated brains were transferred to a fresh 250µl of 4% formaldehyde, and fixed for 50 minutes at room temperature. Samples were rinsed twice in PBS, 0.3% Triton-X-100, then washed twice in PBS, 0.3% Triton-X-100 for 10 minutes. Samples were blocked for 1 hour in PBS, 0.3% Triton-X-100, 10% Normal Goat Serum

(S1000, Vector Labs, containing 0.08% sodium azide). Samples were stored in blocking solution at 4°C.

When used for immunocytochemistry, S2 cells were transfected and cultured on pre-boiled glass coverslips (VWR) in a 6-well plate. Before fixing, the culture medium was removed, and cells were washed with cold PBS, 0.1% Tween-20 for 5 minutes. Cells were fixed with 4% formaldehyde in PBS for 15 minutes at room temperature, washed in PBS, and finally blocked in PBS, 4% BSA (Sigma).

2.5.2 Immunolabelling

For detection of *D42*- and *Toll-7-Gal4*-driven GFP, and for FasII, embryos were stained with antibodies, and labelling was developed with HRP. Embryos were re-hydrated in PBS + 0.1% Triton-X-100 (PBTx) over 1 hour. Primary antibodies were added in PBTx (Table 2.10), and incubated overnight at 4°C. Primary antibody was removed, and embryos were washed 6 x 10 minutes in PBTx. The appropriate biotinylated secondary antibody was added, and incubated for 2 hours at room temperature (Table 2.10). Secondary antibody was removed, and the embryos were washed 6 x 10 minutes in PBTx. Samples were then incubated for 30 minutes with Vecastain ABC reagent (Vector Labs), comprising 5µl Solution A, 5µl Solution B in 990µl PBS. The ABC reagent was removed, and embryos were washed 6 x 10 minutes in PBTx. Embryos were transferred to a 24-well plate, and the PBTx was replaced with 300µl Diaminobenzidine (DAB) solution (Sigma, 1 tablet in 1ml PBTx). To develop the staining, 3µl of a 3% hydrogen peroxide solution was added (Sigma), and the embryos were observed for the emergence of the staining pattern. When required, 5µl of an 8% $NiCl_2$ (Sigma) solution was added, to result in a black staining. The reaction was stopped with thorough washing with PBTx. For double labellings, the process was repeated, allowing the second

reaction to develop in the absence of $NiCl_2$ (brown). Stained embryos were incubated overnight in 50% glycerol in PBTx at 4°C, transferred to 70% glycerol, and stored at 4°C. Embryos were mounted in 70% glycerol.

For detection of antigens with confocal microscopy, embryos, larval and adult brains, and S2 cells were fluorescently labelled. Embryos were re-hydrated as above. All samples were incubated overnight in the appropriate primary antibody at 4°C (Table 2.10). Primary antibody was removed, and samples were washed 6 x 10 minutes in PBTx. Fluorescently-labelled secondary antibody was added, and from this point onwards, samples were kept in the dark. Embryos were incubated in secondary antibody for 2 hours at room temperature, larval and adult brains overnight at 4°C (Table 2.10). Secondary antibody was removed, and samples were washed 6 x 10 minutes in PBTx. Finally, all PBTx was removed, and samples were stored in Vectashield mounting medium (Vector Labs) at 4°C. For staining with anti-cleaved Caspase-3, embryos were first blocked in 1% BSA in PBTx, and were then stained in multiple small aliquots, in 50µl volumes of primary antibody. Samples were then pooled for further staining with secondary antibody and second primary antibody if necessary. To ensure adequate fixing for Caspase samples, the formaldehyde was relatively new for each batch of experiments.

Coverslips of S2 cells were gently transferred to a sheet of Parafilm and placed in a humid chamber. 60µl of primary antibody was added to each coverslip, and the coverslips were incubated overnight on a platform rocker at 4°C. The primary antibody was washed from the cells by returning the coverslips to the 6-well plate, and adding PBTx 3 x 10 minutes. Coverslips were placed back in the humid chamber, and 60µl secondary antibody was added, and incubated in the dark, rocking for 2 hours at room temperature. Coverslips were again

washed 3 x 10 minutes, gently dried, and mounted onto slides with Vectashield + DAPI (Vector Labs).

2.5.3 *In situ* hybridisation

Anti-sense RNA probes were used for *in situ* hybridisation experiments. The pDONR vector includes a T7 RNA polymerase promoter, downstream of the cloning insertion site, therefore *Toll-7* and *Toll-6* entry clones were used as templates to make probes. Since both genes are intronless, the entry clones are cDNA (see Chapter 3). 10µg of pDONR entry clone was linearised by a restriction enzyme that cut in the 5' end of the c DNA: pDONR-Toll-7 was linearised with HindIII, pDONR-Toll-6 with SmaI, in 50µl water, including 5µl 10x restriction buffer and 2µl enzyme. Digestions were carried out overnight at 37°C. DNA was recovered with the phenol/chloroform method. 50µl of DNA was added to 50µl phenol (Sigma), 49µl chloroform (Fisher) and 1µl iso-amylalcohol (Fisher). The samples were vortexed, centrifuged for 5 minutes at 13000rpm, and the aqueous layer was kept. DNA was precipitated by adding 5µl 3M sodium acetate and 150µl ethanol, and chilling for 30 minutes at -80°C. DNA was pelleted at 13000rpm for 10 minutes, washed in 80% ethanol, and dissolved in 20µl water.

Probes were generated in 20µl transcription reactions, including 1µg template DNA, 2µl DIG RNA labelling mix (Roche), 2µl T7 RNA polymerase (USB), 2µl transcription buffer, 1µl RNasin (Promega) in water. The reaction was incubated at 37°C for 2 hours. Transcription was terminated with 1µl DNAse treatment at room temperature for 15 minutes, and inactivated at 65°C for 15 minutes. To purify the RNA probe, 2.5µl 4M LiCl, 0.25µl glycogen (Sigma), and 75µl ethanol were added, and RNA was precipitated overnight at -20°C. The probe was pelleted at 13000rpm for 15 minutes, washed with ethanol, air dried, and dissolved

in 50µl water with 1µl RNasin. Probes were stored at -20°C. Immediately before use, the required volume of probe was denatured at 95°C for 10 minutes and then placed in an ice/ethanol bath for 10 minutes.

Embryos, larval CNS and adult brain preps were fixed as above, except that the formaldehyde was replaced with a 4% paraformaldehyde (BDH) solution, dissolved in PBS. Embryos were gently re-hydrated into PBS, 0.1% Tween-20 (PBTw) over 1 hour, by washing for 15 minutes in 70%, 50%, 30% and 0% methanol in PBTw. All samples were further fixed for 30 minutes with 4% paraformaldehyde in PBTw, and washed 3 x 5 minutes in PBTw. Samples were treated with 125ng/ml Proteinase K in PBTw for 90 seconds at room temperature, and then rinsed twice with 0.2% glycine (Fisher) solution. Samples were then washed 2 x 5 minutes before being fixed again for 30 minutes with 4% paraformaldehyde, and washed again 5 x 5 minutes in PBTw. Samples were rinsed with 50% hybridisation buffer (HB: 50% formamide (MP Biomedicals), 5x SCC buffer, 0.1% Tween-20, 50µg/ml Heparin (Sigma), and 100µg/ml denatured salmon tested DNA (Sigma) in water) in PBTw, and then incubated in HB at 55°C for one hour. The probe was titrated at 1:100, 1:40 and 1:20 in HB at 55°C, added to the samples, and hybridisation proceeded overnight at 55°C. Samples were washed for 20 minutes in HB, then 50% HB in PBTw, then 5 x 20 minutes in PBTx, all at 55°C. Alkaline phosphatase (AP)-conjugated anti-DIG was pre-absorbed with the same tissue as the *in situ* hybridisation sample at a 1:100 dilution, rocking at room temperature for 1 hour, and added to the samples at a final dilution of 1:1000 in PBTw. Samples were incubated for 1 hour at room temperature, and then washed 4 x 20 minutes in PBTw. Samples were then washed 3 x 5 minutes in staining solution (SS: 100mM NaCl, 50mM MgCl, 100mM Tris pH9.5, 0.1% Tween-20). Samples were transferred to a 24-well plate, and developed with 500µl SS with 2.7µl 100mg/ml NBT and 2.1µl 50mg/ml BCIP. Once the samples were suitably developed,

they were washed thoroughly with PBTw, cleared overnight in 50% glycerol in PBTw at 4°C, and then stored in 70% glycerol at 4°C. Samples were mounted and imaged soon after developing.

2.6 Microscopy and imaging

Embryos, and larval and adult CNS samples stained with HRP or AP were mounted whole onto glass slides (VWR). Samples were examined using an Axioplan 2 light microscope (Zeiss) with a 20x lens and a 40x (oil) DIC lens, using Nomarski optics. Dissected embryo samples were also examined with a 63x (oil) DIC lens. Images were taken using a JVC 3CCD camera and Image Grabber software (NeoTech). All images were processed with Photoshop software (Adobe), and figures were compiled with Illustrator (Adobe).

Fluorescent images of larval and adult brains stained with anti-GFP were acquired using a Leica SP2 AOBS laser scanning confocal microscope using a 20x (oil) lens. Images of fixed and fluorescently labelled S2 cells were taken using the 63x (oil) lens on the Leica SP2, at 200Hz and 1024x1024 pixel resolution. Fluorescent images were processed in ImageJ software (NIH).

For apoptosis experiments, embryos stained with anti-cleaved Caspase-3 were scanned using a Radiance 2000 confocal microscope (BioRad). Embryos were oriented so that the ventral nerve cord was closest to the lens, and was horizontal in the centre of the field of view. A 60x (oil) lens was used, with 1.6x zoom, 166lps scanning speed and 512x512 pixel resolution. A 0.25μm z-axis step was used to produce cubic voxels ($0.25\mu m^3$). Gain was maintained at 52.5, offset -0.4 and iris 1.5. The laser power was minimally adjusted to ensure consistency between samples.

2.7 Phenotypic analysis

2.7.1 Adult locomotion

Locomotion phenotypes in adult flies were assessed using the assay developed by Dr Ben Sutcliffe, Dr Manual Forero and Dr Alicia Hidalgo in our Lab (Sutcliffe, 2010). All films were recorded at the same time of day (before 11am). Adult, male, 5-day old flies were collected under CO_2 anaesthesia, their wings were cut with micro scissors, and they were allowed to recover for at least 30 minutes. A petri dish (26mm high, 46mm diameter) was placed on a LP812 light box (Jessops), and a Moticam 2000 (Motic) with a 16mm lens was held 95 mm over the light box and dish. Video was captured with Motic MC Camera 1.1 and Motic Images Plus 2.0 ML software. Flies typically climbed onto the rim of the dish, and walked round and round, and were filmed for 1 minute. Using VirtualDub software (www.virtualdub.org), the first 400 frames were decompressed and saved in AVI format. Frames where the fly had left the arena were discarded. These films were converted to a stack of 400 greyscale TIFF images using ImageJ. The converted films were then processed with the FlyTracker plug-in for ImageJ, developed by M Forero, a modification of the Mtrack2 plug-in from Dr Nico Stuurman, UCSF. Running the program produces a plotted trajectory of the fly's path, a stack of 400 images with the fly's coordinates given for each frame, and a spread sheet giving the fly's speed and distance travelled between frames. By inserting additional formulae, the direct (averaged) distance was determined, as well as the proportion of time the fly was at rest and the speed at which it travelled when moving (Sutcliffe, 2010). A fly was determined to be at rest if it travelled more slowly than 1.5mm/second in any frame.

2.7.2 Axon guidance

Fixed, late stage 17 embryos were stained with anti-FasciclinII (FasII) and examined by light microscopy, to visualise developing motor axons (see above). The ISNb nerve branch was examined in the first 5 abdominal segments (A1-A5) on each side of the embryo. Axonal projections were scored three times for the existence of any targeting phenotype. Because the variability in axon projections was often subtle, and scoring proficiency improved over time, the frequencies obtained on the third time of scoring were used.

2.7.3 Automatic quantification of apoptotic cells

Stacks of confocal images of anti-Caspase 3-labelled embryos were processed using the DeadEasy Caspase plug-in for ImageJ, developed in our lab by Dr Manuel Forero (Forero et al., 2009). DeadEasy Caspase produced a parallel stack to the raw data, with identified cells. The processed stack was compared to the original images, to ensure that cells had been accurately counted, that the background was not producing false positive results, and to identify where signal in the epidermis, axons and gut was affecting the cell count. Identified cells that were not within the ventral nerve cord were excluded by creating a region of interest (ROI) to include only the CNS nerve cord. To remove false positives arising in the epidermis and gut, the ventral-most and dorsal-most slices were processed separately, and areas of non-neuronal signal were manually blacked out before running DeadEasy Caspase. To remove false positives arising from axons, the identified 'cells' in the processed stack were blacked-out, using the Fill tool on ImageJ. The remaining cells were re-counted using the DeadEasy Background Correction tool, devised by M Forero. Finally, labelled dMP2 cells were subtracted, since they are subject to cell-autonomous programmed cell death in stage 17

embryos (Miguel-Aliaga and Thor, 2004). These were identified as large paired cells located close to the midline, in the dorsal cortex of the ventral nerve cord.

2.8 Statistical analysis

Data were collated and analysed using Excel (Microsoft), and statistical tests were carried out using PASW Statistics 18 (IBM). The null hypothesis was for all cases that there was no difference between experimental samples and controls. Data for lethality, axon targeting, and Dorsal localisation were categorical, therefore χ^2 tests were performed. Continuous numerical data were obtained from apoptosis and luciferase assays, and tested for normality, using the shape of the distribution, skewedness and kurtosis. A one-way ANOVA was performed on the data, and a Student's t-test (independent samples, 2 tails) was used for pair-wise comparisons.

CHAPTER 3
TOLL-7 AND *TOLL-6* ARE EXPRESSED IN THE *DROSOPHILA* NERVOUS SYSTEM

3.1 Introduction

In order to characterise the functions of Toll-7 and Toll-6, and to test whether they can serve as DNT receptors, it was crucial to investigate first where the genes are expressed. The aims of this chapter were to determine the expression patterns of *Toll-7* and *Toll-6* by *in situ* hybridisation and by driving GFP expression in *Toll-7*- and *Toll-6*-expressing cells using the Gal4 system. To make RNA probes for *in situ* hybridisation, it was first necessary to generate cDNA clones; to drive GFP expression, suitable Gal4 lines needed to be obtained.

It has been reported previously that *Toll-7* and *Toll-6* are the only paralogues (other than *Toll*) with expression in the embryonic nervous system (Kambris et al., 2002). However, whether expression persists in the larva and adult is unknown.

Neurotrophins are target-derived signalling molecules that act on neurons (Bibel and Barde, 2000). Accordingly, vertebrate neurotrophin expression is found in organs receiving innervation, including the heart, epidermis, muscle and liver (Maisonpierre et al., 1990a). Vertebrate neurotrophin receptors are primarily expressed in neurons, although they can also be detected in non-neuronal tissues, including muscle, the heart and the kidneys, and in a wide range of immune cells (Shelton et al., 1995, Vega et al., 2003).

DNT1 and *DNT2* are expressed in the central nervous system, epidermis and muscle (Zhu et al., 2008, Sutcliffe et al., Submitted). For *Toll-7* and *Toll-6* to function as DNT receptors, they should show complementary patterns of expression.

3.2 Results

I have taken two approaches to describe the expression of *Toll-7* and *Toll-6*: *in situ* hybridisation of mRNA, and using GFP reporters. *In situ* hybridisation labelled the cell bodies expressing *Toll-7* and *Toll-6*. To generate the RNA probes, each of the cDNAs was cloned. To drive GFP in a *Toll-7* pattern, a *Toll-7-Gal4* line was made. To drive GFP expression in a *Toll-6* pattern, I made use of the published *D42-Gal4* line, which carries a Gal4 enhancer trap 7kb upstream of *Toll-6*, and has been previously published as a *Toll-6* reporter (Yeh et al., 1995, Sanyal, 2009).

3.2.1 Generation of *Toll-7* cDNA

The *Toll-7* gene is intronless (Fig 3.1A). It was therefore possible to amplify the full-length coding sequence directly from the genomic DNA by PCR. *Toll-7* coding DNA was amplified from the genomic DNA of *yw* flies, incorporating 5' attB1 and 3' attB2 sites for Gateway cloning (primers 7.8 and 7.9, Table 2.3, materials and methods). The DNA fragment was cloned into pDONR^{221} using Gateway BP Clonase, and the correct clone was identified by restriction digests: digestions by ApaI, and EcoRV (Fig 3.1B). To confirm the clone, the entire coding region was sequenced, and compared to the reference sequence obtained from FlyBase (FBgn0034476) (Fig 3.1C). The sequence revealed three mutations. The two point mutations identified were valine to isoleucine at position 251, and leucine to methionine at position 259. These are fairly conservative changes, and lie close together in the extracellular

domain of Toll-7. There is also a deletion of a glutamine residue close to the C-terminus of the protein. This falls within a short poly-glutamine tract (positions 1414-1426) reducing it from 13 to 12 consecutive glutamine residues. The PCR amplification of *Toll-7* was carried out multiple times, and the observed base pair changes were reasonably reproducible, compatible with naturally occurring polymorphisms. An antisense RNA probe was transcribed from pDONR-Toll-7 using the 3' T7 RNA Polymerase promoter sequence found in pDONR (see section 2.5.3, materials and methods). The *Toll-7* coding sequence was later transferred to pAct-gw-HA by LR gateway cloning. This resulted in an expression clone suitable for constitutive expression of Toll-7 in cultured cells under the actin promoter, and placed an HA tag at the C-terminal.

3.2.2 Generation of a *Toll-7-Gal4* reporter

Since no Gal4 line was available, to drive expression of GFP in a *Toll-7* pattern, it was necessary to generate a promoter-Gal4 fusion construct. To do this, the upstream regulatory DNA of *Toll-7* was cloned into pPTGAL, which contains the Gal4 coding sequence and P-element sequences for transgenesis (Sharma et al., 2002). Upstream of *Toll-7* is 10kb of intergenic DNA. Since this is too large for cloning and transgenesis, I amplified the 5kb immediately upstream of *Toll-7*'s start codon (Fig 3.2A). 5kb of intergenic DNA upstream of *Toll-7* was amplified from *yw* genomic DNA by PCR, incorporating 5' NotI and 3' BamHI restriction sites, using primers 7.15 and 7.14 (Table 2.3, materials and methods). After restriction digestion, the fragment was ligated into pPTGAL, placing it immediately upstream of the *Gal4* coding sequence. To identify the correct clone, restriction digests were carried out, with NotI and BamHI, and ScaI (Fig 3.2B). I sent the finished plasmid to BestGene Inc for transformation into *yw* flies. On receipt of transformed larvae, I mapped the chromosomal

Fig 3.1 - Toll-7 cDNA was cloned into pDONR

A

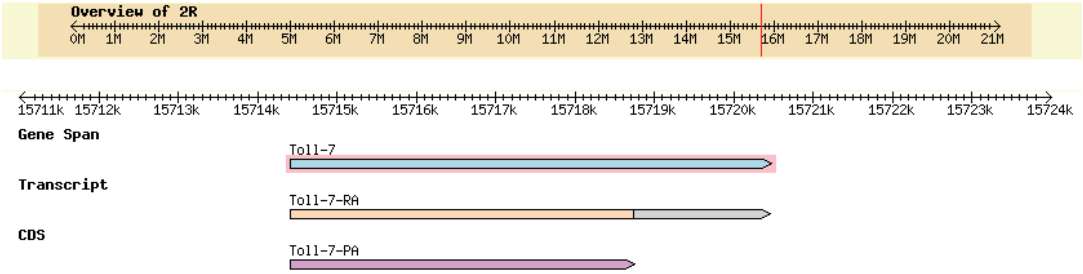

B

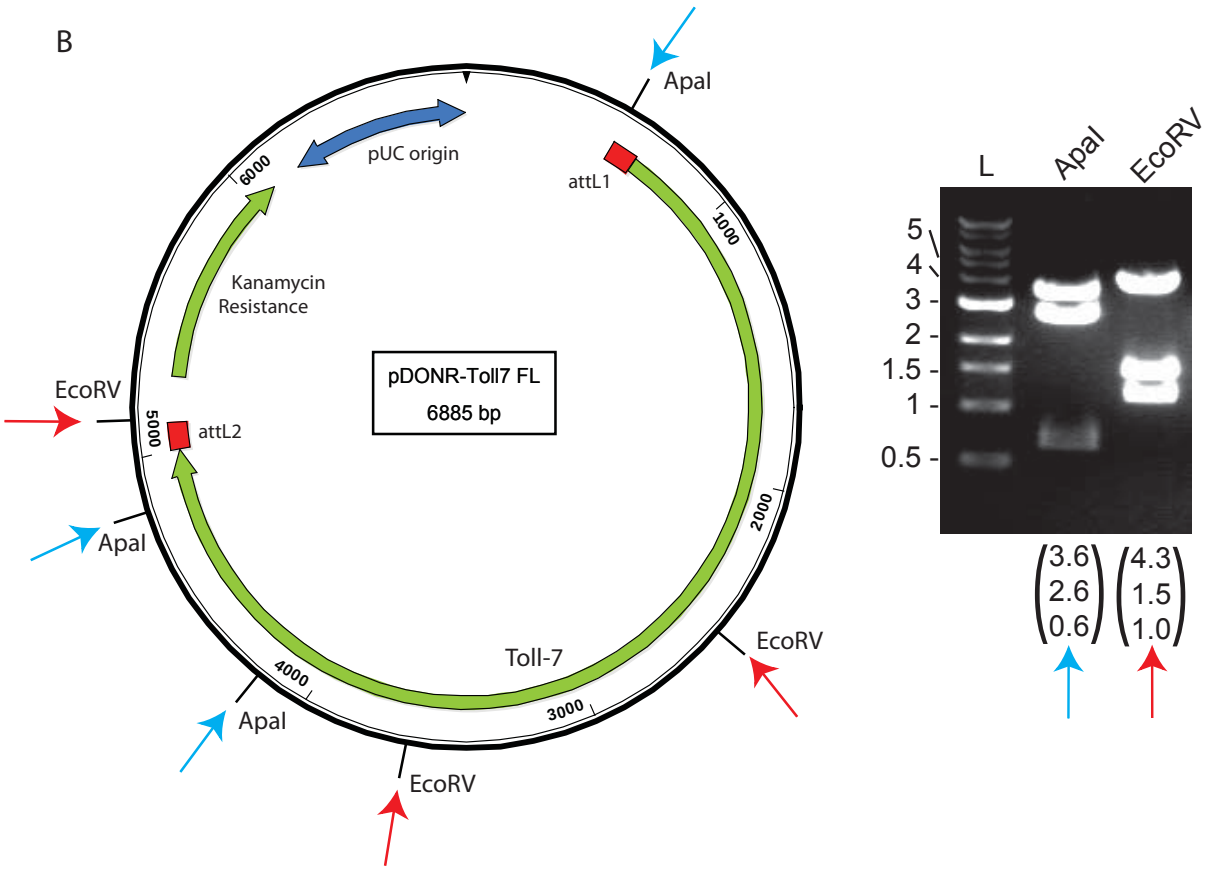

(A) The FlyBase map of the *Toll-7* locus indicated that the gene does not contain introns. (B) *Toll-7* was cloned into pDONR, and restriction digests were used to identify the correct clone. Enzyme sites are indicated on the map, DNA fragments are shown to the right. The predicted fragment sizes are given belpw each lane. (C, over) The sequenced gene region, compared to the predicted *Toll-7* sequence. Mutated residues are highlighted in red. Protein domains are given: Cysteine-rich clusters (CRC) lie C-terminal (CT) and N-terminal (NT) to Leucine-rich repeats (LRR).

Fig 3.1C – Sequence of cloned *Toll-7*

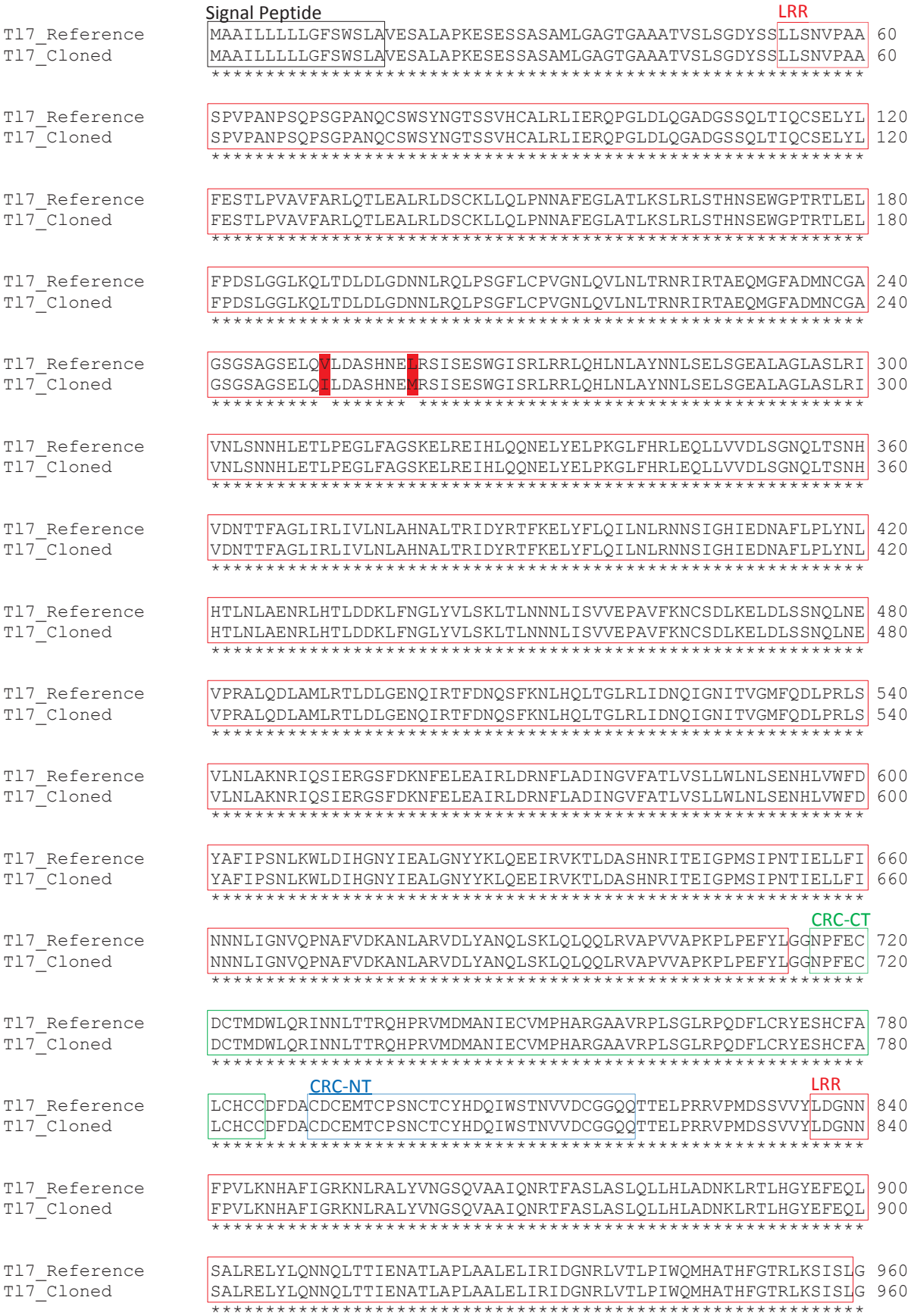


CRC-CT
Tl7_Reference RNQWSCRCQFLQALTSYVADNALIVQDAQDIYCMAASSGTGSAALEDSSSNSGSLEKREL 1020
Tl7_Cloned RNQWSCRCQFLQALTSYVADNALIVQDAQDIYCMAASSGTGSAALEDSSSNSGSLEKREL 1020
Transmembrane
Tl7_Reference DFNATGAACTDYYSGGSMLQHGIPESYIPLLAAALALLFLLVVIAMVFAFRESLRIWLFA 1080
Tl7_Cloned DFNATGAACTDYYSGGSMLQHGIPESYIPLLAAALALLFLLVVIAMVFAFRESLRIWLFA 1080
TIR
Tl7_Reference HYGVRVFGPRCEESEKLYDAVLLHSAKDSEFVCQHLAAQLETGRPPLRVCLQHRDLAHDA 1140
Tl7_Cloned HYGVRVFGPRCEESEKLYDAVLLHSAKDSEFVCQHLAAQLETGRPPLRVCLQHRDLAHDA 1140
Tl7_Reference THYQLLEATRVSRRVVILLTRNFLQTEWARCELRRSVHDALRGRPQKLVIIEEPEVAFEA 1200
Tl7_Cloned THYQLLEATRVSRRVVILLTRNFLQTEWARCELRRSVHDALRGRPQKLVIIEEPEVAFEA 1200
Tl7_Reference ESDIELLPYLKTSAVHRIRRSDRHFWEKLRYALPVDYPTFRGNNYTLELDHHNHERVKQP 1260
Tl7_Cloned ESDIELLPYLKTSAVHRIRRSDRHFWEKLRYALPVDYPTFRGNNYTLELDHHNHERVKQP 1260
Tl7_Reference ASPGLLYRQAPPPAYCGPADAVGIGAVPQVVPVNASVPAEQNYSTATTATPSPRPQRRGE 1320
Tl7_Cloned ASPGLLYRQAPPPAYCGPADAVGIGAVPQVVPVNASVPAEQNYSTATTATPSPRPQRRGE 1320
Tl7_Reference QPGSGSGGNHHLHAQYYQHHGMRPPSEHIYSSIDSDYSTLDNEQHMLMMPGAPGGLAMEA 1380
Tl7_Cloned QPGSGSGGNHHLHAQYYQHHGMRPPSEHIYSSIDSDYSTLDNEQHMLMMPGAPGGLAMEA 1380
Tl7_Reference AQRAQTWRPKREQLHLQQAQAGTLGSKASQAAHQQQQQQQQQQQQQPNPTAVSGQQQGPH 1440
Tl7_Cloned AQRAQTWRPKREQLHLQQAQAGTLGSKASQAAHQQQQQQQQQQQQ-PNPTAVSGQQQGPH 1439
Tl7_Reference VQAYLV 1446
Tl7_Cloned VQAYLV 1445

Fig 3.2 - Generation of Toll-7 Gal4 expression vector

A

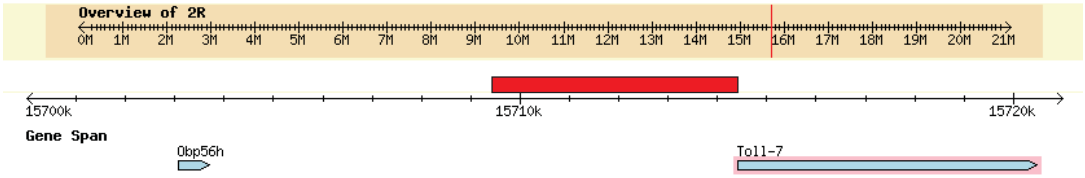

B

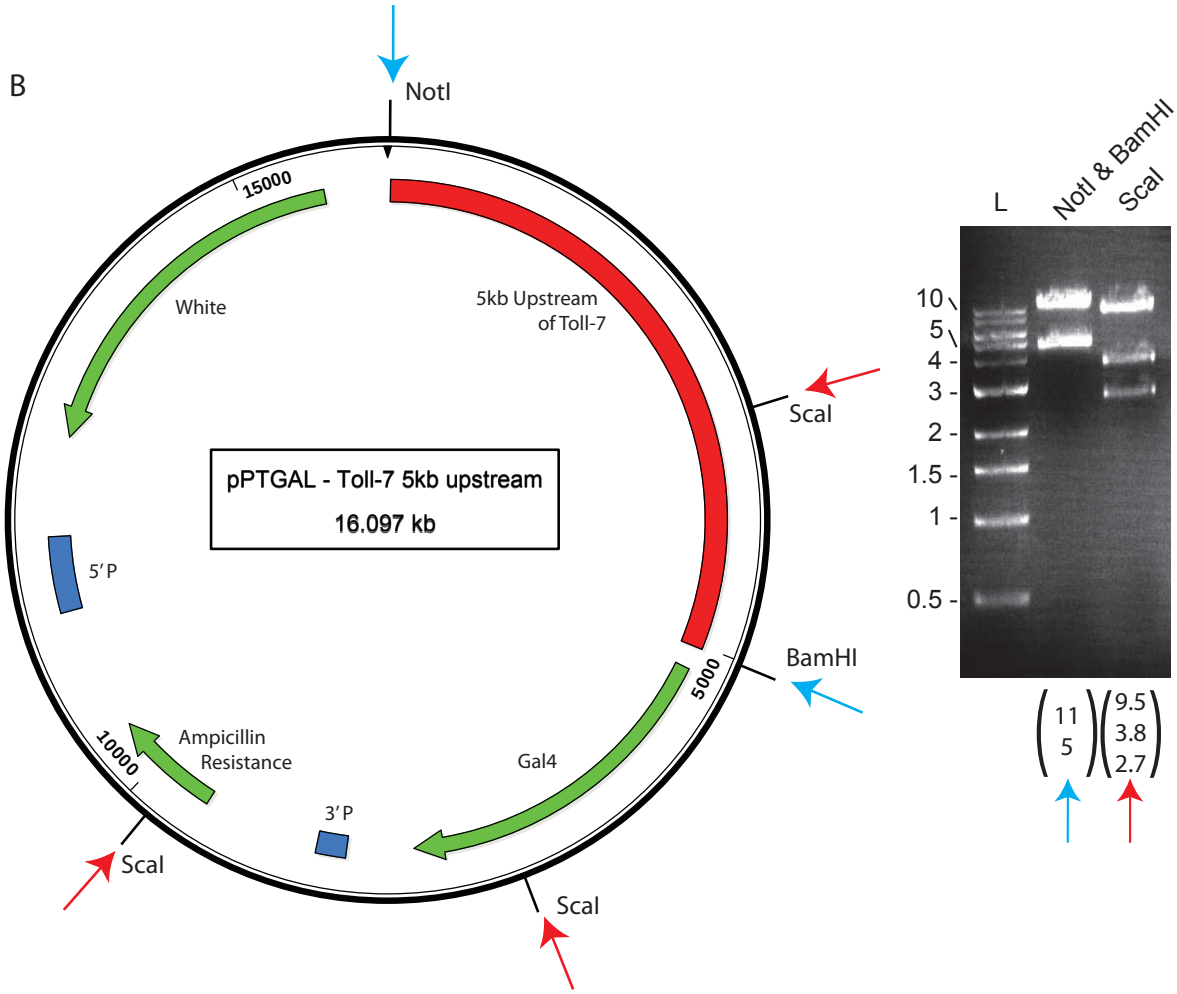

Toll-7-Gal4 expression clone. (A) The 5kb of upstream intergenic DNA cloned is indicated by the red bar. (B) Restriction digests were used to identify the correct clone. Enzyme sites are indicated on the map, DNA fragments are shown to the right. The predicted fragment sizes are given belpw each lane.

location of the transgene, established a balanced stock, and used the resultant line to drive GFP expression (using protocol G, see Fig 2.5 materials and methods).

3.2.3 *Toll-7* expression in the embryonic nervous system

To identify cells expressing *Toll-7* in embryos, *in situ* hybridisation was carried out. *Toll-7* mRNA was detected in the CNS of stage 13 embryos, in a segmentally repeating pattern (Fig 3.3A-B). At this stage, there was expression in stripes in the lateral epidermis (Fig 3.3C). In dissected stage 13 embryos, *Toll-7* was seen in the CNS, and also three bilateral clusters of cells in the thoracic region, which are the precursors of the leg imaginal discs (Fig 3.3D-F). The expression of *Toll-7* at stage 14 was similar to that at stage 13 (Fig 3.3G-K); and CNS cells at the midline were also detected (Fig 3.3L). At stage 15, *Toll-7* expression was seen in the CNS and in lateral epidermal stripes (Fig 3.4A-C). Dissected stage 15 embryos showed a CNS pattern of *Toll-7* expression, including in midline cells, as well as expression in the epidermis and leg imaginal disc precursors (Fig 3.4D-F). By stage 17, *Toll-7* expression was largely restricted to the CNS (Fig 3.4G-I). In late embryos, *Toll-7* mRNA was also detected in the denticles (Fig 3.4J).

I next examined the morphology of cells using the *Toll-7-Gal4* line to drive expression of GAP-GFP. In stage 13 embryos, clusters of segmentally repeating CNS cell bodies were labelled (Fig 3.5A). The labelling of axonal projections identified cells as neurons (Fig 3.5B). Midline cells were labelled dorsally to the VNC, and their large projections identified them as dorsal median (DM) cells (Fig 3.5C). In stage 14, GFP was expressed in more CNS cell bodies, and the longitudinal projections thickened (Fig 3.5D-F). The DM cells were also labelled (Fig 3.5G). In stages 15 to 17, increasing numbers of CNS cells were labelled, GFP expression increased in the longitudinal fascicles, and DM cells were labelled (Fig 3.6A-F). In

stage 15, ISN axons were labelled (Fig 3.6G), and in stage 17, the ISNb motor axons were labelled (Fig 3.6H). Outside of the nervous system, GFP labelled the ring gland (Fig 3.6I) and the fat body (Fig 3.6J) of stage 17 embryos.

3.2.4 *Toll-7* expression in the larval CNS

In situ hybridisation was carried out to characterise expression of *Toll-7* in the larval CNS. In the VNC, expression was most apparent in the thoracic region, particularly in three bilateral clusters which could correspond to the motor neurons for the developing legs (Fig Fig 3.7A-B). *Toll-7* was also expressed in the central brain, and there was strong expression in the optic lobe in a pattern that included the medulla or lamina, and possibly also the precursor cells of the outer proliferation centre (Fig 3.7C-E). In the eye imaginal disc, expression was only detected in the morphogenetic furrow (Fig 3.7F).

Using *Toll-7-Gal4* to drive GAP-GFP, cells were labelled both in the central brain and along the VNC (Fig 3.8A-B). The entire neuropile of the VNC was labelled, and the labelling of individual axons identified the expressing cells as neurons (Fig 3.8C). There was very little expression of GFP in the optic lobe, but in the eye imaginal disc, photoreceptors were labelled with GFP (Fig 3.8D).

3.2.5 *Toll-7* expression the adult brain

Expression of *Toll-7* in the adult brain was also determined by *in situ* hybridisation. *Toll-7* mRNA was detected in the medulla of the optic lobe (Fig 3.9A). In the central brain, *Toll-7* was detected in cells surrounding the antennal nerve, antennal lobe and ventrolateral protocerebrum (Fig 3.9B), and in cells surrounding the ellipsoid and fan-shaped bodies of the central complex (Fig 3.9C-D).

Fig 3.3 - *Toll-7* is expressed in stage 13-14 embrynic CNS

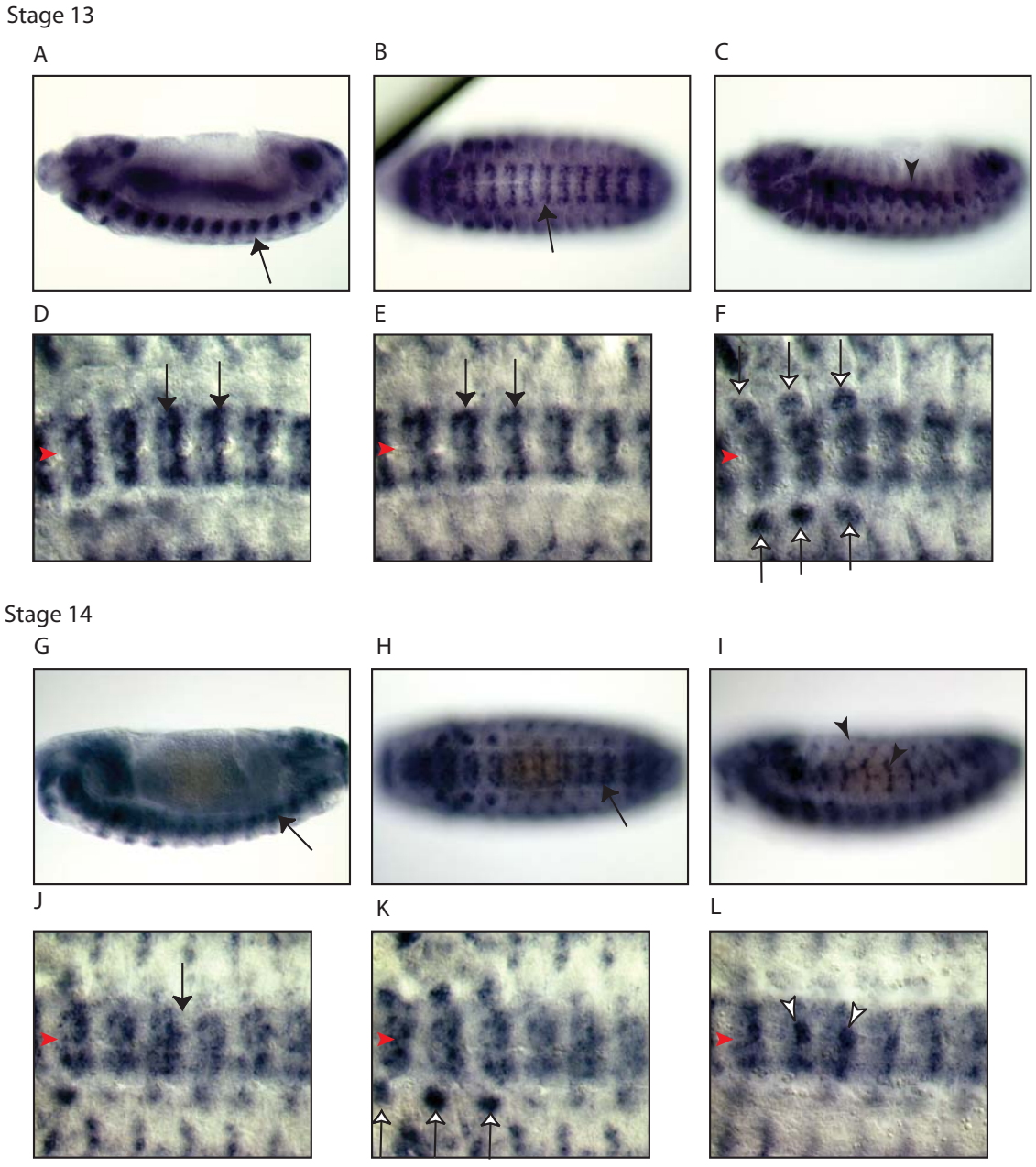

In situ hybridisation showing the distribution of *Toll-7* mRNA. (A-C) Whole mount stage 13 embryo showing *Toll-7* expression in the CNS (arrows) and in the lateral epidermis (arrow heads). (D-F) Dissected stage 13 embryo showing *Toll-7* in a segmentally repeating pattern in the CNS (arrows) and in the primordial leg imaginal discs (white arrows). (G-I) Whole mount stage 14 embryos with *Toll-7* mRNA detected in the CNS (arrows) and lateral and dorsal epidermis (arrow heads). (J-L) Dissected stage 17 embryo showing expression in the CNS (arrows) and leg imaginal disc precursors (white arrows). Cells at the midline are detected (white arrow heads). Ventral midline of dissected samples indicated by red arrow heads, anterior is left.

Fig 3.4 - *Toll-7* is expressed in stage 15-17 embryonic CNS

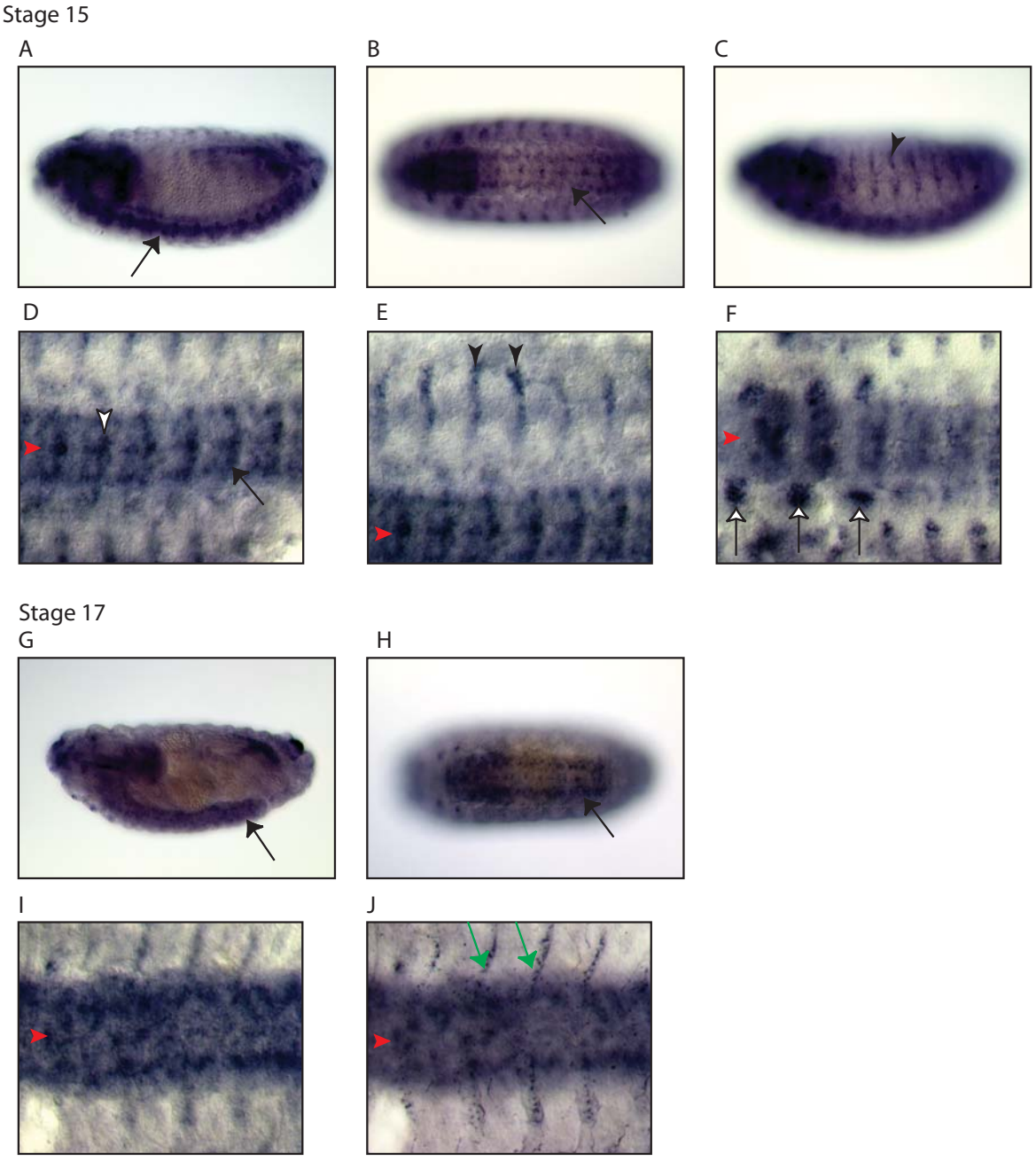

In situ hybridisation showing the distribution of *Toll-7* mRNA. (A-C) Whole mount stage 15 embryo showing *Toll-7* epxression in the CNS (arrows), and in lateral epidermis stripes (arrow heads). (D-E) Dissected stage 15 embryo with *Toll-7* expressed in the CNS (arrows) including midline cells (white arrow heads), lateral epidermis (arrow heads), and the leg imaginal disc primordia (white arrows). (G-H) Whole mount stage 17 embryo showing CNS expression (arrows). (I-J) Dissected stage 17 embryos showing CNS expression, and mRNA detected in the denticles (green arrows). Ventral midline on dissected samples indicated by red arrows heads, anterior is left.

Fig 3.5 - *Toll-7 Gal4* > *UAS-GAP-GFP* labels stage 13-14 embryonic CNS

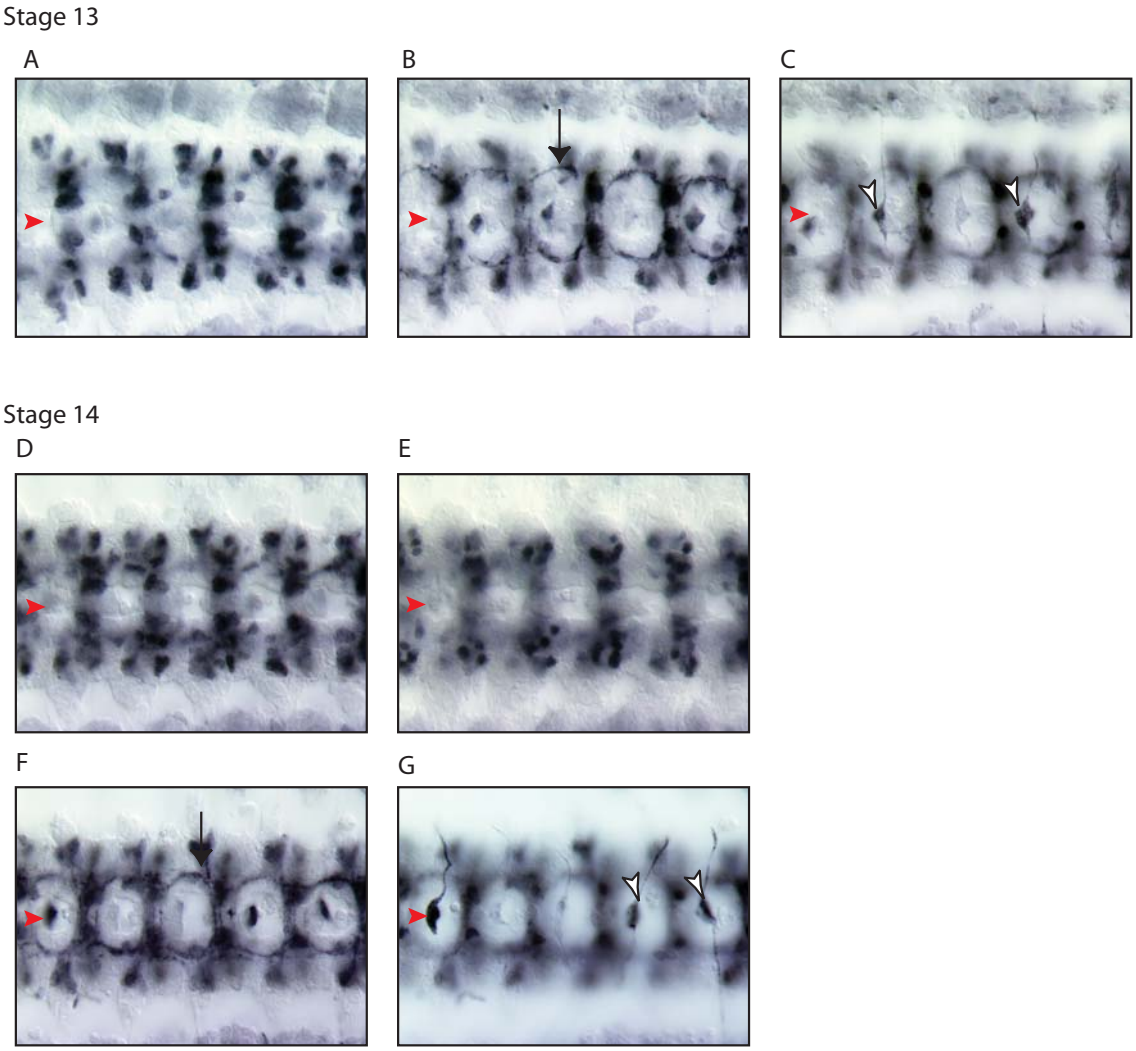

UAS-GAP-GFP driven by *Toll-7-Gal4*, anti-GFP labelling with nickel-enhanced HRP. (A-C) Dissected stage 13 embryo showing expression in clusters of CNS cells with lonitudinal projections (arrow), and the dorsal median (DM) cells (white arrow heads). (D-F) Dissected stage 14 embryo with clusters of CNS cells and longitudinal projections expressing GFP (arrow). (G) GFP labels the DM cells (white arrow head). Ventral midline indicated with red arrow heads, anterior is left.

Fig 3.6 - *Toll-7 Gal4* > *UAS-GAP-GFP* labels stage 15-17 embryonic CNS

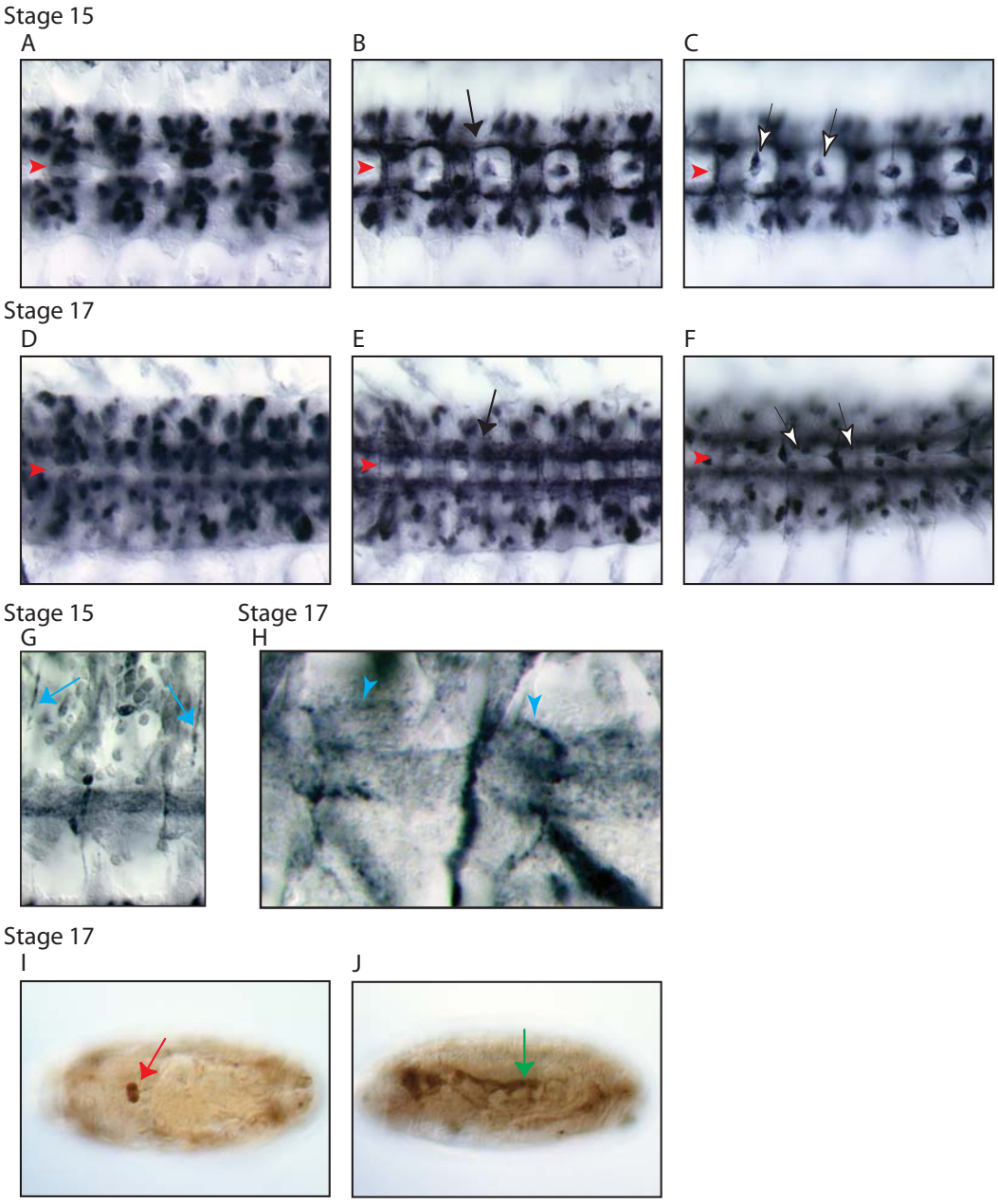

UAS-GAP-GFP driven by *Toll-7 Gal4*, anti GFP labelling with HRP, with (A-H) and without (I-J) nickel enhancment. (A-C) Dissected stage 15, and (D-F) dissected stage 17 embryos showing expression in clusters of cells in the CNS, longitudinal fascicles (arrows), and in the dorsal median (DM) cells (white arrow heads). (G) Dissected stage 15 embryo showing the labelled projection of the ISN dorsolaterally along the body wall (blue arrow). (H) Dissected stage 17 embryo showing GFP expression in the ISNb motor axon (blue arrow head). (I) Dorsal view of whole-mount stage 17 embryo, showing GFP expression in the ring gland (red arrow). (J) Lateral view of a whole-mount stage 17 embryo, showing GFP in the fat body (green arrow). Ventral midline indicated with red arrows heads, anterior is left.

Fig 3.7 - *Toll-7* is expressed in the larval CNS

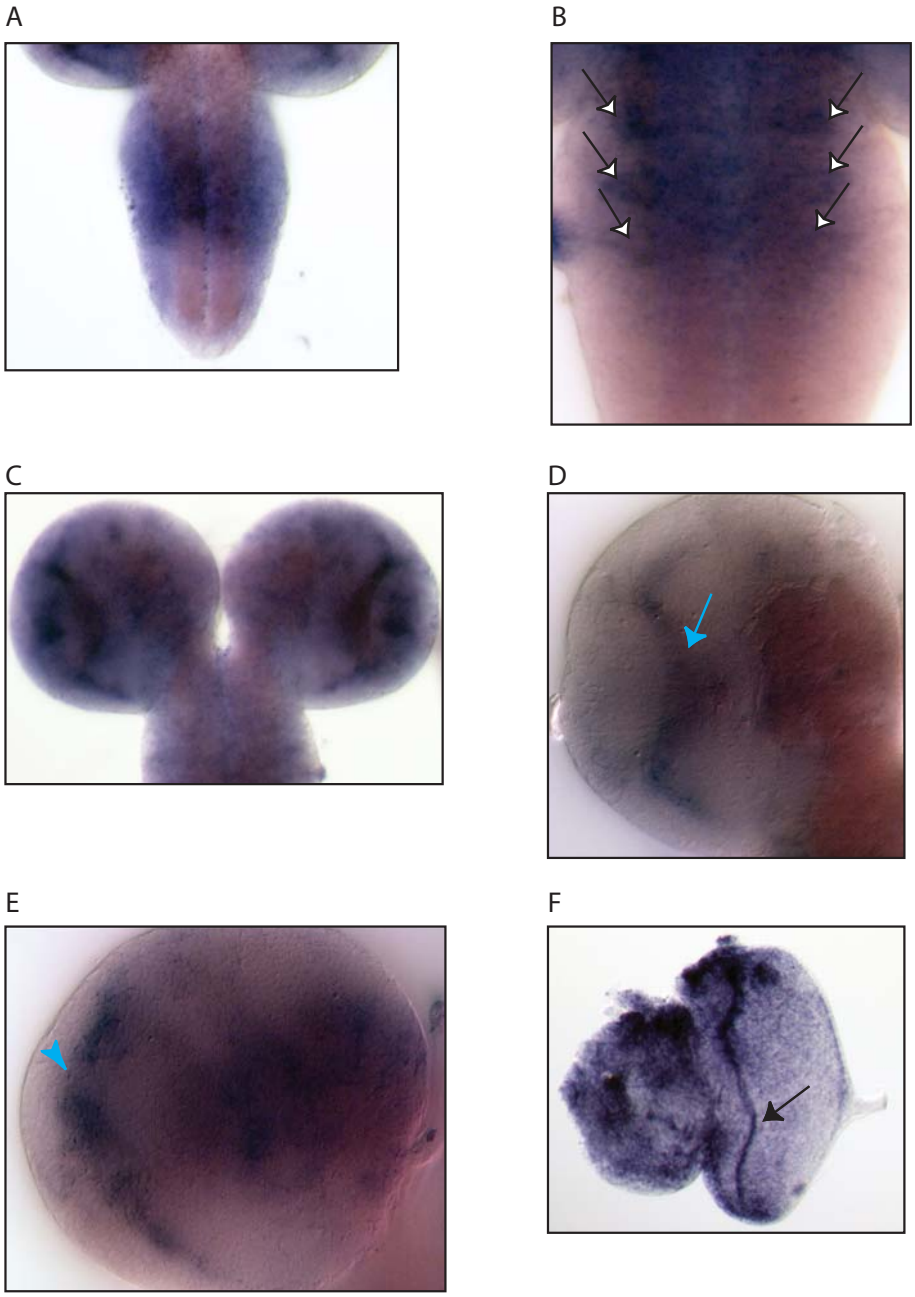

In situ hybridisation showing the distribution of *Toll-7* mRNA in the larval CNS. (A, B) *Toll-7* is expressed more prominently in the thoracic VNC, including three cluster of cells on each side (white arrows). (C-E) *Toll-7* is expressed in the optic lobes, including the medulla or lamina (blue arrow) and and the outer proliferation centre (blue arrow head). (F) Expression of *Toll-7* is limited to the morphogenetic furrow of the eye disc (arrow).

Fig 3.8 - *Toll-7 Gal4* > *UAS-GAP-GFP* labels the larval CNS

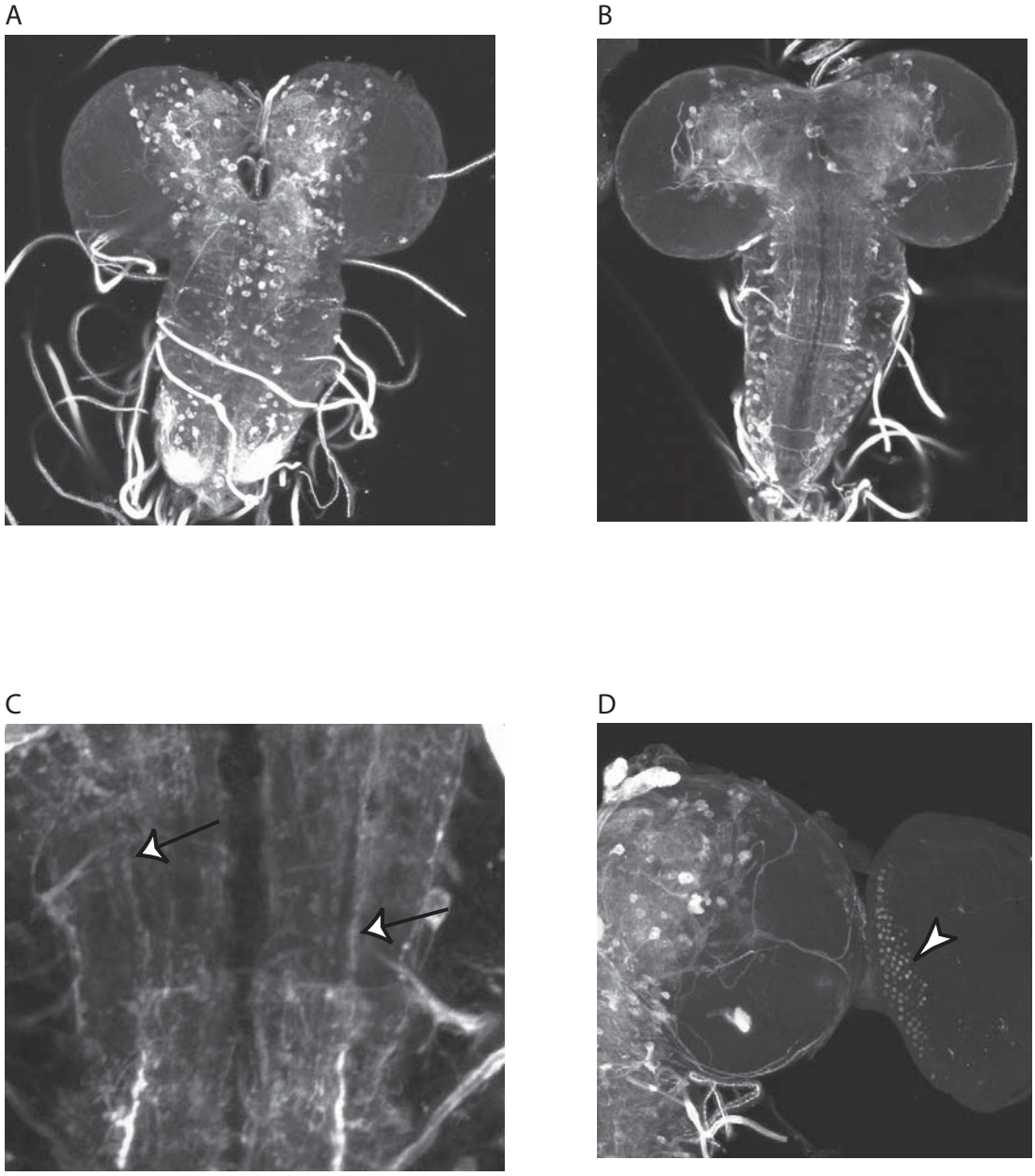

UAS-GAP-GFP drriven by *Toll-7 Gal4*, anti-GFP detected with fluorescence. GFP labels (A) cell bodies and (B) the neuropiles of the central brain and VNC. (C) Individual axons/axon bundles are detected (arrows). (D) Expression is seen in the photoreceptors in the eye imaginal disc (white arrow head).

Toll-7>GAP-GFP was also used to identify cells in the adult brain. GFP labelled cells of the medulla in the adult optic lobe, and they could be seen projecting to the central brain (Fig 3.10A). Posterior to the medulla, the lobula was also detected (Fig 3.10B). In the central brain, there were extensive projections within the ventrolateral protocerebrum, and also the superior medial protocerebrum (Fig 3.10C). The fan-shaped body was very strongly labelled with GFP (Fig 3.10D).

3.2.6 Generation of *Toll-6* cDNA

Like *Toll-7*, the *Toll-6* gene is intronless, so it was possible to amplify the coding DNA directly from genomic DNA of *yw* flies by PCR (Fig 3.11A). The full-length coding sequence was amplified by PCR incorporating 5' attB1 and 3' attB2 sites for Gateway cloning (primers 6.11 and 6.12, Table 2.4, materials and methods). The fragment was cloned into pDONR[221] using Gateway BP Clonase, and the correct clone was identified by restriction digests: digestion by AatII and XhoI, and BglII (Fig 3.11B). To confirm the clone, the entire coding region was sequenced, and compared to the reference sequence obtained from FlyBase (FBgn0036494) (Fig 3.11C). The sequence revealed two point mutations: threonine to alanine at position 252, and serine to threonine at position 1263. These are conservative changes of small amino acids. Thr252Ala falls between LRRs in the extracellular domain, Ser1263Thr is intracellular, but lies outside the signalling TIR domain. It is therefore not anticipated that these mutations will substantially alter the structure or function of the protein. As with *Toll-7* the PCR amplification of *Toll-6* was carried out multiple times, and the observed base pair changes were reasonably reproducible, compatible with naturally occurring polymorphisms. An antisense RNA probe was transcribed from pDONR-Toll-6 using the 3' T7 RNA Polymerase promoter sequence found in pDONR (see section 2.5.3,

Fig 3.9 - *Toll-7* is expressed in the adult brain

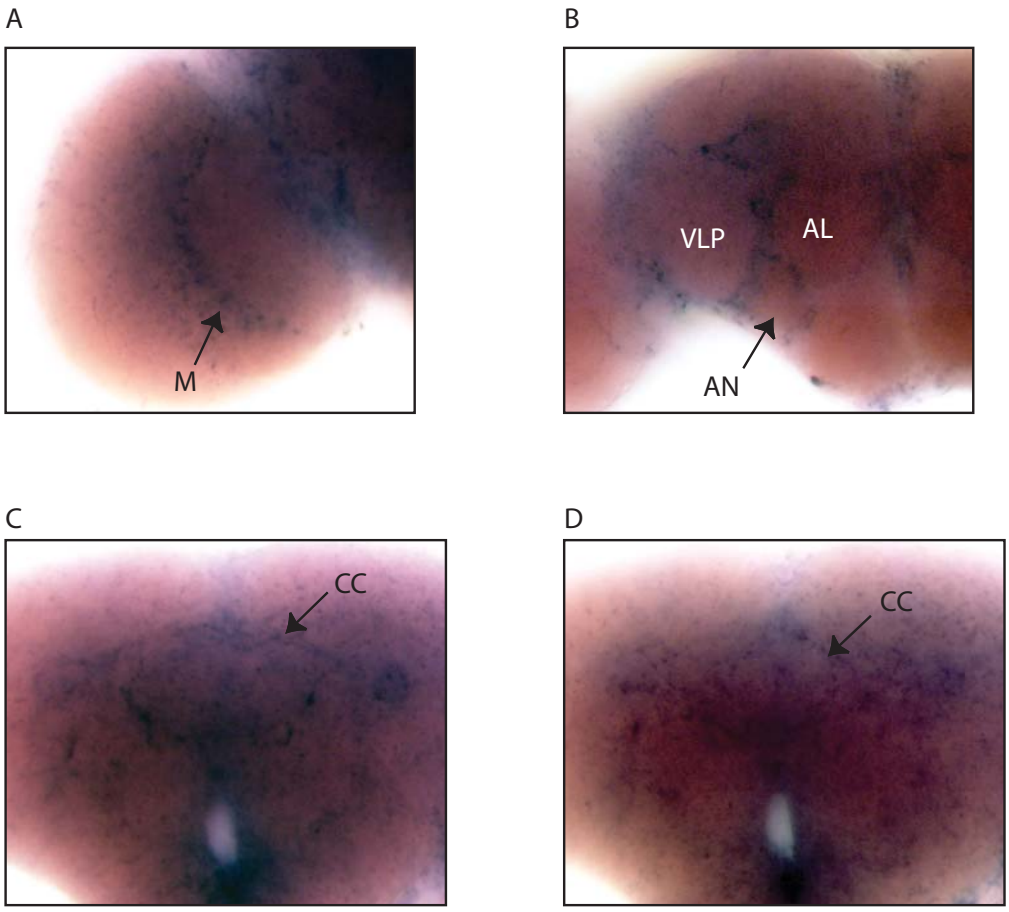

In situ hybridisation showing the distribution of *Toll-7* mRNA. (A) *Toll-7* is expressed in the medulla (M) of the optic lobe. (B) *Toll-7* expression is detected in cells surrounding the antennal nerve (AN), the antennal lobe (AL), and the ventrolateral protocerebrum (VLP). (C) Signal is seen surrounding the fan shaped body and (D) the ellipsoid body of the central complex (CC).

Fig 3.10 - *Toll-7 Gal4* > *UAS-GAP-GFP* labels the adult brain.

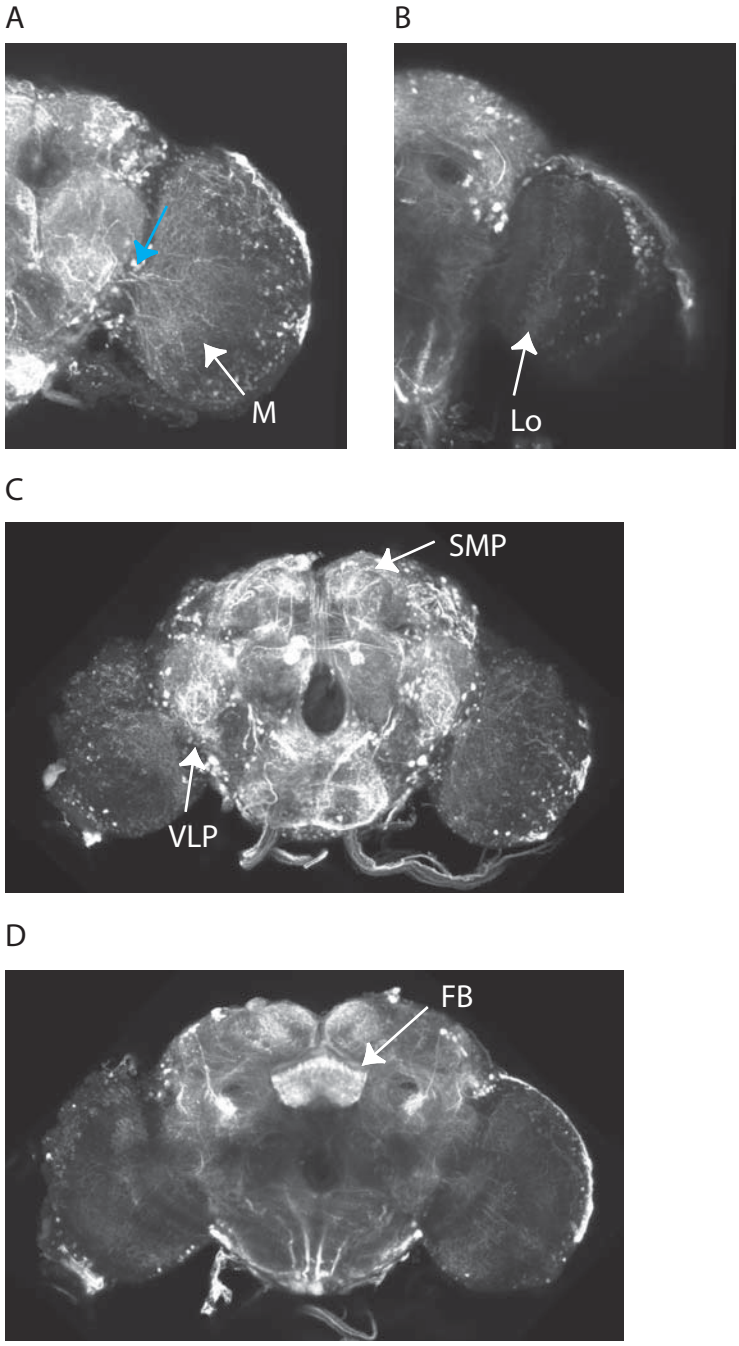

UAS-GAP-GFP driven by *Toll-7-Gal4*, anti-GFP labelling with fluorescence. (A-B) GFP is expressed in the medulla (M) and lobula (Lo) of the optic lobe, with projections to the central brain (blue arrow). (C) GFP labels projections in the ventrolateral protocerebrum (VLP) and the superior medial protocerebrum (SMP). (D) Toll-7 is expressed in cells of the fan shaped body (FB).

materials and methods). The *Toll-6* coding sequence was later transferred to pAct-gw-HA by LR gateway cloning. This resulted in an expression clone suitable for constitutive expression of Toll-6 in cultured cells under the actin promoter, and placed an HA tag at the C-terminal.

3.2.7 *Toll-6* expression in the embryonic CNS

To identify *Toll-6*-expressing cells in embryos, *in situ* hybridisation was carried out. *Toll-6* expression was seen in in early embryos in epidermal stripes (Fig 3.12A-B). *Toll-6* mRNA was detected in stage 13 embryos in segmentally repeating patterns in the developing CNS (Fig 3.12C-D), and also in the dorso-lateral epidermis (Fig 3.12E). In stage 14 embryos, the expression in the CNS became stronger, and *Toll-6* was found at the dorsal margins of the epidermis (Fig 3.12F-J). The CNS expression of *Toll-6* increased in stage 15 embryos (Fig 3.12A-B). Expression outside the CNS was restricted to small clusters of cells lying laterally to the VNC in each segment, which may be a subset of PNS, epidermis or muscle (Fig 3.13A-B). In stages 16 and 17, *Toll-6* was expressed throughout the CNS, including in paired cells close to the midline which could be the dMP2s (Fig 3.13C-F). By Stage 17, expression of *Toll-6* was restricted to the CNS and the small, segmentally repeating clusters of cells (Fig 3.13G-H).

To label the cell membranes of cells that putatively express *Toll-6*, I used the *D42-Gal4* line to drive expression of GAP-GFP. In stage 13 embryos, GFP labelled the CNS (Fig 3.14A) and also a lateral stripe of cells (Fig 3.14B). In stage 14, cells in the ventral epidermis were also labelled (Fig 3.14C-E). In the stage 14 VNC, GFP was expressed in cell bodies and axonal projections, identifying cells as neurons (Fig 3.14F-G). In stage 15 embryos, GFP labelled a subset of cells in the CNS (Fig 3.15A-B). Neuronal projections along the longitudinal connectives and into the periphery were labelled (Fig 3.15C-D). In stage 17 embryos, CNS

Fig 3.11 - Toll-6 coding DNA was cloned into pDONR

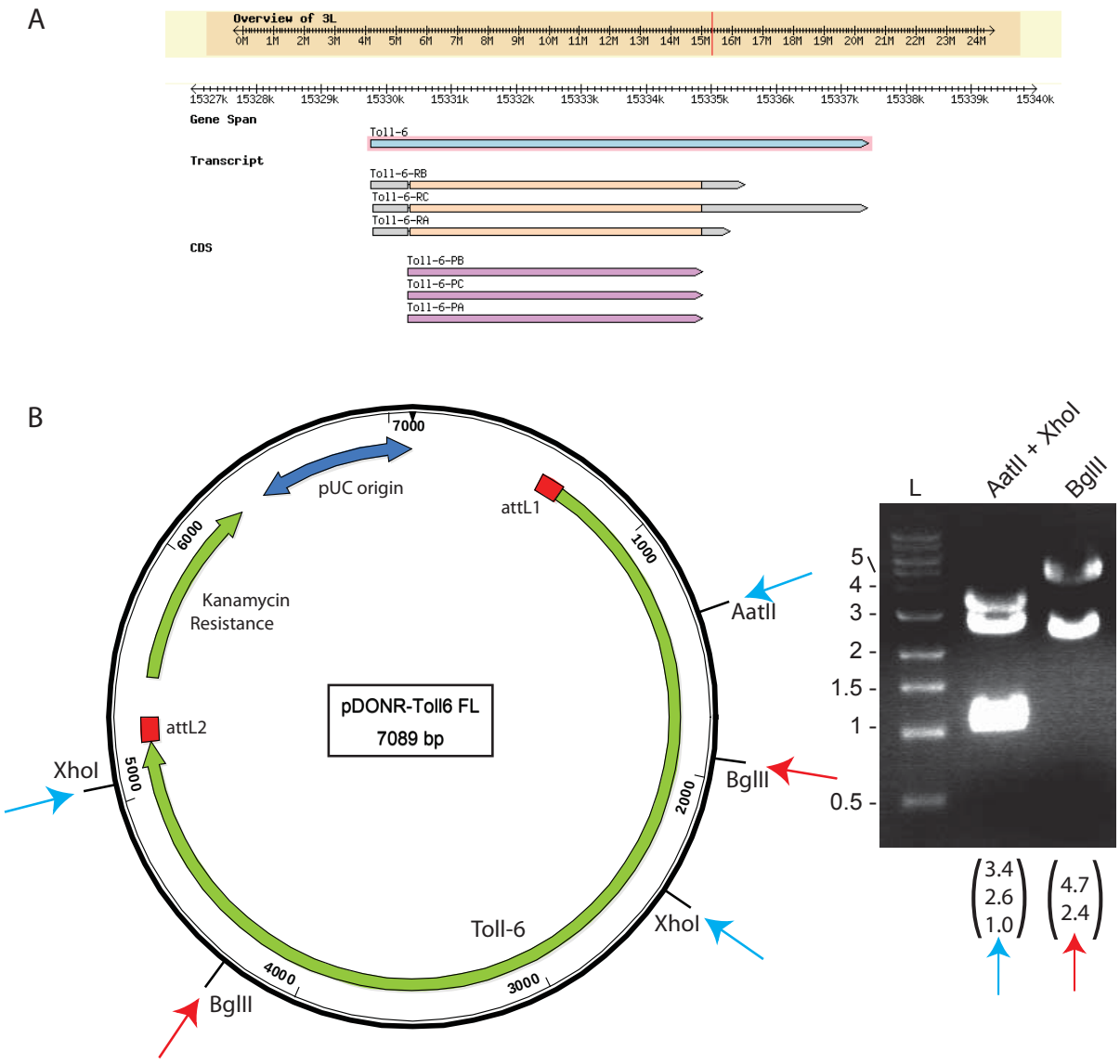

(A) The FlyBase map of the *Toll-6* locus indicated that the gene does not contain introns. (B) *Toll-6* was cloned into pDONR, and restriction digests were used to identify the correct clone. Enzyme sites are indicated on the map, DNA fragments are shown to the right. The predicted fragment sizes are given below each lane. (C, over) The sequenced gene region, compared to the predicted *Toll-6* sequence. Mutated residues are highlighted in red. Protein domains are given: Cysteine-rich clusters (CRC) lie C-terminal (CT) and N-terminal (NT) to Leucine-rich repeats (LRR).

Fig 3.11C – Sequence of cloned *Toll-6*

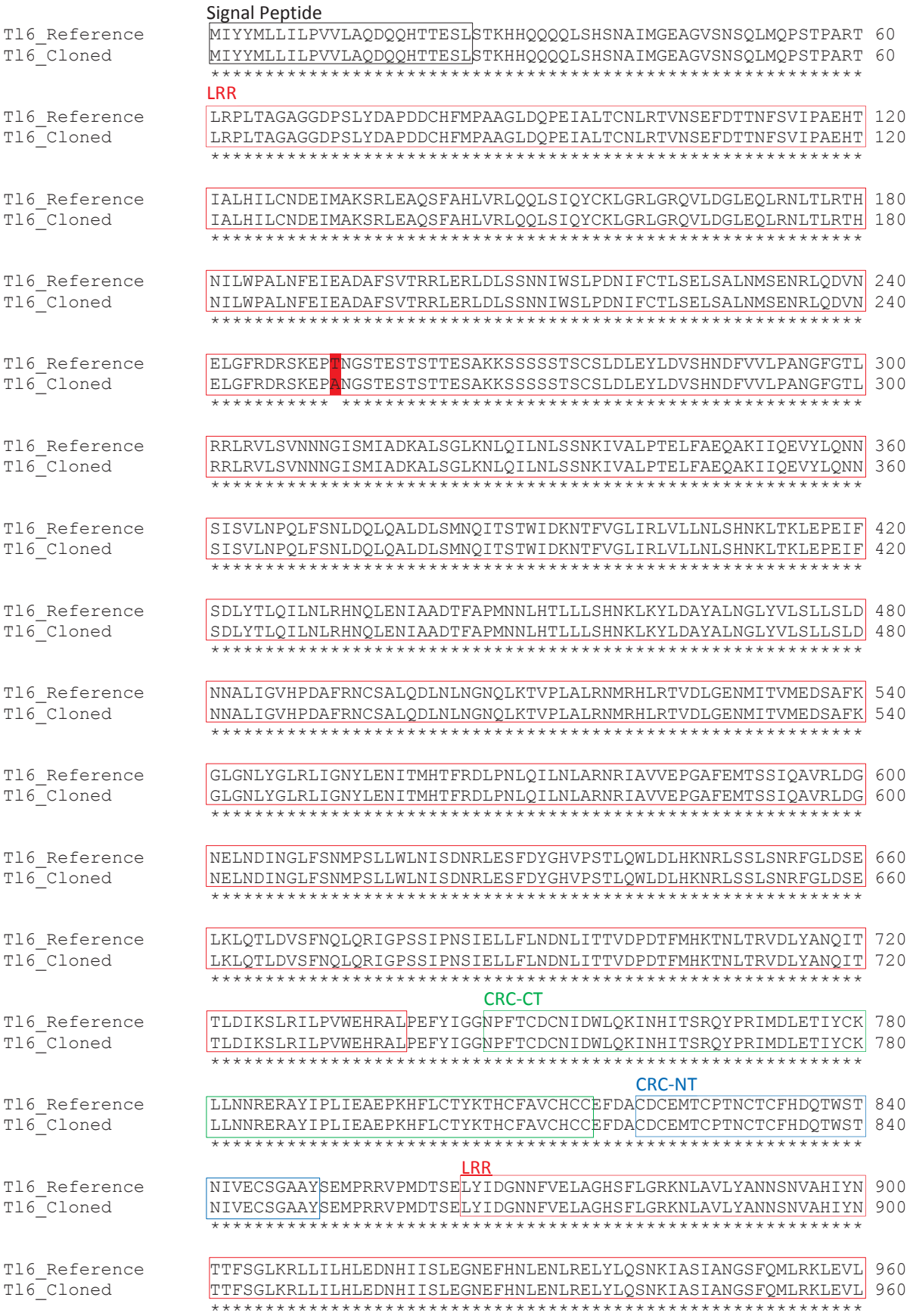


```
                    Signal Peptide
Tl6_Reference       MIYYMLLILPVVLAQDQQHTTESLSTKHHQQQQLSHSNAIMGEAGVSNSQLMQPSTPART 60
Tl6_Cloned          MIYYMLLILPVVLAQDQQHTTESLSTKHHQQQQLSHSNAIMGEAGVSNSQLMQPSTPART 60
                    ************************************************************
                    LRR
Tl6_Reference       LRPLTAGAGGDPSLYDAPDDCHFMPAAGLDQPEIALTCNLRTVNSEFDTTNFSVIPAEHT 120
Tl6_Cloned          LRPLTAGAGGDPSLYDAPDDCHFMPAAGLDQPEIALTCNLRTVNSEFDTTNFSVIPAEHT 120
                    ************************************************************

Tl6_Reference       IALHILCNDEIMAKSRLEAQSFAHLVRLQQLSIQYCKLGRLGRQVLDGLEQLRNLTLRTH 180
Tl6_Cloned          IALHILCNDEIMAKSRLEAQSFAHLVRLQQLSIQYCKLGRLGRQVLDGLEQLRNLTLRTH 180
                    ************************************************************

Tl6_Reference       NILWPALNFEIEADAFSVTRRLERLDLSSNNIWSLPDNIFCTLSELSALNMSENRLQDVN 240
Tl6_Cloned          NILWPALNFEIEADAFSVTRRLERLDLSSNNIWSLPDNIFCTLSELSALNMSENRLQDVN 240
                    ************************************************************

Tl6_Reference       ELGFRDRSKEPTNGSTESTSTTESAKKSSSSSTSCSLDLEYLDVSHNDFVVLPANGFGTL 300
Tl6_Cloned          ELGFRDRSKEPANGSTESTSTTESAKKSSSSSTSCSLDLEYLDVSHNDFVVLPANGFGTL 300
                    ********** ***************************************************

Tl6_Reference       RRLRVLSVNNNGISMIADKALSGLKNLQILNLSSNKIVALPTELFAEQAKIIQEVYLQNN 360
Tl6_Cloned          RRLRVLSVNNNGISMIADKALSGLKNLQILNLSSNKIVALPTELFAEQAKIIQEVYLQNN 360
                    ************************************************************

Tl6_Reference       SISVLNPQLFSNLDQLQALDLSMNQITSTWIDKNTFVGLIRLVLLNLSHNKLTKLEPEIF 420
Tl6_Cloned          SISVLNPQLFSNLDQLQALDLSMNQITSTWIDKNTFVGLIRLVLLNLSHNKLTKLEPEIF 420
                    ************************************************************

Tl6_Reference       SDLYTLQILNLRHNQLENIAADTFAPMNNLHTLLLSHNKLKYLDAYALNGLYVLSLLSLD 480
Tl6_Cloned          SDLYTLQILNLRHNQLENIAADTFAPMNNLHTLLLSHNKLKYLDAYALNGLYVLSLLSLD 480
                    ************************************************************

Tl6_Reference       NNALIGVHPDAFRNCSALQDLNLNGNQLKTVPLALRNMRHLRTVDLGENMITVMEDSAFK 540
Tl6_Cloned          NNALIGVHPDAFRNCSALQDLNLNGNQLKTVPLALRNMRHLRTVDLGENMITVMEDSAFK 540
                    ************************************************************

Tl6_Reference       GLGNLYGLRLIGNYLENITMHTFRDLPNLQILNLARNRIAVVEPGAFEMTSSIQAVRLDG 600
Tl6_Cloned          GLGNLYGLRLIGNYLENITMHTFRDLPNLQILNLARNRIAVVEPGAFEMTSSIQAVRLDG 600
                    ************************************************************

Tl6_Reference       NELNDINGLFSNMPSLLWLNISDNRLESFDYGHVPSTLQWLDLHKNRLSSLSNRFGLDSE 660
Tl6_Cloned          NELNDINGLFSNMPSLLWLNISDNRLESFDYGHVPSTLQWLDLHKNRLSSLSNRFGLDSE 660
                    ************************************************************

Tl6_Reference       LKLQTLDVSFNQLQRIGPSSIPNSIELLFLNDNLITTVDPDTFMHKTNLTRVDLYANQIT 720
Tl6_Cloned          LKLQTLDVSFNQLQRIGPSSIPNSIELLFLNDNLITTVDPDTFMHKTNLTRVDLYANQIT 720
                    ************************************************************
                                                CRC-CT
Tl6_Reference       TLDIKSLRILPVWEHRALPEFYIGGNPFTCDCNIDWLQKINHITSRQYPRIMDLETIYCK 780
Tl6_Cloned          TLDIKSLRILPVWEHRALPEFYIGGNPFTCDCNIDWLQKINHITSRQYPRIMDLETIYCK 780
                    ************************************************************
                                                            CRC-NT
Tl6_Reference       LLNNRERAYIPLIEAEPKHFLCTYKTHCFAVCHCCEFDACDCEMTCPTNCTCFHDQTWST 840
Tl6_Cloned          LLNNRERAYIPLIEAEPKHFLCTYKTHCFAVCHCCEFDACDCEMTCPTNCTCFHDQTWST 840
                    ************************************************************
                                        LRR
Tl6_Reference       NIVECSGAAYSEMPRRVPMDTSELYIDGNNFVELAGHSFLGRKNLAVLYANNSNVAHIYN 900
Tl6_Cloned          NIVECSGAAYSEMPRRVPMDTSELYIDGNNFVELAGHSFLGRKNLAVLYANNSNVAHIYN 900
                    ************************************************************

Tl6_Reference       TTFSGLKRLLILHLEDNHIISLEGNEFHNLENLRELYLQSNKIASIANGSFQMLRKLEVL 960
Tl6_Cloned          TTFSGLKRLLILHLEDNHIISLEGNEFHNLENLRELYLQSNKIASIANGSFQMLRKLEVL 960
                    ************************************************************
```

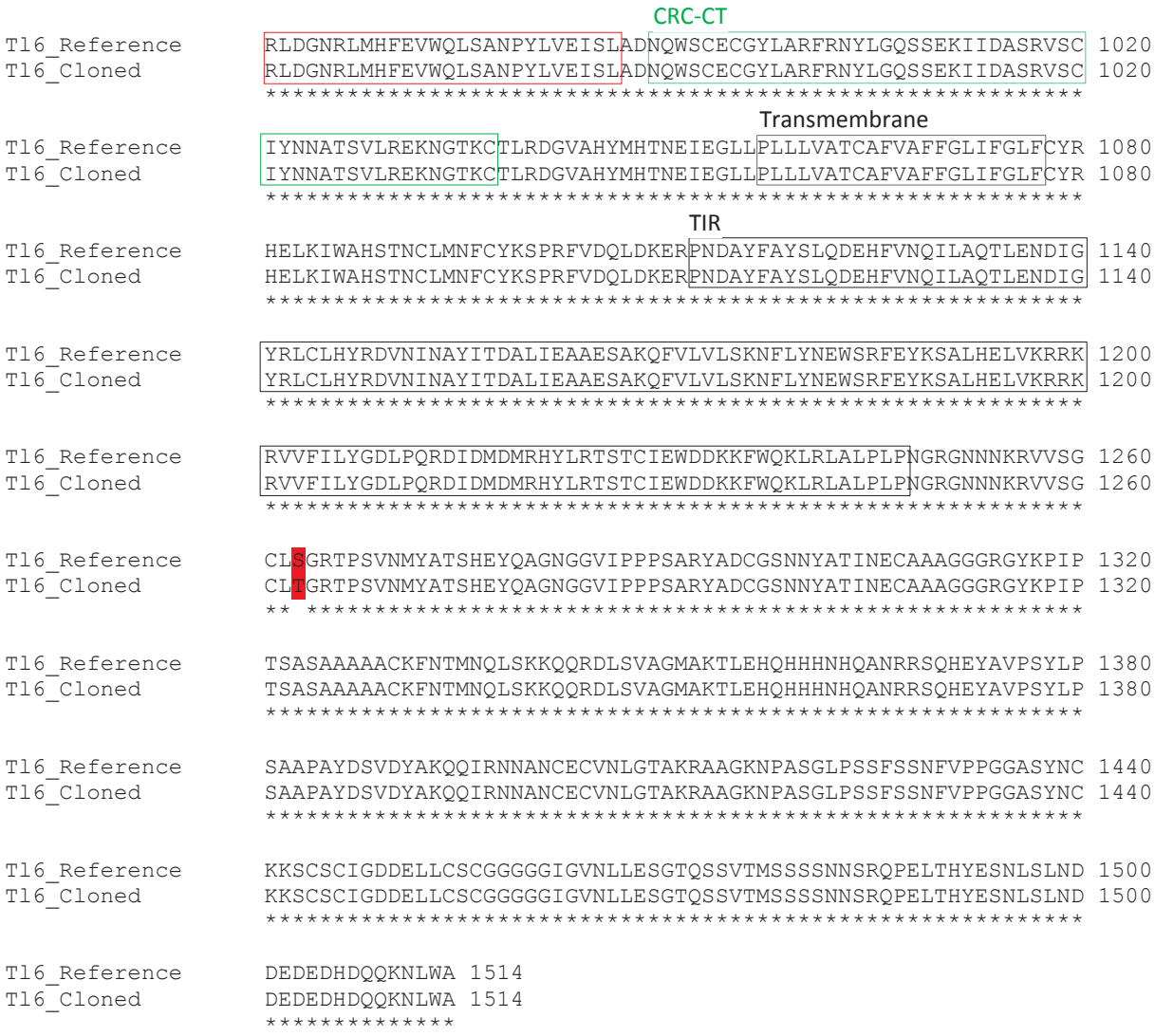
CRC-CT
Transmembrane
TIR
Tl6_Reference RLDGNRLMHFEVWQLSANPYLVEISLADNQWSCECGYLARFRNYLGQSSEKIIDASRVSC 1020
Tl6_Cloned RLDGNRLMHFEVWQLSANPYLVEISLADNQWSCECGYLARFRNYLGQSSEKIIDASRVSC 1020
Tl6_Reference IYNNATSVLREKNGTKCTLRDGVAHYMHTNEIEGLLPLLLVATCAFVAFFGLIFGLFCYR 1080
Tl6_Cloned IYNNATSVLREKNGTKCTLRDGVAHYMHTNEIEGLLPLLLVATCAFVAFFGLIFGLFCYR 1080
Tl6_Reference HELKIWAHSTNCLMNFCYKSPRFVDQLDKERPNDAYFAYSLQDEHFVNQILAQTLENDIG 1140
Tl6_Cloned HELKIWAHSTNCLMNFCYKSPRFVDQLDKERPNDAYFAYSLQDEHFVNQILAQTLENDIG 1140
Tl6_Reference YRLCLHYRDVNINAYITDALIEAAESAKQFVLVLSKNFLYNEWSRFEYKSALHELVKRRK 1200
Tl6_Cloned YRLCLHYRDVNINAYITDALIEAAESAKQFVLVLSKNFLYNEWSRFEYKSALHELVKRRK 1200
Tl6_Reference RVVFILYGDLPQRDIDMDMRHYLRTSTCIEWDDKKFWQKLRLALPLPNGRGNNNKRVVSG 1260
Tl6_Cloned RVVFILYGDLPQRDIDMDMRHYLRTSTCIEWDDKKFWQKLRLALPLPNGRGNNNKRVVSG 1260
Tl6_Reference CLSGRTPSVNMYATSHEYQAGNGGVIPPPSARYADCGSNNYATINECAAAGGGRGYKPIP 1320
Tl6_Cloned CLTGRTPSVNMYATSHEYQAGNGGVIPPPSARYADCGSNNYATINECAAAGGGRGYKPIP 1320
Tl6_Reference TSASAAAAACKFNTMNQLSKKQQRDLSVAGMAKTLEHQHHHNHQANRRSQHEYAVPSYLP 1380
Tl6_Cloned TSASAAAAACKFNTMNQLSKKQQRDLSVAGMAKTLEHQHHHNHQANRRSQHEYAVPSYLP 1380
Tl6_Reference SAAPAYDSVDYAKQQIRNNANCECVNLGTAKRAAGKNPASGLPSSFSSNFVPPGGASYNC 1440
Tl6_Cloned SAAPAYDSVDYAKQQIRNNANCECVNLGTAKRAAGKNPASGLPSSFSSNFVPPGGASYNC 1440
Tl6_Reference KKSCSCIGDDELLCSCGGGGGIGVNLLESGTQSSVTMSSSSNNSRQPELTHYESNLSLND 1500
Tl6_Cloned KKSCSCIGDDELLCSCGGGGGIGVNLLESGTQSSVTMSSSSNNSRQPELTHYESNLSLND 1500
Tl6_Reference DEDEDHDQQKNLWA 1514
Tl6_Cloned DEDEDHDQQKNLWA 1514

expression of GFP increased, as was the labelling of the neuropile (Fig 3.15E-H). Also in stage 17, GFP labelled muscles (Fig 3.15E-F).

3.2.8 *Toll-6* expression in the larval CNS

To determine whether *Toll-6* is expressed in the larval CNS, *in situ* hybridisation was again performed. In the VNC, there was expression throughout the cortex ventrally, and also in cells lying close to the midline dorsally (Fig 3.16A-B). There were high levels of expression in the central brain (Fig 3.16C). In the optic lobes, *Toll-6* was expressed in the lamina and possibly the lamina precursor cells (Fig 3.16D), and weakly in the medulla (Fig 3.16E). In the eye disc, *Toll-6* mRNA was strongly detected in the morphogenetic furrow (Fig 3.16F), but there was no clear expression in the developing retina.

GAP-GFP expression was driven by *D42-Gal4*, to further characterise *Toll-6* expressing cells. In the ventral nerve cord, GFP labelled large paired cells dorsally (Fig 3.17A), and many axons of the dorsal neuropile (Fig 3.17B). More ventrally in the neuropile, individual axons were detectable (Fig 3.17C), confirming that these cells were neurons. GFP was expressed in the central brain, but not in the optic lobes (Fig 3.17D). In the eye imaginal disc, developing photoreceptors were not labelled (Fig 3.17E).

3.2.9 *Toll-6* expression in the adult brain

The distribution of *Toll-6* mRNA in the adult brain was also determined. In the optic lobes, expression was seen in the medulla and more proximally in the lobula (Fig 3.18A). Toll-6 was detected in cells surrounding various central neuropiles, including the antennal nerve and between the ventolateral protocerebrum and antennal lobe (Fig 3,18B). Toll-6 was also

Fig 3.12 - *Toll-6* is expressed in early embryos, and in the stage 13-14 embryonic CNS

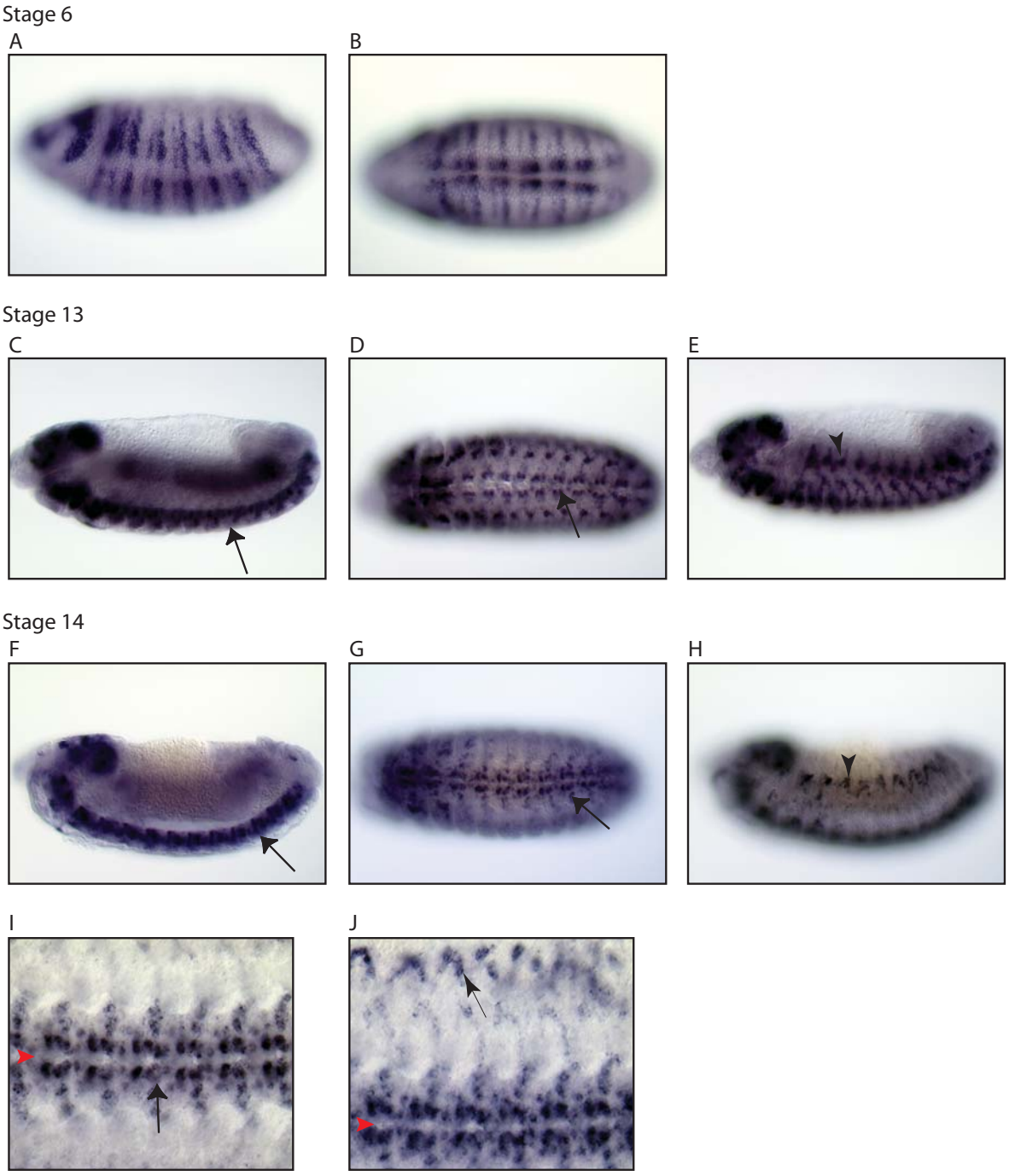

In situ hybridisation showing the distribution of *Toll-6* mRNA. (A-B) Whole mount stage 6 embryo, showing *Toll-6* expression in epidermal stripes. (C-E) Whole mount stage 13 embryo with *Toll-6* expression in the CNS (arrows) and in lateral stripes (arrow head). (F-H) Whole mount and (I-J) dissected stage 14 embryos with *Toll-6* expressed in the CNS (arrows) and in the dorsal epidermis (arrow heads). Ventral midline on dissected samples is indicated (red arrow head), anterior is left.

Fig 3.13 - *Toll-6* is expressed in stage 15-17 embryonic CNS

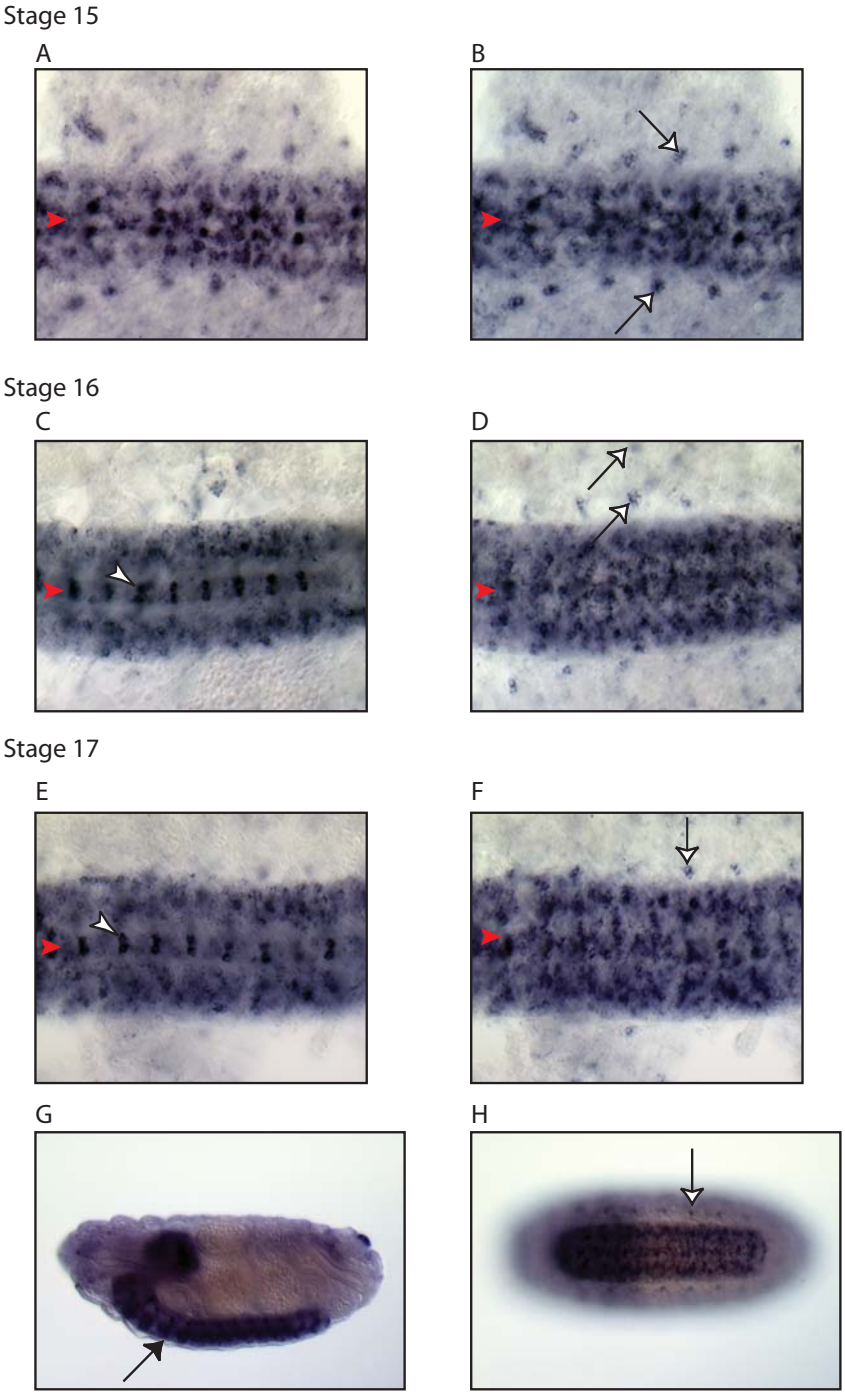

In situ hybridisation showing the distribution of *Toll-6* mRNA. (A-B) Dissected stage 15 embryo showing *Toll-6* expression in the CNS and clusters of cells lateral to the VNC (white arrows). Stage 16 (C-D) and stage 17 (E-F) dissected embryos showing CNS expression. Paired cells close to the midline are detected (white arrow heads), as are lusters of cells outside the CNS (white arrows). (G-H) Whole mount stage 17 embryos showing expression in the CNS (arrow) and in cells clusters outside the CNS (white arrows). Red arrow heads indicate ventral midline of dissected samples, anterior is left.

Fig 3.14 - *D42-Gal4* > *UAS-GAP-GFP* labels stage 13-14 embryonic CNS

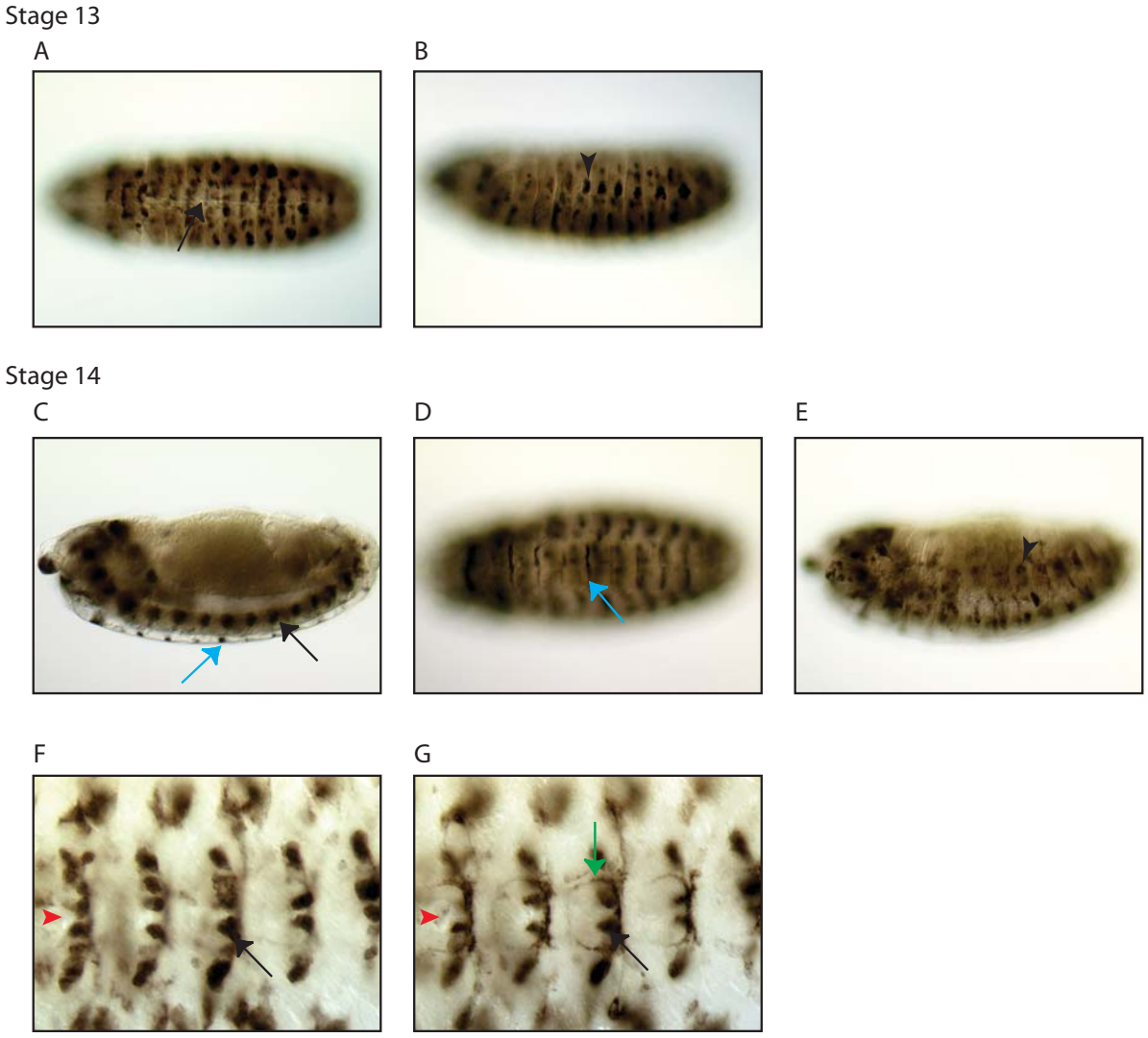

UAS-GAP-GFP driven by *D42-Gal4*, anti-GFP labelling with HRP. (A-B) Whole mount stage 13 embryo showing GFP expression in the CNS (arrow) and the lateral epidermis (arrow head). (C-E) Whole mount stage 14 embryo showing expression in the CNS (arrow), the ventral epidermis (blue arrow), and in the lateral epidermis (arrow head). (F-G) Dissected stage 14 embryos showing GFP labelling cells of the CNS (arrows), including axons projecting longitudinally to the adjacent segment (green arrow). Ventral midline indicated by the red arrow heads, anterior is left.

Fig 3.15 - *D42-Gal4* > *UAS-GAP-GFP* labels stage 15-17 embryonic CNS

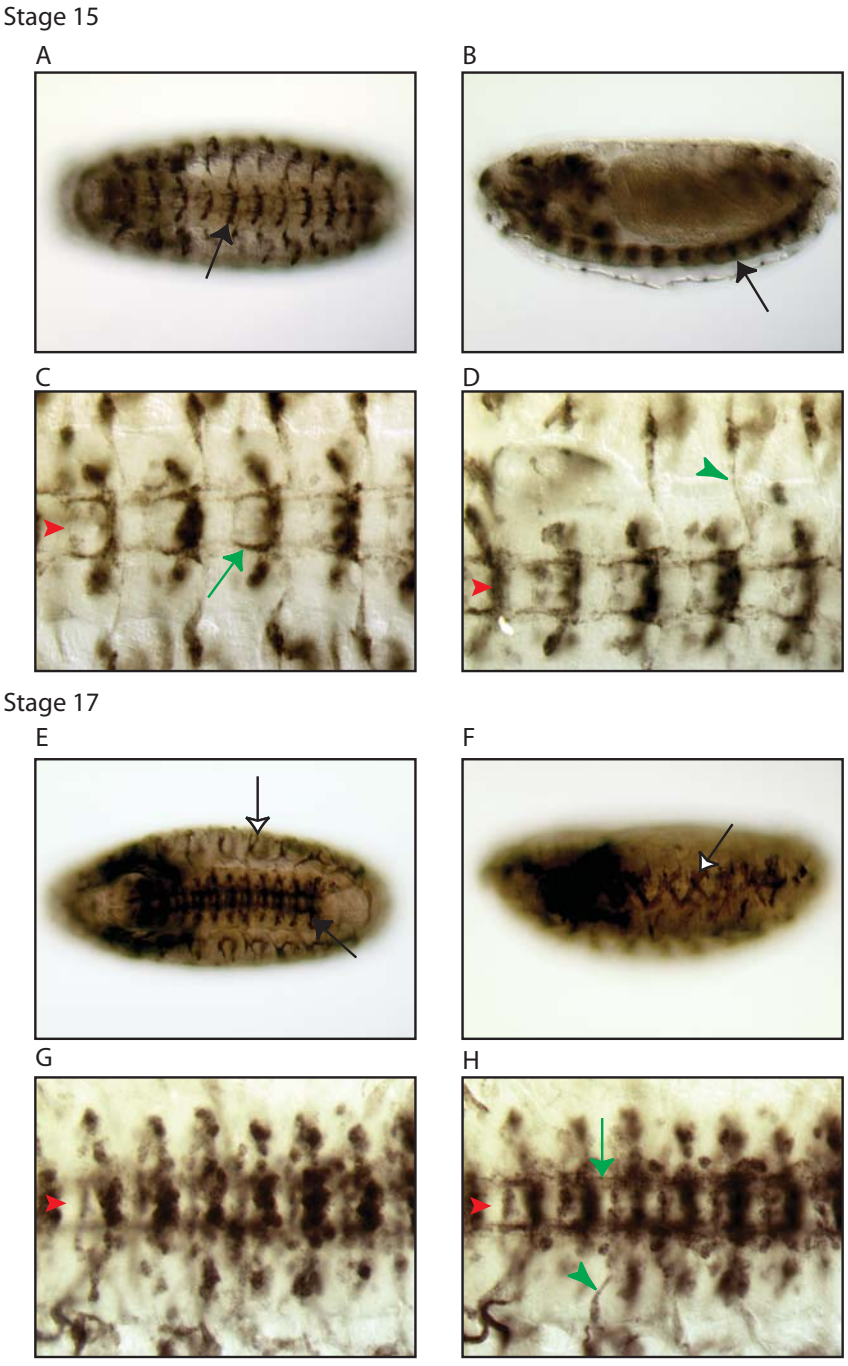

UAS-GAP-GFP driven by *D42-Gal4*, anti GFP detected with HRP. (A-B) Whole mount stage 15 embryo showing GFP expression in the CNS (arrows). (C-D) Dissected stage 15 embryos showing expression in the longitudinal fascicles (green arrow) and axons entering or leaving the CNS (green arrow head). (F-G) Whole mount stage 17 embryo showing GFP is expressed in a subset of muscles (white arrows) and in the CNS (arrow). (H-I) Dissected stage 17 embryo showing GFP labelled longitudinal fascicles (green arrow) and axons entering or leaving the periphery (green arrow head). Ventral midline of dissected samples is indicated (red arrow heads), anterior is left.

Fig 3.16 - *Toll-6* is expressed in the larval CNS

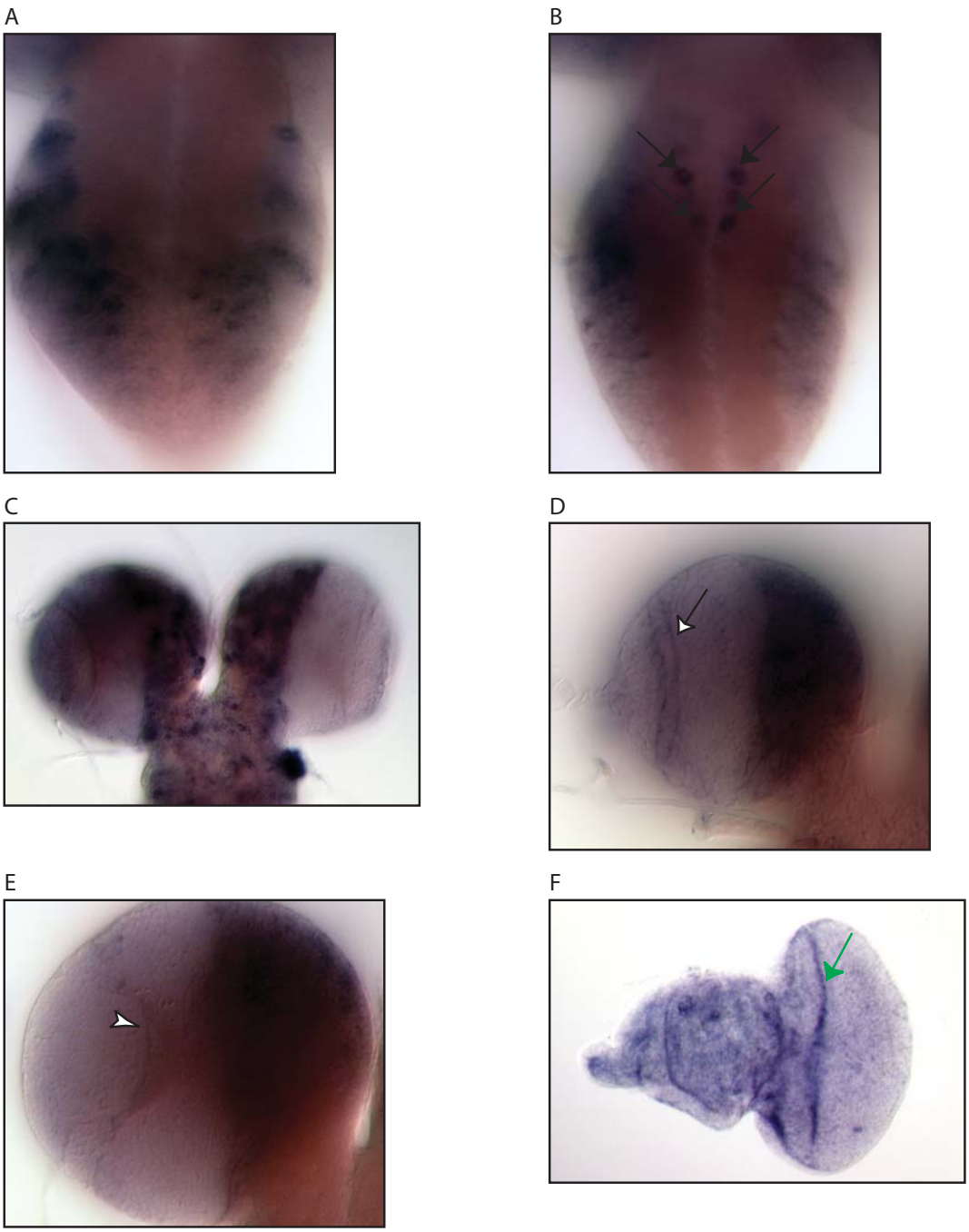

In situ hybridisation showing the distribution of *Toll-6* mRNA. (A) *Toll-6* is expressed widely in the ventral VNC cortex. (B) In the dorsal VNC, cells close to the midline are detected (arrows). (C) *Toll-6* is expressed throughout the larval central brain. (D-E) In the optic lobes, Toll-6 is expressed in cells contributing to the lamina (white arrow) and the medulla (white arrow head). (F) In the eye disc, expression is restricted to the morphogenetic furrow (green arrow).

Fig 3.17 - *D42-Gal4* > *UAS-GAP-GFP* labels neurons in the larval CNS

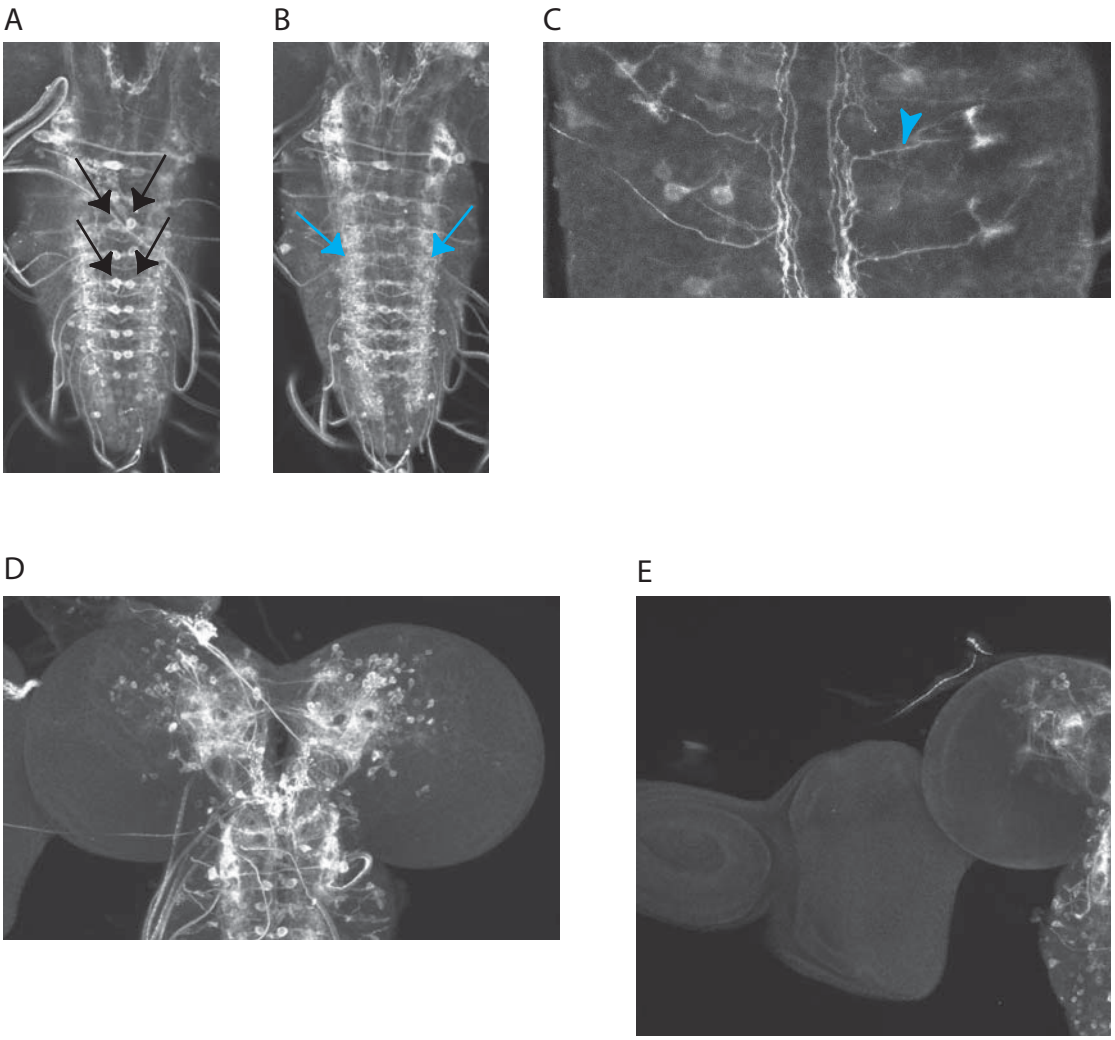

UAS-GAP-GFP driven by *D42-Gal4*, anti-GFP labelling with fluorescence. (A-C) GFP labels the larval VNC, including cells close to the dorsal midline (arrows), the neuropile (blue arrows), and individual axons (blue arrow head). (D) GFP is detected in the central brain, but not the optic lobes. (E) No expression is seen in the eye imaginal disc.

detected in cells surrounding the ellipsoid body and the calyx of the mushroom body (Fig 3.18C-D).

Finally, *D42-Gal4* was used to drive expression of *GAP GFP*, to label cell membranes. GFP labelled cells of the medulla, which were seen projecting to the central brain, as were cells of the lobula, which projected to the contralateral brain (Fig 3.19A-B). Projections were also seen in parts of the antennal lobe and the suboesophageal ganglion (Fig 3.19C). Posteriorly, there were GFP+ cells close to the calyx, though the mushroom body itself was not labelled (Fig 3.19D).

3.2.10 Expression of mCD8-GFP

As well as using GAP-GFP to label cells with *D42-Gal4* and *Toll-7-Gal4*, an alternative membrane-targeted GFP was also used: mCD8-GFP. In the embryos, the patterns of labelling were the same as with GAP-GFP. In the larval brain, mCD8-GFP driven by *Toll-7-Gal4* labelled cell bodies and axons in the VNC (Fig 3.20A). GFP was seen throughout the central brain and optic lobes, in a glial pattern, without obvious cell bodies or axons (Fig 3.20A). *D42>mCD8-GFP* in the larval CNS also labelled cells bodies and axons of the VNC (Fig 3.20B). In the central brain, there was strong GFP expression, and cells were also detected in the optic lobes (Fig 3.20B). Using both *Toll-7-Gal4* and *D42-Gal4* to drive expression of *mCD8-GFP* in the adult brain resulted in a broad pattern of labelling, with a large number of cells and brain region expressing GFP (Fig 3.20C-D).

3.3 Discussion

I have cloned the coding sequences of *Toll-7* and *Toll-6* to generate cDNA for each gene, and from these generated RNA probes and carried out *in situ* hybridisation. I have also generated

Fig 3.18 - *Toll-6* is expressed in the adult brain

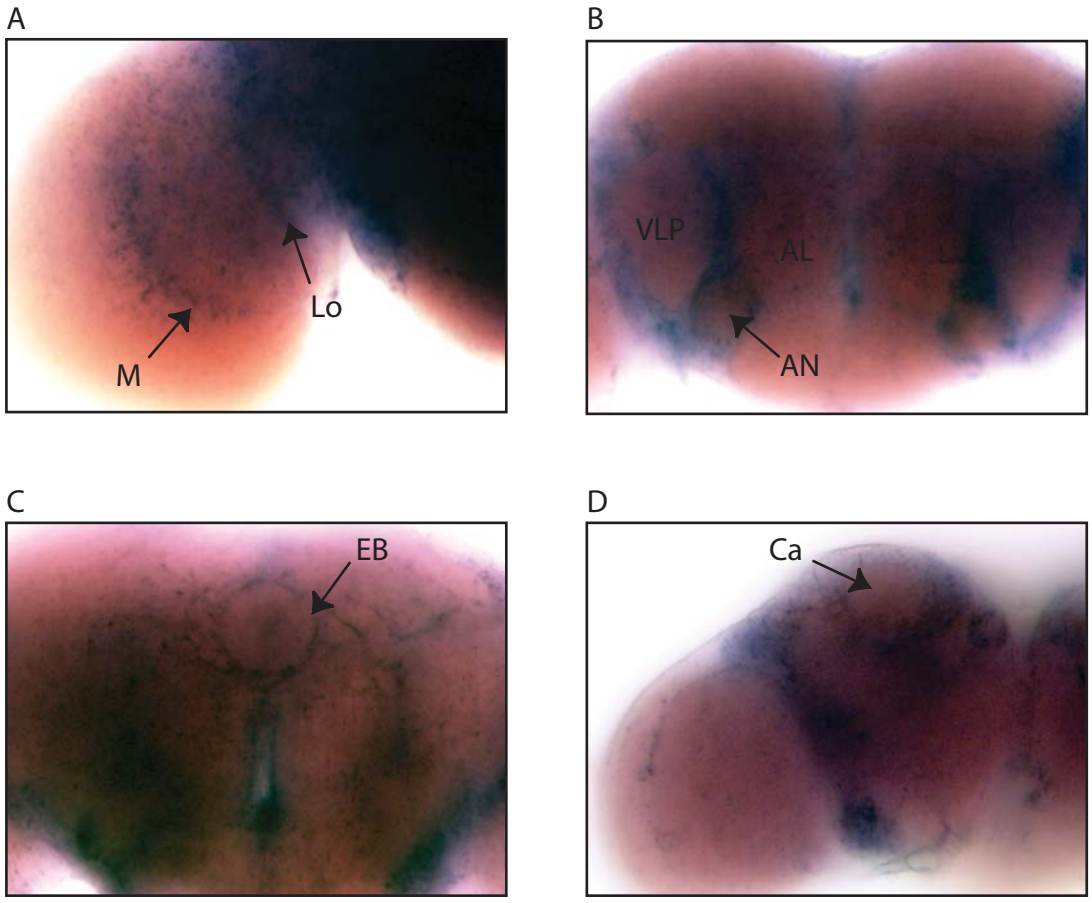

In situ hybridisation showing the distribution of *Toll-6* mRNA. (A) *Toll-6* is expressed in the medulla (M) and lobula (Lo). (B) *Toll-6* expression in the central brain surrounds the antennal nerve (AN), antennal lobe (AL), and the ventrolateral protocerebrum (VLP). (C) Signal is seen around the ellipsoid body (EB). (D) *Toll-6* is dected on the posterior brain, close to the calyx (Ca).

Fig 3.19 - *D42-Gal4* > *UAS-GAP-GFP* labels the adult brain

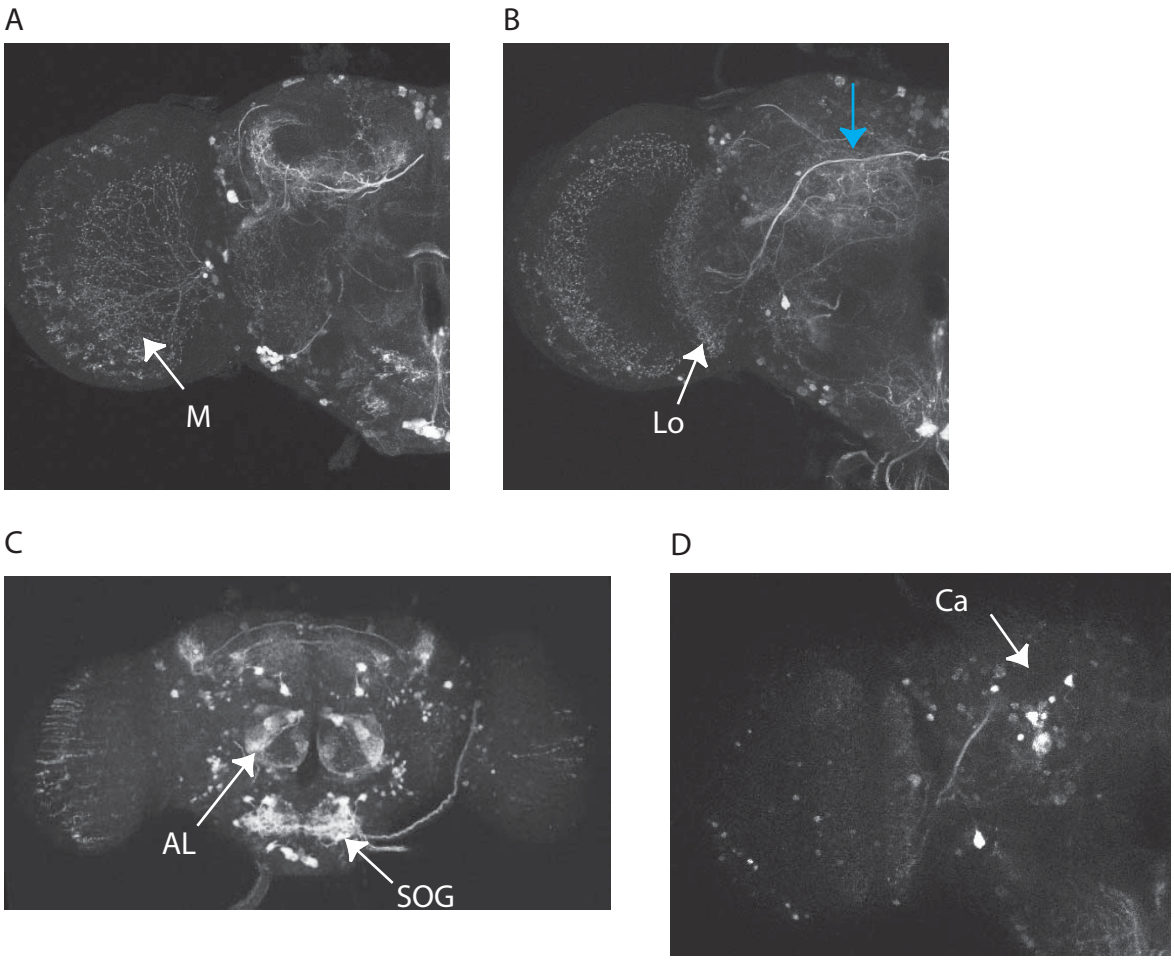

UAS-GAP-GFP driven by *D42-Gal4*, anti-GFP labelling with fluorescence. (A-B) GFP is expressed in the medulla (M) and lobula (Lo) of the optic lobe, with projections to the contralateral brain (blue arrow). (C) GFP labels central brain projection in the antennal lobe (AL) and the suboesophageal ganglion (SOG). (D) On the posterior brain, cells are detected around the calyx.

Fig 3.20 - Labelling of cells with mCD8 GFP

A

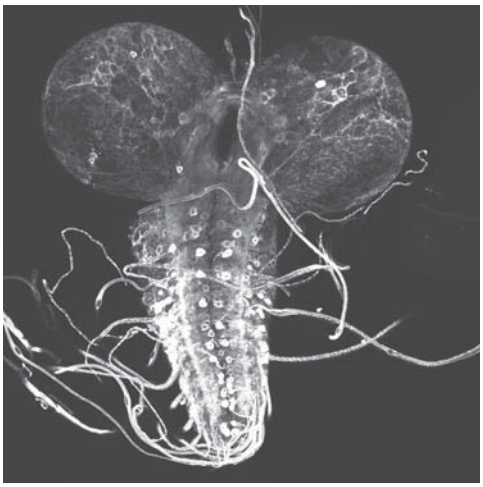

Toll-7 Gal4 > mCD8 GFP

B

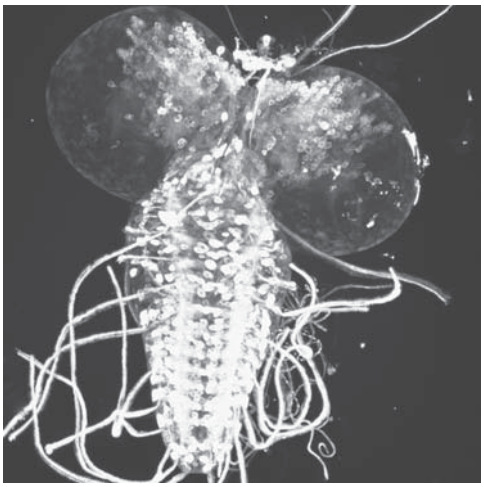

D42-Gal4 > mCD8 GFP

C

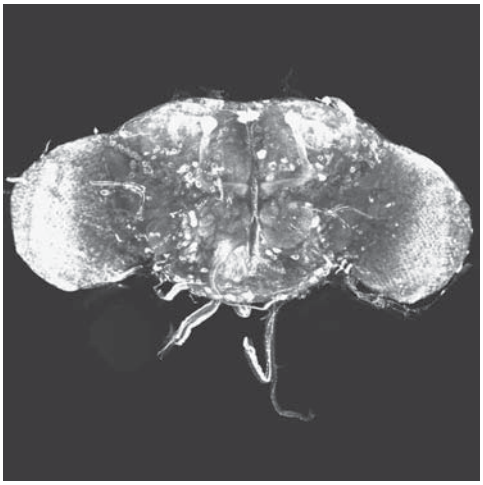

Toll-7 Gal4 > mCD8 GFP

D

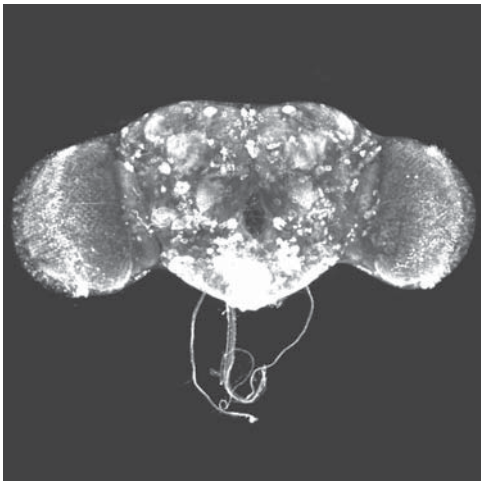

D42-Gal4 > mCD8 GFP

UAS-mCD8-GFP driven by *Toll-7-Gal4* (A, C), or by *D42-Gal4* (B, D). (A) Expression is seen throughout the brain hemispheres and in the VNC of the larval CNS. (B) There is expression in a large number of central brain cells, as well as in the VNC. (C, D) GFP is expressed broadly throughout the adult brain, in many central and optic lobe domains.

a *Toll-7-Gal4* fly line, and used this and the *D42-Gal4* line to examine the morphology of cells by expressing GAP-GFP. In embryos, *Toll-7* and *Toll-6* are expressed in the epidermis and CNS, with expression of both genes largely restricted to the CNS in late embryos. Expression of both *Toll-7* and *Toll-6* continues in the larval and adult CNS. GFP driven by *Toll-7-Gal4* and *D42-Gal4* labels CNS cell bodies and axons from embryos to adults, indicating that expressing cells include neurons.

In situ hybridisation identifies the endogenous expression of a gene. However, signal is restricted to the location of the mRNA: in neurons this is typically the soma. To characterise the cell type, double *in situ* experiments, or co-immunostaining for glial or neuronal markers could have been carried out.

Using Gal4 to drive membrane-targeted GFP can reveal the morphology of cells that normally express *Toll-7* or *Toll-6*. Given the amplification effect of the Gal4/UAS system, it can increase the sensitivity of detection. However, there are two drawbacks of this method. Firstly, the regulation of Gal4 is not identical to that of the gene of interest. In *Toll-7-Gal4*, only a portion of the upstream intergenic region was cloned into a pPTGAL: regulatory elements may have been missed that lie outside of the amplified fragment. And following transformation, the position in the genome of the *Toll-7-Gal4* construct may influence the expression of Gal4. In the D42-enhancer trap, the Gal4-P-element is placed 7kb upstream of *Toll-6*, and oriented on the minus strand (Sanyal, 2009). Therefore, the positional effects of enhancers and repressors could be lost. Since completing this work, the *Drosophila* genome has been re-annotated. A new gene is reported 4kb upstream of *Toll-6*, which lies closer to the D42-Gal4 insertion site. However, it is unclear whether this new sequence encodes a protein, or what its function might be. Secondly, GFP may still be detectable in cells even if *Toll-7* or

Toll-6 are no longer expressed. This perdurance is due to the amplifying effect of Gal4 and the stability of GFP within the cell. The temporal information about expression could be lost.

To overcome the limitations of the *in situ* hybridisation or GFP labelling methods, I combined the results of both to determine the expression of *Toll-7* and *Toll-6*. There was frequently overlap of *in situ* and GFP expression patterns, allowing the morphology of cells expressing GFP to be matched to the cell bodies with mRNA detected.

In embryos, *in situ* hybridisation of *Toll-7* mRNA and *Toll-7>GFP* both strongly labelled the CNS. Both the *in situ* and the GFP expression patterns were segmentally repeating from stage 13, and the CNS labelling became stronger as the embryo developed. The midline cells labelled by *in situ* could be the same midline DM cells labelled by GFP. This large overlap in patterns suggests that *Toll-7-Gal4* is recapitulating the endogenous expression of *Toll-7* mRNA in the CNS, and that Toll-7 is expressed in neurons. Outside of the CNS, the patterns of labelling dis not overlap as clearly. *Toll-7>GFP* did not label the precursors to the leg imaginal discs, as seen with the *in situ*. Conversely, the strong expression of GFP in the fat body and the ring gland was not evident with *in situ* hybridisation. In the larval CNS, there were similar patterns of labelling with *in situ* and *Toll-7>GFP* in the VNC and in the central brain. Again, the overlapping expression suggests that *Toll-7-Gal4* broadly reflected the endogenous expression of *Toll-7*. However, *Toll-7* mRNA detected in the optic lobes was not reflected by GFP expression, and the photoreceptors that are labelled by GFP lacked signal in the *in situ*. In the adult brain, the *in situ* and *Toll-7>GFP* patterns again complemented each other. In the central brain, there was extensive overlap of detection, particularly in the ventrolateral protocerebrum and the central complex. In the optic lobes, mRNA and GFP were both detected in the medulla, although the *Toll-7>GFP* expression in the lobula is not evident in the *in situ*. On the whole, *Toll-7-Gal4* drove expression of GAP-GFP in a cell population

that broadly corresponded to that detected by *in situ* hybridisation. This was particularly the case in the CNS, although there were exceptions outside of the nervous system. Therefore, it is likely that the cells detected by *in situ* were the same as those labelled by GAP-GFP, and that they include neurons.

Toll-6 mRNA was detected in the embryonic CNS, in segmentally repeating stripes at stage 13 increasing to broad expression throughout the VNC at stage 17. This pattern was mirrored by *D42-Gal4*-driven *GAP-GFP* expression, which also labelled the embryonic CNS with increasing intensity as it developed. However, the expression of GFP did not become as widespread as was seen with the *in situ*, suggesting that a subset of *Toll-6*-expressing cells were labelled using *D42-Gal4*. The labelling by GFP of axons indicates that these cells included neurons. Outside the embryonic CNS, *Toll-6* mRNA was detected in clusters of cells that run parallel to the VNC. *D42>GFP* labelled as sub-set of muscle cells, also running parallel to the VNC. However, the labelled muscles lie more laterally than the clusters of cells identified by *in situ*, so it is unlikely that the expression patterns overlap in this instance. In the larval CNS, there is a high degree of overlapping expression in the central brain and VNC. Both *Toll-6* mRNA and *D42>GFP* were detected in these regions, and both methods detected pairs of cells close to the dorsal midline. Therefore, it is likely that the same cells were being detected. Moreover, neither *Toll-6* mRNA nor *D42>GAP-GFP* were detectable in the developing retina. However, the labelling by *in situ* hybridisation of the optic lobes was not reflected by GFP expression. In the adult brain, the pattern of *Toll-6* mRNA and *D42>GAP-GFP* were largely complementary. The same patterns were observed in the optic lobes, with both the medulla and the lobula labelled. In the central brain, there was overlapping expression around the antennal nerve and the antennal lobe. Also, cells surrounding the calyx were seen with both methods, although no axons were labelled in the mushroom body with

GFP. However, the mRNA detected around the ellipsoid body is not reflected by GFP expression. Similarly to *Toll-7-Gal4*, *D42* drove expression in many regions that are labelled by *Toll-6 in situ* hybridisation, particularly in the nervous system. It is therefore likely that both methods were detecting the same cells. Given their morphology, these cells include neurons.

Both *UAS-GAP-GFP* and *UAS-mCD8-GFP* were used to label cells, by crossing lines to *Toll-7-Gal4* and *D42-Gal4*. Both of these GFP proteins are targeted to the membrane, but their patterns of labelling were different in the larval and adult CNS. GAP-GFP is a modified GFP construct, which contains the membrane-anchoring sequence from the GAP-43 protein (Moriyoshi et al., 1996). mCD8-GFP is a fusion protein of GFP and mouse CD8, a trans-membrane lymphocyte marker (Lee and Luo, 1999). In the larval VNC, both versions of GFP labelled cell bodies and axons (compare Fig 3.20A with Fig 3.8, and Fig 3.20B with Fig 3.17). However, the larval brains were differently labelled. With *Toll-7-Gal4*, GAP-GFP only labelled cell bodies and axons in the central brain, whereas mCD8-GFP labelled the entire hemispheres, in an apparently glial pattern. With *D42-Gal4*, GAP-GFP was only expressed in the central brain, but mCD8-GFP was more widely expressed, and was detected in cells of the optic lobes. However, the optic lobe expression of mCD8-GFP does not reflect the *Toll-6 in situ* pattern. In the adult brain, *Toll-7>GAP-GFP* labelled smaller populations of cells than *Toll-7>mCD8-GFP* (compare Fig 3.20C with Fig 3.10). mCD8-GFP was not detected in the fan-shaped body, whereas it was labelled with GAP-GFP and *Toll-7 in situ* hybridisation. Similarly with *D42-Gal4*, the discrete labelling with GAP-GFP contrasted with the broad expression of mCD8-GFP in the adult brain (compare Fig 3.20D with Fig 3.19). Since the *Gal4* drivers were the same, the differences in expression are most likely due to the different versions of GFP. The differences could be due to the length of time the two proteins last

within the cell. It is possible that mCD8-GFP can last longer, and therefore remain at the cell membrane after the expression of Gal4 has been switched off. This could explain why mCD8-GFP labels more cells than GAP-GFP. Alternatively, GAP-GFP could be more rapidly degraded, and its does not reach high enough levels in all cells to be detected. In this chapter, I have used GAP-GFP to label cells, since the patterns of expression more closely reflected the *in situ* patterns. It is intriguing that the two versions of GFP should behave differently, and this fact should be noted in the future when examining gene expression.

The expression of *Toll-7* and *Toll-6* in the adult brain suggests they could play a role in various brain functions. They were found in a number of key brain areas that are involved in the processing and integration of sensory input: the antennal lobe (olfactory), the suboesophageal ganglion (gustatory), and the ventrolateral protocerebrum (auditory, chemosensory and visual) (Masse et al., 2009, Miyazaki and Ito, 2010, Kamikouchi et al., 2006, Miyamoto and Amrein, 2008, Otsuna and Ito, 2006). *Toll-7* and *Toll-6* were also expressed in cells associated with higher brain functions, such as the central complex (central control of locomotion) and the Kenyon cells of the mushroom body (olfactory learning) (Strauss and Heisenberg, 1993, Masse et al., 2009). This suggests that, beyond development, *Toll-7* and *Toll-6* could be involved in higher neuronal functioning.

It was important to describe the expression of *Toll-7* and *Toll-6*, and to determine whether the patterns are consistent with them serving as DNT receptors. Both *Toll-7* and *Toll-6* are expressed in embryonic CNS neurons, and *Toll-7>GAP-GFP* labelled the ISNb motor axon at is muscle target. This complements the embryonic expression of the DNTs, which are found in the muscle (Zhu et al., 2008). In the larval CNS, *DNT1* is expressed in the VNC and the central brain (Sutcliffe, 2010), areas that are overlapped by both *Toll-7* and *Toll-6*. *DNT2* is expressed in the eye imaginal disc, and *DNT1* in the optic lobe, which is complemented by the

expression of *Toll-7* and *Toll-6* in the optic lobe. Similarly, in the adult visual system, *DNT2* is expressed in the retina and *DNT1* in the lamina (Sutcliffe, 2010, Zhu et al., 2008). *Toll-7* and *Toll-6* are expressed in the medulla, and *Toll-6* also in the lobula complex, which are downstream of the *DNT*-expressing tissues. Moreover, *Toll-7>GFP* and *D42>GFP* both reveal axons projecting from the optic lobes into the central brain. *Toll-7* and *Toll-6* are expressed in neurons, including those that project to *DNT*-expressing tissues, and others that overlap with *DNT*-expressing neurons. Therefore, the expression patterns of *Toll-7* and *Toll-6* are compatible with them serving as DNT receptors.

Toll-6 and *Toll-7* are broadly expressed in the *Drosophila* CNS, in patterns that are consistent with them interacting with the DNTs. In the following chapters I will look at the functional interactions between the Tolls and the DNTs, and the CNS functions of Toll-7 and Toll-6.

CHAPTER 4
TOLL-7 AND *TOLL-6* GENETICALLY INTERACT WITH THE DNTS

4.1 Introduction

Toll-7 and *Toll-6* are expressed in the *Drosophila* CNS from embryos to the adult, in patterns that often complement the expression of *DNT1* and *DNT2*. The aims of this chapter were to test if these two protein families interact in flies, by using two conventional genetic approaches. Firstly, genetic interactions between the mutant alleles of the *Toll*s and the *DNT*s were analysed. Secondly, genetic rescue experiments were carried out to attempt to rescue the lethality of spz^{2} and $DNT1^{41}DNT2^{e03444}$ double mutants.

For this, it was important to generate loss of function, null alleles for *Toll-7* and *Toll-6*. Since fly lines were available with P-element transposons close to the start of each gene, mutants could be generated by P-element excision (Adams and Sekelsky, 2002). P-elements are transposable elements, that are often found near to the 5' end of genes (Spradling et al., 1995). Inducing the excision of a P-element (so-called 'hopping-out') can lead to a number of possible outcomes, which can have varying effects on the function of the nearby gene (Adams and Sekelsky, 2002). This can be done by expressing *Δ2-3 Transposase*, which induces the mobilisation of P-elements from the genome (Robertson et al., 1988). One possible outcome is an imprecise excision, when some of the genomic DNA flanking the insertion is also removed (Daniels et al., 1985, Salz et al., 1987). This creates a small deletion in the chromosome. Screening by PCR can identify flies carrying deletions that, if large enough,

could have resulted in the loss of part or all of the gene's coding sequence. Sequencing can then be used to confirm the precise nature of the lesion.

Mutant alleles of *DNT1* and *DNT2* interact *in vivo*, and this can be seen by looking at lethality (Sutcliffe, 2010). $DNT1^{41}DNT2^{e03444}$ mutants can be maintained as a viable homozygous stock. However, $DNT1^{41}DNT2^{eo3444}$ homozygotes are semi-lethal as progeny of a heterozygous stock, when balanced over the *TM6B* chromosome and maintained at 18°C. Under these conditions, there are very few homozygous, Tb^{+} pupae (survival index ≈ 0). With $DNT1^{41}$/*TM6B* and $DNT2^{e03444}$/*TM6B* single mutants, homozygous Tb^{+} pupae can be counted at near wild-type rates (survival index ≈ 1). The genetic interaction between *DNT1* and *DNT2* was revealed by a survival index <1. Thus, by counting the number of *TM6B* and Tb^{+} pupae in combinations of *Toll-7, Toll-6* and *DNT* double mutants, kept at 18°C, potential genetic interactions can be tested. For details on how the survival index is calculated, see section 2.1.5, materials and methods. In addition to $DNT1^{41}$ and $DNT2^{e03444}$ there is a hypomorphic allele of *spz*. The spz^{2} allele encodes a protein with a single amino acid substitution in the pro-domain (Weber et al., 2007), and around 7% of flies pupate as homozygotes. It is unknown whether *DNT1*, *DNT2*, *Toll-7* or *Toll-6* also genetically interact with *spz*.

Genetic rescue experiments provide further information about the relationships between genes, and shared signalling pathways. And a key experiment to test whether Toll-7 and Toll-6 are receptors for DNT1 and DNT2 is to test if overexpression of constitutively active forms of the receptors can rescue the mutant phenotypes of the DNT mutants. *Toll-7* and *Toll-6* are paralogues of *Toll*, and share the same general protein structure. Therefore the molecularly characterised constitutively active *Toll* receptors, which signal in the absence of ligand, can be used as a guide to generate activated *Toll-7* and *Toll-6*. The deletion of the entire extracellular domain results in a constitutively active Toll receptor: $Toll^{\Delta LRR}$ (Winans and Hashimoto,

1995). Truncating *Toll-7* and *Toll-6* in the same way may also produce activated receptors. Alternatively, the $Toll^{10b}$ mutant allele encodes a protein with an amino acid substitution of cysteine to tyrosine in the extracellular domain (Schneider et al., 1991). This cysteine is within the Cys-rich cluster lying closest to the membrane, and is thought to play a role in inhibiting Toll signalling in the absence of ligand (Hu et al., 2004). The auto-inhibition is released when the cysteine is mutated. The cysteine is in a conserved position in Toll-7 and Toll-6, and it is anticipated that mutating the equivalent residue in these genes will create constitutively active receptors.

4.2 Results

4.2.1 Generation of *Toll-7* null alleles by P-element imprecise excision

A P-element mobilisation and PCR screen was carried out by Janine Fenton, the technician in our lab, before I arrived. *GE17034* flies carry a P-element 383bp upstream of the ATG start codon of *Toll-7*. The P-element was mobilised by expressing *Δ2-3 transposase*, and the mutated chromosome was recovered and balanced stocks were established, using genetic protocol H (Fig 2.6, materials and methods). P-element mobilisation of these flies generated 129 lines representing unique excision events, identified as white-eyed males. 72 of these lines were screened by PCR using primers 7.1-7.7 (Table 2.3, materials and methods), identifying 6 as potential mutants, including $Toll\text{-}7^{P8}$ and $Toll\text{-}7^{P114}$. A region of genomic DNA was amplified by PCR, with forward primer 7.2 and reverse primer 7.4, which are located either side of the original P-element insertion site. In wild-type flies, these primers amplify a 2.1kb fragment of DNA. The amplified fragments in these mutants were smaller ($Toll\text{-}7^{P8}$ = 1.2kb, $Toll\text{-}7^{P114}$ = 1.6kb), indicating a deletion of the genome (Fig 4.1A). To molecularly characterise the break-points in these mutant lines, the genomic DNA fragment

was sequenced by J Fenton. In both cases, the deletion removed the ATG start codon of *Toll-7*, the signal peptide, and the first few amino acids (Fig 4.1B). They are therefore protein null alleles, and will be used throughout this work.

4.2.2 Generation of *Toll-6* null alleles by P-element imprecise excision

A P-element mobilisation was carried out with the help of Janine Fenton and Sarah Quail, an undergraduate student. *GE26951* flies carry a P-element 154 base-pairs upstream of the ATG start codon of *Toll-6*, which was excised using Protocol I (Fig 2.7, materials and methods). 505 stocks were established from white-eyed males, representing unique excision events of the *GE26951* P-element. Of these lines, 366 were screened by PCR for a deletion in the genomic DNA using primers 6.1-6.10 (Table 2.4, materials and methods). 10 lines were identified as potential mutants, including $Toll\text{-}6^{26}$ and $Toll\text{-}6^{31}$. A region of genomic DNA was amplified by PCR, with forward primer 6.2 and reverse primer 6.8, which are located either side of the original P-element insertion site. In wild-type flies, these primers amplify a 3.4kb fragment of DNA. The fragment amplified in these mutants were smaller ($Toll\text{-}6^{26}$ = 1.9kb, $Toll\text{-}6^{31}$ = 1.6kb), indicating a deletion in the genome (Fig 4.2A). To molecularly identify the break-points in these lines, genomic DNA fragment was sequenced by J Fenton. In both cases, the deletion eliminates the initiating ATG start codon for *Toll-6*, and uncovers the sequences encoding the signal peptide and the first few amino acids (Fig 4.2B). These are therefore protein null alleles.

4.2.3 Genetic interactions between *Toll-7*, *Toll-6*, *DNT1* and *DNT2*

Using the survival index to measure viability, I tested whether there are functional interactions between the DNTs and Toll-7 and Toll-6. $DNT1^{41}$, $Toll\text{-}7^{P8}$ and $Toll\text{-}7^{P114}$ single

Fig 4.1 - *Toll-7* mutagenesis by imprecise P-element excision

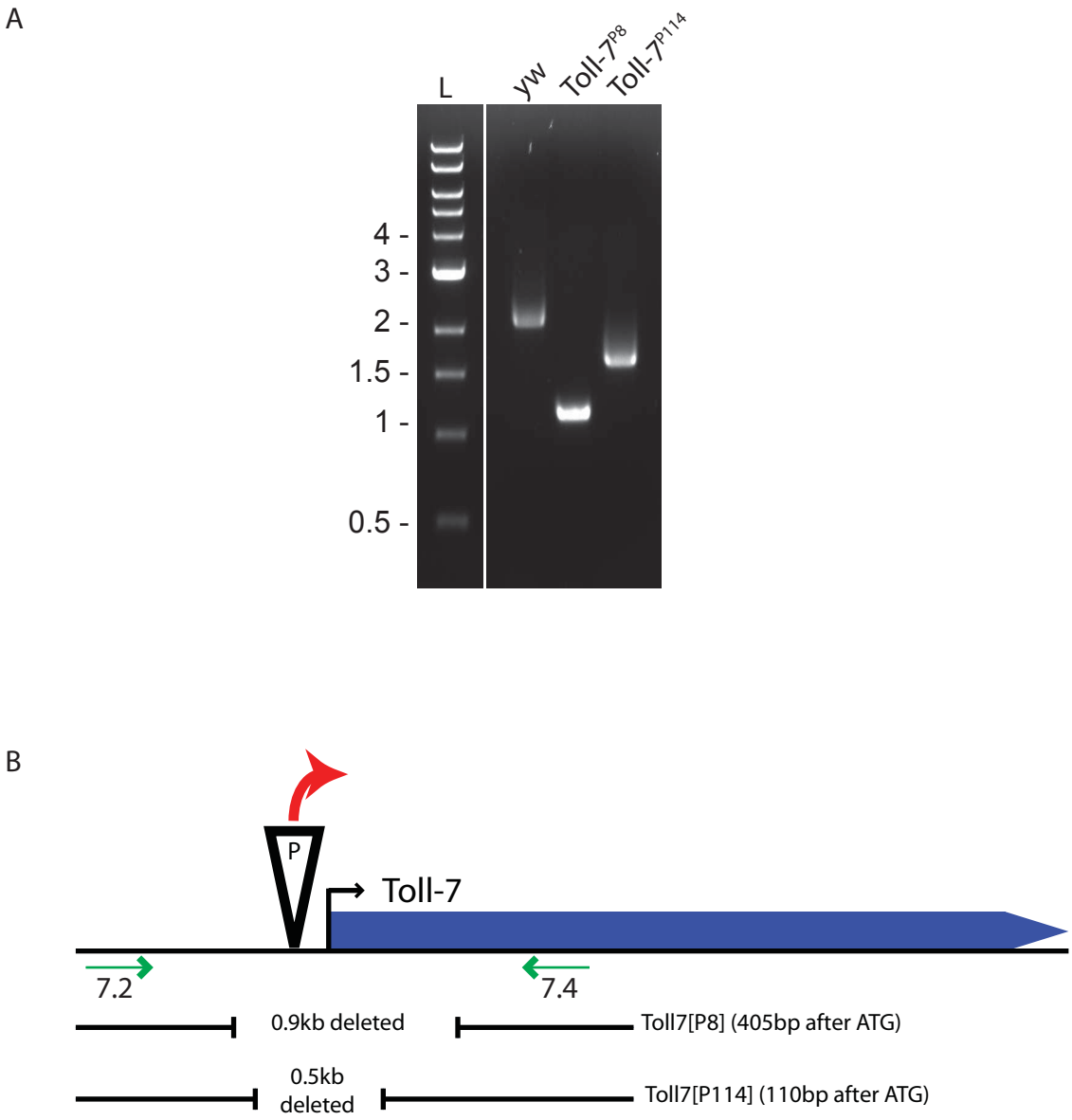

Mutant alleles of *Toll-7* were generated by P-element mobilisation. (A) PCR of genomic DNA revealed two lines with deletions. (B) Sequencing confirmed that the deletions uncovered the start codon of *Toll-7* and the first few amino acids. Primer sites used in (A) are indicated by green arrows. The forward primer was 7.2, located 1kb upstream of the start of *Toll-7*; the reverse primer was 7.4, located 1kb into the *Toll-7* gene.

Fig 4.2 - Toll-6 mutagenesis by imprecise P-element excision

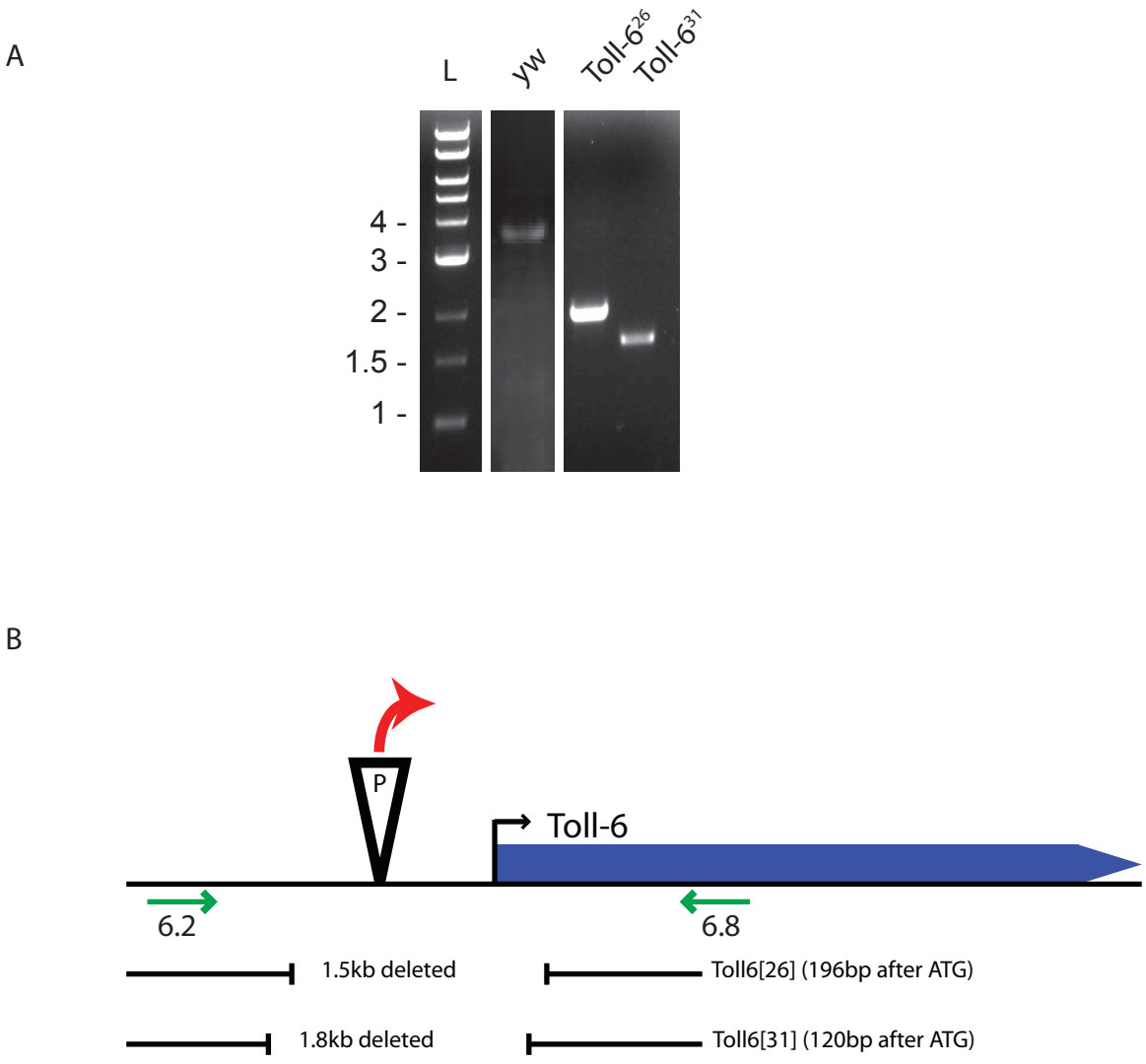

Mutant alleles of *Toll-6* were generated by P-element mobilisation. (A) PCR of genomic DNA revealed two lines with deletions. (B) Sequencing confirmed that the deletions uncovered the start codon of *Toll-6* and the first few amino acids. Primer sites used in (A) are indicated by green arrows. The forward primer is 6.2, located 2kb upstream of the start of *Toll-6*; the reverse primer is 6.8, located 1.9kb into the *Toll-6* coding sequence.

mutants showed a reduced viability to approximately half that of controls (Fig 4.3A). The *DNT2*^{e03444} mutant showed slightly reduced viability compared to controls, while *Toll-6*^{26} and *Toll-6*^{31} mutant alleles showed no effect on viability (Fig 4.3A).

I next looked at various combinations of alleles for *Toll-6*, *Toll-7* and the *DNT*s. As previously reported (Sutcliffe, 2010), *DNT2*^{e03444}*DNT1*$^{41/}$*TM6B* double mutants had a greatly reduced viability. Similarly, *Toll-7*^{P8}*Toll-6*^{26}*/SM6aTM6B* and *Toll-7*^{P114}*Toll-6*^{31}*/SM6aTM6B* double mutants were semi-lethal, with a very low survival index (Fig 4.3B). Loss of the two receptors phenocopied the loss of the two DNTs. I observed a similar reduction in viability in *DNT1*^{41}*Toll-6*^{26}*/TM6B* and *Toll-7*^{P114}*;DNT2*^{e03444}*/SM6aTM6B* double mutants (Fig 4.3B). This suggests removing one DNT and one Toll is the equivalent of removing both DNTs or both Tolls, that there could be two ligand-receptor pairs. This could indicate functional interactions between DNT1 and Toll-7, and between DNT2 and Toll-6. The survival index of the *DNT2*^{e03444}*Toll-6*^{26}*/SM6aTM6B* double mutants was similar to *DNT2*^{e03444}*/TM6B* and *Toll-6*^{31}*/TM6B* single mutants (Fig 4.3A, B). This is consistent with the notion that these genes are components in the same signalling pathway. *Toll-7*^{P114}*;DNT1*^{41}*/SM6aTM6B* double mutants showed a strongly reduced viability (Fig 4.3B). This was much lower than either of the single mutants, and could point to promiscuity of binding.

Finally, I combined alleles of *DNT1*, *DNT2*, *Toll-7* and *Toll-6* with *spz*. The *spz*^{2} allele had a low survival index (Fig 4.3C). The combination of *spz*^{2} and *DNT2*^{e03444} showed a slightly reduced viability, while *spz*^{2}*DNT1*^{41} double mutants were fully lethal (Fig 4.3C). When placed in a *spz*^{2} mutant background, both *Toll-7*^{P8} and *Toll-6*^{26} mutant alleles were lethal (Fig 4.3C). This is consistent with Toll-6 and Toll-7 playing roles in DNT signalling.

Fig 4.3 - Toll-7 and Toll-6 genetically interact with DNTs

A

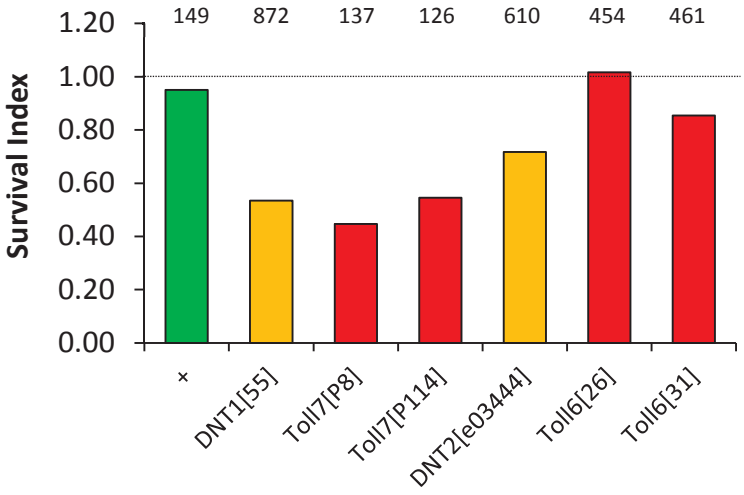

B

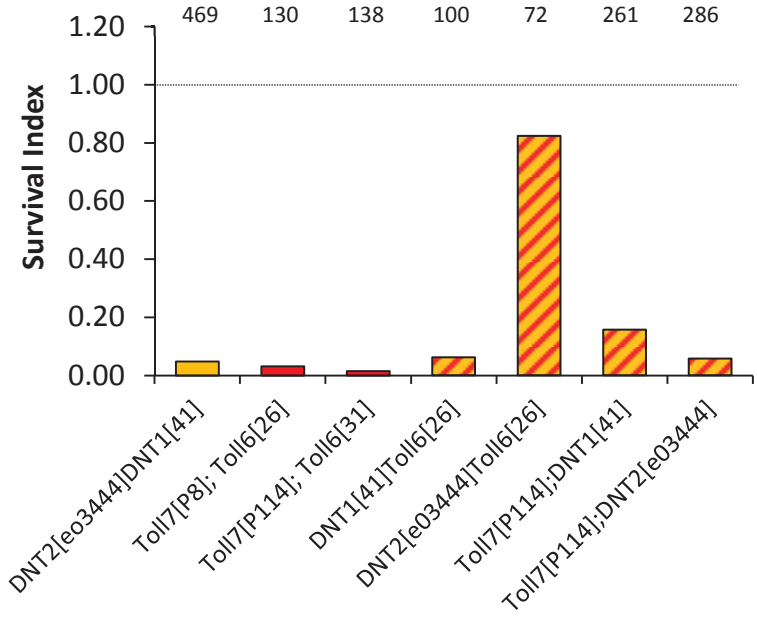

C

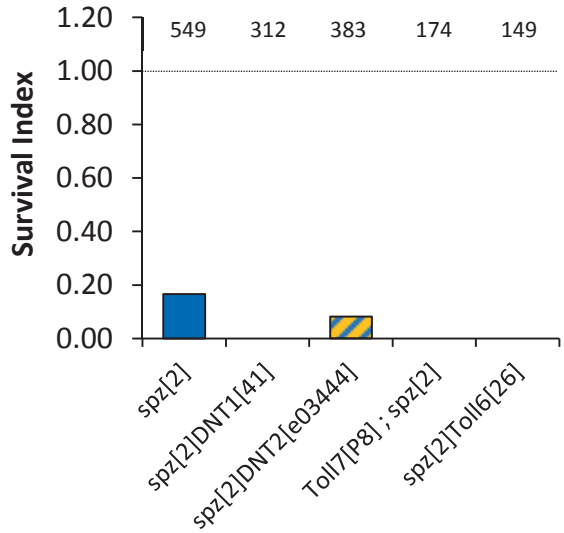

Fig 4.3 – Toll-7 and Toll-6 genetically interact with DNTs
Graphs showing the survival index of *Toll* and *DNT* mutants. (A) Control flies have a survival index of approximately 1 (green bar). Single mutant flies have mild/no lethality phenotype. (B) Double mutant flies all show strongly reduced viability, except $DNT2^{e03444}Toll\text{-}6^{26}$, indicating genetic interaction between *Toll-7*, *Toll-6*, *DNT1* and *DNT2*. (C) The semi-lethal phenotype of spz^{2} is enhanced in the lethal combinations with *DNT1*, *Toll-7* and *Toll-6*. Orange indicates *DNT1* and *DNT2* mutants, red indicates *Toll-7* and *Toll-6* mutants, blue indicates *spz* mutants, double mutants are coloured accordingly. Total numbers of pupae counted is indicated above bars. Full genotypes, from left to right are: (A) $+/TM6B$, $DNT1^{55}/TM6B$, $Toll\text{-}7^{P8}$;$+/SM6aTM6B$; $Toll\text{-}7^{P114}$;$+/SM6aTM6B$, $DNT2^{e03444}/TM6B$, $Toll\text{-}6^{26}/TM6B$, $Toll\text{-}6^{31}/TM6B$, (B) $DNT2^{e03444}DNT1^{41}/TM6B$, $Toll\text{-}7^{P8}$;$Toll\text{-}6^{26}/SM6aTM6B$, $Toll\text{-}7^{P114}$;$Toll\text{-}6^{31}/SM6aTM6B$; $DNT1^{41}Toll6^{26}/TM6B$, $DNT1^{e03444}Toll\text{-}6^{26}/TM6B$, $Toll\text{-}7^{P114}$;$DNT1^{41}/SM6aTM6B$, $Toll\text{-}7^{P114}$;$DNT2^{e03444}/SM6aTM6B$, (C) $spz^{2}/TM6B$, $spz^{2}DNT1^{41}/TM6B$, $spz^{2}DNT2^{e03444}/TM6B$, $Toll\text{-}7^{P8}$;$spz^{2}/SM6aTM6B$, $spz^{2}Toll\text{-}6^{26}/TM6B$

4.2.4 Rescue of *Toll-7Toll-6* mutant lethality by activated *Toll-7* and *Toll-6*

Two versions of constitutively active *Toll-7* and *Toll-6* receptor constructs were made, following the example of the activated Toll constructs: $Toll^{\Delta LRR}$ and $Toll^{10b}$. For details on how the constructs were generated, see section 2.2.9, materials and methods. Similarly to $Toll^{\Delta LRR}$, the extracellular domain of *Toll-7* and *Toll-6* was deleted, yielding $Toll\text{-}7^{\Delta LRR}$ and $Toll\text{-}6^{\Delta LRR}$. The constructs were placed into expression clones downstream of UAS, with an attB sequence in the clone for φC31-mediated fly transgenesis. $Toll^{10b}$ is a constitutively active *Toll* allele, with a cysteine to tyrosine point mutation in the extracellular domain. The equivalent cysteine residue was mutated in *Toll-7* (Cys 993) and *Toll-6* (Cys 1020), yielding $Toll\text{-}7^{Cys\text{-}Tyr}$ and $Toll\text{-}6^{Cys\text{-}Tyr}$ constructs. These were placed into P-element-containing expression clones downstream of UAS, for Transposase-mediated fly transgenesis. Expression of the constitutively active receptors in flies was driven using the Gal4/UAS system (see methods).

I first asked whether activated *Toll-7* and *Toll-6* constructs can rescue the receptor double mutant phenotype. $Toll\text{-}7^{P8}Toll\text{-}6^{26}$ double mutants display a semi-lethal phenotype at 18°C in an *SM6aTM6B*-balanced stock. I expressed either $Toll\text{-}7^{\Delta LRR}$, $Toll\text{-}6^{\Delta LRR}$ or $Toll\text{-}7^{Cys\text{-}Tyr}$ in cholinergic neurons with the *ChaGal4* driver, in a $Toll\text{-}7^{P8};Toll\text{-}6^{26}/SM6aTM6B$ double mutant background. The *ChaGal4* driver was used, because it drives expression in a large proportion of neurons. The pan-neuronal *elavGal4* driver could not be recombined with *Toll-6* mutant alleles, and was therefore not used in rescue experiments with *Toll-7Toll-6* double mutants. $Toll\text{-}6^{\Delta LRR}$ and $Toll\text{-}7^{\Delta LRR}$ partially, but significantly, rescued the lethality of the receptor double mutants; expressing $Toll\text{-}7^{Cys\text{-}Tyr}$ rescued the mutants slightly more than the ΔLRR receptors (Fig 4.4). Unfortunately, I was unable to generate the fly stocks to test the

effect of *Toll-6*$^{Cys\text{-}Tyr}$ on lethality. Expressing activated receptors in neurons partially rescued the *Toll-7*^{P8}*Toll-6*^{31} double mutant lethality, indicating that to some extent, this is a nervous system phenotype and that the receptors are functional.

4.2.5 Rescue of *DNT* mutant lethality by activated *Toll-7* and *Toll-6*

I next tested whether expressing activated *Toll-7* or *Toll-6* receptors could rescue the semi-lethal phenotype of the *DNT1*^{41}*DNT2*^{e03444} double mutant. Activated receptor constructs were expressed in all neurons with the *elavGal4* driver, in a *DNT2*^{e03444}*DNT1*^{41}*/TM6B* double mutant background. *Toll-7*$^{\Delta LRR}$ and *Toll-6*$^{\Delta LRR}$ rescued the lethality of *DNT1DNT2* double mutant (Fig 4.5A). *Toll-7*$^{Cys\text{-}Tyr}$ and *Toll-6*$^{Cys\text{-}Tyr}$ also rescued the *DNT1DNT2* double mutant lethality, above the rescue by ΔLRR constructs (Fig 4.5A). Moreover, neuronal expression of *UAS-Toll*^{10b}, the *Toll* equivalent of the Cys-Tyr constructs, also rescued the *DNT1DNT2* double mutant lethality. These rescues indicate that Toll-7 and Toll-6 share a common function with the DNTs, and are acting downstream of the ligands.

Spz is also a DNT, so I asked whether activating Toll-7 or Toll-6 in neurons could rescue the lethality of *spz* mutants. Therefore activated receptors were expressed in all neurons in a *spz*^{2} mutant background. *Toll-7*$^{\Delta LRR}$ and *Toll-6*$^{\Delta LRR}$ both rescued the semi-lethality of *spz*^{2} (Fig 4.5B). This result, together with the rescue of *DNT1*^{41}*DNT2*^{e03444} lethality will *Toll*^{10b}, shows that activated receptors can substitute for each other, and suggests that DNTs and Tolls share the same signalling pathways.

4.3 Discussion

In this chapter (with the help of Janine Fenton and Sarah Quail) I have generated null mutants of *Toll-7* and *Toll-6* by imprecise excision of P-elements. Using genetic interactions, I have

Fig 4.4 – Constitutively active receptors rescue Toll-7Toll-6 mutant lethality

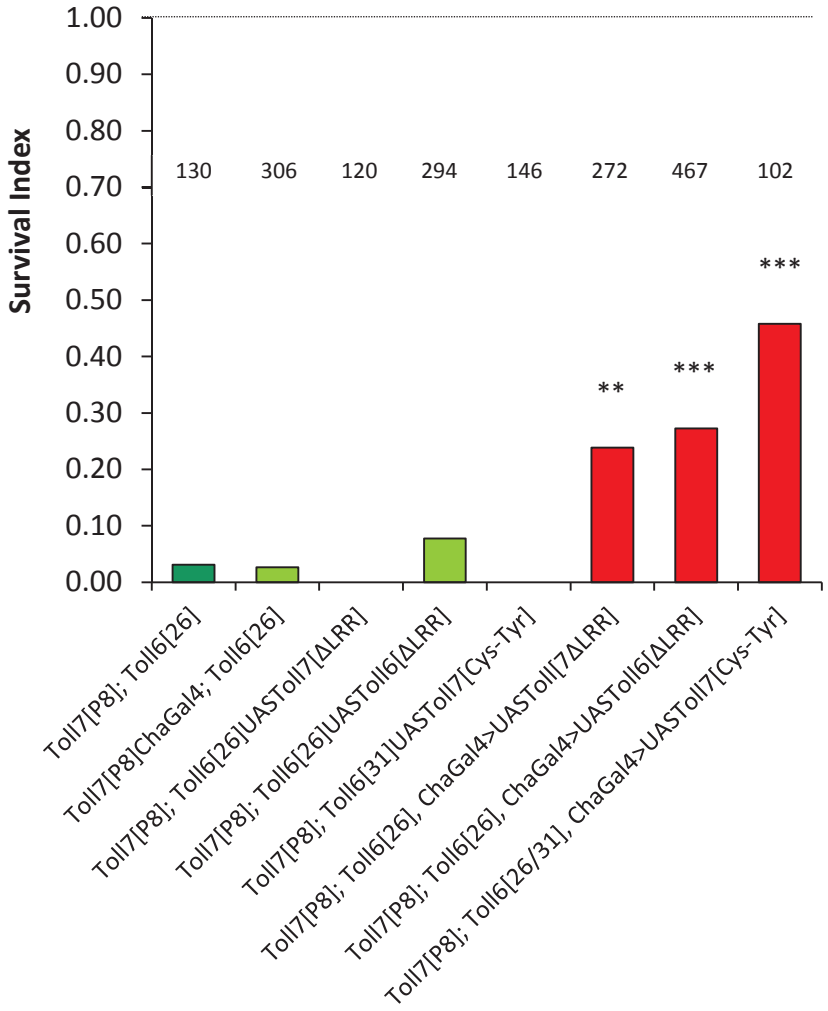

The survival index of *Toll-7Toll-6* mutants indicates a semi-lethal phenotype. This is rescued by expression in cholinergic neurons of *Toll-6$^{\Delta LRR}$*, *Toll-7$^{\Delta LRR}$*, or *Toll-7$^{Cys\text{-}Tyr}$*. Controls in green, rescues in red, **p<0.01, ***p<0.001 Fisher's exact test compared to *Toll7^{P8};Toll6^{26}*, total numbers of counted pupae indicated above bars, full genotypes from left to right are *Toll-7^{P8};Toll-6^{26}/SM6aTM6B, Toll-7^{P8}ChaGal4;Toll-6^{26}/SM6aTM6B, Toll-7^{P8};Toll-6^{26}UASToll-7$^{\Delta LRR}$/SM6aTM6B, Toll-7^{P8};Toll-6^{26}UASToll-6$^{\Delta LRR}$/SM6aTM6B, Toll-7^{P8};Toll-6^{31}UASToll-7$^{Cys\text{-}Tyr}$/SM6aTM6B, Toll-7^{P8}ChaGal4;Toll-6^{26}/SM6aTM6B x Toll-7^{P8};Toll-6^{26}UASToll-7$^{\Delta LRR}$/SM6aTM6B, Toll-7^{P8}ChaGal4;Toll-6^{26}/SM6aTM6B x Toll-7^{P8};Toll-6^{26}UASToll-6$^{\Delta LRR}$/SM6aTM6B, Toll-7^{P8}ChaGal4;Toll-6^{26}/SM6aTM6B x Toll-7^{P8};Toll-6^{31}UASToll-7$^{Cys\text{-}Tyr}$/SM6aTM6B*

Fig 4.5 - Constitutively active *Toll* paralogues rescue *DNT* mutant lethality

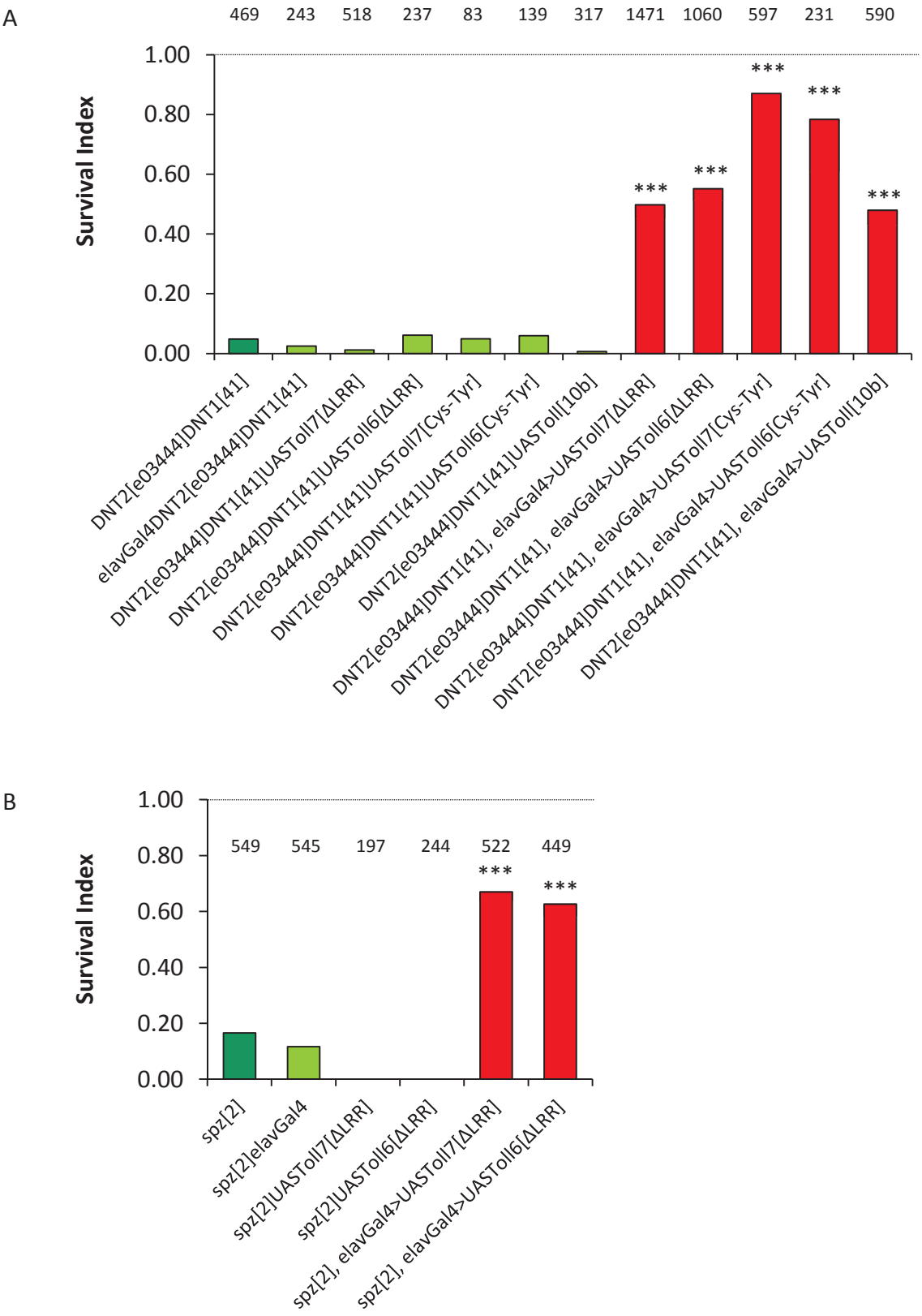

Fig 4.5 - Constitutively active *Toll* paralogues rescue *DNT* mutant lethality
(A) The survival index of *DNT1DNT2* mutants indicates a semi-lethal phenotype. This is rescued by expression in all neurons of constitutively active receptors. (B) *Toll-7*$^{\Delta LRR}$ and *Toll-6*$^{\Delta LRR}$ *rescue* the lethality of *spz*^{2} mutants. Mutants in dark green, controls in light green, rescues in red, ***p<0.001 compared to (A) *DNT2*^{e03444}*DNT1*^{41}, or (B) *spz*^{2}, Fisher's exact test, total numbers of pupae counted indicated above bars, full genotypes from left to right are (A) *DNT2*^{e03444}*DNT1*^{41}/*TM6B, elavGal4DNT2*^{e03444}*DNT1*^{41}/*TM6B, DNT2*^{e03444}*DNT1*^{41}*UASToll-7*$^{\Delta LRR}$/*TM6B, DNT2*^{e03444}*DNT1*^{41}*UASToll-6*$^{\Delta LRR}$/*TM6B, UASToll-7*$^{Cys\text{-}Tyr}$/*UASToll-7*$^{Cys\text{-}Tyr}$*;DNT2*^{e03444}*DNT1*^{41}/*TM6B, DNT2*^{e03444}*DNT1*^{41}*UASToll-6*$^{Cys\text{-}Tyr}$/*TM6B, UASToll*^{10b}/*UASToll10b;DNT2*^{e03444}*DNT1*^{41}/*TM6B, elavGal4DNT2*^{e03444}*DNT1*^{41}/*TM6B x DNT2*^{e03444}*DNT1*^{41}*UASToll-7*$^{\Delta LRR}$/*TM6B, elavGal4DNT2*^{e03444}*DNT1*^{41}/*TM6B x DNT2*^{e03444}*DNT1*^{41}*UASToll-6*$^{\Delta LRR}$/*TM6B, elavGal4DNT2*^{e03444}*DNT1*^{41}/*TM6B x UASToll-7*$^{Cys\text{-}Tyr}$/*UASToll-7*$^{Cys\text{-}Tyr}$*;DNT2*^{e03444}*DNT1*^{41}/*TM6B, elavGal4DNT2*^{e03444}*DNT1*^{41}/*TM6B x DNT2*^{e03444}*DNT1*^{41}*UASToll-6*$^{Cys\text{-}Tyr}$/*TM6B, elavGal4DNT2*^{e03444}*DNT1*^{41}/*TM6B x UASToll10b/UASToll*^{10b}*;DNT2*^{e03444}*DNT1*^{41}/*TM6B*, (B) *spz*^{2}/*TM6B, elavGal4spz*^{2}/*TM6B, UASToll-7*$^{\Delta LRR}$*spz*^{2}/*TM6B, UASToll-6*$^{\Delta LRR}$*spz*^{2}/*TM6B, elavGal4spz*^{2}/*TM6B x UASToll-7*$^{\Delta LRR}$*spz*^{2}/*TM6B, elavGal4spz*^{2}/*TM6B x UASToll-6*$^{\Delta LRR}$*spz*^{2}/*TM6B.*

shown that *Toll-7Toll-6* double mutants phenocopy *DNT1DNT2* double mutants, and that the genes interact *in vivo*. These experiments suggest an interaction between Toll-7 and DNT1, and Toll-6 and DNT2. I have also generated constitutively active receptor constructs by removing the extracellular domain or mutating a conserved cysteine residue, and have obtained transgenic flies to express the activated receptors using the Gal4/UAS system. I finally showed that expressing constitutively active receptors in the nervous system rescues the semi-lethal phenotype of *Toll-7Toll-6*, *DNT1DNT2*, and *spz* mutants.

DNT1DNT2 mutants are viable, and can survive as a homozygous stock. The semi-lethal phenotype is revealed when heterozygous flies balanced with TM6B are crossed and maintained at 18°C. The lower temperature apparently sensitises the alleles, resulting in the observed lethality. It is unusual for temperature-sensitive effects to manifest at lower temperature: most conditional alleles show their phenotype at higher temperatures. However, temperature can have broad, non-specific effects on neuronal structure and function, beyond specific temperature-sensing pathways. At the NMJ, higher temperatures promote axonal branching, synaptic transmission and corresponding enhancement of locomotion (Sigrist et al., 2003, Zhong and Wu, 2004). These effects, as well as temperature-dependent plastic changes in the central brain, are correlated with changes in ion channel activity and cAMP signalling (Peng et al., 2007). It is possible that the 18°C condition is restricting neuronal function, and that this is enhancing the interaction between DNTs and Tolls. Lower temperatures have also been shown to enhance phenotypes of NFκB mutant alleles in flies (Ayyar et al., 2007). Spz is known to signal through the NFκB paralogues Dorsal and Dif (Manfruelli et al., 1999, Meng et al., 1999). Therefore the low temperature-sensitivity of NFκB may be contributing to the lethal phenotype seen with this assay. Although it is not entirely clear why lower temperature sensitises this phenotype, it has been a useful assay to

employ. The results are reproducible (Sutcliffe, 2010), and have revealed functional interactions between Toll-7 and Toll-6 and the DNTs.

Looking at various double mutant combinations of *DNT1*, *DNT2*, *Toll-6* and *Toll-7*, I have seen a genetic interaction between the ligands and the receptors. To some extent, the data suggest that there are two parallel signalling pathways. Removing both ligands causes the same lethal phenotype as removing both receptors (Fig 4.6A). Lethality is also seen on removing *DNT1* and *Toll-6*, or *DNT2* and *Toll-7* (Fig 4.6B). Therefore, in a *DNT1* mutant background, loss of *Toll-6* phenocopies loss of *DNT2*; in a *DNT2* mutant background, loss of *Toll-7* phenocopies loss of *DNT1*. This is consistent with DNT1 and Toll-7 acting as one ligand receptor pair, DNT2 and Toll-6 acting as another pair. Moreover, removing *DNT2* and *Toll-6* does not enhance the phenotype of *DNT2* or *Toll-6* single mutants, consistent with them acting in the same pathway. The semi-lethal interaction of *Toll-7* with *DNT1*, however, demonstrates that this represents a simplified model. The fact that the *Toll-7DNT1* double mutant phenotype is stronger than the single mutants could be explained by promiscuity in ligand-receptor interactions. This is seen in some other contexts, including the binding of vertebrate neurotrophins to the Trk family of receptors (Reichardt, 2006). The spz^{2} allele interacts differently with $DNT2^{e03444}$ and $Toll\text{-}6^{26}$, which further suggests that the relationships between the ligands and receptors are not straight-forward pairings.

The *Toll-7Toll-6* double mutant semi-lethality over *SM6aTM6B* at 18°C is partially rescued by expressing $Toll\text{-}7^{\Delta LRR}$, $Toll\text{-}6^{\Delta LRR}$ and $Toll\text{-}7^{Cys\text{-}Tyr}$ in neurons. This means that, to some extent, the lethality is due to a loss of *Toll-7* and *Toll-6* in the nervous system. However, the rescue is not to control viability. This could because *ChaGal4*, specific to cholinergic neurons, is not driving expression in all the neurons required for survival. It is possible that a higher degree of rescue might have been reached if the activated receptors were expressed in

Fig 4.6 - Semi-lethal combinations of alleles indicate functional interactions between DNTs and Tolls

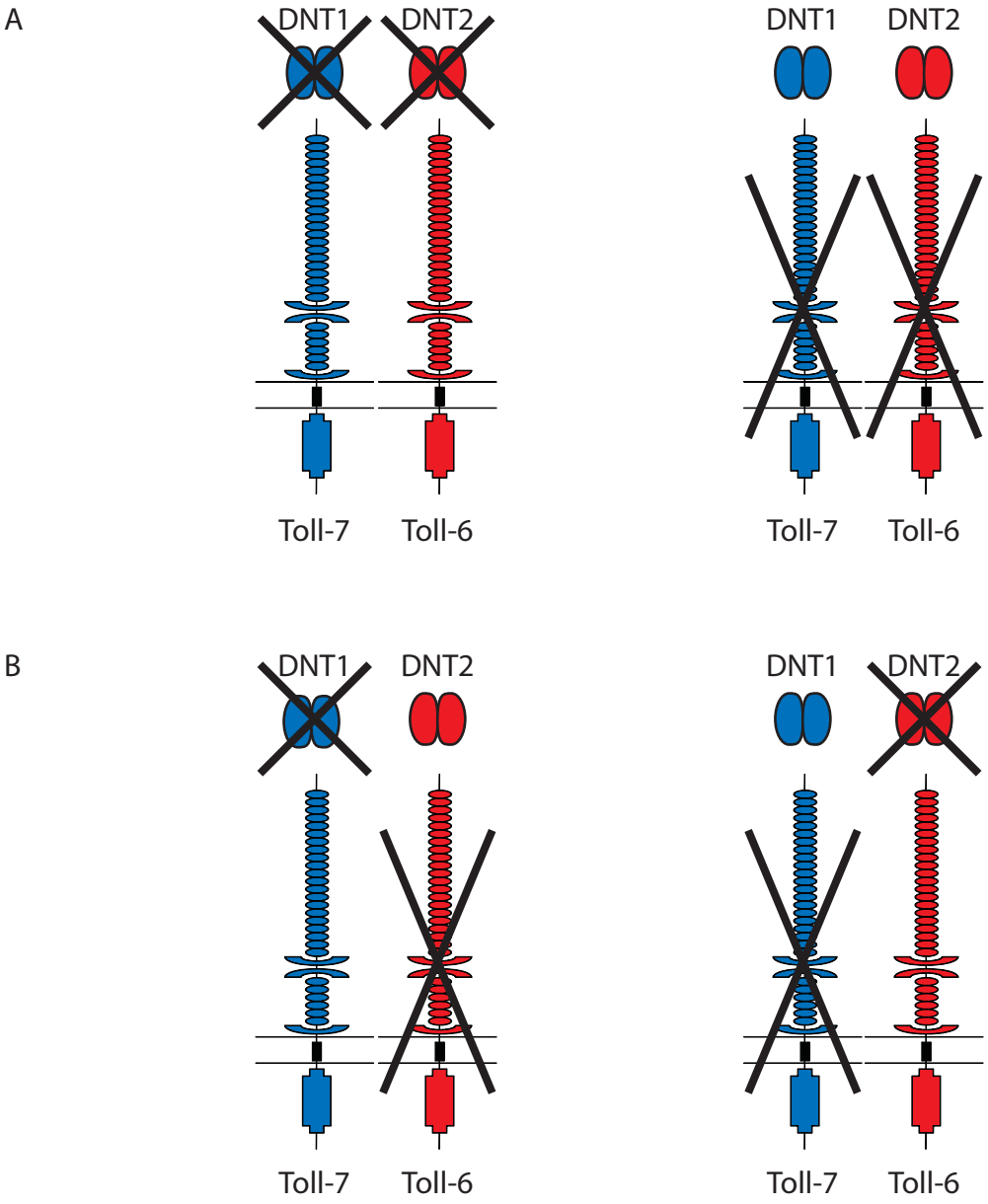

Various combinations of mutant alleles of *DNT1, DNT2, Toll-6* and *Toll-7* result in a semi-lethal phenotype. (A) Loss of both ligands and loss of both receptors results in the same phenotype. (B) Loss of DNT1 and Toll-6, or loss of DNT2 and Toll-7, effectively knocks out both signalling pathways, and results in a semi-lethal phenotype.

an alternative or larger subset of neurons. Unfortunately, the pan-neuronal *elavGal4* driver did not recombine with null alleles of *Toll-6.* Additionally, the levels of expression are likely to exceed the endogenous activation of Toll-7 and Toll-6 *in vivo*, which may disrupt normal neuronal functions. Finally, signalling outside the nervous system may also be important for viability, and the partial rescue of survival could reflect this.

Some conclusions can be drawn from the small, but significant rescues of the *Toll-7Toll-6* double mutant lethality. The rescues indicate that the ΔLRR activated receptor constructs are functional, and that removing the extracellular domain is an effective strategy to activate the receptors. Moreover, as shown by the rescue with *Toll-7*$^{Cys\text{-}Tyr}$ activated receptor, conserved cysteine residues close to the membrane could be involved in silencing the unbound receptor. The greater effect of *Toll-7*$^{Cys\text{-}Tyr}$ than *Toll-7*$^{\Delta LRR}$ suggests that the mutated receptor might be more effective in signalling than the truncated form. The fact that Toll-7 and Toll-6 could be constitutively activated in the same way as Toll, suggests that the Toll paralogues share common activation mechanisms.

Activating Toll-7 or Toll-6 in neurons partially rescues the lethality of *DNT1DNT2* double mutants and *spz* mutants. This again demonstrates that the lethality phenotype is due, at least in part, to neuronal dysfunction. The incomplete rescue could again be due to insufficient or dysregulated expression of the activated receptors. The rescue of *DNT1DNT2* double mutants was stronger than the rescue of the *Toll-7Toll-6* double mutants, which might reflect the use of the more widely expressing *elavGal4* driver, compared to *ChaGal4* used earlier. However the endogenous control of expression levels was lost, and any non-neuronal requirements of *Toll-7* and *Toll-6* were not met. Another explanation of the incomplete rescue could be that *Toll-7* and *Toll-6* are not the only DNT receptors, and that activation of additional receptors may be required to fully rescue the *DNT* mutant phenotype. The Cys-Tyr activated receptors appeared

to more strongly rescue *DNT1DNT2* double mutant lethality than the ΔLRR receptors, similar to the effect seen in *Toll-7Toll-6* double mutants. Intriguingly, the rescue by *Toll*^{10b} was more similar to the ΔLRR versions of *Toll-7* and *Toll-6* than the Cys-Tyr receptors. This could be due to a positional effect of *UAS-Toll*^{10b} in the genome, or could point to differences in signalling between Toll, Toll-7 and Toll-6.

The significant rescues of *DNT* mutant lethality phenotypes by constitutively active *Toll-7* and *Toll-6* show that the receptors share a common signalling pathway with the DNTs: activating signalling compensates for a loss of the ligands. Toll is known to signal through the NFκB homologues Dorsal and Dif (Moussian and Roth, 2005, Meng et al., 1999). Since activated *Toll*, *Toll-6* and *Toll-7* all rescue *DNT* mutant lethality, it is likely that Toll-7 and Toll-6 also signal through NFκB. These rescues also show that the receptors are acting downstream of the DNTs. Spz binds to Toll to activate signalling (Weber et al., 2003). Activating *Toll-7* and *Toll-6* rescues the *spz* phenotype, and *Toll*^{10b} rescues the *DNT1DNT2* phenotype. It has also been shown that neuronal expression of *DNT1* and *DNT2* rescues the *spz* lethality, and that expressing spz rescues the *DNT2DNT1* phenotype (Sutcliffe, 2010). These results are compatible with promiscuous or redundant relationships between the ligands and the receptors.

Lethality is a gross, non-specific phenotype, and doesn't indicate what molecular or cellular processes are disrupted. Therefore, in the following chapter, I will examine what are the CNS functions of *Toll-7* and *Toll-6*, and whether these are compatible with them serving as DNT receptors.

CHAPTER 5
TOLL-7 AND *TOLL-6* FUNCTION IN THE NERVOUS SYSTEM

5.1 Introduction

In the previous chapters, I have shown that *Toll-7* and *Toll-6* are expressed in the *Drosophila* nervous system, and that the receptors genetically interact with the DNTs. The aims of this chapter were to characterise the functions of *Toll-7* and *Toll-6* in the nervous system, testing for phenotypes also found in *DNT* mutants. I tested for locomotion phenotypes, and the roles of the receptors in axon targeting and cell survival. Finally, rescue experiments tested whether constitutively active receptors can rescue the cell death phenotype of the DNTs.

Drosophila behaviour has long been used as a read-out of nervous system function (Heisenberg, 1997). Adult locomotion lends itself to the investigation of gene function, since it can be easily tested, and requires the coordination of a large number of inputs and outputs. Locomotion phenotypes can result from dysfunction in a wide range of processes, from neuromuscular communication to central control mechanisms. Locomotion is disrupted if there are changes to the muscle (Gilsohn and Volk, 2010), or if there is dysfunction in the motor neuron at the NMJ (Wan et al., 2000, Wagh et al., 2006). Sensory input, including visual and proprioceptive signal, are required for normal locomotion (Keller et al., 2002). Control of motor neuron excitability influences the ability of flies to move normally (Ping et al., 2011). And in the brain, the Central Complex plays a pivotal role in the central control of locomotion, including initiation, speed and direction (Strauss and Heisenberg, 1993, Strauss, 2002). And beyond the function of specific genes, the fly's sex, age, food availability, light

levels all influence the level of activity (Martin et al., 1999). Therefore, I will test if *Toll-7* and *Toll-6* mutants show locomotion phenotypes.

Motor neurons send their axons out of the CNS to their targets – muscle. Once a motor axon has found its target, it establishes synapses (the NMJ), and the contraction of the muscle is brought under neuronal control. The embryonic development of the muscle and the targeting of motor axons occur simultaneously, and muscles form independently of innervation (Bate, 1993, Broadie and Bate, 1993). Motor neurons reach their muscle targets in a series of steps. Firstly, pioneer motor axons exit the VNC and project to the periphery towards the muscle, follower neurons then fasciculate along the pioneer axons to establish the segmental and intersegmental nerves, and finally axons branch off to target to specific muscle fibres where an NMJ is established (Sánchez-Soriano and Prokop, 2005, Landgraf and Thor, 2006). The projection of motor axons from the CNS does not require muscle, but synaptogenesis does depend on the normal differentiation of muscle fibres (Prokop et al., 1996). Looking for defects in the intersegmental nerve b (ISNb) frequently identifies genes that play a role in axon targeting (Dorsten and VanBerkum, 2008, Meyer and Moussian, 2009). ISNb is made up of the motor axons from the RP1, RP3, RP4, RP5 and V neurons, and they target the ventral longitudinal muscles 6, 7, 12, and 13 (Landgraf et al., 1997). These RP neurons all originate from the same neuroblast (NB3-1), while the V neuron is the only motor neuron originating from NB5-2 (Schmid et al., 1999). The dendritic arbours of motor neurons are myotopically mapped, and the dendrites corresponding to the ISNb axons are found together in the adjacent anterior hemisegment (Landgraf et al., 2003). Motor neurons can be labelled with anti-Fasciclin II (FasII) antibodies. FasII is a highly specific marker of the axons and growth cones of a subset of motor neurons, including the ISNb nerve branch, and does not label sensory or interneurons (Van Vactor et al., 1993). Therefore, staining with anti-FasII can

reveal misrouting phenotypes of the ISNb nerve branch as it targets the embryonic muscle. Thus, I will test if motor axon targeting required *Toll-7* and *Toll-6*

One of the fundamental aspects of neuronal development is whether the cell should survive or die. Apoptosis is a form of programmed cell death and is characterised by the condensation of the nucleus and other organelles, and the membrane-bound fragmentation of the cell (Kerr et al., 1972). Apoptosis is genetically controlled, and involves a host of pro-apoptotic genes, initiator and effector Caspases, and inhibitors (Xu et al., 2009). The process in flies broadly reflects the apoptosis pathways in vertebrates, though species differences include the relative importance of Cytochrome C involvement (Kornbluth and White, 2005). Caspase-3 is the most potent effector of cell death, and is homologous to DrICE in flies (Degterev et al., 2003, Xu et al., 2009). Antibodies raised against the activated vertebrate Caspase-3 also recognise activated *Drosophila* DrICE (Muro et al., 2006, Bond et al., 2008). Apoptosis is an important feature of nervous system development across species (Buss et al., 2006), and in flies 25-50% of cells in the developing CNS are lost in this way (White et al., 1994, Rogulja-Ortmann et al., 2007). Therefore, I will test whether apoptosis levels change in *Toll-7* and *Toll-6* mutants, and whether activated forms of the receptors can rescue the excess cell death of *DNT* mutants.

DNT mutant flies show locomotion defects, and mutant embryos show axon targeting defects and increased neuronal cell death (Zhu et al., 2008, Sutcliffe et al., Submitted). To test if the Tolls can function as DNT receptors, it is important to investigate whether *Toll-7* and *Toll-6* mutants show similar phenotypes to the *DNT* mutants.

5.2 Results

5.2.1 *Toll-7* and *Toll-6* are required for normal locomotion behaviour

I tested the locomotion phenotype of adult flies using the paradigm developed by Ben Sutcliffe, Manuel Forero and Alicia Hidalgo (Sutcliffe et al., Submitted). Adult flies had their wings clipped, and were allowed to recover for 30 minutes. They were filmed for one minute after being placed in the centre of a petri dish, and the films were processed using FlyTracker software. The software produced a plotted trajectory of the fly's path, and also a detailed read-out of various behavioural parameters. Flies were controlled for age, sex and food quality. Filming was always carried out at the same time of day, between 9.30am and 11.00am.

When placed in the petri dish, *yw* control flies invariably walked to the edge, climbed the walls of the dish, and walked on the rim of the dish. This produced a characteristic circular trajectory (Fig 5.1A). When tested in the same way, the trajectories of *Toll-7*$^{P8/P114}$ and *Toll-6*$^{26/31}$ single mutants showed that they travel a much shorter distance than the controls, over an equal period of time (Fig 5.1B, C). *Toll-7*$^{P8/P114}$*;Toll-6*$^{26/31}$ double mutants behaved similarly to the single mutants (Fig 5.1D). Mutant flies would not always travel far enough to reach the rim, but would remain on the bottom of the petri dish. They rarely completed a full circuit of the dish, so the circular trajectory of the controls was lost. When the total distance travelled was quantified, all of the mutants showed a greatly reduced path length, compared to controls (Fig 5.2A).

The reduction in distance travelled by the mutants could be attributed to at least two behavioural phenotypes. The first is time resting. This was defined as a frame of the film where a fly travelled less than 1.5mm, and included frames where a fly was grooming or

motionless. When I observed the flies, it was clear that the mutants showed an increase in resting behaviour. Quantifying the proportion of time spent resting confirmed this (Fig 5.2B).

The increased time resting was accompanied by an additional phenotype: mutant flies walked more slowly than the *yw* controls. The average walking speeds of the flies were compared, ignoring the frames when the fly was resting. *Toll-7*$^{P8/P114}$, *Toll-6*$^{26/31}$, and *Toll-7*$^{P8/P114}$*;Toll-6*$^{26/31}$ all travelled at slower average speeds compared to *yw* (Fig 5.2C). The FlyTracker software measured the speed of the flies in each of the frames recorded. I pooled all of these values, to produce a histogram showing the distribution of walking speeds for each genotype (Fig 5.2D). The single and double mutant flies spent a larger proportion of time walking slowly, whereas the controls were able to walk at higher speeds.

Toll-7 and *Toll-6* are therefore required for normal locomotion behaviour. Single and double mutant flies did not travel as far as controls in a set period of time, and this was due to an increased amount of time at rest, and an inability to walk as quickly as control flies.

5.2.2 *Toll-7* and *Toll-6* are required for axon targeting

To test if *Toll-7* and *Toll-6* are involved in axon targeting, the ISNb motor axons were examined as they target to muscles 6, 7, 12, and 13. Motor axons were stained with anti-FasII, and abdominal segments A1 to A5 were examined in late stage 17 embryos, where the prototypical axonal pattern consists of three projections. The most lateral of these lies in the cleft of muscles 12 and 13; the projection between muscles 13 and 6 is often thicker and shorter than the others, and the projection between muscles 6 and 7 is often the faintest (Fig 5.3A). The phenotypes that I looked for were fan, loss of 1 projection, loss of 2 or more projections, and misrouting (Zhu et al., 2008). The fan phenotype is recognised by multiple thin projections originating at the cleft of muscles 13 and 6, and along with the loss of 1

Fig 5.1 - *Toll-7* and *Toll-6* mutant flies travel less far than control flies

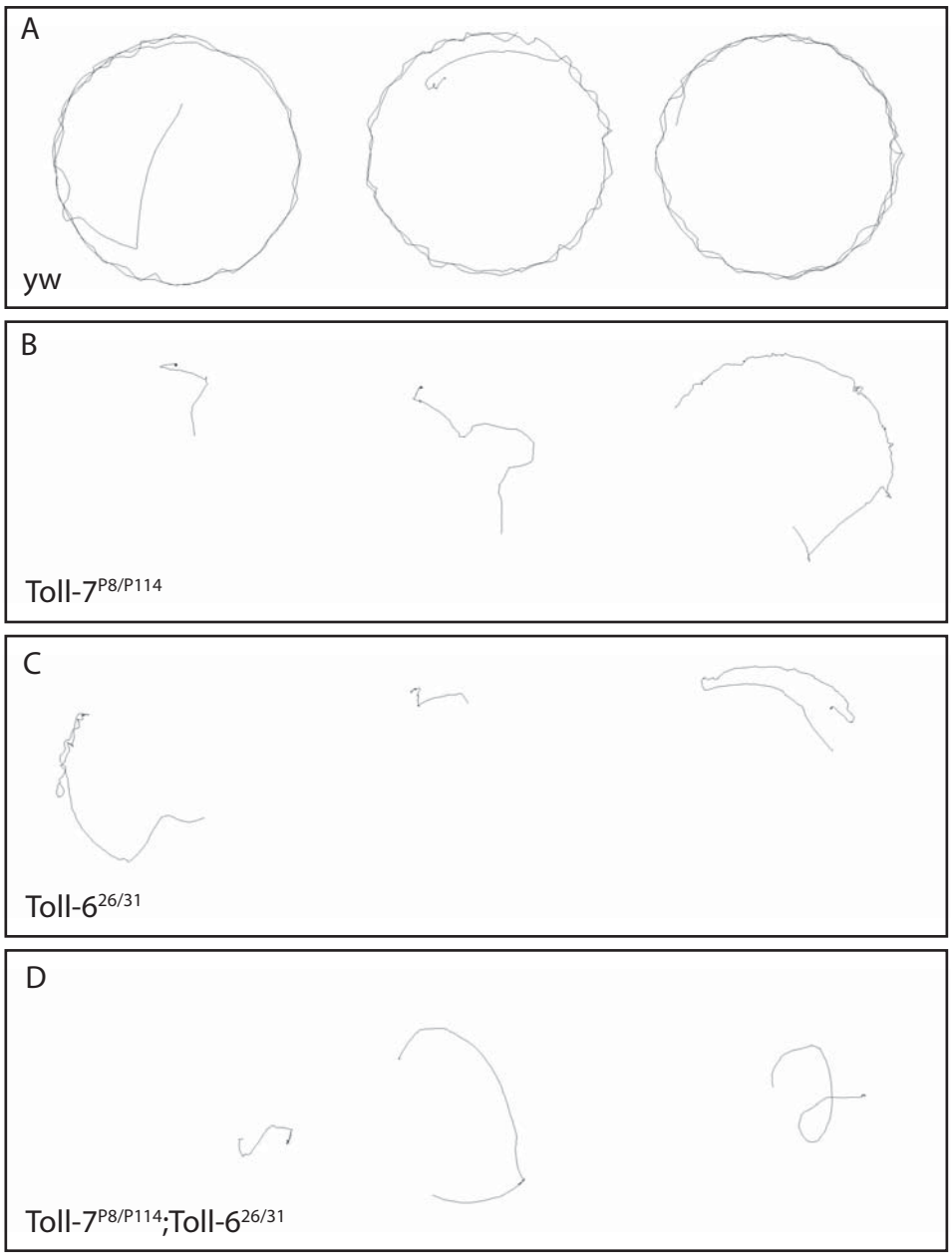

(A-D) Representative trajectories of adult flies of the given genotype, recorded over an equal amount of time, when placed in the centre of a petri dish. (A) *yw* control flies typically travel to the rim of the dish, and continue to walk around it. (B) *Toll-7* and (C) *Toll-6* single mutants and (D) double mutants have reduced trajectory lengths.

Fig 5.2 – *Toll-7* and *Toll-6* mutants show locomotion phenotypes

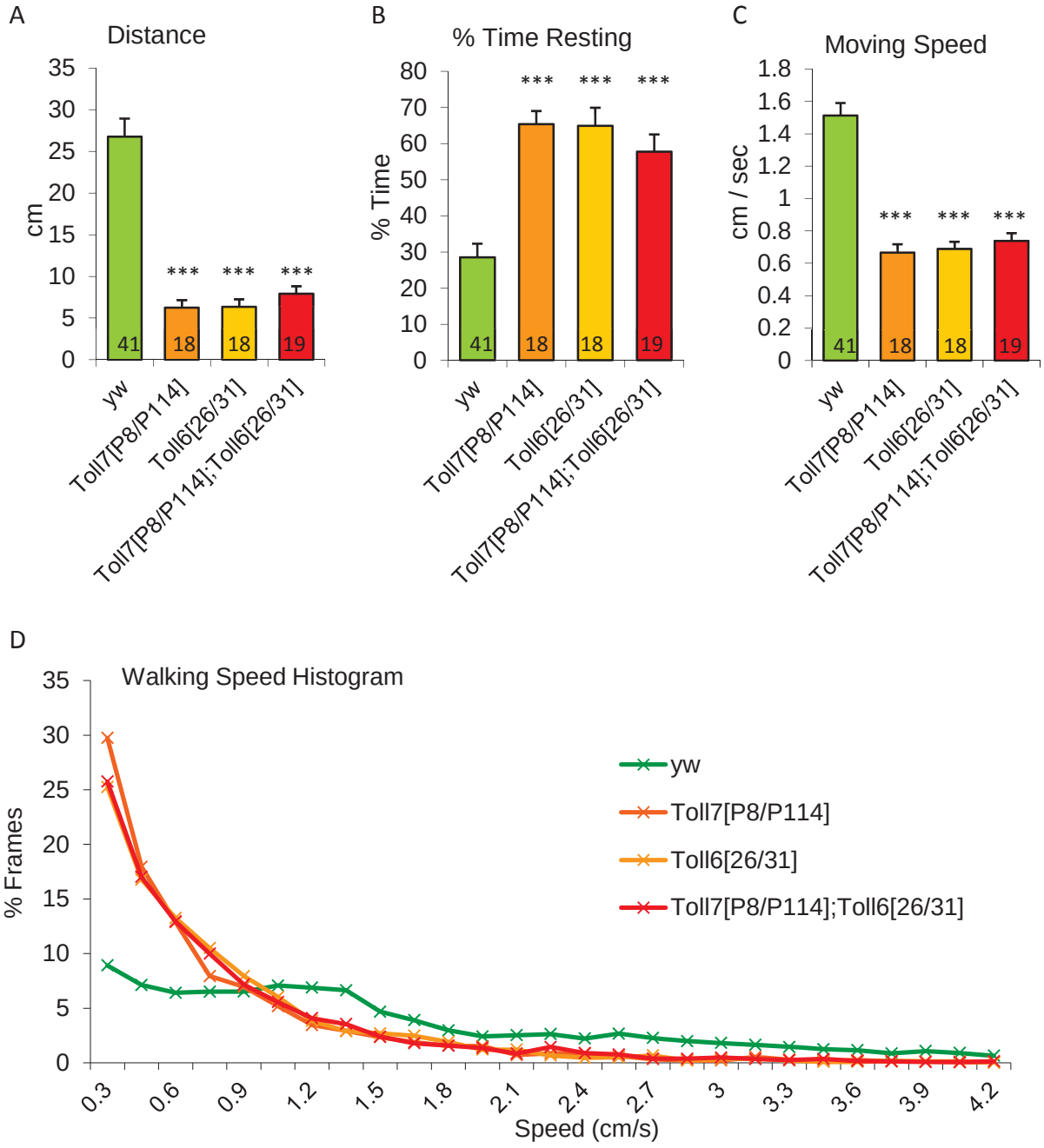

Toll-7 and *Toll-6* single and double mutants travel a shorter distance during a set period of time, quantified in (A). The reduced distance travelled by mutant flies is comprised of at least two components. (B) Mutants spend a greater proportion of time resting. (C) Mutant flies walk at a slower average speed. Mean shown +/- SEM, numbers given in bars, ***p<0.001 Students t-test. (D) A histogram showing the distribution of speeds travelled by flies in each frame. Mutant flies travel more at slower speeds, while control flies are more able to travel at faster speeds.

projection, does not reproducibly vary between genotypes (Fig 5.3B). Misrouting refers to the errant projection of an axon to the wrong muscle, to another nerve, to the next hemisegment, or following a path that substantially deviates from the classical pattern. When comparing genotypes, misrouting and loss of 2 or more projections were combined, as these were the phenotypes that varied according to genotype.

In *yw* controls, 20% of hemisegments showed a misrouting phenotype. In *Toll-6*$^{26/31}$ and *Toll-6*$^{31/DfXG4}$ mutant embryos, there was an increase in the proportion of hemisegments showing misrouting (Fig 5.3C, E). While the rate of misrouting increased, the aberrant projections looked similar to the misrouted axons seen in controls. In *Toll-7*$^{P8/P114}$ and *Toll-7*$^{P114/DfBSC22}$ mutant embryos, a much stronger increase in the proportion of aberrant hemisegment was observed (Fig 5.3C, E). To eliminate the contribution of genetic background to the phenotypes, two transheterozygote combinations were used for each gene: one using different null alleles, the other placing a null allele in *trans* over a deficiency. The fact the same phenotypes were observed in each case confirms that the effects are gene-specific. *Toll-7*$^{P8/P114}$ and *Toll-7*$^{P114/DfBSC22}$ mutants showed more severe misrouting phenotypes, including projections forming loops and misrouting further from the target, which were not seen in control flies. *Toll-7*$^{P8/P114}$ and *Toll-7*$^{P114/DfBSC22}$ mutants also showed the loss of 2 or more projections phenotype, which was never seen in controls. In some instances, the entire ISNb nerve branch was missing (Fig 5.3D). This means Toll-7 has the greater influence over axon targeting to muscles 6, 7, 12 and 13. *Toll-7*$^{P8/P114}$*;Toll-6*$^{26/31}$ double mutants also showed the more severe misrouting phenotypes and losses of 2 or more projections. In the double mutants, there were significantly more aberrant hemisegments compared to *Toll-7*$^{P8/P114}$ single mutants (Fig 5.3E). Therefore, *Toll-7* and *Toll-6* are required for the targeting of the ISNb motor axons.

Fig 5.3 - *Toll-6* and *Toll-7* promote axon targeting

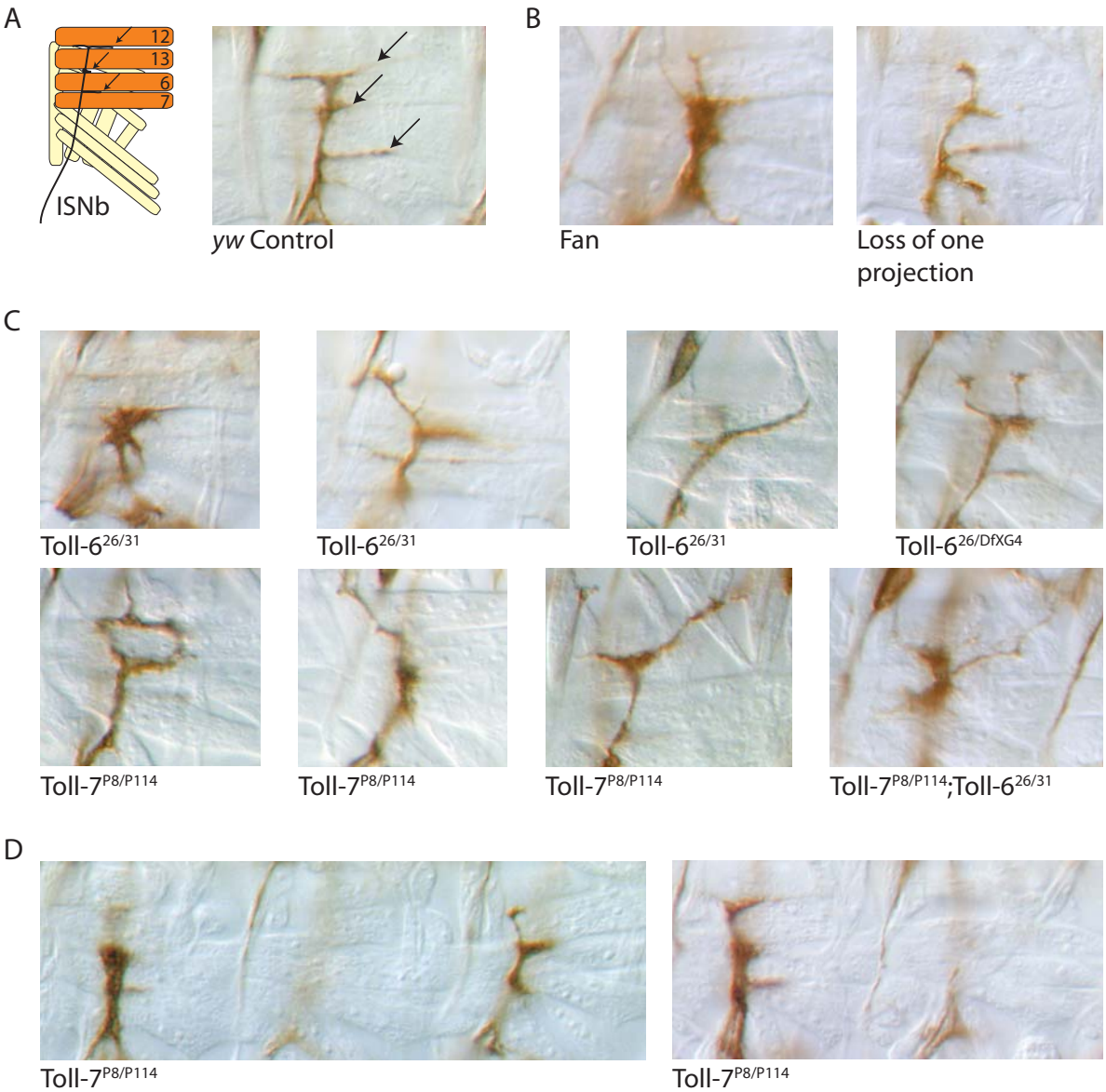

Fig 5.3 – *Toll-6* and *Toll-7* promote axon targeting
ISNb motor neurons target to muscles 6, 7, 12 and 13, and are visualised with anti-FasII in stage 17 embryos. (A) A diagram showing the targeting of ISNb to the muscle, and on the right a control hemisegment showing the typical pattern of projections (arrows). (B) Fan and loss of one projection phenotypes did not vary with genotype. (C) Misrouting in *Toll-6* and *Toll-7* single and double mutants. (D) Loss of the entire ISNb nerve in *Toll-7* mutant embryos. (E) Quantification of misrouting phenotypes. Number of hemisegments given in the bars, *$p<0.05$ ***$p<0.001$ χ^2 test, black asterisks compared to *yw*, red compared to $Toll\text{-}7^{P8/P114}$, for statistics, misrouting and loss of 2+ projections are considered together.

5.2.3 *Toll-7* and *Toll-6* can promote cell survival in the CNS

To analyse the role of *Toll-7* and *Toll-6* in cell survival, I carried out an immunofluorescent staining of activated Caspase-3, to detect apoptotic cells in the stage 17 embryonic VNC by confocal microscopy. To process the stacks of images, I used the DeadEasy Caspase plugin from ImageJ (Forero et al., 2009), which produced a parallel stack of white Caspase-positive cells on a black background. The software also returned the number of cells counted (Fig 5.4A, and see section 2.7.3, materials and methods). Since the number of apoptotic cells varies greatly between developmental stages, late stage 17 embryos were examined, where wild-type samples typically have 110-120 apoptotic cells (Rogulja-Ortmann et al., 2007, Sutcliffe, 2010, Pennack, 2008).

To test whether *Toll-7* and *Toll-6* are required for cell survival in the *Drosophila* embryonic VNC, I counted Caspase-positive cells in *Toll-7* and *Toll-6* mutants. *Toll-7*$^{P8/P114}$ and *Toll-6*$^{26/31}$ mutant embryos both showed an increase in the number of apoptotic cells compared to controls (Fig 5.4B, C). The same result was obtained when looking at *Toll-7*$^{P8/DfBSC22}$ and *Toll-6*$^{26/DfXG4}$ mutants, with alleles in *trans* over deficiencies, therefore genetic background is unlikely to have contributed to the phenotype (Fig 5.4C). The increase in cell death in *Toll-6* and *Toll-7* mutants shows that these genes are required for cell survival in the developing VNC.

I next tested whether *Toll-7* and *Toll-6* were sufficient to maintain cell survival, by expressing constitutively active receptors in the all neurons in the developing VNC. First, the *Toll-7*$^{\Delta LRR}$ and *Toll-6*$^{\Delta LRR}$ activated receptors were expressed in all neurons using *elavGal4*, in otherwise wild-type embryos. *Toll-7*$^{\Delta LRR}$ had no effect on the number of apoptotic cells, while *Toll-6*$^{\Delta LRR}$ increased the amount of cell death in the VNC (Fig 5.5A, C). This result was not consistent

with *Toll-7* and *Toll-6* being able to promote cell survival. I next tested whether Cys-Tyr activated receptors could maintain cell survival. Expressing *Toll-7*$^{Cys\text{-}Tyr}$ and *Toll-6*$^{Cys\text{-}Tyr}$ in all neurons in otherwise wild-type embryos reduced the amount of cell death compared to *yw* (Fig 5.5B, D). Therefore, activated *Toll-7* and *Toll-6* prevent naturally occurring cell death, indicating that the receptors can promote cell survival.

5.2.4 Activated *Toll-7* and *Toll-6* rescue the *DNT1* and *DNT2* mutant phenotypes

The above analyses show that *Toll-7* and *Toll-6* mutant phenotypes resemble those of *DNT1* and *DNT2* mutants. The crucial test of whether Toll-7 and Toll-6 can function as DNT receptors is to test if activated receptors can rescue the phenotype of *DNT* mutants. *DNT1* and *DNT2* are both required for cell survival, since mutant embryos showed an increase in apoptosis (Fig 5.6A, C, see also Zhu et al., 2008). To test whether activated *Toll-7* and *Toll-6* receptors could rescue this phenotype, I expressed *Toll-7*$^{Cys\text{-}Tyr}$ in all neurons in *DNT1*^{41} mutant embryos, and *Toll-6*$^{Cys\text{-}Tyr}$ in neurons of *DNT2*$^{e03444/Df6092}$ mutants. In both cases, the amount of cell death was rescued to below control levels (Fig 5.6B, D). The rescue of the cell death phenotype is evidence that Toll-7 and Toll-6 functionally interact with the DNTs.

5.3 Discussion

I have shown that *Toll-7* and *Toll-6* mutants exhibit abnormal adult behaviour, and loss of these genes causes axon targeting defects and increases cell death in the developing CNS. Expression of activated *Toll-7* and *Toll-6* in neurons reduces the amount of naturally occurring cell death, and also rescues the phenotype of the *DNT* mutants. Therefore, *Toll-7*

Fig 5.4 - *Toll-7* and *Toll-6* are required for cell survival in the embryonic VNC

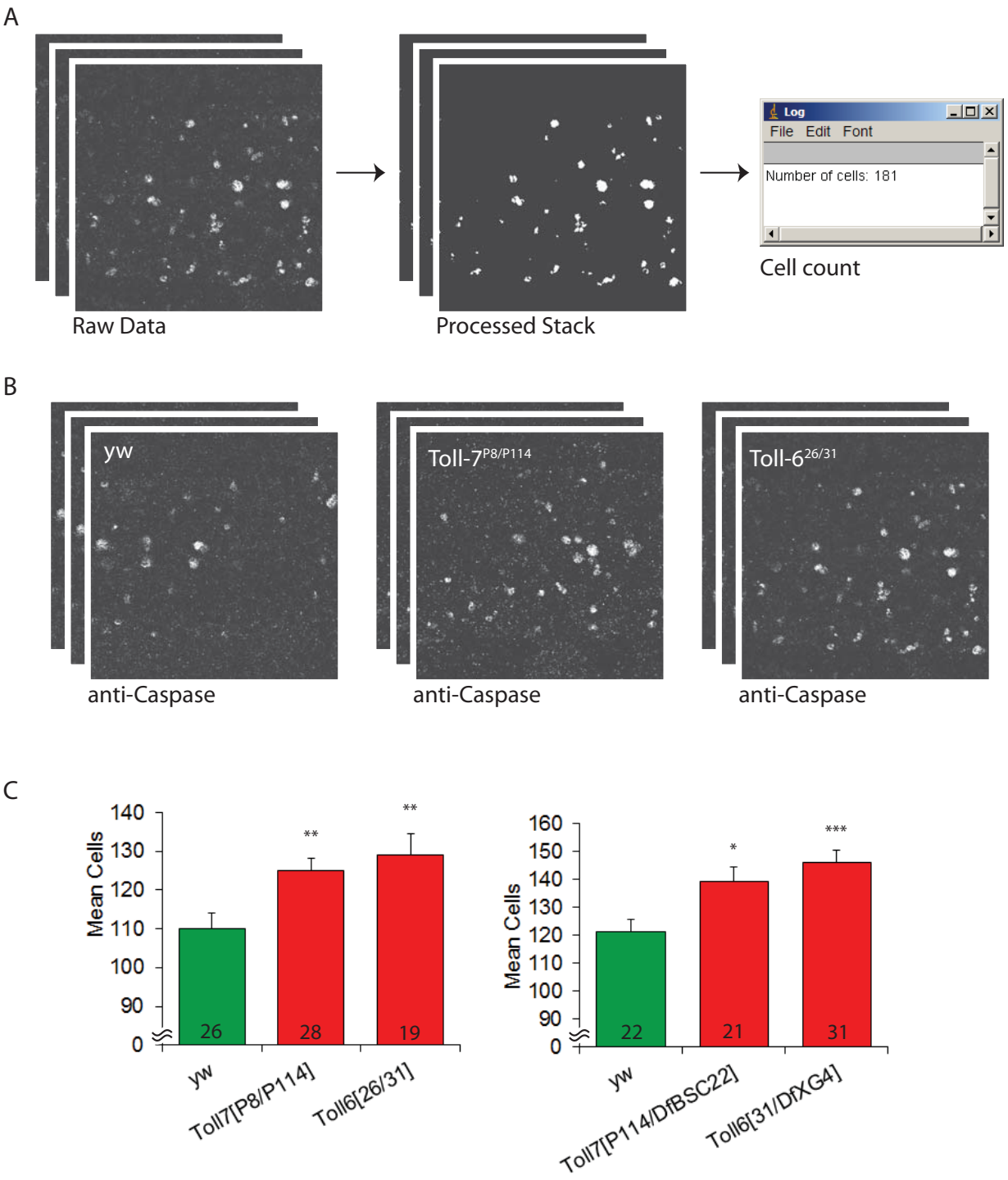

(A) Stage 17 embryonic VNCs were stained with anti-cleaved Caspase-3, and detected with confocal miscroscopy. DeadEasy software produced a parallel stack of images, where cells are identified from background, and a count of cell number is given. (B) Representative samples of *yw*, *Toll-7*$^{P8/P114}$ and *Toll-6*$^{26/31}$ embryos stained with anti-cleaved Caspase-3. (C) *Toll-7* and *Toll-6* mutants show increased apoptosis in the developing CNS. Mean cells shown +/- SEM, numbers given in bars, *p<0.05 **p<0.01 ***p<0.001 Students t-test, numbers given in bars.

Fig 5.5 - *Toll-7* and *Toll-6* activated with Cys-Tyr mutations, but not ΔLRR, reduce naturally occuring cell death

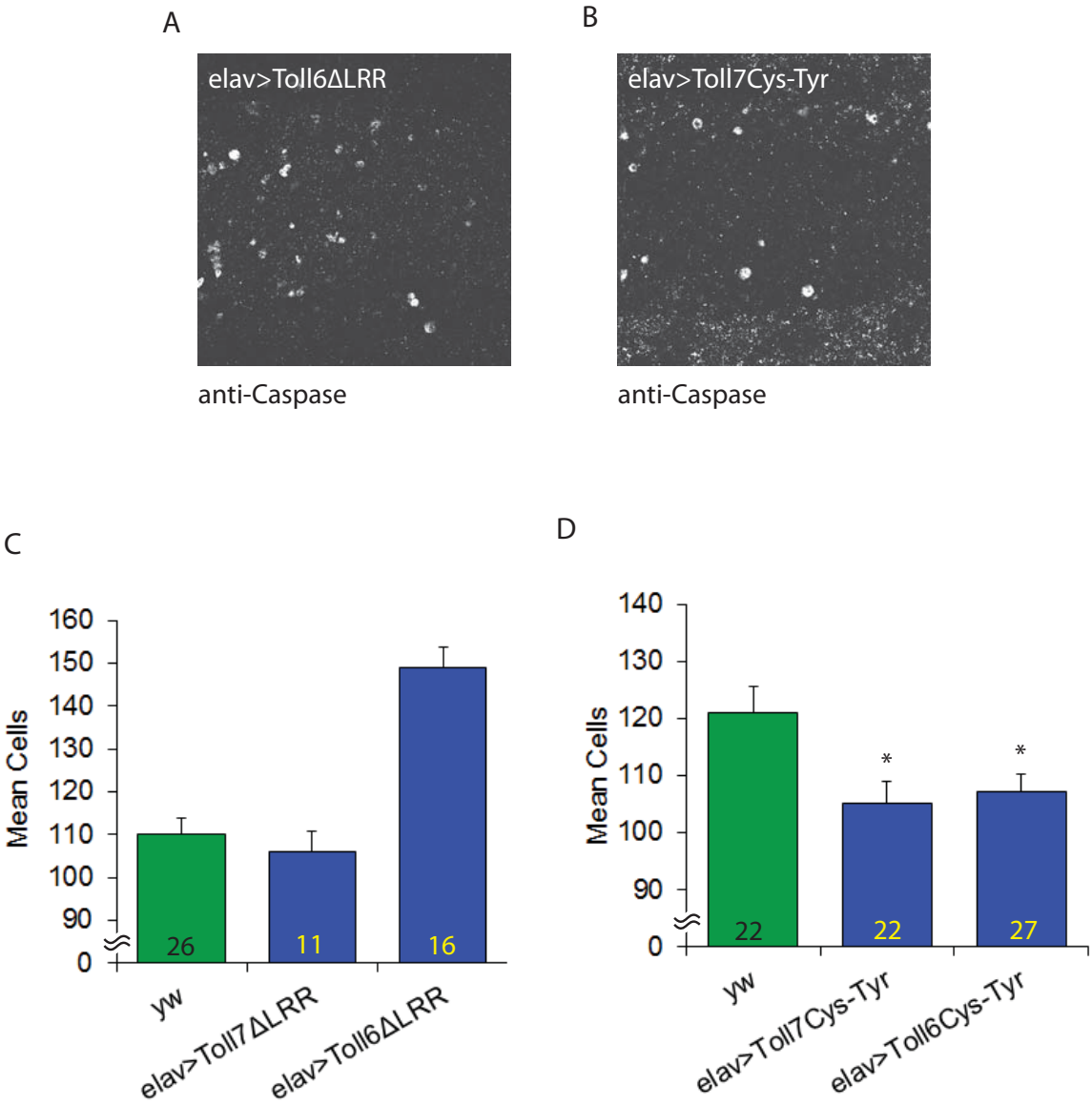

Apoptosis was quantified in embryos with neuronal expression of activated *Toll-7* and *Toll-6* receptors. Representative samples are shown for (A) *elav>Toll-6*$^{\Delta LRR}$ and (B) *elav>Toll-7*$^{Cys\text{-}Tyr}$ (C) *Toll-7*$^{\Delta LRR}$ had no effect, while *Toll-6*$^{\Delta LRR}$ increased cell death in the embryonic VNC. (D) Expressing *Toll-6*$^{Cys\text{-}Tyr}$ and *Toll-7*$^{Cys\text{-}Tyr}$ in all neurons reduced the number of apoptotic cells. Mean cells shown +/- SEM, numbers given in bars, *p<0.05 Students t-test. Full genotypes from left to right are (C) *yw, elavGal4 x UASToll-7*$^{\Delta LRR}$, *elavGal4 x UASToll-6*$^{\Delta LRR}$, (D) *yw, elavGal4 x UASToll-7*$^{Cys\text{-}Tyr}$, *elavGal4 x UASToll-6*$^{Cys\text{-}Tyr}$

Fig 5.6 - Activated *Toll-7* and *Toll-6* rescue the *DNT1* and *DNT2* mutant phenotype

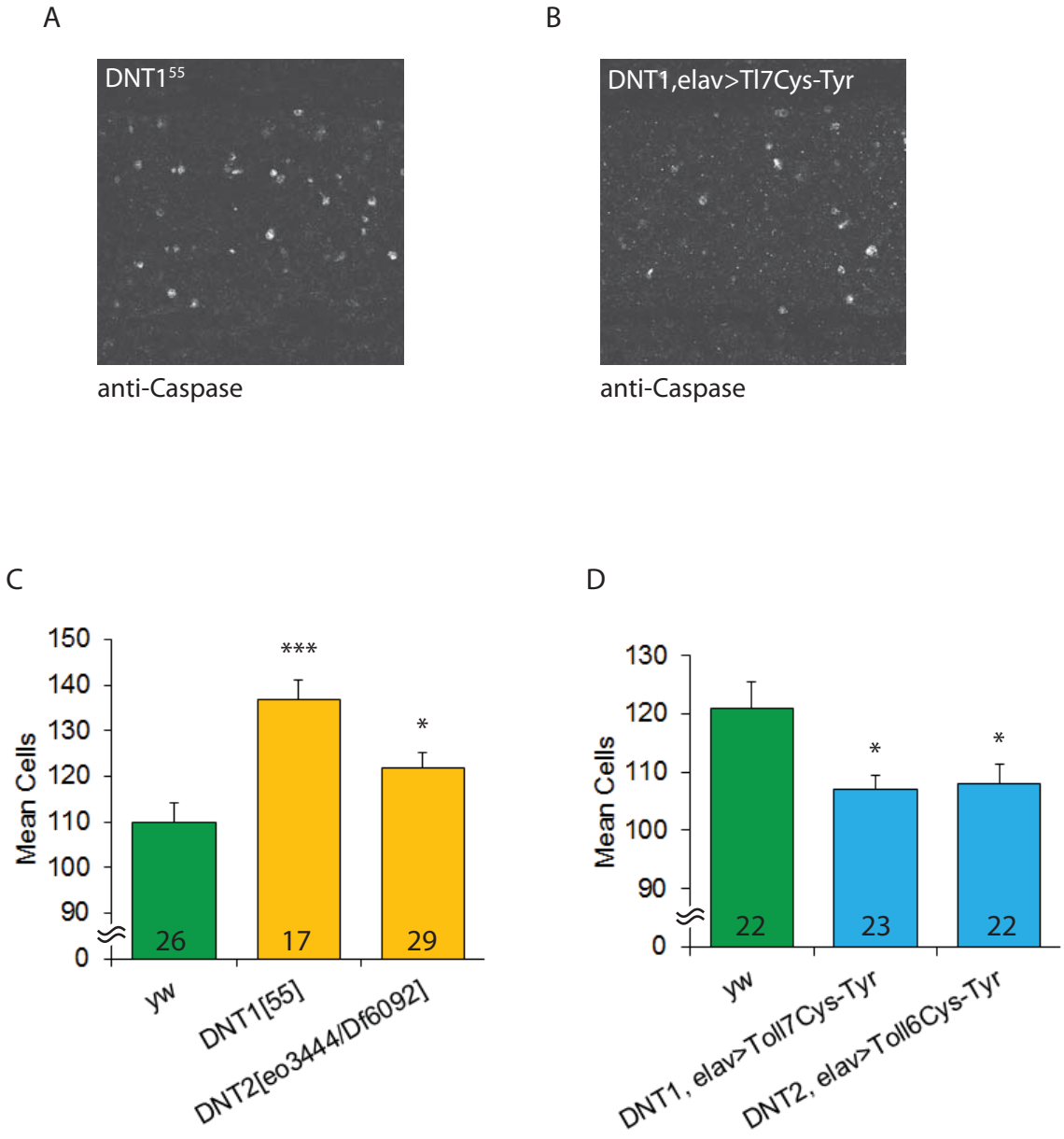

Expression of activated receptors rescues the increased apoptosis seen in *DNT* mutants. Representative sampled are shown for (A) *DNT1*^{55} and (B) *DNT1, elav>Toll-7*$^{Cys\text{-}Tyr}$. (C) *DNT1* and *DNT2* mutants have more cell death in the embryonic VNC than *yw* controls. (D) Expressing *Toll-7*$^{Cys\text{-}Tyr}$ in all neurons in *DNT1* mutants, and *Toll-6*$^{Cys\text{-}Tyr}$ neurons of *DNT2* mutants reduces the amount of apoptosis to below control levels. Mean cells shown +/- SEM, numbers given in bars, *p<0.05 ***p<0.001 Students t-test. Full genotpyes in (D), from left to right are *yw, DNT1*^{41}*elavGal4 x UASToll-7*$^{Cys\text{-}Tyr}$*;DNT1*^{41}*, DNT2*^{e03444}*elavGal4 x Df6092UASToll-6*$^{Cys\text{-}Tyr}$*/TM6BlacZ.*

and *Toll-6* are necessary for normal development and function of the *Drosophila* CNS, and these data are consistent with them serving as DNT receptors.

I observed a locomotion phenotype in *Toll-7* and *Toll-6* single and double mutant adult flies, but I am unable to attribute the effects to a specific adult function. The phenotype may be due to an underlying developmental defect, which is manifested in the behaving adult. Equally, I cannot directly attribute the adult phenotype to the specific developmental defects identified in mutant embryos, since during metamorphosis, the *Drosophila* nervous system undergoes extensive remodelling (Tissot and Stocker, 2000). Moreover, the axon targeting defects that I identified were to muscles that go on to form the larval body wall. The motor neurons that target the adult legs first arise in the larva, and the central complex that controls locomotion behaviour forms in the pupa (Baek and Mann, 2009, Pereanu et al., 2011). It is therefore unclear whether the behavioural phenotypes are due to loss of *Toll-7* and *Toll-6* in the adult CNS, or result from a nervous system that is dysfunctional because of defects in development.

Adult *Toll-7* and *Toll-6* mutant flies do not travel as far as *yw* controls over the same amount of time, and this is partly due to a reduction in walking speed. This could be due to a reduced contractility of muscle fibres. However, reduced walking speed coupled with increased time resting is reminiscent of the behavioural phenotypes of flies with a defective central complex (Strauss and Heisenberg, 1993). Both *Toll-7* and *Toll-6* are expressed in the adult brain, in cells surrounding the central complex, and could therefore be important in the central control of locomotion. Alternatively, the expression of both genes in a broad range of brain regions might point to a more global neurological deficit. Interestingly, *Toll-7* is expressed in clusters of cells in the larval VNC that could correspond to the developing motor neurons of the leg, which are present in larval stages (Truman, 1990). A potential role for *Toll-7* in adult motor neurons could also be contributing to the locomotion phenotype.

Toll-7 and *Toll-6* are required for the normal targeting of the ISNb nerve branch to muscles 6, 7, 12 and 13. Like all neurons, ISNb projections are subject to various long- and short-range guidance cues (Tessier-Lavigne and Goodman, 1996, Dickson, 2002). ISNb is also a well-studied nerve branch, and genes identified that permit axon targeting include extracellular matrix components, extracellular proteases, cell recognition molecules, receptor phosphatases, and transcription factors (Meyer and Moussian, 2009, Serpe and O'Connor, 2006, Abrell and Jäckle, 2001, Sun et al., 2001, Desai et al., 1997, Madden et al., 1999). The role of the Toll receptor in axon targeting has also been studied. Toll was reported to act non-cell-autonomously in neurons to inhibit axon targeting, and to regulate motor neuron number and muscle fibre development (Rose et al., 1997, Halfon et al., 1995). However, *Toll* expression has since been demonstrated in embryonic neurons (Sutcliffe et al., Submitted), making it likely that Toll also functions cell-autonomously. *Toll-7* and *Toll-6* are also expressed in neurons, and are therefore acting cell-autonomously to promote axon targeting.

The misrouting phenotypes of *Toll-7* and *Toll-6* mutants are strongly reminiscent of those seen in *DNT1* and *DNT2* mutants (Zhu et al., 2008). The morphologies of aberrant ISNb projections in *Toll-7* and *Toll-6* mutants were similar to those in DNT mutants: projections to incorrect muscles or neighbouring hemisegments, formation of axon loops, and of losses of 2 or more projections. Loss of *DNT1* more severely affected ISNb than loss of *DNT2*, and double mutants showed significantly more misrouting than either single mutant (Zhu et al., 2008). *Toll-7* phenocopies *DNT1* in the lethality assay of genetic interaction. Similarly, *Toll-7* mutants show a stronger misrouting phenotype than *Toll-6* mutants, and the double mutants are still more severe. *GFP* driven by *Toll-7-Gal4* specifically labels the ISNb nerve branch, so it is not surprising that *Toll-7* mutants show a phenotype in these axons. Therefore, the axon guidance phenotypes and lethality phenotypes are in accordance, and point to an interaction of

DNT2 with Toll-6 and DNT1 with Toll-7. To strengthen this, the SNa nerve branch could be examined for misrouting phenotypes in *Toll-7* and *Toll-6* mutants. It has been shown that loss of *DNT2* has a stronger effect on SNa misrouting than loss of *DNT1* (Zhu et al., 2008).

In the previous chapter, I generated two versions of constitutively active *Toll-7* and *Toll-6*: the ΔLRR form and the Cys-Tyr form. When rescuing lethality, they behaved similarly. However, when they were expressed in neurons in the embryonic CNS, only the Cys-Tyr versions were able to reduce the levels of apoptosis. This was an unexpected result, and indicates that two types of receptor are not functioning in the same way. This could be due to differences in the way the two proteins are expressed: the truncated forms might not be optimally transcribed of translated, or they might be accumulating within the cell. Alternatively, they might be downregulated or rapidly removed from the membrane before they can have an effect on cell survival, but are able still able to influence animal viability. Cell survival and animal viability might reflect separate aspects of Toll signalling. Importantly, the lethality assay involves counting pupae, which is a much later stage of development than the embryos assayed here: this could also affect how the transgenes affect different phenotypes.

During the course of the project, the different activated receptor versions were made at different times. Similarly, the generation of fly lines used in cell death rescue experiments took some time. Consequently, apoptosis assay experiments were carried out in two batches. Inevitably, the properties of the confocal laser change over time, which affects the detection of immunolabelling. To negate this effect, a *yw* control sample was tested for each batch of experiments. Both of the control counts of apoptotic cells that I obtained are in accordance with the 110-120 range found by other members of the lab (Pennack, 2008, Sutcliffe, 2010). The fact that the increases in apoptosis seen in *Toll-7*$^{P8/P114}$ and *Toll-6*$^{26/31}$ compared to their

control are mirrored by the increase seen in *Toll-7*$^{P8/DfBSC22}$ and *Toll-6*$^{26/DfXG4}$ compared to their own control, further validates this approach.

Loss of *Toll-7* and *Toll-6* resulted in increased cell death in the embryonic VNC compared to controls; however the changes observed were somewhat modest. It is possible that Toll-7 and Toll-6 are compensating for each other in these single mutants, and that the double mutant would show a stronger phenotype. This was the case with axon guidance, where the *Toll-7Toll-6* double mutant showed the strongest phenotype. The potential for redundancy could also explain why the *DNT1* and *DNT2* mutants show a greater amount of cell death compared to *Toll-7* and *Toll-6.* Similarly, there is more apoptosis in *spz*^{2} mutants than in *Toll*$^{r3/Dfro80b}$ mutants (Zhu et al., 2008). Nevertheless, the increases in apoptosis seen here are broadly comparable to those produced previously in the lab (Zhu et al., 2008). Equally, the relatively subtle effect of activating *Toll-7* and *Toll-6* is similar to previous results following activation of *Toll* (Zhu et al., 2008).

There is extensive cell death in the *Drosophila* embryonic CNS, and in some contexts this may be pre-determined (White et al., 1994, Rogulja-Ortmann et al., 2007, Miguel-Aliaga and Thor, 2009). This could mean that not all cells are subject to a non-cell-autonomous control of survival. However, it is clear that neurotrophism is an important aspect of the development of the fly's CNS (Hidalgo, 2002, Hidalgo et al., 2006, Zhu et al., 2008). Importantly, all results here are significant, and the ability of *Toll-7* and *Toll-6* to modulate neuronal survival demonstrates that cell number is plastic.

Toll-7 and *Toll-6* are both necessary and sufficient for cell survival in the developing CNS. *Toll-7* and *Toll-6* show the same loss- and gain-of-function phenotypes as *DNT1* and *DNT2* indicating that they serve common functions (Zhu et al., 2008). The rescue of *DNT1* and

DNT2 by neuronal expression of *Toll-7*$^{Cys\text{-}Tyr}$ and *Toll-6*$^{Cys\text{-}Tyr}$, respectively, shows that the ligands and the receptors share a common signalling pathway. Moreover, the rescue data indicate that *Toll-7* and *Toll-6* act downstream of the DNTs. This is consistent with them functioning as DNT receptors.

Altogether, in this chapter I have shown that *Toll-7* and *Toll-6* carry out important functions in the CNS. During development, they control cell survival and targeting, and they are required for locomotion behaviour in the adult. The phenotypes of *Toll-7* and *Toll-6* mutants closely resemble those of *DNT1* and *DNT2* mutants. In addition, mutant alleles of *Toll*s and *DNT*s interact, and activated Toll receptors rescues *DNT* mutant phenotypes. With overlapping and complementary patterns of expression, *Toll-7* and *Toll-6* could function as DNT receptors. In the next chapter, I will test this directly, by carrying out signalling assays in cell culture.

CHAPTER 6
DNT1 AND DNT2 ACTIVATE NFκB SIGNALLING THROUGH TOLL-7 AND TOLL-6

6.1 Introduction

Toll-7 and *Toll-6* are expressed in the *Drosophila* CNS, and are required for neuronal survival and targeting. The *Tolls* genetically interact with the *DNTs*, and constitutively active receptors rescue *DNT* mutant phenotypes. My aims in this chapter were to test in cell culture whether Toll-7 and Toll-6 signal through NFκB, and whether they can be activated by DNT1 and DNT2. By testing the effect of each DNT on cells expressing either Toll receptor, I aimed to test ligand-receptor interactions.

There are a number of ways to test whether two proteins function as a ligand-receptor pair. Competition binding assays can be carried out in cell culture, but this does not prove that binding is functional. Similarly, *in vitro* assays such as surface plasmon resonance can demonstrate protein-protein interactions, but again this does not produce functional evidence. Testing signalling in cultured cells has the advantage that the read-out of ligand binding demonstrates a functional interaction. Given that the read-out of NFκB signalling can also be complemented with *in vivo* tests, this was considered the best approach. I therefore tested whether DNT1 and DNT2 can activate NFκB signalling through Toll-7 and Toll-6.

In order to investigate whether DNT1 and DNT2 can signal through Toll-7 and Toll-6 in cultured cells, it is first necessary to obtain recombinant DNT protein. DNT1, DNT2 and Spz possess a cystine-knot (CK) domain that is structurally homologous to neurotrophin family,

and an N-terminal pro-domain (DeLotto and DeLotto, 1998, Mizuguchi et al., 1998, Zhu et al., 2008). To signal, the CK of Spz is cleaved from the pro-domain by Easter or SPE *in vivo* (DeLotto and DeLotto, 1998, Jang et al., 2006), and it is likely that DNT1 and DNT2 maturation also involves the cleavage of their CK from the pro-domain. DNT1 possesses an additional domain C-terminal to the cys-knot (CTD), also called DNT1 CK+3' (Zhu et al., 2008, Sutcliffe et al., Submitted). It is unclear whether this extra domain remains with the CK or is also endogenously cleaved. Both the CK and the CK + CTD proteins are functional *in vivo*, though they can produce different results in different experimental paradigms (Pennack, 2008, Sutcliffe, 2010).

Functional DNT1 and DNT2 CKs can be expressed *in vivo* under the Gal4/UAS system, as can the CK of Spz (Zhu et al., 2008, Hu et al., 2004). However, in cell culture experiments, the Spz pro-domain is required for the expression and secretion of a functional protein (Weber et al., 2007). Recombinant full-length Spz protein can be produced in E. coli, or by using the Baculovirus expression system (Hoffmann et al., 2008, Weber et al., 2003, DeLotto and DeLotto, 1998). Alternatively, small quantities of DNT protein can be produced in *Drosophila* S2 cells transfected in a 6-well plate (Arnot et al., 2010). The advantage of Baculovirus expression is that it uses insect cells to generate protein which is folded and secreted into the cell supernatant, and can be harvested under native conditions. It is therefore more likely to yield a protein that shows correct folding.

During dorsoventral patterning, Toll signalling leads to the activation of Dorsal, an NFκB homologue (Moussian and Roth, 2005). In the innate immune response, Toll also activates Dif, and Dorsal and Dif can act redundantly in some contexts (Manfruelli et al., 1999, Meng et al., 1999). Both *dorsal* and *Dif* are expressed in the nervous system (Cantera et al., 1999, Mindorff et al., 2007). Toll-7 and Toll-6 share the same intracellular domain as Toll, so it is

most likely that they also signal through these NFκB homologues. Indeed, *elavGal4>Toll-7*$^{\Delta LRR}$ and *elavGal4>Toll-6*$^{\Delta LRR}$ rescue the *spz*^{2} mutant semi-lethality, and *elavGal4>Toll*^{10b} rescues the *DNT1*^{41}*DNT2*^{e03444} mutant semi-lethality, providing further evidence that Tolls share intracellular signalling pathways (see Chapter 4).

NFκB signalling can be measured using two methods: testing for nuclear localisation of NFκB protein, or with the use of reporter plasmids. When Dorsal is activated, it translocates to the nucleus, following the phosphorylation and degradation of Cactus (Rushlow et al., 1989, Steward, 1989, Roth et al., 1989, Verma et al., 1995). Expressing *Toll*^{10b} in cell culture activates Dorsal, and this can be quantified by visualising the nuclear localisation of Dorsal by immunocytochemistry (Kubota et al., 1993). Alternatively, the use of a reporter plasmid can be used to quantify NFκB signalling in cultured cells. The most convenient reporter is Luciferase, and kits are commercially available for the quantification of Luciferase activity, using luminescence as a read-out. To measure Dorsal activity, a number of reporters are available, including *zen-Luciferase*, *snail-Luciferase*, and *twist-Luciferase* (Reach et al., 1996, Ratnaparkhi et al., 2008). It has been shown previously that the most responsive reporter to Dorsal is *snail-Luciferase*, and the strength of the luminescence signal can be augmented by adding *dorsal* cDNA (Ratnaparkhi et al., 2008). To measure Dif activation, a *drosomycin-Luciferase* reporter can be used (Tauszig et al., 2000). An advantage of the drosomycin reporter is the availability of a S2 cell line stably-transfected with this plasmid (Weber et al., 2003). In experiments using either *snail-Luciferase* or *drosomycin-Luciferase*, a control plasmid is also transfected: *actin-Renilla*. This plasmid encodes the Renilla Firefly gene, and is constitutively expressed under the actin promoter. Renilla Firefly activity is also measured by luminescence, but it uses a different substrate and requires different buffer conditions. In this way, the Firefly and Renilla readings can be obtained independently. By co-transfecting

with *actin-Renilla*, which does not respond to Dorsal or Dif, experimental Firefly readings can be normalised, which takes into account differences in transfection efficiency and cell number.

6.2 Results

6.2.1 Expression of recombinant DNT1

To express DNT1 protein using the Baculovirus system, cDNA was first cloned into pFastBac vectors, and then shuttled in to the Baculovirus bacmid using the Bac-to-Bac method using DH10Bac E. coli (Invitrogen) (see materials and methods). The isolated bacmid was then given to the Baculovirus Facility at the Department of Biochemistry, University of Cambridge, who carried a time-course of expression from two cell lines. The Baculovirus facility then returned samples of cell pellets and supernatants generated during the time-course. To test for the production of DNT protein, the supernatant samples were tested by western blot, probing for the His-tag included in the constructs. Only the supernatants were assayed for presence of His-tagged DNT1. For the protein to be functional, it must be folded correctly, and subsequently secreted from the cells. Protein that accumulates in inclusion bodies is likely to be misfolded, and therefore not suitable for cell signalling assays. Protease recognition sequences were included in expression constructs, so that the pro-domain could be cleaved from the CK to generate mature DNT proteins. Expression of DNT proteins using Baculovirus was undertaken in collaboration with Dr Jukka Aurikko and Prof Nick Gay at the Department of Biochemistry, University of Cambridge.

To produce mature DNT1 protein, I first generated constructs encoding DNT1 CK and DNT1 CK+CTD. In flies, the CK and the CK+CTD can be expressed without the endogenous pro-

domain (Zhu et al., 2008). So that the protein would be secreted from cells, and could be identified by western blot, an exogenous EGT signal peptide (SP) and protein tags were included at the N-terminal. The final constructs therefore encoded: EGT SP–FLAG-His-Thrombin–DNT1 CK and EGT SP–FLAG-His-Thrombin–DNT1 CK+CTD. However, western blot of all the supernatant samples from the time-course failed to detect any His-tagged DNT protein (Fig 6.1B). Since Spz requires its pro-domain to be expressed in cultured cells (Weber et al., 2007), a construct was cloned that contained the endogenous DNT1 Pro-domain + CK. Evidence from our lab has shown previously that the CTD can be spontaneously cleaved in cell culture (Zhu et al., 2008). Therefore, to ensure the His-tag remained with the CK, it was placed at the C-terminal of the CK, and the CTD was removed, resulting in DNT1 Pro+CK–TEV-His. However, none of the DNT1 Pro+CK time-course supernatant samples contained a His-tagged protein detectable by western blot (Fig 6.1B). My collaborators routinely produce recombinant Spz using the Baculovirus system, with a construct encoding the Spz pro-domain, followed by a His-tag and TEV protease sequence, with the Spz CK at the C-terminal (Weber et al., 2003). Using this as a template, the DNT1 CK+CTD was cloned and substituted for the Spz CK. The resultant construct was: Spz Pro–His-TEV–DNT1 CK+CTD. However, once again, His-tagged protein could not be detected in supernatant samples from the Baculovirus time-course (Fig 6.1B). Another member of the Gay lab, Dr Chris Arnot, produced smaller quantities of Spz protein in cells cultured in a 6-well plate, which were sufficient for signalling assays (Arnot, 2009). I therefore cloned a full-length DNT1 construct suitable for protein expression from small cultures of S2 cells. The final construct contained the endogenous pro-domain, a TEV protease sequence, His and V5 tags, and the CK + CTD. To test for the production and secretion of DNT1 from S2 cells, a sample from transfected cells was tested by western blot, probing for the presence of a

V5-tagged protein. V5-tagged DNT1 was detected as a band of ≈40kDa (Fig 6.1C). This size is consistent with the CK and the CTD remaining together after expression. The predicted size of the CK+CTD according to the amino acid sequence is ≈46kDa, also seen previously in our lab (Zhu et al., 2008). The reduced size could reflect a partial proteolysis of the C-terminal of the protein, since the V5 tag is attached to the DNT1 CK at its N-terminal.

6.2.2 Expression of recombinant DNT2

As with DNT1, constructs encoding DNT2 were generated for expression using the Baculovirus system and from S2 cells. To produce mature DNT2, a construct was generated that included an EGT signal peptide, FLAG and His tags, and a thrombin protease N-terminal to the DNT2 CK. Baculovirus was then made which contained the EGT SP–FLAG-His-Thrombin–DNT2 CK construct, and given to the Baculovirus facility for generation of time-course samples. However, none of the supernatant samples yielded a His-tagged protein detectable by western blot (Fig 6.2B). Next, a full-length DNT2 construct was made, with C-terminal TEV and His sequences, which included the endogenous pro-domain. Again, the supernatant samples from the Baculovirus time-course were probed by western blot for the presence of His-tagged protein. On this occasion, protein was detected as a band of ≈41kDa, which corresponds to the size of full-length DNT2 (Fig 6.2B). According to the time course samples, the optimum conditions for expression of DNT2 with Baculovirus are using Sf9 cells, using a multiple of infection of 10, and culturing the cells for 4 days before protein purification. Finally, a construct was made for expression of full-length DNT2 from small cultures of S2 cells. Similarly to DNT1, this placed TEV and tag sequences between the pro-domain and CK of the protein, resulting in DNT2 Pro–TEV-His-V5–DNT2 CK. This was transfected into S2 cells, and the supernatant was probed for the presence of V5-tagged

protein by western blot. V5-tagged DNT2 was detected as a band of ≈13kDa (Fig 6.2C). This size corresponds to the tagged DNT2 CK, and suggests that the pro-domain is spontaneously cleaved under these culture conditions.

6.2.3 Expression and purification of DNT2 using Baculovirus

Protein expression with Baculovirus, and the subsequent investigation of recombinant DNT2 protein, was carried out in collaboration with Dr Jukka Aurikko and Prof Nick Gay at the Department of Biochemistry, University of Cambridge. To produce recombinant DNT2 on a large scale, 2l cultures of Sf9 cells were infected, and protein purification was carried out after 4 days (see Section 2.4.1, materials and methods). To test whether DNT2 was purified, a sample of the eluate was run on SDS-PAGE, alongside a sample of the original supernatant. All protein was stained with Coomassie. In the original supernatant, there were no specific proteins visible. In the purified sample, which had been significantly concentrated from the original supernatant, specific protein species were visible. Protein corresponding to full-length DNT2 was barely detectable at 41kDa. Instead, proteins of ~13kDa and ~28kDa were seen (Fig 6.3A). To identify these proteins, they were blotted to a PVDF membrane and sent for Edman sequencing of their N-terminals at the Protein and Nucleic Acid Chemistry Facility, at the Department of Biochemistry, University of Cambridge. The N-terminal sequence of the 28kDa fragment was ‘HSSPPPCGLY’, which is found at the start of the DNT2 pro-domain after removal of the signal peptide (Fig 6.3B, C). The N-terminal sequence of the 13kDa fragment was ‘$^{S}/_{H}$PGRXT’, which aligns to ‘SPGRST’, found in DNT2 just upstream of the six conserved cysteine residues that comprise the CK (Fig 6.3B, C). These results show that the 28kDa protein is the DNT2 pro-domain and the 13kDa protein is the DNT2 CK, and that they are most likely spontaneously cleaved under Baculovirus expression conditions. To

Fig 6.1 - Recombinant DNT1 protein expression

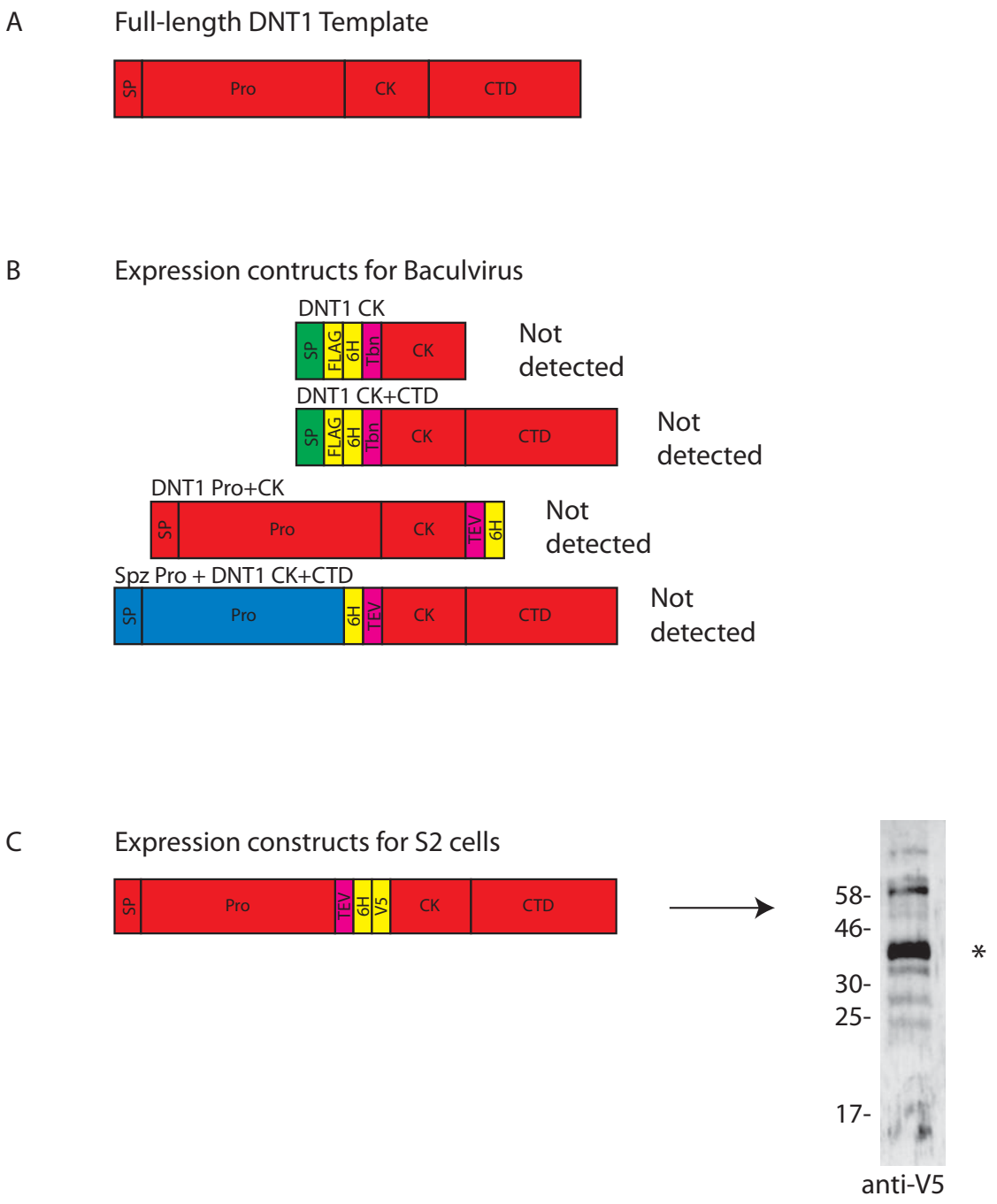

(A) Full-length DNT1 consists of a signal peptide (SP), a pro-domain (Pro), a Cys-knot (CK), and a C-terminal domain (CDT). (B) Constructs were made to express DNT1 using Baculovirus. None of these produced protein that could be detected by western blot in the culture supernatant. (C) Full-length DNT1 was expressed in S2 cells, and secreted into the supernatant as a cleaved CK+CTD protein, detected by western blot (* right).

Fig 6.2 - Recombinant DNT2 protein expression

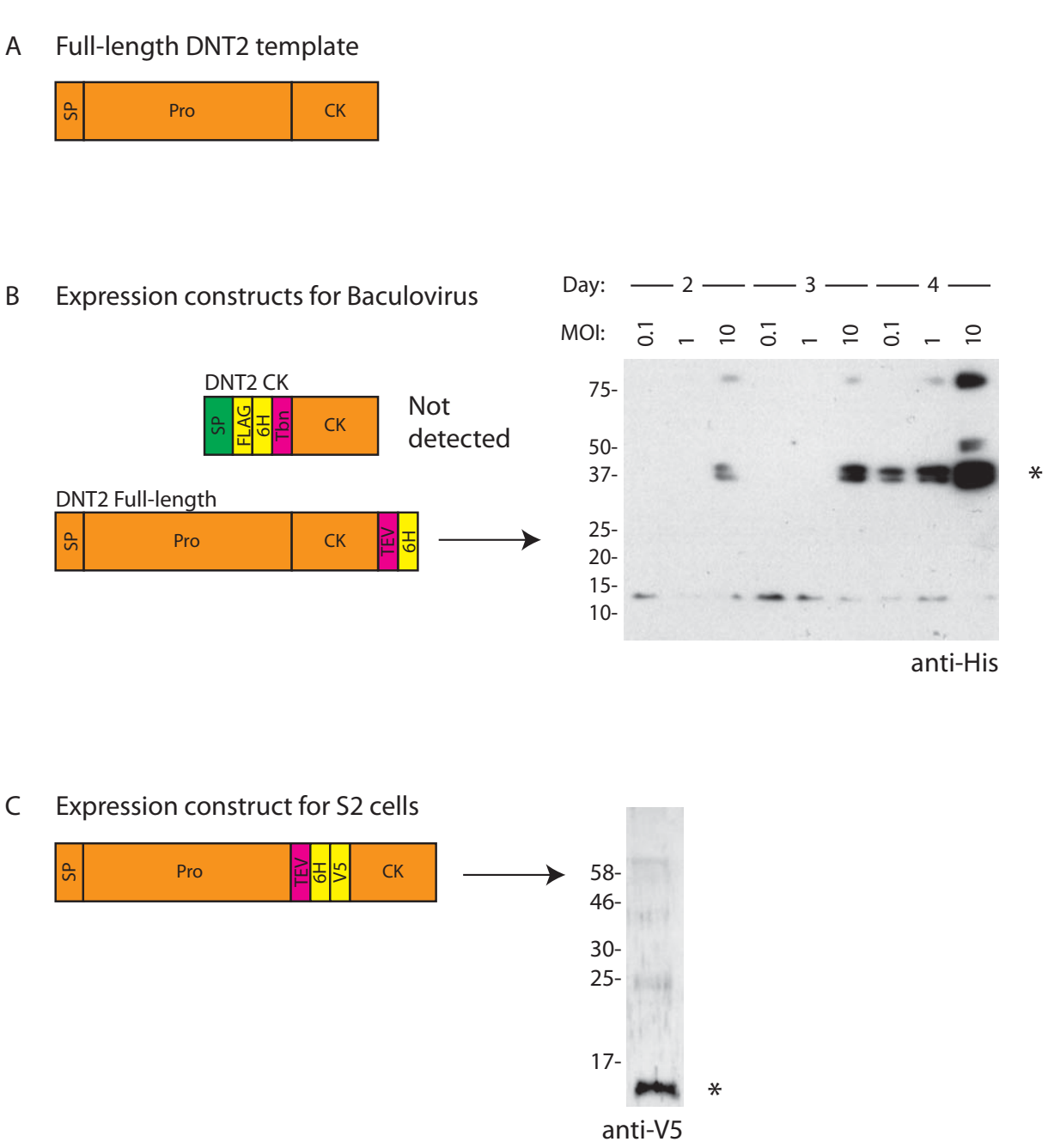

(A) Full-length DNT2 consists of a signal peptide (SP), a pro-domain (Pro), and a Cys-knot domain (CK). (B) Constructs were made to express DNT2 using Baculovirus. No protein was detected when the tagged CK was expressed alone. Tagged full-length DNT2 was detected in the cell supernatant by western blot (* right). The optimum conditions for expression were infecting with an MOI of 10, and culturing for 4 days. (C) Full-length DNT2 was expressed in S2 cells, and secreted as a cleaved CK protein in to supernatant, detected by western blot (* right).

remove the pro-domain, a sample of the purified DNT2 was treated with 1:100 Trypsin for 30mins at 37°C. This effectively degraded the pro-domain, and left the 13kDa CK intact (Fig 6.4A). Under non-reducing conditions, the protein was detected as ~26kDa, indicating that the CK normally exists as a disulphide-linked dimer (Fig 6.4A). Trypsin treatment could also damage the CK, so an alternative method was sought that could separate the two purified domains under less harsh conditions. To do this, the purified protein sample was passed through a size-exclusion column. This fractionates the proteins according to molecular weight. Protein is detected as it exits the chromatography column by UV absorbance at 280nm. In the purified sample, DNT2 CK had the lowest molecular weight, and was therefore anticipated to elute last. To identify the protein eluting in the final fractions, samples were run on SDS-PAGE and stained with Coomassie (Fig 6.4B). The final fractions contained a number of protein species, which was contrary to the expectation that proteins would elute according to size. The largest protein, approximately 75kDa, was an unidentified contaminant that also appeared in the time-course and purified samples. The three strongest bands were ~41kDa, ~28kDa and ~13kDa (Fig 6.4B). These sizes correspond to the full-length DNT2, the pro-domain, and the CK. The proteins ran at the same molecular weight under native conditions (through the size-exclusion column), but separated into three species under denaturing, reducing conditions (SDS-PAGE). This is consistent with the DNT2 CK being cleaved from the pro-domain, but them remaining attached under native conditions. Under denaturing conditions, the pro-domain and CK dissociated and were detected separately. Some full-length DNT2, which remained uncleaved, was detected as a band at the predicted 41kDa. This indicates that the fraction collected from the size-exclusion column corresponded to ~41kDa, and included cleaved and intact DNT2 protein. Altogether, DNT2 can be

produced using Baculovirus. The full-length protein is spontaneously cleaved to yield the pro-domain, and the dimerising CK.

6.2.4 Expression of Toll-7 and Toll-6 in S2 cells

To test whether DNTs can activate Toll-7 or Toll-6 signalling, it is first necessary to express the receptors in S2 cells, and test whether they are targeted to the membrane. Wild-type Toll-7 and Toll-6 receptors with C-terminal HA tags were expressed in cells using the pAct-Toll-7-HA and pAct-Toll-6-HA plasmids (see Sections 3.2.1 and 3.2.6, Chapter 3). To test whether the proteins can be detected at the membrane, S2 cells were transfected, and after 48 hours were fixed and labelled with anti-HA. Fig 6.5 shows that, although there was cytoplasmic signal, both Toll-7 and Toll-6 localised to the membrane in S2 cells.

6.2.5 Constitutively active Toll-7 and Toll-6 signal through NFκB

To confirm that Toll-$7^{Cys\text{-}Tyr}$ and Toll-$6^{Cys\text{-}Tyr}$ are functional as constitutively active receptors, and to test whether they signal through NFκB, I tested whether their expression in S2 cells can induce the activation of NFκB reporter plasmids. Activation of Dorsal was tested by transfecting S2 cells with the *snail-Luciferase* reporter, Dif activation was tested in cells stably transfected with the *drosomycin-Luciferase* reporter. Activated receptors were transfected using pUAS-Toll-$7^{Cys\text{-}Tyr}$ and pUAS-Toll-$6^{Cys\text{-}Tyr}$ (see materials and methods). The expression of the activated receptors was therefore under the control of Gal4. By co-transfecting pMT-Gal4, the expression of Gal4 could be activated by adding 1mM $CuSO_4$ to the cell medium, which binds the metallothionine promoter. Thus, expression of Toll-$7^{Cys\text{-}Tyr}$ and Toll-$6^{Cys\text{-}Tyr}$ was induced by adding Cu^{2+} to cultured cells. To test whether the expression of activated receptors can activate NFκB, the reporter activity in cells in which expression

Fig 6.3 - Expression of DNT2 using Baculovirus

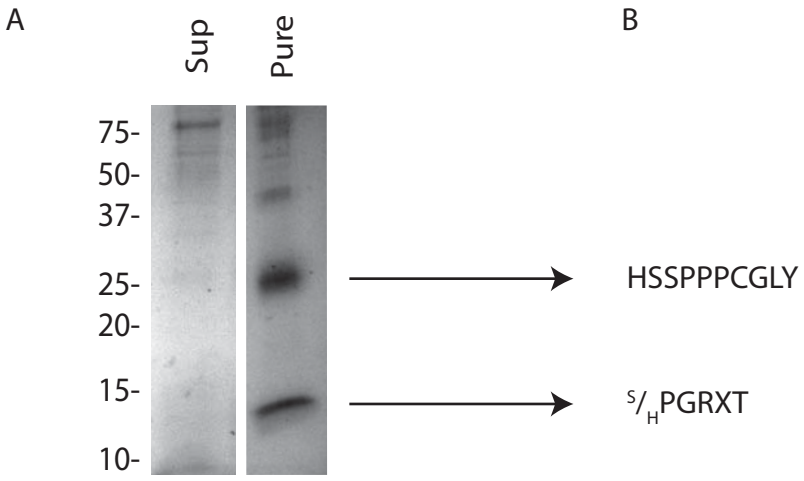

C

DNT2 sequence

28kDa fragment

MTKSIKRPPPFSCKQVLLTYVILAYTVAAHSSPPPCGLYGAPPCQFLPAPPGQTPTCARPGK

TYCEHADNYPTYLIKSLVRKWGYEAATLLVDETWEDFAAVAWHDTPVFYDPKSIFPPRDPA

AQDFNGYSYQTPFGGNPQRPSGGGNPLFVSNPSTEAPTYLLYTSSGGGHRSGHRYNSQG

GGTSSSGGHLYINQSDKSTPYNATLWLKRLVRDLSRKQRQPDEVQAEVVEPVNEQTEEAE

13kDa fragment

EQDNPAEDHPQSKRDVSLNMDLLDIVGVEAPNPLKKRSRTKRQSPGRSTLCQTTSQFITPQ

AALNSRGNWMFVVNEQNTARQMVKAELCASNTCSNLCELPNGYNSRCEQKFVQKRLIALQ

TEV 6His

GNGQNLYTDTFWFPSCCVCTIAAN ENLYFQG HHHHHH

The Cys-knot of DNT2 is spontaneously cleaved after expression using Baculovirus. (A) Purification of DNT2 from a 2l culture yields two proteins of ~13kDa and ~28kDa. Lane marked 'Sup' is from the original cell culture supernatant, 'Pure' is after purification with Ni-NTA. (B) Edman (N-terminal) sequencing results obtained from the two purified proteins. (C) The N-terminal sequences obtained are found in DNT2, and are underlined and in yellow. The six conserved cysteine residues that form the DNT2 CK are highlighted in red, TEV protease and 6His tag sequences are at the C-terminal.

Fig 6.4 - DNT2 CK dimerises, and remains associated with the pro-domain

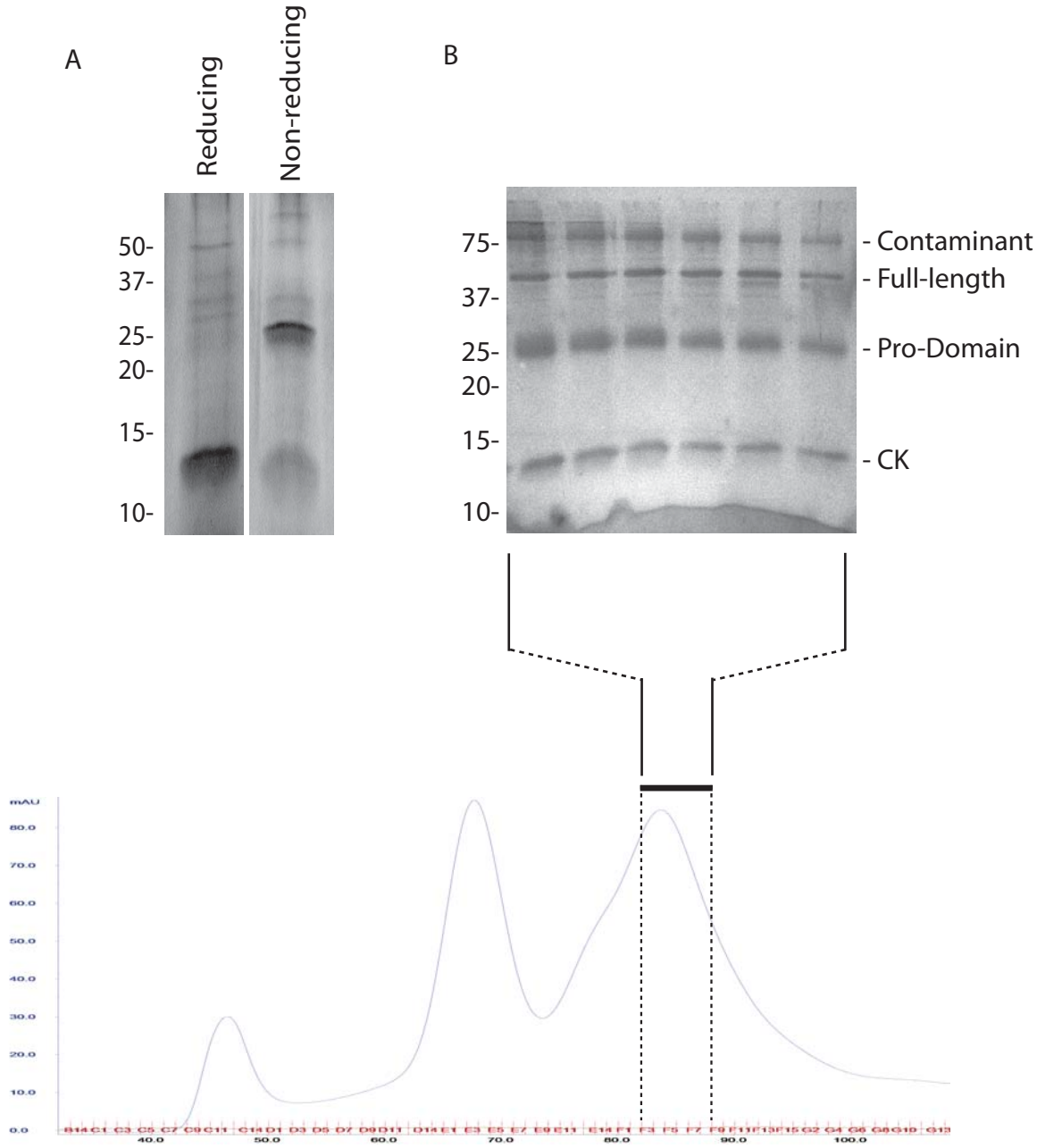

(A) After treatment with trypsin, the DNT2 pro-domain is degraded, and only the CK is detectable. Running the protein in non-reducing conditions reveals it normally exists as a dimer. Protein gel shown, stained with Coomassie. (B) Purified DNT2 was passed through a size-exclusion column, eluted protein was detected by UV absorbance. Lower molecular weight proteins elute last, and are detected on the right of the chromatogram (below). The indicated fractions were run on SDS-PAGE and stained with Coomassie. The proteins corresponding in size to full-length DNT2, the cleaved pro-domain, and the CK all elute together. A high molecular-weight contaminant is also detected.

Fig 6.5 - Toll-7 and Toll-6 localise to the membrane of S2 cells

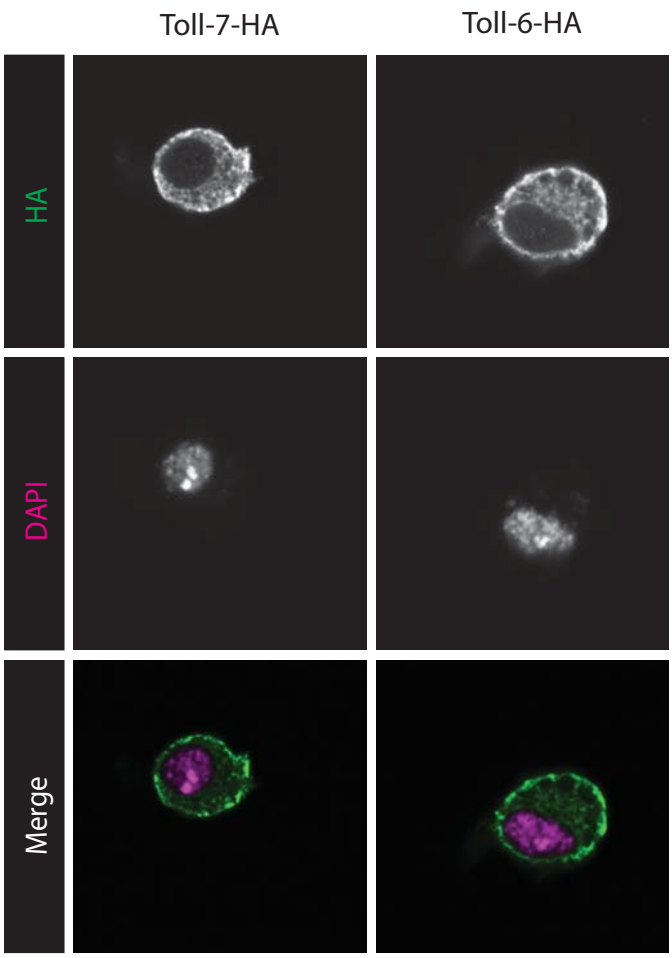

Confocal images of S2 cells expressing HA-tagged Toll-7 and Toll-6. Anti-HA staining is shown, with the nuclear marker DAPI.

was induced by Cu^{2+} was normalised against cells not receiving Cu^{2+}. This generated a relative Luciferase value, which indicated the effect of inducing gene expression with Cu^{2+}. The relative Luciferase activity of cells transfected with both pMT-Gal4 and pUAS-Toll-$7^{Cys\text{-}Tyr}$ or pUAS-Toll-$6^{Cys\text{-}Tyr}$ was compared to cells transfected with only the pMT-Gal4 or only the pUAS plasmid. These singly-transfected cells, and cells transfected with an empty pDONR vector, served as negative controls, since there was no expression of activated receptors (green bars, Fig 6.6A, B).

When Toll-$6^{Cys\text{-}Tyr}$ and Toll-$7^{Cys\text{-}Tyr}$ expression was induced in cells carrying the *snail-Luciferase* there was a modest but significant increase in the Luciferase activity compared to negative control (Fig 6.6A). Toll-$6^{Cys\text{-}Tyr}$ and Toll-$7^{Cys\text{-}Tyr}$ also induced the activation of *drosomycin-Luciferase* (Fig 6.6B). The small increase in Luciferase activity in cell expressing only pMT-Gal-4 is not significantly different from cells transfected with the empty pDONR vector ($p=0.17$). These results confirm that the Cys-Tyr activated receptors are functional. The activation of both NFκB reporters also shows that Toll-7 and Toll-6 can signal through Dorsal and Dif.

6.2.6 DNT1 activates NFκB via Toll-7

To test whether DNT1 can signal through Toll-7 or Toll-6 to activate Dorsal, recombinant protein was added to S2 cells expressing wild-type receptors, and NFκB activity was quantified using the *snail-Luciferase* reporter. The DNT1 CK+CTD protein purified from S2 cell expression used was. Because the amounts of DNT1 produced by S2 cells was small, and consequently the purification process was not highly stringent, a reliable concentration of DNT1 protein could not by obtained. Therefore, all of the protein purified from one 6-well plate culture was used in each batch of experiments. S2 cells were transfected with Toll-7 or

Fig 6.6 – Constitutively active Toll-7 and Toll-6 signal through NFκB

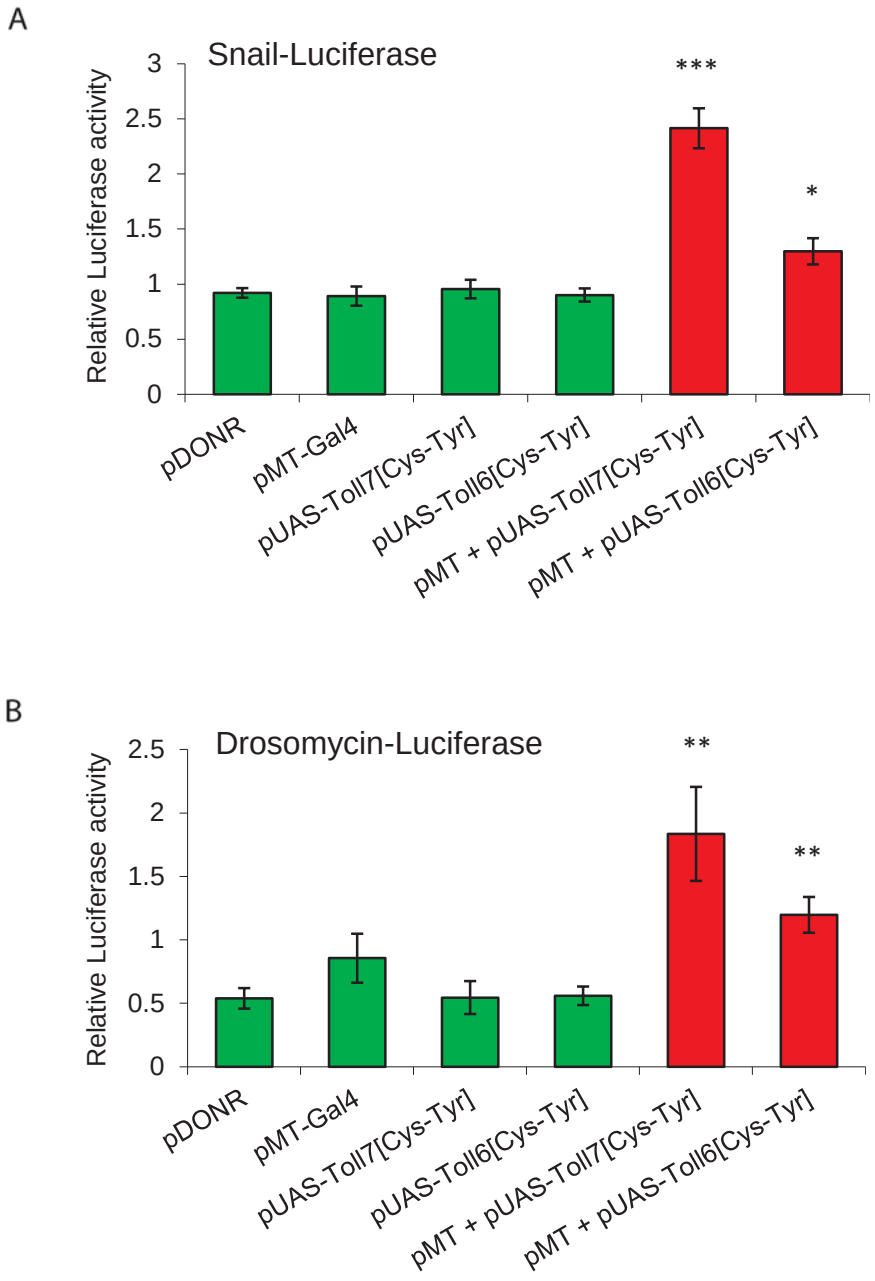

Graphs showing the luciferase activity of cells treated with 1mM $CuSO_4$, relative to untreated cells. *Toll-7*$^{Cys\text{-}Tyr}$ and *Toll-6*$^{Cys\text{-}Tyr}$ are expressed only when pUAS expression plasmids are co-transfected with *pMT-Gal4* (red bars). (A) Cells transfected with the Snail-Luciferase reporter of Dorsal activation and *Dorsal* cDNA. (B) Cells transfected with the Drosomycin-Luciferase reporter of Dif activation. Mean effect ± SEM shown, n≥3, *p<0.05 **p<0.01 ***p<0.001 Student's t-test compared to pDONR.

Toll-6 expression plasmids, *snail-Luciferase*, and the *actin-Renilla* control plasmid, and cultured for 48 hours. *dorsal* cDNA was co-transfected, to increase the *snail-Luciferase* signal. DNT1 CK+CTD was added to the cells, and the Luciferase assay was carried out after 24 hours. However, adding DNT1 did not induce the activation of the *snail-Luciferase* in cells expressing Toll-7 or Toll-6 (Fig 6.7).

An alternative way to test for the activation of Dorsal is to visualise the localisation of Dorsal protein within a cell, by immunocytochemistry. S2 cells were transfected with wild-type Toll-7 or Toll-6, and cultured for 48 hours. Because Dorsal is normally expressed at very low levels in S2 cells, *dorsal* cDNA was co-transfected into cells to be able to detect it by immunostaining. DNT1 CK+CTD purified from S2 cell expression was added, and cells were fixed and labelled with anti-Dorsal after 90 minutes. Cells were examined by confocal microscopy, and the localisation of Dorsal was recorded. Dorsal was determined to be nuclear if there was strong signal in the nucleus (identified by DAPI co-staining), and signal excluded from the cytoplasm (Fig 6.8A). The percentage of cells expressing Toll-7 or Toll-6 with nuclear Dorsal, compared to non-nuclear, was then recorded. DNT1 CK+CTD slightly increased the nuclear localisation of Dorsal in S2 cells expressing Toll-6, although this was not statistically significant (Fig 6.8B). In cells expressing Toll-7, DNT1 CK+CTD significantly induced the proportion of cells with nuclear Dorsal (Fig 6.8B). This shows that DNT1 can activate Dorsal signalling, through at least Toll-7.

To test whether DNT1 could also activate Dif through Toll-7 or Toll-6, recombinant protein was added to cells that carried a Dif reporter plasmid. Wild-type Toll-7 or Toll-6 was transfected into stably-transfected *drosomycin-Luciferase* cells, with the *actin-Renilla* control plasmid. Cells were cultured for 48 hours, and DNT1 CK+CTD purified from S2 cell expression was added. After 24 hours, the Luciferase activity was assayed. In cells transfected

with the empty pDONR vector or with pAct-Toll-6, DNT1 CK+CTD had no effect. In cells expressing Toll-7, DNT1 CK+CTD produced a significant increase in Luciferase activity compared to cells treated with PBS (1.9-fold increase in luminescence, $p<0.05$) (Fig 6.9). This shows that DNT1 can activate Dif signalling through Toll-7.

6.2.7 DNT2 activates NFκB via Toll-7 and Toll-6

To test whether DNT2 can also activate NFκB through Toll-7 or Toll-6, the stably-transfected *drosomycin-Luciferase* cell line was used to test for activation of Dif. DNT2 CK, purified from Baculovirus was used. Since the protein was produced in large amounts, and was relatively pure, a reliable concentration of DNT2 protein could by obtained, and therefore a set amount of DNT2 could be added to cells. S2 cells, stably transfected with *drosomycin-Luciferase*, were also transfected with pAct-Toll-7 or pAct-Toll-6, as well as the *actin-Renilla* control plasmid. After 48 hours, 50nM DNT2 CK was added, and Luciferase activity was determined after a further 24 hours. Adding DNT2 CK to cells transfected with the empty pDONR vector, but without Toll-7 or Toll-6, increased the amount of Luciferase activity compared to PBS-treated cells (Fig 6.9). This suggests that DNT2 can activate Dif through proteins endogenously expressed in S2 cells. When either wild-type Toll-7 or Toll-6 was expressed in S2 cells, addition of DNT2 CK also resulted in a strong induction of the Luciferase reporter (Fig 6.9). Moreover, adding DNT2 CK increased Luciferase activity more in cells expressing either Toll-7 or Toll-6, compared to cells transfected with pDONR. This indicates that DNT2 can signal through Toll-7 and Toll-6 to activate Dif.

Fig 6.7 – DNT1 has no effect on a Dorsal reporter

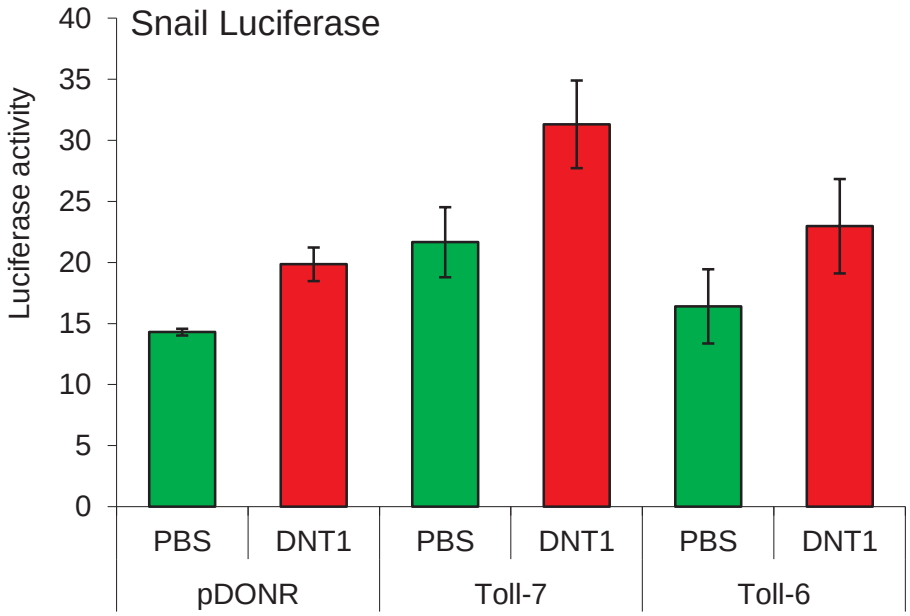

A graph showing no effect on a Dorsal reporter after adding DNT1 to S2 cells expressing Toll-7 and Toll-6. Cells were co-transfected with *Dorsal* cDNA, control cells were transfected with the empty pDONR vector. Mean Luciferase activity is shown ± SEM, n≥3, none of the values are significantly different, Student's t-test

Fig 6.8 - DNT1 signals through Toll-7 to induce the nuclear localisation of Dorsal

A

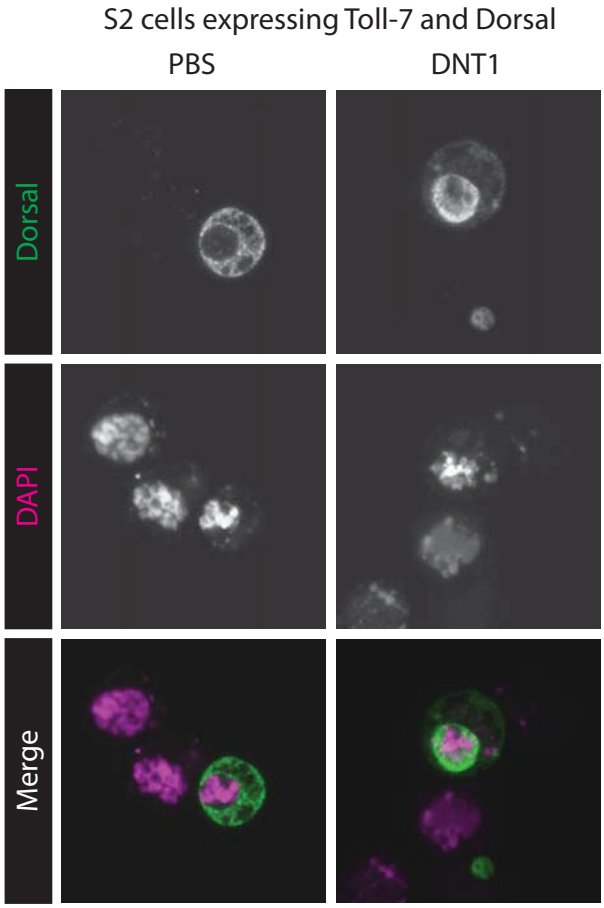

B

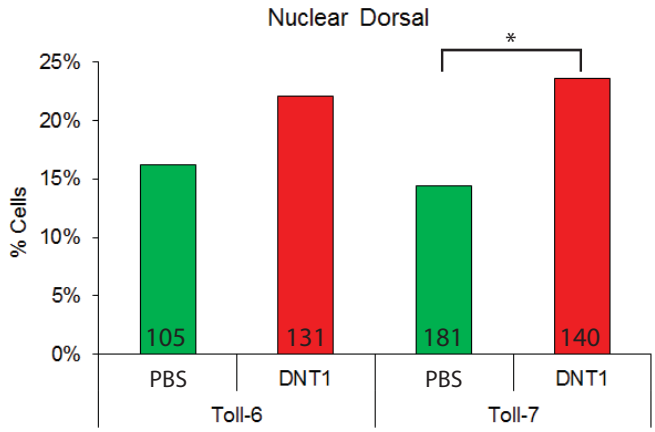

When activated, Dorsal translocates to the nucleus. (A) S2 cells expressing Toll-7 and Dorsal were stained with anti-Dorsal and DAPI, and detected with confocal microscopy. Adding DNT1 lead to the nuclear localisation of Dorsal. (B) Quantification of the effect of DNT1 on Dorsal localisation, in cells expressin Toll-6 and Toll-7. Numbers given in bars, *p<0.05 chi-squared test compared to PBS control.

Fig 6.9 – DNT1 and DNT2 activate Dif through Toll-7 and Toll-6

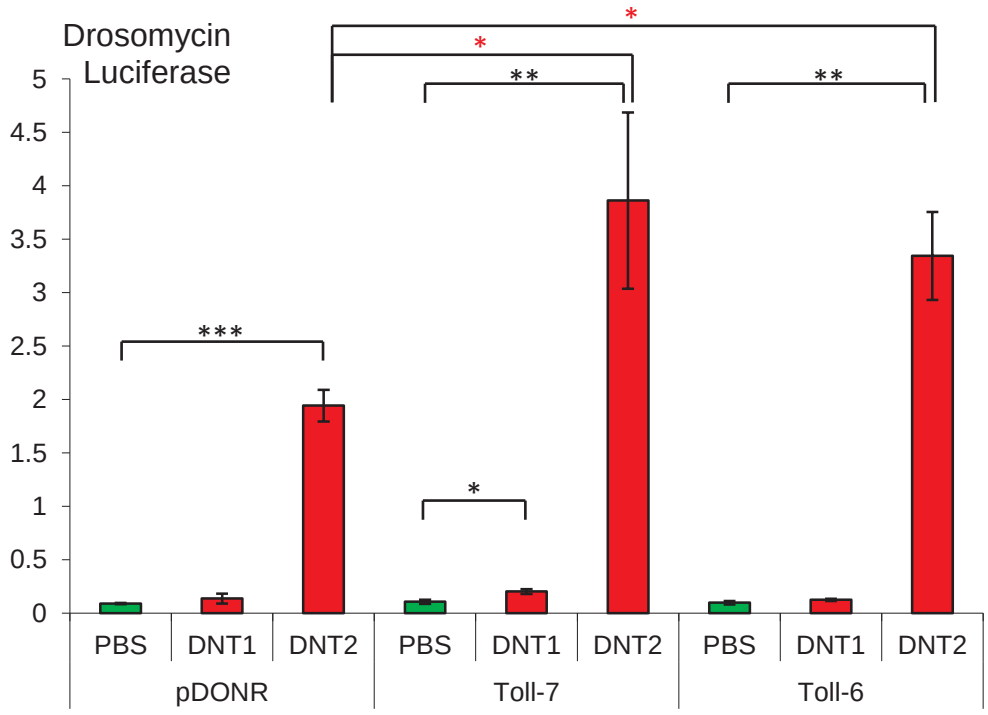

A graph showing the luciferase activity in cells transfected with a Dif reporter. DNT1 and DNT2 were added to cells expressing Toll-7 and Toll-6. Control cells were transfected with the empty pDONR vector. Mean Luciferase activity is shown ± SEM, n≥3, *p<0.05 **p< 0.01 ***p<0.001 Student's t-test, black asterisks compared to PBS control for each receptor (green bars), red asterisks compared to pDONR + DNT1.

6.3 Discussion

In this chapter, I have used cell culture to demonstrate that Toll-6 and Toll-7 can signal through NFκB. Expressing DNT1 using Baculovirus and in S2 cells revealed that the pro-domain and the CTD are both required for the secretion of DNT1 from cultured cells. It is likely that DNT1's pro-domain is also spontaneously cleaved, and that the CTD remains attached to the CK (see also Zhu et al., 2008). Using the Baculovirus expression system, I have produced recombinant DNT2 protein. Similarly to DNT1, the pro-domain is required for secretion of DNT2 from cultured insect cells. The CK is spontaneously cleaved from the pro-domain *in vitro*, though biochemical data are consistent with the two peptides remaining associated under native conditions. DNT1 signalled through Toll-7 to induce the nuclear localisation of Dorsal and the activation of a Dif reporter plasmid. DNT2 signalled through both Toll-7 and Toll-6 to activate Dif signalling.

Expressing constitutively active Toll-7 and Toll-6 in S2 cells lead to the activation of reporters of both Dorsal and Dif activity. The effects seen were modest, although they were significant. Given more time, I could have better optimised the conditions for this experiment; it is likely that transfection conditions could be improved, particularly given the large number of plasmids involved in each transfection. One strategy to improve this could be to establish cells lines stably transfected with all of the common plasmids, reducing the amount of DNA needed for transient transfections. It is interesting to note that Toll-$7^{Cys\text{-}Tyr}$ produced a stronger effect than Toll-$6^{Cys\text{-}Tyr}$. It is not clear why the two paralogues should have behaved differently in this context, when they produced similar results in the rescue of cell death and lethality. It is known that Toll can activate both Dif and Dorsal, and the choice of NFκB paralogue used depends on the context (Manfruelli et al., 1999, Meng et al., 1999). Equally,

Toll-9 has also been shown to activate Dif (Ooi et al., 2002), and Toll-8 (Tollo) can interact with Relish (Ayyar et al., 2007). It is therefore not surprising that Toll-6 and Toll-7 can signal through NFκB. Whether the receptors employ Dif or Dorsal *in vivo* is likely to depend on the cell type and context.

The effects on NFκB signalling of DNT1 and DNT2 are not comparable. DNT2 was obtained using the Baculovirus system, in large quantities with high purity. DNT1 was obtained from small-scale cultures of S2 cells, and was not purified in sufficient quantities to be visible on a Coomassie-stained protein gel. Producing recombinant DNT1 protein was not as simple as initially anticipated. By the time the optimum arrangement of protein domains was discovered for expression in S2 cells, there was not enough time to express it in larger quantities using Baculovirus. I would anticipate that, had I obtained Baculovirus-expressed DNT1, the data relating to the effect of DNT1 on S2 cells may have been statistically significant, less equivocal, and comparable to those obtained with DNT2. However, in the attempt to express and purify DNT ligands, some of their biochemical characteristics have been revealed.

In vivo, functional CK isoforms of Spz, DNT1 and DNT2 can be expressed without the endogenous pro-domain (Hu et al., 2004, Zhu et al., 2008). However, attempts to directly produce DNT1-CK and DNT2-CK in cultured insect cells using the Baculovirus system did not yield any protein. Mature DNT2 was only purified from culture supernatant when the full-length construct was expressed. In the case of DNT1, the endogenous pro-domain and CTD were both required for the expression and secretion of the mature protein. The requirement of the pro-domain for secretion in the Baculovirus expression paradigm is also seen with Spz (Weber et al., 2007). Similarly, the pro-domain is necessary for the expression and secretion of the Spz homologue, NGF, from cultured cells (Suter et al., 1991). Moreover, the secretion of different vertebrate neurotrophins is regulated by their pro-domains: mature NGF is

secreted from cultured cells when expressed with its endogenous pro-domain, but is retained in cells when fused to the BDNF pro-domain (Nomoto et al., 2007). This suggests that the secretion of Spz homologues can be regulated by interactions with the pro-domain, and may explain why DNT1 CK+CTD was not detectable when fused to the Spz pro-domain.

DNT expression clones were generated that included either a TEV or Thrombin protease recognition sequence. It was anticipated that the pro-domain would remain attached to the CK, and that a directed proteolysis would be required to yield mature DNT protein, since this is the case with Spz (Weber et al., 2003). However, biochemical analysis of purified DNT proteins suggest that the pro-domains are spontaneously cleaved from these Spz paralogues.

When full-length DNT1 was expressed in S2 cells, the size of the V5-tagged protein detected by Western blot corresponded to the cys-knot plus much of the CTD. While both the pro-domain and the CTD are required for protein secretion, the persistence of the CTD suggests that it could play a role in DNT1 signalling. The long CTD is unique to DNT1 within the Spz family, however it is conserved between invertebrate species, which could also indicate that it is functionally important (Parker et al., 2001, Wilson, 2009). *In vivo*, both DNT1 CK and DNT1 CK+CTD can promote cell survival (Zhu et al., 2008). However, in axon targeting, at the larval NMJ, and in behavioural assays, expression of DNT1 CK+CTD gave clearer phenotypes (Pennack, 2008, Sutcliffe, 2010). Therefore, the CTD of DNT1 is functionally important, and is a characteristic unique to DNT1 within the neurotrophin family.

When full-length DNT2 was expressed using Baculovirus, the CK was spontaneously cleaved from the pro-domain, which separated on a reducing, denaturing gel. Under native conditions, through a size-exclusion column, the cleaved pro-domain and cys-knot eluted in the same fractions as the intact full-length DNT2. This suggests that after cleavage, the pro-domain and

cys-knot could remain attached. Similarly, the pro-domain and CK of Spz remain together after cleavage, and separate on binding to Toll (Weber et al., 2007). In Spz, this is due interaction of charged residues on the pro-domain and CK (Arnot et al., 2010), though it is unclear if the same happens with DNT2.

The effect of DNT1 on Luciferase reporters in S2 cells was very weak. As mentioned above, this is probably due to the quality of the recombinant DNT1 protein obtained. There was only enough time to produce DNT1 on a small scale, using S2 cells. The total amount of DNT1 secreted into the cell medium would have been relatively small from the outset. And the methods of purifying protein from these small volumes were more likely to result in protein loss, compared to Baculovirus-expressed protein: for example, using NiNTA spin columns with small volumes, compared to 1 hour incubation with NiNTA-agarose with Baculovirus. Moreover, although the purification process isolated DNT1 from most of the protein contaminants in the supernatant, the level of purity was likely to be much lower than Bacolvirus-produced DNT2. To mitigate this, each time the experiment was repeated, a fresh batch of DNT1 was produced, and all of the protein was used up on each occasion. In this way, the maximum amount of DNT1 was added to the cells as was possible. However, either because of a small amount of DNT1, or a larger amount of contaminating protein, the effects seen with DNT1 are much smaller than those of DNT2. Given more time, I would return to the Baculovirus system to produce DNT1 in large quantities. This would be likely to greatly improve the strength of the response of Luciferase reporters in S2 cells to DNT1. Because the effects of DNT1 were less robust than those of DNT2, I looked at an additional measure of NFκB activation. The induction of nuclear localisation of Dorsal protein, together with the activation of the *drosomycin-Luciferase* reporter, show that DNT1 can activate NFκB signalling through Toll-7.

DNT2 is able to significantly activate *drosomycin-Luciferase* in S2 cells, even when no Toll receptor was transfected. The same effect is seen when Spz is added to S2 cells that have not been transfected with Toll, and is due to endogenous Toll expression in this cell line (Weber et al., 2003). DNT2 rescues Spz mutant lethality, which could point to promiscuity in DNT/Toll binding (Sutcliffe, 2010). Therefore, DNT2 could be signalling through Toll to activate NFκB, or through promiscuous binding to an additional, endogenously expressed receptor. To test these hypotheses, experiments could be repeated that included RNAi targeting each of the receptors.

DNT2 activated Dif signalling in cells transfected with Toll-7 and Toll-6, at significantly higher levels than in untransfected cells. This indicates DNT2 signals through Toll-7 and Toll-6 to activate NFκB. Activation of both receptors by DNT2 suggests that there is promiscuity of binding between the DNTs and the Tolls. However, the DNT2 results do not provide any evidence of for a specific relationship to Toll-7 or Toll-6. And the results with DNT1 are not strong enough to rule out similarly promiscuous binding. One way to approach this question would be to assess the binding affinities of the DNTs to Toll-7 and Toll-6. To do this would require DNT1 protein of a comparable amount and purity to DNT2, that is, expressed using Baculovirus. With high-quality DNT1, binding affinities could be tested *in vitro* using surface plasmon resonance, or in culture by producing dose-response curves for NFκB activation. However, the specificity of binding and NFκB activation in cell culture would not necessarily reflect all of the *in vivo* signalling events. In the fly, whether a DNT binds to a Toll will depend on their expression patterns and amount of protein available to signal. Also, the endogenous signalling pathway will depend on the presence of Dif, Dorsal, or some other factor, within the cell.

In this chapter, I have demonstrated that DNTs signal through Tolls in cell culture. Together with the patterns of expression, genetic interactions, shared phenotypes and rescue experiments, my results support a role for Toll-7 and Toll-6 functioning in the CNS as DNT receptors.

CHAPTER 7
DISCUSSION

7.1 Summary of results

The aims of this thesis were to investigate the functions of Toll-7 and Toll-6 in the *Drosophila* CNS, and to test whether they could function as DNT receptors. I first examined the expression patterns of *Toll-7* and *Toll-6* in embryos, and in the larval and adult CNS, by *in situ* hybridisation and by *Gal4*-driven expression of *GAP-GFP*. In embryos, *Toll-7* mRNA was detected in the CNS and in the epidermis, and also in clusters cells in the thorax that are most likely the leg primordia. By the end of embryogenesis, *Toll-7* expression was largely restricted to the leg primordia, and the CNS – where mRNA was most strongly detected. *Toll-7* mRNA was also detected in the larval CNS and the adult brain, both in central brain regions and the optic lobes. I generated a *Toll-7-Gal4* fly line, and used it to drive expression of membrane-targeted *GAP-GFP*. There was significant overlap of the *in situ* and GFP expression patterns, particularly in the CNS. The labelling of axons by GFP identified cells as neurons. *Toll-6* mRNA was detected in the embryonic CNS and epidermis. In late embryos, *Toll-6* expression was distributed in the CNS and small clusters of cells lateral to the VNC, which could be epidermis, PNS or muscle. *In situ* hybridisation revealed expression of *Toll-6* in the larval CNS and in the adult brain, in both the central brain and optic lobes. Using the *D42 Gal4* driver, which is inserted upstream of *Toll-6*, to drive expression of *GAP-GFP*, a population of cells was labelled that frequently overlapped with the *in situ* pattern. Axonal projections revealed these cells as neurons. Therefore, these data indicate that *Toll-7* and *Toll-6* are expressed in neurons in the *Drosophila* CNS, from embryos to adults

I next investigated the functions of the receptors, and tested whether they can interact with the DNTs. To do this, I generated null mutant alleles, with the help of Janine Fenton and Sarah Quail, and generated constitutively active receptor constructs for gain-of-function transgenic flies. To test for a lethality phenotype, *Toll-7* and *Toll-6* single and double mutant flies were balanced over *TM6B* or *SM6aTM6B* as heterozygotes, and kept at 18°C. The survival index of the $Toll\text{-}7^{P8}$ and $Toll\text{-}7^{P114}$ mutants was slightly reduced, and that of $Toll\text{-}6^{26}$ and $Toll\text{-}6^{31}$ mutants was not reduced, compared to controls; but $Toll\text{-}7^{P8}Toll\text{-}6^{26}$ and $Toll\text{-}7^{P114}Toll\text{-}6^{31}$ double mutants show a semi-lethal phenotype. Similarly, $DNT1^{41}$ single mutants showed a reduced survival index and $DNT2^{e03444}$ showed a wild-type survival index, and the $DNT1^{41}DNT2^{e03444}$ double mutants showed a semi-lethal phenotype. I also investigated genetic interactions between *DNT*s and *Toll*s, by combining *Toll-7*, *Toll-6* and *DNT* mutant alleles. $Toll\text{-}7^{P114}DNT2^{e03444}$ and $Toll\text{-}6^{26}DNT1^{41}$ double mutants were semi-lethal over TM6B at 18°C, suggesting an interaction between Toll-7 and DNT1, and Toll-6 and DNT2. The semi-lethality of spz^{2} mutants was rescued by expressing activated forms of *Toll-7* and *Toll-6* in neurons, revealing that Toll-7 and Toll-6 can function like Toll, most likely by activating NFκB. Finally, expressing constitutively active *Toll-7* and *Toll-6* in neurons rescued the $DNT1^{41}DNT2^{e03444}$ double mutant semi-lethality. This demonstrates that Toll-7 and Toll-6 can function downstream of DNT1 and DNT2, which is consistent with them serving as receptors for the DNTs. The rescue of lethality by expressing activated receptors in neurons demonstrates that *Toll-7* and *Toll-6* have important cell-autonomous functions in neurons.

To investigate the functions of *Toll-7* and *Toll-6* in the *Drosophila* nervous system, I tested for locomotion, axon targeting and cell survival phenotypes. $Toll\text{-}7^{P8/P114}$ and $Toll\text{-}6^{26/31}$ single and double mutant adults show locomotion phenotypes: they walk more slowly than controls, and spend more time resting. Therefore the receptors are required for normal locomotion in

adults. I next investigated a role for *Toll-7* and *Toll-6* in axon targeting, by looking at anti-FasII-labelled ISNb motor axons in single and double mutant embryos. In *Toll-6*$^{26/31}$ and *Toll-6*$^{26/DfXG4}$ single mutants, there was in increase in the frequency of misrouting phenotypes compared to controls. In *Toll-7*$^{P8/P114}$ and *Toll-7*$^{P114/DfBSC22}$ single mutants, there was increased misrouting, and also hemisegments in which all of the stereotypic ISNb projections were lost. In *Toll-7*$^{P8/P114}$*Toll-6*$^{26/31}$ double mutants, the misrouting and loss of projection phenotypes were further increased. I also tested whether *Toll-7* and *Toll-6* can regulate cell survival in the embryonic CNS. In *Toll-7*$^{P8/P114}$, *Toll-7*$^{P114/DfBSC22}$, *Toll-6*$^{26/31}$ and *Toll-6*$^{31/DfXG4}$ mutants, there was an increase in apoptosis in the embryonic VNC, indicating that *Toll-7* and *Toll-6* are required for cell survival. Expressing activated receptors in neurons rescued naturally occurring cell death to below control levels, showing that the receptors can promote cell survival. And most importantly, the increased cell death phenotype of *DNT1*^{41} and *DNT2*$^{e03444/Df6092}$ mutant embryos was rescued by expressing *Toll-7*$^{Cys\text{-}Tyr}$ and *Toll-6*$^{Cys\text{-}Tyr}$ in neurons. These results indicate that *Toll-7* and *Toll-6* are required for normal fly behaviour, and axon targeting and cell survival in the developing CNS. The rescue of DNT mutant phenotypes by activated receptors is evidence that Toll-7 and Toll-6 functionally interact with the DNTs *in vivo*, and act downstream of the ligands.

Finally, to test whether DNT1 and DNT2 can signal through Toll-7 and Toll-6, I carried out signalling assays in cell culture. To do this, it was first necessary to generate recombinant DNT protein. After unsuccessful attempts with the Baculovirus system, recombinant DNT1 was expressed in S2 cells. For expression and secretion from cells, DNT1's endogenous pro-domain and CTD are required, though in cultured cells the pro-domain appeared to be spontaneously cleaved, yielding mature DNT1 CK+CTD protein. DNT2 was produced using the Baculovirus expression system. As with DNT1, DNT2's pro-domain was required for the

expression and secretion of DNT2 from insect cells, though it is also cleaved in culture. Biochemical analysis is consistent with the pro-domain being spontaneously cleaved from the DNT2 CK, but that the two domains remain associated under native conditions. Expressing *Toll-7*$^{Cys\text{-}Tyr}$ and *Toll-6*$^{Cys\text{-}Tyr}$ in S2 cells resulted in the activation of Dif and Dorsal. DNT1 activated the Dif reporter and induced the nuclear localisation of Dorsal, signalling through Toll-7. DNT2 strongly activated the Dif reporter, and can signal through Toll-7 and Toll-6.

Altogether, my data show that *Toll-7* and *Toll-6* are expressed in the *Drosophila* CNS; that they function to control adult behaviour, axon targeting and cell survival; and that they can function both *in vivo* and in cell culture as DNT receptors.

7.2 Toll-7 and Toll-6 function in the *Drosophila* CNS

Toll-7 and *Toll-6* are expressed in the CNS, from embryos to adults. Previous reports have shown *Toll-7*, *Toll-6* and Toll are expressed in the CNS; none of the other paralogues have been described in the nervous system (Kambris et al., 2002, Zhu et al., 2008). *Toll-7Toll-6* double mutants are semi-lethal, and this phenotype can be partially rescued by expressing activated receptors in neurons. This shows that, to some extent, *Toll-7* and *Toll-6* are required in the nervous system for viability. However, the incomplete rescue suggests that the receptors might be also required in other tissues.

Toll-7 and *Toll-6* are required for normal adult behaviour. Locomotion is frequently used as a phenotypic readout of neuronal function (Strauss, 2002). Although the adult phenotype cannot be attributed to an adult function of the genes, the phenotype of slow walking and frequent resting are reminiscent of defects in the central complex, where both receptors are expressed (Strauss and Heisenberg, 1993, Strauss, 2002).

Toll-7 and *Toll-6* promote axon targeting and cell survival in the developing CNS, since single and double mutants show axon targeting phenotypes and increased apoptosis. *Toll-7* mutants showed a stronger misrouting phenotype of the ISNb motor axons, consistent with the expression pattern of *Toll-7>GAP-GFP*, in which the ISNb projections were specifically labelled. *Toll-7* and *Toll-6* mutants show an increase in apoptotic cell number in the developing CNS, and expressing $Toll\text{-}7^{Cys\text{-}Tyr}$ and $Toll\text{-}6^{Cys\text{-}Tyr}$ in neurons rescued naturally occurring cell death. *Toll* mutants also show axon targeting defects in embryos and larvae (Rose et al., 1997, Halfon et al., 1995). Halfon et al. reported the loss of the innervation of muscles 6 and 7, which coincided with loss of the corresponding RP3 neurons. Increased neuronal apoptosis in *Toll* mutants has also been shown (Zhu et al., 2008). Altogether, *Toll*, *Toll-7* and *Toll-6* share common functions, and play important roles in the development of the *Drosophila* nervous system.

Drosophila motor neurons project to their muscle targets in a well-defined and highly stereotypic pattern (Landgraf et al., 1997, Landgraf and Thor, 2006). It is possible that this reflects a hard-wired pattern of development, in which genetically-encoded cell-autonomous factors determine the survival and targeting of developing motor neurons. However, there is evidence that motor neurons may also be subject to trophic and tropic regulation. In wild-type embryos, Eve^{+} and $HB9^{+}$ motor neurons can undergo apoptosis (Rogulja-Ortmann et al., 2007). And in *DNT* mutant embryos, there is a further loss of these motor neurons and their peripheral projections (Zhu et al., 2008). In *Toll-7* mutants, the increase in CNS apoptosis is accompanied by losses in entire ISNb motor nerve branches. This is consistent with *Toll-7* promoting the survival of motor neurons, and could be confirmed by investigating whether the exccess apoptotic cells in *Toll-7* mutants also express motor neuron markers. Although motor neurons can project to the periphery in the absence of muscle, synaptogenesis requires

the presence of fully-differentiated muscle, and muscle precursors direct the defasciculation and targeting of motor axons (Prokop et al., 1996, Landgraf et al., 1999). When their normal targets are ablated, motor axons can ectopically target to alternative muscles (Sink and Whitington, 1991, Cash et al., 1992). Conversely, when individual motor neurons are ablated, neighbouring axons can innervate the deprived muscle (Chang and Keshishian, 1996). These results are consistent with tropic interactions between muscles and motor neurons. The robustness of neuronal development in *Drosophila* is revealed by the stereotypic pattern of axonal targeting. Developmental plasticity – the ability of neurons and their targets to signal to each other and fine-tune innervation – could represent a key element of the development of the *Drosophila* nervous system.

Since *Toll-7* and *Toll-6* are expressed in the larval and adult CNS, it would be interesting in the future to investigate the functions of the receptors at these later stages. By expressing activated receptors, and by using RNAi to knock-down *Toll-7* and *Toll-6* after embryonic development, larval and adult functions of the receptors could be revealed. For example, it would be interesting to examine the roles of *Toll-7* and *Toll-6* at the larval NMJ. This is a model synapse, and has been used to investigate structural plasticity and electrophysiological properties of *Drosophila* neurons, including in *DNT* mutants (Hebbar et al., 2006, Baines and Pym, 2006, Sutcliffe et al., Submitted).

7.3 Different versions of activated receptors do not function equally

To test the function of Toll-7 and Toll-6, constitutively active receptor constructs were made, following the example of two different published versions of constitutively active Toll receptors (Schneider et al., 1991, Winans and Hashimoto, 1995). *Toll-7*$^{Cys\text{-}Tyr}$ and *Toll-6*$^{Cys\text{-}Tyr}$ were made by mutating a cysteine residue to tyrosine in the third CRC in the extracellular

domain. The equivalent mutation in this conserved cysteine in Toll is responsible for the dominant activation seen in the *Toll*^{10b} allele (Schneider et al., 1991). *Toll-7*$^{\Delta LRR}$ and *Toll-6*$^{\Delta LRR}$ were also made, where all of the LRRs and CRCs were deleted. These are equivalent deletions to the *Toll*$^{\Delta LRR}$ construct, which also signals in the absence of ligand (Winans and Hashimoto, 1995). It was anticipated that the different versions of each activated receptor would produce similar effects *in vivo*. In the rescue of lethality of both *Toll-7Toll-6* and *DNT1DNT2* double mutants, expression of both Cys-Tyr and ΔLRR receptors resulted in an increased survival index; although the Cys-Tyr versions produced the stronger rescue of *DNT1DNT2* semi-lethality. This suggested that the structural changes thought to be involved in Toll activation – that ligand binding releases receptor auto-inhibition (Hu et al., 2004) – are shared by Toll-7 and Toll-6. However, only expression of the Cys-Tyr receptors reduced naturally occurring cell death in the embryonic CNS. In contrast, expressing *Toll-7*$^{\Delta LRR}$ produced no effect, and *Toll-6*$^{\Delta LRR}$ resulted in an increase in the number of apoptotic cells. In cell culture, expression of both *Toll*^{10b} and *Toll*$^{\Delta LRR}$ results in the activation of the *drosomycin-Luciferase* reporter (Sun et al., 2002, Sun et al., 2004, Hu et al., 2004). However, in a previous report that generated *ΔLRR* versions of all Toll paralogues, only *Toll*$^{\Delta LRR}$ and *Toll-5*$^{\Delta LRR}$ were shown to activate *drosomycin-Luciferase* (Tauszig et al., 2000). It is interesting that when I expressed *Toll-7*$^{Cys\text{-}Tyr}$ and *Toll-6*$^{Cys\text{-}Tyr}$ in S2 cells, they were able to activate *drosomycin-Luciferase*. This suggests that different versions of activated *Toll-7* and *Toll-6* do not function in the same way. The constitutive activity of Toll$^{\Delta LRR}$ is partly due to a cysteine residue at the protein's N-terminal: when this is removed or mutated, the level of activity falls to below that of Toll^{10b} (Hu et al., 2004). This cysteine is not conserved in *Toll-7* or *Toll-6*, and could explain the apparently lower level of activity of the *ΔLRR* receptors. The different *in vivo* results could be due to differences in how the proteins are expressed at the membrane.

If the ΔLRR receptors are less effective at activating cell signalling, they may not be able to rescue phenotypes that require stronger levels of signalling, but are still able to rescue phenotypes that require weaker signalling. It is possible that this is behind the observed differences on cell death and lethality seen when expressing *Toll-7*$^{\Delta LRR}$ and *Toll-6*$^{\Delta LRR}$ in neurons. A similar situation exists in the control of neuronal survival and outgrowth by NFκB: low levels of NFκB activation can promote neurite outgrowth, whereas stronger activation is required to promote cell survival (Gutierrez et al., 2005). *Toll-7*$^{Cys\text{-}Tyr}$ and *Toll-6*$^{Cys\text{-}Tyr}$ rescued mutant semi-lethality and naturally occurring cell death *in vivo*, and activate NFκB signalling in cultured cells: they therefore represent the more efficient versions of constitutively active receptor.

7.4 Toll-7 and Toll-6 function as DNT receptors

As well as describing the functions of Toll-7 and Toll-6 in the *Drosophila* CNS, an aim of my thesis was to test whether they can serve as receptors for DNT1 and DNT2. To investigate this possibility, I looked at a number of criteria. Firstly, DNTs are expressed in neuronal targets, such as muscle, and have non-cell-autonomous effects on neurons (Zhu et al., 2008). Both *Toll-7* and *Toll-6* are expressed in CNS neurons, in patterns that complement and overlap expression of the DNTs, such as in motor neurons (Zhu et al., 2008, Sutcliffe et al., Submitted). Secondly, DNT mutants have defects in CNS development and function. Like *DNT1* and *DNT2*, *Toll-7* and *Toll-6* are required in neurons for viability at 18°C, where there is genetic interaction between the ligands and the receptors. Moreover, both Tolls and DNTs are required for normal adult locomotion, they promote axon targeting, and they are necessary and sufficient for cell survival. Thirdly, expressing activated forms *Toll-7* and *Toll-6* in neurons rescued *DNT1DNT2* double mutant semi-lethality, and also rescued the increased

apoptosis seen in the CNS of *DNT1* and *DNT2* mutants. This indicates that the receptors are functioning downstream of the ligands. Fourthly, in cell culture, I showed that DNT1 can activate NFκB signalling through Toll-7, and DNT2 through Toll-7 and Toll-6. Altogether, these data provide evidence that Toll-7 and Toll-6 can function as DNT receptors, both *in vivo* and in cell culture.

The possibility exists that are two ligand/receptor pairs. The expression patterns of *Toll-7* and *Toll-6* do not reveal an obvious pairing. The receptors are expressed in broadly overlapping patterns, and it is possible that some neurons express both *Toll-7* and *Toll-6*. The strongest evidence for specific interactions came from lethality assays. These experiments suggest that DNT1 and Toll-7 interact, and that DNT2 and Toll-*6* interact. This set of relationships is supported by data from axon targeting phenotypes: both *DNT1* and *Toll-7* have stronger misrouting phenotypes in the ISNb projections, whereas *DNT2* and *Toll-6* have a relatively weaker phenotype (for *DNT* phenotypes, see also Zhu et al., 2008). On the other hand, *Toll-7DNT1* double mutants – putatively two members of one signalling pathway – have a stronger lethality phenotype than either single mutant. This suggests there are additional interactions between the ligands and the receptors. And in cell death experiments, *DNT1* mutants have a stronger phenotype than *DNT2*, whereas *Toll-7* mutants have slightly less cell death than *Toll-6*. In cell culture, DNT1 appears to function through Toll-7, but it is anticipated that the weak effects seen through Toll-6 would become stronger and significant had higher quality, Baculovirus-derived protein been available. Using DNT2 from Baculovirus shows that the ligand can signal through both Toll-7 and Toll-6. Therefore, it is possible that some promiscuity exists in DNT and Toll binding.

Previous work in our lab has shown that the DNTs are functionally redundant: expressing activated *spz* rescues the *DNT1DNT2* mutant phenotype, and activated *DNT1* and *DNT2*

rescue *spz* (Sutcliffe et al., Submitted). Similarly, I have shown that expressing activated *Toll-7* and *Toll-6* can partially rescue the *spz* mutant semi-lethality, and that $Toll^{10b}$ partially rescues *DNT1DNT2*. *In vivo*, a number of factors most likely determine which DNT signals through which receptor. Primarily, the endogenous receptor will be expressed where it can detect the relevant DNT. And if there is ligand/receptor promiscuity, binding could be influenced by the relative abundance of each DNT. Binding of vertebrate neurotrophins to their receptors is also promiscuous, and is regulated by alternative splicing and the co-expression of additional receptors (Clary and Reichardt, 1994, Strohmaier et al., 1996, Roux and Barker, 2002). Although there are no splice variants of intronless *Toll-7* and *Toll-6*, it is unknown whether post-translational modifications or co-receptor expression could also regulate ligand/receptor specificity between the Tolls and the DNTs.

To further characterise the biochemical relationships between the DNT1, DNT2, Toll-7 and Toll-6, additional experiments could be carried out in cell culture and *in vitro*. This would require much larger amounts of higher purity recombinant DNT1 protein than were produced during this thesis. By also expressing Toll-7 and Toll-6 proteins, *in vitro* experiments using surface plasmon resonance could determine the binding affinities of the ligands and the receptors. And biophysical techniques, potentially including protein crystallisation, could characterise the nature of DNT/Toll binding.

7.5 Toll-7 and Toll-6 signal through NFκB

I have shown that Toll-7 and Toll-6 signal through NFκB paralogues, Dorsal and Dif. Toll is known to activate both Dorsal and Dif, depending on the signalling context (Manfruelli et al., 1999, Meng et al., 1999, Moussian and Roth, 2005). Equally, Toll-9 has also been shown to activate Dif (Ooi et al., 2002), and Toll-8 (Tollo) can interact with Relish, a third *Drosophila*

NFκB paralogue (Ayyar et al., 2007). And all vertebrate TLRs signal through NFκB (Kawai and Akira, 2007). It is most likely that, *in vivo*, whether Toll-7 and Toll-6 signal through Dorsal, Dif or heterodimers will depend on which are present in the cell. Heterodimerisation of Dorsal or Dif with Relish, enhances the innate immune response (Han and Ip, 1999, Tanji et al., 2010). It would be interesting to test whether DNT/Toll signalling can also activate Relish. Although it is most likely that Toll-7 and Toll-6 activate NFκB *in vivo*, this remains to be tested. To do this, NFκB could be activated by expression of *dTRAF2* in *Toll-7* and *Toll-6* mutants, to rescue lethality or cell death phenotypes (Cha et al., 2003).

The activation of NFκB by neurotrophins is conserved from flies to humans. Vertebrate neurotrophins activate NFκB through Trks and $p75^{NTR}$, to promote cell survival and neurite outgrowth (Foehr et al., 2000, Carter et al., 1996). The activation of NFκB by neurotrophins can be measured by nuclear localisation of NFκB protein subunits or with a reporter plasmid, and its effect on cell survival and axon growth have been attributed to its actions in the nucleus (Foehr et al., 2000, Carter et al., 1996, Gutierrez and Davies, 2011). NFκB regulates multiple aspects of neuronal development and function, and is implicated in diseases including epilepsy, Alzheimer's disease and cancer (Mattson and Meffert, 2006). Neuronal NFκB can be activated by glutamatergic transmission and increases in intracellular Ca^{2+}, which results in the nuclear localisation of NFκB and the regulation of transcription (Guerrini et al., 1995, Wellmann et al., 2001, Meffert et al., 2003). NFκB can then regulate synaptic plasticity by modifying neuronal structure and receptor expression (Gutierrez et al., 2005, Boersma et al., 2011, O'Mahony et al., 2006). NFκB activation is associated with transcriptional regulation and the induction of long-term memory in crabs, therefore role of NFκB in synaptic plasticity is conserved across animals (Freudenthal and Romano, 2000). In

all of these examples, NFκB activation results in its nuclear localisation and the regulation of transcription.

NFκB was the first transcription factor to be found in synapses, but its potential functions outside the nucleus remain relatively unexplored (Kaltschmidt et al., 1993). In flies misexpression of Dorsal protein in photoreceptors can cause it to ectopically localise to axons, which is correlated with axon targeting defects (Mindorff et al., 2007). Indeed, Dorsal has been shown to function in muscle to regulate glutamate receptor density, without localising to the nucleus to regulate transcription (Heckscher et al., 2007). Moreover, TLR-3 and TLR-8 can function in vertebrate axons to inhibit outgrowth, and these effects have been shown to be independent of NFκB (Cameron et al., 2007, Ma et al., 2006). Therefore, it is possible that Toll signalling could regulate multiple aspects of neuronal development and function, through canonical NFκB signalling in the nucleus, through alternative NFκB functions near the cell membrane, or through as-yet uncharacterised pathways that do not involve NFκB. In the future, it would be very interesting dissect the downstream signalling pathways activated in DNT/Toll signalling.

7.6 Crosstalk between the nervous and immune systems

The characterisation of *Drosophila* Tolls as DNT receptors raises some important questions about the functions of TLRs in the vertebrate nervous system. All human TLRs have been detected in neurons (Zhou et al., 2009), and their activation can influence neuronal cell number and morphology (Okun et al., 2011). TLRs bind a number of endogenous ligands, many of which are released by damaged or necrotic tissue (Sloane et al., 2010). TLRs can also be activated by secreted endogenous ligands, such as HMGB1, which can promote neurite outgrowth by binding its alternative receptor, RAGE (Yang et al., 2005, Hori et al., 1995).

And there is evidence that TLRs could play a role in normal neuronal functioning: TLR3 knock-out mice show cognitive defects, suggesting signalling is important also in the absence of infection (Okun et al., 2010a). However, the endogenous ligands of TLRs in the undamaged, 'sterile' brain are unknown. Toll and neurotrophin families are found in humans and in flies, and Tolls have neuronal functions in both animals. It is therefore compelling to test whether vertebrate neurotrophins constitute a family of endogenous vertebrate TLR ligands, and to investigate whether the relationship between Tolls and neurotrophins is conserved across animals.

There are reports of cross-talk between the TLR and neurotrophin signalling pathways in immune cells. In dendritic cells – initiators of the innate and adaptive immune responses – TLR4 signalling can up-regulate the expression of NGF and $p75^{NTR}$ (Jiang et al., 2008). NGF/$p75^{NTR}$ signalling can then enhance the maturation of LPS-stimulated dendritic cells, to promote the release of cytokines and to activate T-cells of the adaptive immune system (Jiang et al., 2007). It would be interesting to test whether TLR signalling in neurons can also interact with neurotrophin/$p75^{NTR}$/Trk signalling pathways, and explore the effect of TLR signalling on neuronal function both in health and in inflammation.

The generation of mature Spz protein is through a proteolytic cascade, which involves different zymogens in dorsoventral patterning and immunity; it is unknown what proteases normally cleave pro-Spz for it to function as a neurotrophin, or how DNT1 and DNT2 are endogenously processed. Proteolytic cascades are also seen in the vertebrate coagulation cascade, where circulating factors in the blood are sequentially activated, resulting in the formation of a fibrin clot. The key mechanism of vertebrate coagulation – an amplifying proteolytic cascade – is also seen in invertebrates. An analogous process occurs in the horseshoe crab, but instead of the cascade converging on fibrin activation, Coagulagen is

cleaved and goes on to form a clot (Osaki and Kawabata, 2004). In vertebrates, the protease Plasmin plays an important role in the control of blood coagulation by breaking down the fibrin clot. Plasmin is itself activated by a protease, tissue Plasminogen Activator (tPA). In the vertebrate CNS, the tPA/Plasmin proteolytic cascade results in the cleavage of BDNF – a structural homologue of Coagulogen (Pang et al., 2004). And this process is directly regulated by the secretion of tPA from neurons in response to neuronal activity, which is a key mechanism in the regulation of LTP (Nagappan et al., 2009). There is an intriguing similarity between the mechanisms that control haemostasis and neurotrophin signalling, at the centre of which are Cys-knot proteins.

Spz plays a central role in the *Drosophila* innate immune system, and the aggregation of Coagulogen is part of the horseshoe crab's immune response (Bergner et al., 1996). Immune functions of Cys-knot proteins are conserved across animals, and neurotrophins are involved in multiple aspects of mammalian innate and adaptive immune responses (Vega et al., 2003). BDNF is involved in the development of the pre-implantation mouse embryo (Kawamura et al., 2007), and Spz has a well-defined role in the establishment of the dorsoventral axis in early *Drosophila* embryos (Moussian and Roth, 2005). And the structure and function of vertebrate and *Drosophila* neurotrophins are conserved. These are disparate functions, and the co-option of one signalling pathway to a different physiological system, raises an important point. In the end, it is the result of signalling that matters, not the means. It matters far more that neurons and immune cells can respond to extracellular signals, than it matters that neurotrophins convey those signals. Vertebrate and *Drosophila* neurotrophins are structural homologues; they both promote the survival, targeting and function of neurons; and they activate NFκB signalling. In vertebrates, neurotrophins signal through Trk and $p75^{NTR}$, whereas in *Drosophila*, they signal through Tolls.

7.7 Implications

My thesis has established roles for Toll-7 and Toll-6 in the development and function of the *Drosophila* nervous system. I have also shown that Tolls can function as neurotrophin receptors. This introduces a different class of protein to the neurotrophin receptors, which in vertebrates includes Trks, $p75^{NTR}$ and Sortilin. It is now compelling to examine whether the neurotrophin/Toll relationship is conserved, by testing whether vertebrate neurotrophins can bind and signal through TLRs. The characterisation of neuronal functions of Tolls, homologues to vertebrate immune receptors, also sheds more light on the link between the nervous and immune systems. And in *Drosophila*, the identification of receptors for DNT1 and DNT2 allows the continued and more detailed investigation of *Drosophila* neurotrophin signalling.

REFERENCES

ABRELL, S. & JÄCKLE, H. 2001. Axon guidance of Drosophila SNb motoneurons depends on the cooperative action of muscular Krüppel and neuronal capricious activities. Mech Dev, 109, 3-12.

ADAMS, M. D., CELNIKER, S. E., HOLT, R. A., EVANS, C. A., GOCAYNE, J. D., AMANATIDES, P. G., SCHERER, S. E., LI, P. W., HOSKINS, R. A., GALLE, R. F., GEORGE, R. A., LEWIS, S. E., RICHARDS, S., ASHBURNER, M., HENDERSON, S. N., SUTTON, G. G., WORTMAN, J. R., YANDELL, M. D., ZHANG, Q., CHEN, L. X., BRANDON, R. C., ROGERS, Y. H., BLAZEJ, R. G., CHAMPE, M., PFEIFFER, B. D., WAN, K. H., DOYLE, C., BAXTER, E. G., HELT, G., NELSON, C. R., GABOR, G. L., ABRIL, J. F., AGBAYANI, A., AN, H. J., ANDREWS-PFANNKOCH, C., BALDWIN, D., BALLEW, R. M., BASU, A., BAXENDALE, J., BAYRAKTAROGLU, L., BEASLEY, E. M., BEESON, K. Y., BENOS, P. V., BERMAN, B. P., BHANDARI, D., BOLSHAKOV, S., BORKOVA, D., BOTCHAN, M. R., BOUCK, J., BROKSTEIN, P., BROTTIER, P., BURTIS, K. C., BUSAM, D. A., BUTLER, H., CADIEU, E., CENTER, A., CHANDRA, I., CHERRY, J. M., CAWLEY, S., DAHLKE, C., DAVENPORT, L. B., DAVIES, P., DE PABLOS, B., DELCHER, A., DENG, Z., MAYS, A. D., DEW, I., DIETZ, S. M., DODSON, K., DOUP, L. E., DOWNES, M., DUGAN-ROCHA, S., DUNKOV, B. C., DUNN, P., DURBIN, K. J., EVANGELISTA, C. C., FERRAZ, C., FERRIERA, S., FLEISCHMANN, W., FOSLER, C., GABRIELIAN, A. E., GARG, N. S., GELBART, W. M., GLASSER, K., GLODEK, A., GONG, F., GORRELL, J. H., GU, Z., GUAN, P., HARRIS, M., HARRIS, N. L., HARVEY, D., HEIMAN, T. J., HERNANDEZ, J. R., HOUCK, J., HOSTIN, D., HOUSTON, K. A., HOWLAND, T. J., WEI, M. H., IBEGWAM, C., et al. 2000. The genome sequence of Drosophila melanogaster. Science, 287, 2185-95.

ADAMS, M. D. & SEKELSKY, J. J. 2002. From sequence to phenotype: reverse genetics in Drosophila melanogaster. Nat Rev Genet, 3, 189-98.

ALOE, L. & LEVI-MONTALCINI, R. 1977. Mast cells increase in tissues of neonatal rats injected with the nerve growth factor. Brain Res, 133, 358-66.

ALVARADO, D., RICE, A. H. & DUFFY, J. B. 2004. Bipartite inhibition of Drosophila epidermal growth factor receptor by the extracellular and transmembrane domains of Kekkon1. Genetics, 167, 187-202.

ANDERSON, K. V., JÜRGENS, G. & NÜSSLEIN-VOLHARD, C. 1985. Establishment of dorsal-ventral polarity in the Drosophila embryo: genetic studies on the role of the Toll gene product. Cell, 42, 779-89.

ANDERSON, K. V. & NÜSSLEIN-VOLHARD, C. 1984. Information for the dorsal--ventral pattern of the Drosophila embryo is stored as maternal mRNA. Nature, 311, 223-7.

ARBOUR, N. C., LORENZ, E., SCHUTTE, B. C., ZABNER, J., KLINE, J. N., JONES, M., FREES, K., WATT, J. L. & SCHWARTZ, D. A. 2000. TLR4 mutations are associated with endotoxin hyporesponsiveness in humans. Nat Genet, 25, 187-91.

ARNOT, C. J. 2009. Signalling mechanisms of the Toll ectodomain and its extracellular ligand Spätzle. University of Cambridge.

ARNOT, C. J., GAY, N. J. & GANGLOFF, M. 2010. Molecular mechanism that induces activation of Spätzle, the ligand for the Drosophila Toll receptor. J Biol Chem, 285, 19502-9.
ARÉVALO, J. C., YANO, H., TENG, K. K. & CHAO, M. V. 2004. A unique pathway for sustained neurotrophin signaling through an ankyrin-rich membrane-spanning protein. EMBO J, 23, 2358-68.
AURIKKO, J. P., RUOTOLO, B. T., GROSSMANN, J. G., MONCRIEFFE, M. C., STEPHENS, E., LEPPÄNEN, V. M., ROBINSON, C. V., SAARMA, M., BRADSHAW, R. A. & BLUNDELL, T. L. 2005. Characterization of symmetric complexes of nerve growth factor and the ectodomain of the pan-neurotrophin receptor, p75NTR. J Biol Chem, 280, 33453-60.
AYYAR, S., PISTILLO, D., CALLEJA, M., BROOKFIELD, A., GITTINS, K., GOLDSTONE, C. & SIMPSON, P. 2007. NF-kappaB/Rel-mediated regulation of the neural fate in Drosophila. PLoS One, 2, e1178.
BACKER, J. M., MYERS, M. G., SHOELSON, S. E., CHIN, D. J., SUN, X. J., MIRALPEIX, M., HU, P., MARGOLIS, B., SKOLNIK, E. Y. & SCHLESSINGER, J. 1992. Phosphatidylinositol 3'-kinase is activated by association with IRS-1 during insulin stimulation. EMBO J, 11, 3469-79.
BAEK, M. & MANN, R. S. 2009. Lineage and birth date specify motor neuron targeting and dendritic architecture in adult Drosophila. J Neurosci, 29, 6904-16.
BAIG, M. A. & KHAN, M. A. 1996. The induction of neurotrophin and TRK receptor mRNA expression during early avian embryogenesis. Int J Dev Neurosci, 14, 55-60.
BAINES, R. A. & PYM, E. C. 2006. Determinants of electrical properties in developing neurons. Semin Cell Dev Biol, 17, 12-9.
BAKER, N. E. & YU, S. Y. 2001. The EGF receptor defines domains of cell cycle progression and survival to regulate cell number in the developing Drosophila eye. Cell, 104, 699-708.
BALDWIN, A. N., BITLER, C. M., WELCHER, A. A. & SHOOTER, E. M. 1992. Studies on the structure and binding properties of the cysteine-rich domain of rat low affinity nerve growth factor receptor (p75NGFR). J Biol Chem, 267, 8352-9.
BAMJI, S. X., MAJDAN, M., POZNIAK, C. D., BELLIVEAU, D. J., ALOYZ, R., KOHN, J., CAUSING, C. G. & MILLER, F. D. 1998. The p75 neurotrophin receptor mediates neuronal apoptosis and is essential for naturally occurring sympathetic neuron death. J Cell Biol, 140, 911-23.
BARDE, Y. A. 1994. Neurotrophic factors: an evolutionary perspective. J Neurobiol, 25, 1329-33.
BARDE, Y. A., EDGAR, D. & THOENEN, H. 1982. Purification of a new neurotrophic factor from mammalian brain. EMBO J, 1, 549-53.
BARKER, P. A. 2007. High affinity not in the vicinity? Neuron, 53, 1-4.
BARTUS, R. T., DEAN, R. L., BEER, B. & LIPPA, A. S. 1982. The cholinergic hypothesis of geriatric memory dysfunction. Science, 217, 408-14.
BATE, M. 1993. The mesoderm and its derivatives. In: BATE, M. & MARTINEZ ARIAS, A. (eds.) The development of Drosophila melanogaster. New York: CSHL Press.
BECK, G., MUNNO, D. W., LEVY, Z., DISSEL, H. M., VAN-MINNEN, J., SYED, N. I. & FAINZILBER, M. 2004. Neurotrophic activities of trk receptors conserved over 600 million years of evolution. J Neurobiol, 60, 12-20.

BENITO-GUTIÉRREZ, E., GARCIA-FERNÀNDEZ, J. & COMELLA, J. X. 2006. Origin and evolution of the Trk family of neurotrophic receptors. Mol Cell Neurosci, 31, 179-92.
BERGMANN, A., STEIN, D., GEISLER, R., HAGENMAIER, S., SCHMID, B., FERNANDEZ, N., SCHNELL, B. & NÜSSLEIN-VOLHARD, C. 1996. A gradient of cytoplasmic Cactus degradation establishes the nuclear localization gradient of the dorsal morphogen in Drosophila. Mech Dev, 60, 109-23.
BERGNER, A., OGANESSYAN, V., MUTA, T., IWANAGA, S., TYPKE, D., HUBER, R. & BODE, W. 1996. Crystal structure of a coagulogen, the clotting protein from horseshoe crab: a structural homologue of nerve growth factor. EMBO J, 15, 6789-97.
BERKEMEIER, L. R., WINSLOW, J. W., KAPLAN, D. R., NIKOLICS, K., GOEDDEL, D. V. & ROSENTHAL, A. 1991. Neurotrophin-5: a novel neurotrophic factor that activates trk and trkB. Neuron, 7, 857-66.
BERND, P. 2008. The role of neurotrophins during early development. Gene Expr, 14, 241-50.
BETTENCOURT, R., TANJI, T., YAGI, Y. & IP, Y. T. 2004. Toll and Toll-9 in Drosophila innate immune response. J Endotoxin Res, 10, 261-8.
BIBEL, M. & BARDE, Y. A. 2000. Neurotrophins: key regulators of cell fate and cell shape in the vertebrate nervous system. Genes Dev, 14, 2919-37.
BIBEL, M., HOPPE, E. & BARDE, Y. A. 1999. Biochemical and functional interactions between the neurotrophin receptors trk and p75NTR. EMBO J, 18, 616-22.
BLÖCHL, A., BLUMENSTEIN, L. & AHMADIAN, M. R. 2004. Inactivation and activation of Ras by the neurotrophin receptor p75. Eur J Neurosci, 20, 2321-35.
BLÖCHL, A. & BLÖCHL, R. 2007. A cell-biological model of p75NTR signaling. J Neurochem, 102, 289-305.
BOERSMA, M. C., DRESSELHAUS, E. C., DE BIASE, L. M., MIHALAS, A. B., BERGLES, D. E. & MEFFERT, M. K. 2011. A requirement for nuclear factor-kappaB in developmental and plasticity-associated synaptogenesis. J Neurosci, 31, 5414-25.
BOND, D., PRIMROSE, D. A. & FOLEY, E. 2008. Quantitative evaluation of signaling events in Drosophila S2 cells. Biol Proced Online, 10, 20-8.
BOOTH, G. E., KINRADE, E. F. & HIDALGO, A. 2000. Glia maintain follower neuron survival during Drosophila CNS development. Development, 127, 237-44.
BOSSING, T., UDOLPH, G., DOE, C. Q. & TECHNAU, G. M. 1996. The embryonic central nervous system lineages of Drosophila melanogaster. I. Neuroblast lineages derived from the ventral half of the neuroectoderm. Dev Biol, 179, 41-64.
BOTHWELL, M. 1995. Functional interactions of neurotrophins and neurotrophin receptors. Annu Rev Neurosci, 18, 223-53.
BOTHWELL, M. 2006. Evolution of the neurotrophin signaling system in invertebrates. Brain Behav Evol, 68, 124-32.
BRAND, A. H. & PERRIMON, N. 1993. Targeted gene expression as a means of altering cell fates and generating dominant phenotypes. Development, 118, 401-15.
BRIDGHAM, J. T., WILDER, J. A., HOLLOCHER, H. & JOHNSON, A. L. 2003. All in the family: evolutionary and functional relationships among death receptors. Cell Death Differ, 10, 19-25.
BROADIE, K. & BATE, M. 1993. Muscle development is independent of innervation during Drosophila embryogenesis. Development, 119, 533-43.

BRUNO, M. A. & CUELLO, A. C. 2006. Activity-dependent release of precursor nerve growth factor, conversion to mature nerve growth factor, and its degradation by a protease cascade. Proc Natl Acad Sci U S A, 103, 6735-40.
BUCHON, N., POIDEVIN, M., KWON, H. M., GUILLOU, A., SOTTAS, V., LEE, B. L. & LEMAITRE, B. 2009. A single modular serine protease integrates signals from pattern-recognition receptors upstream of the Drosophila Toll pathway. Proc Natl Acad Sci U S A, 106, 12442-7.
BULLOCH, A. G., DIEP, C. Q., LOGAN, C. C., BULLOCH, E. S., ROBBINS, S. M., HISLOP, J. & SOSSIN, W. S. 2005. Ltrk is differentially expressed in developing and adult neurons of the Lymnaea central nervous system. J Comp Neurol, 487, 240-54.
BUSS, R. R., SUN, W. & OPPENHEIM, R. W. 2006. Adaptive roles of programmed cell death during nervous system development. Annu Rev Neurosci, 29, 1-35.
CALDEIRA, M. V., MELO, C. V., PEREIRA, D. B., CARVALHO, R., CORREIA, S. S., BACKOS, D. S., CARVALHO, A. L., ESTEBAN, J. A. & DUARTE, C. B. 2007. Brain-derived neurotrophic factor regulates the expression and synaptic delivery of alpha-amino-3-hydroxy-5-methyl-4-isoxazole propionic acid receptor subunits in hippocampal neurons. J Biol Chem, 282, 12619-28.
CAMERON, J. S., ALEXOPOULOU, L., SLOANE, J. A., DIBERNARDO, A. B., MA, Y., KOSARAS, B., FLAVELL, R., STRITTMATTER, S. M., VOLPE, J., SIDMAN, R. & VARTANIAN, T. 2007. Toll-like receptor 3 is a potent negative regulator of axonal growth in mammals. J Neurosci, 27, 13033-41.
CAMPENOT, R. B. 1977. Local control of neurite development by nerve growth factor. Proc Natl Acad Sci U S A, 74, 4516-9.
CAMPOS, A. R., FISCHBACH, K. F. & STELLER, H. 1992. Survival of photoreceptor neurons in the compound eye of Drosophila depends on connections with the optic ganglia. Development, 114, 355-66.
CAMPOS-ORTEGA, J. A. & HARTENSTEIN, V. 1985. The embryonic development of Drosophila melanogaster, Berlin, Springer-Verlag.
CANTARELLA, G., LEMPEREUR, L., PRESTA, M., RIBATTI, D., LOMBARDO, G., LAZAROVICI, P., ZAPPALÀ, G., PAFUMI, C. & BERNARDINI, R. 2002. Nerve growth factor-endothelial cell interaction leads to angiogenesis in vitro and in vivo. FASEB J, 16, 1307-9.
CANTERA, R., ROOS, E. & ENGSTRÖM, Y. 1999. Dif and cactus are colocalized in the larval nervous system of Drosophila melanogaster. J Neurobiol, 38, 16-26.
CARTER, B. D., KALTSCHMIDT, C., KALTSCHMIDT, B., OFFENHÄUSER, N., BÖHM-MATTHAEI, R., BAEUERLE, P. A. & BARDE, Y. A. 1996. Selective activation of NF-kappa B by nerve growth factor through the neurotrophin receptor p75. Science, 272, 542-5.
CASH, S., CHIBA, A. & KESHISHIAN, H. 1992. Alternate neuromuscular target selection following the loss of single muscle fibers in Drosophila. J Neurosci, 12, 2051-64.
CHA, G. H., CHO, K. S., LEE, J. H., KIM, M., KIM, E., PARK, J., LEE, S. B. & CHUNG, J. 2003. Discrete functions of TRAF1 and TRAF2 in Drosophila melanogaster mediated by c-Jun N-terminal kinase and NF-kappaB-dependent signaling pathways. Mol Cell Biol, 23, 7982-91.
CHANG, T. N. & KESHISHIAN, H. 1996. Laser ablation of Drosophila embryonic motoneurons causes ectopic innervation of target muscle fibers. J Neurosci, 16, 5715-26.

CHAO, M. V. 2003. Neurotrophins and their receptors: a convergence point for many signalling pathways. Nat Rev Neurosci, 4, 299-309.
CHAO, M. V., BOTHWELL, M. A., ROSS, A. H., KOPROWSKI, H., LANAHAN, A. A., BUCK, C. R. & SEHGAL, A. 1986. Gene transfer and molecular cloning of the human NGF receptor. Science, 232, 518-21.
CHAO, M. V., RAJAGOPAL, R. & LEE, F. S. 2006. Neurotrophin signalling in health and disease. Clin Sci (Lond), 110, 167-73.
CHAPMAN, B. S. 1995. A region of the 75 kDa neurotrophin receptor homologous to the death domains of TNFR-I and Fas. FEBS Lett, 374, 216-20.
CHEN, G., FERNANDEZ, J., MISCHE, S. & COUREY, A. J. 1999. A functional interaction between the histone deacetylase Rpd3 and the corepressor groucho in Drosophila development. Genes Dev, 13, 2218-30.
CHEN, G. Y. & NUÑEZ, G. 2010. Sterile inflammation: sensing and reacting to damage. Nat Rev Immunol, 10, 826-37.
CHEN, K. S., NISHIMURA, M. C., ARMANINI, M. P., CROWLEY, C., SPENCER, S. D. & PHILLIPS, H. S. 1997. Disruption of a single allele of the nerve growth factor gene results in atrophy of basal forebrain cholinergic neurons and memory deficits. J Neurosci, 17, 7288-96.
CHEN, Z. Y., BATH, K., MCEWEN, B., HEMPSTEAD, B. & LEE, F. 2008. Impact of genetic variant BDNF (Val66Met) on brain structure and function. Novartis Found Symp, 289, 180-8; discussion 188-95.
CHEN, Z. Y., JING, D., BATH, K. G., IERACI, A., KHAN, T., SIAO, C. J., HERRERA, D. G., TOTH, M., YANG, C., MCEWEN, B. S., HEMPSTEAD, B. L. & LEE, F. S. 2006. Genetic variant BDNF (Val66Met) polymorphism alters anxiety-related behavior. Science, 314, 140-3.
CHITTKA, A., AREVALO, J. C., RODRIGUEZ-GUZMAN, M., PÉREZ, P., CHAO, M. V. & SENDTNER, M. 2004. The p75NTR-interacting protein SC1 inhibits cell cycle progression by transcriptional repression of cyclin E. J Cell Biol, 164, 985-96.
CHO, Y. S., STEVENS, L. M. & STEIN, D. 2010. Pipe-dependent ventral processing of Easter by Snake is the defining step in Drosophila embryo DV axis formation. Curr Biol, 20, 1133-7.
CHUANG , H. H., PRESCOTT, E. D., KONG, H., SHIELDS, S., JORDT, S. E., BASBAUM, A. I., CHAO, M. V. & JULIUS, D. 2001. Bradykinin and nerve growth factor release the capsaicin receptor from PtdIns(4,5)P2-mediated inhibition. Nature, 411, 957-62.
CLARY, D. O. & REICHARDT, L. F. 1994. An alternatively spliced form of the nerve growth factor receptor TrkA confers an enhanced response to neurotrophin 3. Proc Natl Acad Sci U S A, 91, 11133-7.
COHEN-CORY, S. & FRASER, S. E. 1995. Effects of brain-derived neurotrophic factor on optic axon branching and remodelling in vivo. Nature, 378, 192-6.
COVACEUSZACH, S., CAPSONI, S., UGOLINI, G., SPIRITO, F., VIGNONE, D. & CATTANEO, A. 2009. Development of a non invasive NGF-based therapy for Alzheimer's disease. Curr Alzheimer Res, 6, 158-70.
COVACU, R., ARVIDSSON, L., ANDERSSON, A., KHADEMI, M., ERLANDSSON-HARRIS, H., HARRIS, R. A., SVENSSON, M. A., OLSSON, T. & BRUNDIN, L. 2009. TLR activation induces TNF-alpha production from adult neural stem/progenitor cells. J Immunol, 182, 6889-95.

CREEDON, D. J., JOHNSON, E. M. & LAWRENCE, J. C. 1996. Mitogen-activated protein kinase-independent pathways mediate the effects of nerve growth factor and cAMP on neuronal survival. J Biol Chem, 271, 20713-8.
CROWDER, R. J. & FREEMAN, R. S. 1998. Phosphatidylinositol 3-kinase and Akt protein kinase are necessary and sufficient for the survival of nerve growth factor-dependent sympathetic neurons. J Neurosci, 18, 2933-43.
CROWLEY, C., SPENCER, S. D., NISHIMURA, M. C., CHEN, K. S., PITTS-MEEK, S., ARMANINI, M. P., LING, L. H., MCMAHON, S. B., SHELTON, D. L. & LEVINSON, A. D. 1994. Mice lacking nerve growth factor display perinatal loss of sensory and sympathetic neurons yet develop basal forebrain cholinergic neurons. Cell, 76, 1001-11.
CUELLO, A. C., BRUNO, M. A., ALLARD, S., LEON, W. & IULITA, M. F. 2010. Cholinergic involvement in Alzheimer's disease. A link with NGF maturation and degradation. J Mol Neurosci, 40, 230-5.
DANIELS, S. B., MCCARRON, M., LOVE, C. & CHOVNICK, A. 1985. Dysgenesis-induced instability of rosy locus transformation in Drosophila melanogaster: analysis of excision events and the selective recovery of control element deletions. Genetics, 109, 95-117.
DAVEY, F. & DAVIES, A. M. 1998. TrkB signalling inhibits p75-mediated apoptosis induced by nerve growth factor in embryonic proprioceptive neurons. Curr Biol, 8, 915-8.
DAVOLI, C., MARCONI, A., SERAFINO, A., IANNONI, C., MARCHEGGIANO, A. & RAVAGNAN, G. 2002. Expression of nerve growth factor-like polypeptides and immunoreactivity related to the two types of neurotrophin receptors in earthworm tissues. Cell Mol Life Sci, 59, 527-39.
DEARBORN, R. & KUNES, S. 2004. An axon scaffold induced by retinal axons directs glia to destinations in the Drosophila optic lobe. Development, 131, 2291-303.
DEGTEREV, A., BOYCE, M. & YUAN, J. 2003. A decade of caspases. Oncogene, 22, 8543-67.
DELOTTO, Y. & DELOTTO, R. 1998. Proteolytic processing of the Drosophila Spätzle protein by easter generates a dimeric NGF-like molecule with ventralising activity. Mech Dev, 72, 141-8.
DESAI, C. J., KRUEGER, N. X., SAITO, H. & ZINN, K. 1997. Competition and cooperation among receptor tyrosine phosphatases control motoneuron growth cone guidance in Drosophila. Development, 124, 1941-52.
DICKSON, B. J. 2002. Molecular mechanisms of axon guidance. Science, 298, 1959-64.
DISSING, M., GIORDANO, H. & DELOTTO, R. 2001. Autoproteolysis and feedback in a protease cascade directing Drosophila dorsal-ventral cell fate. EMBO J, 20, 2387-93.
DOBROWSKY, R. T. & CARTER, B. D. 1998. Coupling of the p75 neurotrophin receptor to sphingolipid signaling. Ann N Y Acad Sci, 845, 32-45.
DOLAN, J., WALSHE, K., ALSBURY, S., HOKAMP, K., O'KEEFFE, S., OKAFUJI, T., MILLER, S. F., TEAR, G. & MITCHELL, K. J. 2007. The extracellular leucine-rich repeat superfamily; a comparative survey and analysis of evolutionary relationships and expression patterns. BMC Genomics, 8, 320.
DONOVAN, M. J., MIRANDA, R. C., KRAEMER, R., MCCAFFREY, T. A., TESSAROLLO, L., MAHADEO, D., SHARIF, S., KAPLAN, D. R., TSOULFAS, P. & PARADA, L. 1995. Neurotrophin and neurotrophin receptors in vascular smooth

muscle cells. Regulation of expression in response to injury. Am J Pathol, 147, 309-24.
DORSTEN, J. N. & VANBERKUM, M. F. 2008. Frazzled cytoplasmic P-motifs are differentially required for axon pathway formation in the Drosophila embryonic CNS. Int J Dev Neurosci, 26, 753-61.
DOWNES, C. E. & CRACK, P. J. 2010. Neural injury following stroke: are Toll-like receptors the link between the immune system and the CNS? Br J Pharmacol, 160, 1872-88.
DRIER, E. A., HUANG, L. H. & STEWARD, R. 1999. Nuclear import of the Drosophila Rel protein Dorsal is regulated by phosphorylation. Genes Dev, 13, 556-68.
EDENFELD, G., STORK, T. & KLÄMBT, C. 2005. Neuron-glia interaction in the insect nervous system. Curr Opin Neurobiol, 15, 34-9.
EDWARDS, R. H., SELBY, M. J., GARCIA, P. D. & RUTTER, W. J. 1988. Processing of the native nerve growth factor precursor to form biologically active nerve growth factor. J Biol Chem, 263, 6810-5.
EGAN, M. F., KOJIMA, M., CALLICOTT, J. H., GOLDBERG, T. E., KOLACHANA, B. S., BERTOLINO, A., ZAITSEV, E., GOLD, B., GOLDMAN, D., DEAN, M., LU, B. & WEINBERGER, D. R. 2003. The BDNF val66met polymorphism affects activity-dependent secretion of BDNF and human memory and hippocampal function. Cell, 112, 257-69.
EL CHAMY, L., LECLERC, V., CALDELARI, I. & REICHHART, J. M. 2008. Sensing of 'danger signals' and pathogen-associated molecular patterns defines binary signaling pathways 'upstream' of Toll. Nat Immunol, 9, 1165-70.
ELDON, E., KOOYER, S., D'EVELYN, D., DUMAN, M., LAWINGER, P., BOTAS, J. & BELLEN, H. 1994. The Drosophila 18 wheeler is required for morphogenesis and has striking similarities to Toll. Development, 120, 885-99.
ENGLISH, J., PEARSON, G., WILSBACHER, J., SWANTEK, J., KARANDIKAR, M., XU, S. & COBB, M. H. 1999. New insights into the control of MAP kinase pathways. Exp Cell Res, 253, 255-70.
ERNFORS, P., IBÁÑEZ, C. F., EBENDAL, T., OLSON, L. & PERSSON, H. 1990. Molecular cloning and neurotrophic activities of a protein with structural similarities to nerve growth factor: developmental and topographical expression in the brain. Proc Natl Acad Sci U S A, 87, 5454-8.
ERNSBERGER, U. 2009. Role of neurotrophin signalling in the differentiation of neurons from dorsal root ganglia and sympathetic ganglia. Cell Tissue Res, 336, 349-84.
ESPOSITO, D., PATEL, P., STEPHENS, R. M., PEREZ, P., CHAO, M. V., KAPLAN, D. R. & HEMPSTEAD, B. L. 2001. The cytoplasmic and transmembrane domains of the p75 and Trk A receptors regulate high affinity binding to nerve growth factor. J Biol Chem, 276, 32687-95.
EVANS, T. A., HARIDAS, H. & DUFFY, J. B. 2009. Kekkon5 is an extracellular regulator of BMP signaling. Dev Biol, 326, 36-46.
FELTEN, D. L., FELTEN, S. Y., CARLSON, S. L., OLSCHOWKA, J. A. & LIVNAT, S. 1985. Noradrenergic and peptidergic innervation of lymphoid tissue. J Immunol, 135, 755s-765s.
FENG, D., KIM, T., OZKAN, E., LIGHT, M., TORKIN, R., TENG, K. K., HEMPSTEAD, B. L. & GARCIA, K. C. 2010. Molecular and structural insight into proNGF engagement of p75NTR and sortilin. J Mol Biol, 396, 967-84.

FERNANDEZ, N. Q., GROSSHANS, J., GOLTZ, J. S. & STEIN, D. 2001. Separable and redundant regulatory determinants in Cactus mediate its dorsal group dependent degradation. Development, 128, 2963-74.
FERRANDON, D., IMLER, J. L., HETRU, C. & HOFFMANN, J. A. 2007. The Drosophila systemic immune response: sensing and signalling during bacterial and fungal infections. Nat Rev Immunol, 7, 862-74.
FIGUROV, A., POZZO-MILLER, L. D., OLAFSSON, P., WANG, T. & LU, B. 1996. Regulation of synaptic responses to high-frequency stimulation and LTP by neurotrophins in the hippocampus. Nature, 381, 706-9.
FISCHBACH, K. F. & TECHNAU, G. 1984. Cell degeneration in the developing optic lobes of the sine oculis and small-optic-lobes mutants of Drosophila melanogaster. Dev Biol, 104, 219-39.
FISCHER, W., WICTORIN, K., BJÖRKLUND, A., WILLIAMS, L. R., VARON, S. & GAGE, F. H. 1987. Amelioration of cholinergic neuron atrophy and spatial memory impairment in aged rats by nerve growth factor. Nature, 329, 65-8.
FOEHR, E. D., LIN, X., O'MAHONY, A., GELEZIUNAS, R., BRADSHAW, R. A. & GREENE, W. C. 2000. NF-kappa B signaling promotes both cell survival and neurite process formation in nerve growth factor-stimulated PC12 cells. J Neurosci, 20, 7556-63.
FORERO, M. G., PENNACK, J. A., LEARTE, A. R. & HIDALGO, A. 2009. DeadEasy caspase: automatic counting of apoptotic cells in Drosophila. PLoS One, 4, e5441.
FRADE, J. M., RODRÍGUEZ-TÉBAR, A. & BARDE, Y. A. 1996. Induction of cell death by endogenous nerve growth factor through its p75 receptor. Nature, 383, 166-8.
FREUDENTHAL, R. & ROMANO, A. 2000. Participation of Rel/NF-kappaB transcription factors in long-term memory in the crab Chasmagnathus. Brain Res, 855, 274-81.
GANGLOFF, M., MURALI, A., XIONG, J., ARNOT, C. J., WEBER, A. N., SANDERCOCK, A. M., ROBINSON, C. V., SARISKY, R., HOLZENBURG, A., KAO, C. & GAY, N. J. 2008. Structural insight into the mechanism of activation of the Toll receptor by the dimeric ligand Spätzle. J Biol Chem, 283, 14629-35.
GAVALDÀ, N., GUTIERREZ, H. & DAVIES, A. M. 2009. Developmental switch in NF-kappaB signalling required for neurite growth. Development, 136, 3405-12.
GAY, N. J. & GANGLOFF, M. 2007. Structure and function of Toll receptors and their ligands. Annu Rev Biochem, 76, 141-65.
GEHLER, S., GALLO, G., VEIEN, E. & LETOURNEAU, P. C. 2004. p75 neurotrophin receptor signaling regulates growth cone filopodial dynamics through modulating RhoA activity. J Neurosci, 24, 4363-72.
GENTRY, J. J., RUTKOSKI, N. J., BURKE, T. L. & CARTER, B. D. 2004. A functional interaction between the p75 neurotrophin receptor interacting factors, TRAF6 and NRIF. J Biol Chem, 279, 16646-56.
GERTTULA, S., JIN, Y. S. & ANDERSON, K. V. 1988. Zygotic expression and activity of the Drosophila Toll gene, a gene required maternally for embryonic dorsal-ventral pattern formation. Genetics, 119, 123-33.
GHIGLIONE, C., CARRAWAY, K. L., AMUNDADOTTIR, L. T., BOSWELL, R. E., PERRIMON, N. & DUFFY, J. B. 1999. The transmembrane molecule kekkon 1 acts in a feedback loop to negatively regulate the activity of the Drosophila EGF receptor during oogenesis. Cell, 96, 847-56.

GILLESPIE, S. K. & WASSERMAN, S. A. 1994. Dorsal, a Drosophila Rel-like protein, is phosphorylated upon activation of the transmembrane protein Toll. Mol Cell Biol, 14, 3559-68.
GILSOHN, E. & VOLK, T. 2010. Slowdown promotes muscle integrity by modulating integrin-mediated adhesion at the myotendinous junction. Development, 137, 785-94.
GLOOR, G. B., PRESTON, C. R., JOHNSON-SCHLITZ, D. M., NASSIF, N. A., PHILLIS, R. W., BENZ, W. K., ROBERTSON, H. M. & ENGELS, W. R. 1993. Type I repressors of P element mobility. Genetics, 135, 81-95.
GOETHALS, S., YDENS, E., TIMMERMAN, V. & JANSSENS, S. 2010. Toll-like receptor expression in the peripheral nerve. Glia, 58, 1701-9.
GONG, Y., CAO, P., YU, H. J. & JIANG, T. 2008. Crystal structure of the neurotrophin-3 and p75NTR symmetrical complex. Nature, 454, 789-93.
GOODMAN, C. S. & DOE, C. Q. 1993. Embryonic development of the Drosophila central nervous system. In: BATE, M. & MARTINEZ ARIAS, A. (eds.) The development of Drosophila melanogaster. New York: CSHL Press.
GOTTAR, M., GOBERT, V., MATSKEVICH, A. A., REICHHART, J. M., WANG, C., BUTT, T. M., BELVIN, M., HOFFMANN, J. A. & FERRANDON, D. 2006. Dual detection of fungal infections in Drosophila via recognition of glucans and sensing of virulence factors. Cell, 127, 1425-37.
GUERRINI, L., BLASI, F. & DENIS-DONINI, S. 1995. Synaptic activation of NF-kappa B by glutamate in cerebellar granule neurons in vitro. Proc Natl Acad Sci U S A, 92, 9077-81.
GUNDERSEN, R. W. & BARRETT, J. N. 1979. Neuronal chemotaxis: chick dorsal-root axons turn toward high concentrations of nerve growth factor. Science, 206, 1079-80.
GUTIERREZ, H. & DAVIES, A. M. 2011. Regulation of neural process growth, elaboration and structural plasticity by NF-κB. Trends Neurosci, 34, 316-25.
GUTIERREZ, H., HALE, V. A., DOLCET, X. & DAVIES, A. 2005. NF-kappaB signalling regulates the growth of neural processes in the developing PNS and CNS. Development, 132, 1713-26.
GÄRTNER, A., POLNAU, D. G., STAIGER, V., SCIARRETTA, C., MINICHIELLO, L., THOENEN, H., BONHOEFFER, T. & KORTE, M. 2006. Hippocampal long-term potentiation is supported by presynaptic and postsynaptic tyrosine receptor kinase B-mediated phospholipase Cgamma signaling. J Neurosci, 26, 3496-504.
HAHN, U. K., FRYER, S. E. & BAYNE, C. J. 1996. An invertebrate (Molluscan) plasma protein that binds to vertebrate immunoglobulins and its potential for yielding false-positives in antibody-based detection systems. Dev Comp Immunol, 20, 39-50.
HALFON, M. S., HASHIMOTO, C. & KESHISHIAN, H. 1995. The Drosophila toll gene functions zygotically and is necessary for proper motoneuron and muscle development. Dev Biol, 169, 151-67.
HALFON, M. S. & KESHISHIAN, H. 1998. The Toll pathway is required in the epidermis for muscle development in the Drosophila embryo. Dev Biol, 199, 164-74.
HALLBÖÖK, F., IBÁÑEZ, C. F. & PERSSON, H. 1991. Evolutionary studies of the nerve growth factor family reveal a novel member abundantly expressed in Xenopus ovary. Neuron, 6, 845-58.
HALLBÖÖK, F., WILSON, K., THORNDYKE, M. & OLINSKI, R. P. 2006. Formation and evolution of the chordate neurotrophin and Trk receptor genes. Brain Behav Evol, 68, 133-44.

HAMANOUE, M., MIDDLETON, G., WYATT, S., JAFFRAY, E., HAY, R. T. & DAVIES, A. M. 1999. p75-mediated NF-kappaB activation enhances the survival response of developing sensory neurons to nerve growth factor. Mol Cell Neurosci, 14, 28-40.
HAN, J. H., LEE, S. H., TAN, Y. Q., LEMOSY, E. K. & HASHIMOTO, C. 2000. Gastrulation defective is a serine protease involved in activating the receptor toll to polarize the Drosophila embryo. Proc Natl Acad Sci U S A, 97, 9093-7.
HAN, Z. S. & IP, Y. T. 1999. Interaction and specificity of Rel-related proteins in regulating Drosophila immunity gene expression. J Biol Chem, 274, 21355-61.
HANISCH, U. K., JOHNSON, T. V. & KIPNIS, J. 2008. Toll-like receptors: roles in neuroprotection? Trends Neurosci, 31, 176-82.
HARTENSTEIN, V. 1993. Atlas of Drosophila development. In: BATE, M. & MARTINEZ ARIAS, A. (eds.) The development of Drosophila melanogaster. New York: CSHL Press.
HASHIMOTO, C., GERTTULA, S. & ANDERSON, K. V. 1991. Plasma membrane localization of the Toll protein in the syncytial Drosophila embryo: importance of transmembrane signaling for dorsal-ventral pattern formation. Development, 111, 1021-8.
HE, X. L. & GARCIA, K. C. 2004. Structure of nerve growth factor complexed with the shared neurotrophin receptor p75. Science, 304, 870-5.
HEBBAR, S., HALL, R. E., DEMSKI, S. A., SUBRAMANIAN, A. & FERNANDES, J. J. 2006. The adult abdominal neuromuscular junction of Drosophila: a model for synaptic plasticity. J Neurobiol, 66, 1140-55.
HECHT, P. M. & ANDERSON, K. V. 1993. Genetic characterization of tube and pelle, genes required for signaling between Toll and dorsal in the specification of the dorsal-ventral pattern of the Drosophila embryo. Genetics, 135, 405-17.
HECKSCHER, E. S., FETTER, R. D., MAREK, K. W., ALBIN, S. D. & DAVIS, G. W. 2007. NF-kappaB, IkappaB, and IRAK control glutamate receptor density at the Drosophila NMJ. Neuron, 55, 859-73.
HEISENBERG, M. 1997. Genetic approaches to neuroethology. Bioessays, 19, 1065-73.
HEMPSTEAD, B. L., MARTIN-ZANCA, D., KAPLAN, D. R., PARADA, L. F. & CHAO, M. V. 1991. High-affinity NGF binding requires coexpression of the trk proto-oncogene and the low-affinity NGF receptor. Nature, 350, 678-83.
HIDALGO, A. 2002. Interactive nervous system development: control of cell survival in Drosophila. Trends Neurosci, 25, 365-70.
HIDALGO, A. & BRAND, A. H. 1997. Targeted neuronal ablation: the role of pioneer neurons in guidance and fasciculation in the CNS of Drosophila. Development, 124, 3253-62.
HIDALGO, A. & FFRENCH-CONSTANT, C. 2003. The control of cell number during central nervous system development in flies and mice. Mech Dev, 120, 1311-25.
HIDALGO, A., LEARTE, A. R., MCQUILTON, P., PENNACK, J. & ZHU, B. 2006. Neurotrophic and gliatrophic contexts in Drosophila. Brain Behav Evol, 68, 173-80.
HOFFMANN, A., FUNKNER, A., NEUMANN, P., JUHNKE, S., WALTHER, M., SCHIERHORN, A., WEININGER, U., BALBACH, J., REUTER, G. & STUBBS, M. T. 2008. Biophysical characterization of refolded Drosophila Spätzle, a cystine knot protein, reveals distinct properties of three isoforms. J Biol Chem, 283, 32598-609.
HOHN, A., LEIBROCK, J., BAILEY, K. & BARDE, Y. A. 1990. Identification and characterization of a novel member of the nerve growth factor/brain-derived neurotrophic factor family. Nature, 344, 339-41.

HOLGADO-MADRUGA, M., MOSCATELLO, D. K., EMLET, D. R., DIETERICH, R. & WONG, A. J. 1997. Grb2-associated binder-1 mediates phosphatidylinositol 3-kinase activation and the promotion of cell survival by nerve growth factor. Proc Natl Acad Sci U S A, 94, 12419-24.
HORI, O., BRETT, J., SLATTERY, T., CAO, R., ZHANG, J., CHEN, J. X., NAGASHIMA, M., LUNDH, E. R., VIJAY, S. & NITECKI, D. 1995. The receptor for advanced glycation end products (RAGE) is a cellular binding site for amphoterin. Mediation of neurite outgrowth and co-expression of rage and amphoterin in the developing nervous system. J Biol Chem, 270, 25752-61.
HU, X., YAGI, Y., TANJI, T., ZHOU, S. & IP, Y. T. 2004. Multimerization and interaction of Toll and Spätzle in Drosophila. Proc Natl Acad Sci U S A, 101, 9369-74.
HUANG, A. M., RUSCH, J. & LEVINE, M. 1997. An anteroposterior Dorsal gradient in the Drosophila embryo. Genes Dev, 11, 1963-73.
HUANG, E. J. & REICHARDT, L. F. 2001. Neurotrophins: roles in neuronal development and function. Annu Rev Neurosci, 24, 677-736.
HUANG, E. J. & REICHARDT, L. F. 2003. Trk receptors: roles in neuronal signal transduction. Annu Rev Biochem, 72, 609-42.
HUANG, H. R., CHEN, Z. J., KUNES, S., CHANG, G. D. & MANIATIS, T. 2010. Endocytic pathway is required for Drosophila Toll innate immune signaling. Proc Natl Acad Sci U S A, 107, 8322-7.
HUGHES, A. L., MESSINEO-JONES, D., LAD, S. P. & NEET, K. E. 2001. Distinction between differentiation, cell cycle, and apoptosis signals in PC12 cells by the nerve growth factor mutant delta9/13, which is selective for the p75 neurotrophin receptor. J Neurosci Res, 63, 10-9.
IMLER, J. L. & HOFFMANN, J. A. 2001. Toll receptors in innate immunity. Trends Cell Biol, 11, 304-11.
INDO, Y., TSURUTA, M., HAYASHIDA, Y., KARIM, M. A., OHTA, K., KAWANO, T., MITSUBUCHI, H., TONOKI, H., AWAYA, Y. & MATSUDA, I. 1996. Mutations in the TRKA/NGF receptor gene in patients with congenital insensitivity to pain with anhidrosis. Nat Genet, 13, 485-8.
IWASAKI, A. & MEDZHITOV, R. 2004. Toll-like receptor control of the adaptive immune responses. Nat Immunol, 5, 987-95.
JAARO, H., BECK, G., CONTICELLO, S. G. & FAINZILBER, M. 2001. Evolving better brains: a need for neurotrophins? Trends Neurosci, 24, 79-85.
JACK, C. S., ARBOUR, N., MANUSOW, J., MONTGRAIN, V., BLAIN, M., MCCREA, E., SHAPIRO, A. & ANTEL, J. P. 2005. TLR signaling tailors innate immune responses in human microglia and astrocytes. J Immunol, 175, 4320-30.
JACKSON, A. C., ROSSITER, J. P. & LAFON, M. 2006. Expression of Toll-like receptor 3 in the human cerebellar cortex in rabies, herpes simplex encephalitis, and other neurological diseases. J Neurovirol, 12, 229-34.
JAN, Y. N. & JAN, L. Y. 1993. The peripheral nervous system. In: BATE, M. & MARTINEZ ARIAS, A. (eds.) The development of Drosophila melanogaster. Ney York: CSHL Press.
JANEWAY, C. A. 1989. Approaching the asymptote? Evolution and revolution in immunology. Cold Spring Harb Symp Quant Biol, 54 Pt 1, 1-13.
JANG, I. H., CHOSA, N., KIM, S. H., NAM, H. J., LEMAITRE, B., OCHIAI, M., KAMBRIS, Z., BRUN, S., HASHIMOTO, C., ASHIDA, M., BREY, P. T. & LEE, W.

J. 2006. A Spätzle-processing enzyme required for toll signaling activation in Drosophila innate immunity. Dev Cell, 10, 45-55.
JIANG, Y., CHEN, G., ZHANG, Y., LU, L., LIU, S. & CAO, X. 2007. Nerve growth factor promotes TLR4 signaling-induced maturation of human dendritic cells in vitro through inducible p75NTR 1. J Immunol, 179, 6297-304.
JIANG, Y., CHEN, G., ZHENG, Y., LU, L., WU, C., ZHANG, Y., LIU, Q. & CAO, X. 2008. TLR4 signaling induces functional nerve growth factor receptor p75NTR on mouse dendritic cells via p38MAPK and NF-kappa B pathways. Mol Immunol, 45, 1557-66.
JING, S., TAPLEY, P. & BARBACID, M. 1992. Nerve growth factor mediates signal transduction through trk homodimer receptors. Neuron, 9, 1067-79.
JOHNSON, D., LANAHAN, A., BUCK, C. R., SEHGAL, A., MORGAN, C., MERCER, E., BOTHWELL, M. & CHAO, M. 1986. Expression and structure of the human NGF receptor. Cell, 47, 545-54.
KALTSCHMIDT, C., KALTSCHMIDT, B. & BAEUERLE, P. A. 1993. Brain synapses contain inducible forms of the transcription factor NF-kappa B. Mech Dev, 43, 135-47.
KAMBRIS, Z., BILAK, H., D'ALESSANDRO, R., BELVIN, M., IMLER, J. L. & CAPOVILLA, M. 2003. DmMyD88 controls dorsoventral patterning of the Drosophila embryo. EMBO Rep, 4, 64-9.
KAMBRIS, Z., BRUN, S., JANG, I. H., NAM, H. J., ROMEO, Y., TAKAHASHI, K., LEE, W. J., UEDA, R. & LEMAITRE, B. 2006. Drosophila immunity: a large-scale in vivo RNAi screen identifies five serine proteases required for Toll activation. Curr Biol, 16, 808-13.
KAMBRIS, Z., HOFFMANN, J. A., IMLER, J. L. & CAPOVILLA, M. 2002. Tissue and stage-specific expression of the Tolls in Drosophila embryos. Gene Expr Patterns, 2, 311-7.
KAMIKOUCHI, A., SHIMADA, T. & ITO, K. 2006. Comprehensive classification of the auditory sensory projections in the brain of the fruit fly Drosophila melanogaster. J Comp Neurol, 499, 317-56.
KANDA, H., IGAKI, T., KANUKA, H., YAGI, T. & MIURA, M. 2002. Wengen, a member of the Drosophila tumor necrosis factor receptor superfamily, is required for Eiger signaling. J Biol Chem, 277, 28372-5.
KAO , S., JAISWAL, R. K., KOLCH, W. & LANDRETH, G. E. 2001. Identification of the mechanisms regulating the differential activation of the mapk cascade by epidermal growth factor and nerve growth factor in PC12 cells. J Biol Chem, 276, 18169-77.
KAPLAN, D. R., HEMPSTEAD, B. L., MARTIN-ZANCA, D., CHAO, M. V. & PARADA, L. F. 1991. The trk proto-oncogene product: a signal transducing receptor for nerve growth factor. Science, 252, 554-8.
KAPLAN, D. R. & MILLER, F. D. 2000. Neurotrophin signal transduction in the nervous system. Curr Opin Neurobiol, 10, 381-91.
KATO, K., FORERO, M. G., FENTON, J. C. & HIDALGO, A. 2011. The Glial Regenerative Response to Central Nervous System Injury Is Enabled by Pros-Notch and Pros-NFκB Feedback. PLoS Biol, 9, e1001133.
KAWAI, T. & AKIRA, S. 2007. Signaling to NF-kappaB by Toll-like receptors. Trends Mol Med, 13, 460-9.
KAWAMURA, K., KAWAMURA, N., FUKUDA, J., KUMAGAI, J., HSUEH, A. J. & TANAKA, T. 2007. Regulation of preimplantation embryo development by brain-derived neurotrophic factor. Dev Biol, 311, 147-58.

KAWAMURA, K., KAWAMURA, N., MULDERS, S. M., SOLLEWIJN GELPKE, M. D. & HSUEH, A. J. 2005. Ovarian brain-derived neurotrophic factor (BDNF) promotes the development of oocytes into preimplantation embryos. Proc Natl Acad Sci U S A, 102, 9206-11.
KEITH, F. J. & GAY, N. J. 1990. The Drosophila membrane receptor Toll can function to promote cellular adhesion. EMBO J, 9, 4299-306.
KELLER, A., SWEENEY, S. T., ZARS, T., O'KANE, C. J. & HEISENBERG, M. 2002. Targeted expression of tetanus neurotoxin interferes with behavioral responses to sensory input in Drosophila. J Neurobiol, 50, 221-33.
KERR, J. F., WYLLIE, A. H. & CURRIE, A. R. 1972. Apoptosis: a basic biological phenomenon with wide-ranging implications in tissue kinetics. Br J Cancer, 26, 239-57.
KHURSIGARA, G., ORLINICK, J. R. & CHAO, M. V. 1999. Association of the p75 neurotrophin receptor with TRAF6. J Biol Chem, 274, 2597-600.
KIM, S., CHUNG, S., YOON, J., CHOI, K. W. & YIM, J. 2006. Ectopic expression of Tollo/Toll-8 antagonizes Dpp signaling and induces cell sorting in the Drosophila wing. Genesis, 44, 541-9.
KIMURA, M. T., IRIE, S., SHOJI-HOSHINO, S., MUKAI, J., NADANO, D., OSHIMURA, M. & SATO, T. A. 2001. 14-3-3 is involved in p75 neurotrophin receptor-mediated signal transduction. J Biol Chem, 276, 17291-300.
KLEIN, R., JING, S. Q., NANDURI, V., O'ROURKE, E. & BARBACID, M. 1991. The trk proto-oncogene encodes a receptor for nerve growth factor. Cell, 65, 189-97.
KLEVE, C. D., SILER, D. A., SYED, S. K. & ELDON, E. D. 2006. Expression of 18-wheeler in the follicle cell epithelium affects cell migration and egg morphology in Drosophila. Dev Dyn, 235, 1953-61.
KOLESNIKOV, T. & BECKENDORF, S. K. 2007. 18 wheeler regulates apical constriction of salivary gland cells via the Rho-GTPase-signaling pathway. Dev Biol, 307, 53-61.
KONG, Y. & LE, Y. 2011. Toll-like receptors in inflammation of the central nervous system. Int Immunopharmacol, 11, 1407-14
KORNBLUTH, S. & WHITE, K. 2005. Apoptosis in Drosophila: neither fish nor fowl (nor man, nor worm). J Cell Sci, 118, 1779-87.
KORTE, M., CARROLL, P., WOLF, E., BREM, G., THOENEN, H. & BONHOEFFER, T. 1995. Hippocampal long-term potentiation is impaired in mice lacking brain-derived neurotrophic factor. Proc Natl Acad Sci U S A, 92, 8856-60.
KUBOTA, K., KEITH, F. J. & GAY, N. J. 1993. Relocalization of Drosophila dorsal protein can be induced by a rise in cytoplasmic calcium concentration and the expression of constitutively active but not wild-type Toll receptors. Biochem J, 296 (Pt 2), 497-503.
KUJA-PANULA, J., KIILTOMÄKI, M., YAMASHIRO, T., ROUHIAINEN, A. & RAUVALA, H. 2003. AMIGO, a transmembrane protein implicated in axon tract development, defines a novel protein family with leucine-rich repeats. J Cell Biol, 160, 963-73.
KUMAR, H., KAWAI, T. & AKIRA, S. 2009. Toll-like receptors and innate immunity. Biochem Biophys Res Commun, 388, 621-5.
LANDGRAF, M., BAYLIES, M. & BATE, M. 1999. Muscle founder cells regulate defasciculation and targeting of motor axons in the Drosophila embryo. Curr Biol, 9, 589-92.

LANDGRAF, M., BOSSING, T., TECHNAU, G. M. & BATE, M. 1997. The origin, location, and projections of the embryonic abdominal motorneurons of Drosophila. J Neurosci, 17, 9642-55.
LANDGRAF, M., JEFFREY, V., FUJIOKA, M., JAYNES, J. B. & BATE, M. 2003. Embryonic origins of a motor system: motor dendrites form a myotopic map in Drosophila. PLoS Biol, 1, E41.
LANDGRAF, M. & THOR, S. 2006. Development of Drosophila motoneurons: specification and morphology. Semin Cell Dev Biol, 17, 3-11.
LATHIA, J. D., OKUN, E., TANG, S. C., GRIFFIOEN, K., CHENG, A., MUGHAL, M. R., LARYEA, G., SELVARAJ, P. K., FFRENCH-CONSTANT, C., MAGNUS, T., ARUMUGAM, T. V. & MATTSON, M. P. 2008. Toll-like receptor 3 is a negative regulator of embryonic neural progenitor cell proliferation. J Neurosci, 28, 13978-84.
LAUKKANEN, M. L., OKER-BLOM, C. & KEINÄNEN, K. 1996. Secretion of green fluorescent protein from recombinant baculovirus-infected insect cells. Biochem Biophys Res Commun, 226, 755-61.
LEE, R., KERMANI, P., TENG, K. K. & HEMPSTEAD, B. L. 2001. Regulation of cell survival by secreted proneurotrophins. Science, 294, 1945-8.
LEE, T. & LUO, L. 1999. Mosaic analysis with a repressible cell marker for studies of gene function in neuronal morphogenesis. Neuron, 22, 451-61.
LEHNARDT, S. 2010. Innate immunity and neuroinflammation in the CNS: the role of microglia in Toll-like receptor-mediated neuronal injury. Glia, 58, 253-63.
LEIBROCK, J., LOTTSPEICH, F., HOHN, A., HOFER, M., HENGERER, B., MASIAKOWSKI, P., THOENEN, H. & BARDE, Y. A. 1989. Molecular cloning and expression of brain-derived neurotrophic factor. Nature, 341, 149-52.
LEMAITRE, B., NICOLAS, E., MICHAUT, L., REICHHART, J. M. & HOFFMANN, J. A. 1996. The dorsoventral regulatory gene cassette spätzle/Toll/cactus controls the potent antifungal response in Drosophila adults. Cell, 86, 973-83.
LEMOSY, E. K., KEMLER, D. & HASHIMOTO, C. 1998. Role of Nudel protease activation in triggering dorsoventral polarization of the Drosophila embryo. Development, 125, 4045-53.
LEMOSY, E. K., TAN, Y. Q. & HASHIMOTO, C. 2001. Activation of a protease cascade involved in patterning the Drosophila embryo. Proc Natl Acad Sci U S A, 98, 5055-60.
LEON, A., BURIANI, A., DAL TOSO, R., FABRIS, M., ROMANELLO, S., ALOE, L. & LEVI-MONTALCINI, R. 1994. Mast cells synthesize, store, and release nerve growth factor. Proc Natl Acad Sci U S A, 91, 3739-43.
LESSMANN, V., GOTTMANN, K. & MALCANGIO, M. 2003. Neurotrophin secretion: current facts and future prospects. Prog Neurobiol, 69, 341-74.
LEVASHINA, E. A., LANGLEY, E., GREEN, C., GUBB, D., ASHBURNER, M., HOFFMANN, J. A. & REICHHART, J. M. 1999. Constitutive activation of toll-mediated antifungal defense in serpin-deficient Drosophila. Science, 285, 1917-9.
LEVI-MONTALCINI, R. 1987. The nerve growth factor 35 years later. Science, 237, 1154-62.
LEVI-MONTALCINI, R., SKAPER, S. D., DAL TOSO, R., PETRELLI, L. & LEON, A. 1996. Nerve growth factor: from neurotrophin to neurokine. Trends Neurosci, 19, 514-20.

LEVINE, E. S., CROZIER, R. A., BLACK, I. B. & PLUMMER, M. R. 1998. Brain-derived neurotrophic factor modulates hippocampal synaptic transmission by increasing N-methyl-D-aspartic acid receptor activity. Proc Natl Acad Sci U S A, 95, 10235-9.
LI, L., QIU, L., SONG, L., SONG, X., ZHAO, J., WANG, L., MU, C. & ZHANG, H. 2009. First molluscan TNFR homologue in Zhikong scallop: molecular characterization and expression analysis. Fish Shellfish Immunol, 27, 625-32.
LI, Y. X., ZHANG, Y., LESTER, H. A., SCHUMAN, E. M. & DAVIDSON, N. 1998. Enhancement of neurotransmitter release induced by brain-derived neurotrophic factor in cultured hippocampal neurons. J Neurosci, 18, 10231-40.
LIGOXYGAKIS, P., BULET, P. & REICHHART, J. M. 2002a. Critical evaluation of the role of the Toll-like receptor 18-Wheeler in the host defense of Drosophila. EMBO Rep, 3, 666-73.
LIGOXYGAKIS, P., PELTE, N., HOFFMANN, J. A. & REICHHART, J. M. 2002b. Activation of Drosophila Toll during fungal infection by a blood serine protease. Science, 297, 114-6.
LINNARSSON, S., BJÖRKLUND, A. & ERNFORS, P. 1997. Learning deficit in BDNF mutant mice. Eur J Neurosci, 9, 2581-7.
LOEB, D. M., STEPHENS, R. M., COPELAND, T., KAPLAN, D. R. & GREENE, L. A. 1994. A Trk nerve growth factor (NGF) receptor point mutation affecting interaction with phospholipase C-gamma 1 abolishes NGF-promoted peripherin induction but not neurite outgrowth. J Biol Chem, 269, 8901-10.
LU, B., PANG, P. T. & WOO, N. H. 2005. The yin and yang of neurotrophin action. Nat Rev Neurosci, 6, 603-14.
LUCINI, C., CASTALDO, L., LAMANNA, C., MARUCCIO, L., VEGA, J. A. & GARGIULO, G. 1999. Neuronal and non-neuronal Trk neurotrophin receptor-like proteins in Eisenia foetida (Annelida Oligochaeta). Neurosci Lett, 261, 163-6.
LUCKOW, V. A., LEE, S. C., BARRY, G. F. & OLINS, P. O. 1993. Efficient generation of infectious recombinant baculoviruses by site-specific transposon-mediated insertion of foreign genes into a baculovirus genome propagated in Escherichia coli. J Virol, 67, 4566-79.
LUO, C., SHEN, B., MANLEY, J. L. & ZHENG, L. 2001. Tehao functions in the Toll pathway in Drosophila melanogaster: possible roles in development and innate immunity. Insect Mol Biol, 10, 457-64.
MA, Y., LI, J., CHIU, I., WANG, Y., SLOANE, J. A., LÜ, J., KOSARAS, B., SIDMAN, R. L., VOLPE, J. J. & VARTANIAN, T. 2006. Toll-like receptor 8 functions as a negative regulator of neurite outgrowth and inducer of neuronal apoptosis. J Cell Biol, 175, 209-15.
MADDEN, K., CROWNER, D. & GINIGER, E. 1999. LOLA has the properties of a master regulator of axon-target interaction for SNb motor axons of Drosophila. Dev Biol, 213, 301-13.
MAGGIRWAR, S. B., SARMIERE, P. D., DEWHURST, S. & FREEMAN, R. S. 1998. Nerve growth factor-dependent activation of NF-kappaB contributes to survival of sympathetic neurons. J Neurosci, 18, 10356-65.
MAHADEO, D., KAPLAN, L., CHAO, M. V. & HEMPSTEAD, B. L. 1994. High affinity nerve growth factor binding displays a faster rate of association than p140trk binding. Implications for multi-subunit polypeptide receptors. J Biol Chem, 269, 6884-91.
MAISONPIERRE, P. C., BELLUSCIO, L., FRIEDMAN, B., ALDERSON, R. F., WIEGAND, S. J., FURTH, M. E., LINDSAY, R. M. & YANCOPOULOS, G. D.

1990a. NT-3, BDNF, and NGF in the developing rat nervous system: parallel as well as reciprocal patterns of expression. Neuron, 5, 501-9.
MAISONPIERRE, P. C., BELLUSCIO, L., SQUINTO, S., IP, N. Y., FURTH, M. E., LINDSAY, R. M. & YANCOPOULOS, G. D. 1990b. Neurotrophin-3: a neurotrophic factor related to NGF and BDNF. Science, 247, 1446-51.
MALENKA, R. C. & NICOLL, R. A. 1999. Long-term potentiation--a decade of progress? Science, 285, 1870-4.
MAMIDIPUDI, V., LI, X. & WOOTEN, M. W. 2002. Identification of interleukin 1 receptor-associated kinase as a conserved component in the p75-neurotrophin receptor activation of nuclear factor-kappa B. J Biol Chem, 277, 28010-8.
MANDAI, K., GUO, T., ST HILLAIRE, C., MEABON, J. S., KANNING, K. C., BOTHWELL, M. & GINTY, D. D. 2009. LIG family receptor tyrosine kinase-associated proteins modulate growth factor signals during neural development. Neuron, 63, 614-27.
MANFRUELLI, P., REICHHART, J. M., STEWARD, R., HOFFMANN, J. A. & LEMAITRE, B. 1999. A mosaic analysis in Drosophila fat body cells of the control of antimicrobial peptide genes by the Rel proteins Dorsal and DIF. EMBO J, 18, 3380-91.
MAROSO, M., BALOSSO, S., RAVIZZA, T., LIU, J., ARONICA, E., IYER, A. M., ROSSETTI, C., MOLTENI, M., CASALGRANDI, M., MANFREDI, A. A., BIANCHI, M. E. & VEZZANI, A. 2010. Toll-like receptor 4 and high-mobility group box-1 are involved in ictogenesis and can be targeted to reduce seizures. Nat Med, 16, 413-9.
MARTIN, J. R., ERNST, R. & HEISENBERG, M. 1999. Temporal pattern of locomotor activity in Drosophila melanogaster. J Comp Physiol A, 184, 73-84.
MARTIN-ZANCA, D., OSKAM, R., MITRA, G., COPELAND, T. & BARBACID, M. 1989. Molecular and biochemical characterization of the human trk proto-oncogene. Mol Cell Biol, 9, 24-33.
MASSE, N. Y., TURNER, G. C. & JEFFERIS, G. S. 2009. Olfactory information processing in Drosophila. Curr Biol, 19, R700-13.
MATSUDA, H., KANNAN, Y., USHIO, H., KISO, Y., KANEMOTO, T., SUZUKI, H. & KITAMURA, Y. 1991. Nerve growth factor induces development of connective tissue-type mast cells in vitro from murine bone marrow cells. J Exp Med, 174, 7-14.
MATTSON, M. P. & MEFFERT, M. K. 2006. Roles for NF-kappaB in nerve cell survival, plasticity, and disease. Cell Death Differ, 13, 852-60.
MAZUREK, N., WESKAMP, G., ERNE, P. & OTTEN, U. 1986. Nerve growth factor induces mast cell degranulation without changing intracellular calcium levels. FEBS Lett, 198, 315-20.
MCDONALD, N. Q., LAPATTO, R., MURRAY-RUST, J., GUNNING, J., WLODAWER, A. & BLUNDELL, T. L. 1991. New protein fold revealed by a 2.3-A resolution crystal structure of nerve growth factor. Nature, 354, 411-4.
MEAKIN, S. O. & MACDONALD, J. I. 1998. A novel juxtamembrane deletion in rat TrkA blocks differentiative but not mitogenic cell signaling in response to nerve growth factor. J Neurochem, 71, 1875-88.
MEAKIN, S. O., MACDONALD, J. I., GRYZ, E. A., KUBU, C. J. & VERDI, J. M. 1999. The signaling adapter FRS-2 competes with Shc for binding to the nerve growth factor receptor TrkA. A model for discriminating proliferation and differentiation. J Biol Chem, 274, 9861-70.

MEDZHITOV, R., PRESTON-HURLBURT, P. & JANEWAY, C. A. 1997. A human homologue of the Drosophila Toll protein signals activation of adaptive immunity. Nature, 388, 394-7.
MEFFERT, M. K., CHANG, J. M., WILTGEN, B. J., FANSELOW, M. S. & BALTIMORE, D. 2003. NF-kappa B functions in synaptic signaling and behavior. Nat Neurosci, 6, 1072-8.
MENG, X., KHANUJA, B. S. & IP, Y. T. 1999. Toll receptor-mediated Drosophila immune response requires Dif, an NF-kappaB factor. Genes Dev, 13, 792-7.
MEYER, F. & MOUSSIAN, B. 2009. Drosophila multiplexin (Dmp) modulates motor axon pathfinding accuracy. Dev Growth Differ, 51, 483-98.
MI, S., LEE, X., SHAO, Z., THILL, G., JI, B., RELTON, J., LEVESQUE, M., ALLAIRE, N., PERRIN, S., SANDS, B., CROWELL, T., CATE, R. L., MCCOY, J. M. & PEPINSKY, R. B. 2004. LINGO-1 is a component of the Nogo-66 receptor/p75 signaling complex. Nat Neurosci, 7, 221-8.
MICERA, A., LAMBIASE, A., STAMPACHIACCHIERE, B., BONINI, S. & LEVI-SCHAFFER, F. 2007. Nerve growth factor and tissue repair remodeling: trkA(NGFR) and p75(NTR), two receptors one fate. Cytokine Growth Factor Rev, 18, 245-56.
MIGUEL-ALIAGA, I. & THOR, S. 2004. Segment-specific prevention of pioneer neuron apoptosis by cell-autonomous, postmitotic Hox gene activity. Development, 131, 6093-105.
MIGUEL-ALIAGA, I. & THOR, S. 2009. Programmed cell death in the nervous system--a programmed cell fate? Curr Opin Neurobiol, 19, 127-33.
MINDORFF, E. N., O'KEEFE, D. D., LABBÉ, A., YANG, J. P., OU, Y., YOSHIKAWA, S. & VAN MEYEL, D. J. 2007. A gain-of-function screen for genes that influence axon guidance identifies the NF-kappaB protein dorsal and reveals a requirement for the kinase Pelle in Drosophila photoreceptor axon targeting. Genetics, 176, 2247-63.
MING, G., SONG, H., BERNINGER, B., INAGAKI, N., TESSIER-LAVIGNE, M. & POO, M. 1999. Phospholipase C-gamma and phosphoinositide 3-kinase mediate cytoplasmic signaling in nerve growth cone guidance. Neuron, 23, 139-48.
MINICHIELLO, L. 2009. TrkB signalling pathways in LTP and learning. Nat Rev Neurosci, 10, 850-60.
MINICHIELLO, L., CALELLA, A. M., MEDINA, D. L., BONHOEFFER, T., KLEIN, R. & KORTE, M. 2002. Mechanism of TrkB-mediated hippocampal long-term potentiation. Neuron, 36, 121-37.
MISHRA, B. B., MISHRA, P. K. & TEALE, J. M. 2006. Expression and distribution of Toll-like receptors in the brain during murine neurocysticercosis. J Neuroimmunol, 181, 46-56.
MITCHAM, J. L., PARNET, P., BONNERT, T. P., GARKA, K. E., GERHART, M. J., SLACK, J. L., GAYLE, M. A., DOWER, S. K. & SIMS, J. E. 1996. T1/ST2 signaling establishes it as a member of an expanding interleukin-1 receptor family. J Biol Chem, 271, 5777-83.
MIYAKE, K. 2003. Innate recognition of lipopolysaccharide by CD14 and toll-like receptor 4-MD-2: unique roles for MD-2. Int Immunopharmacol, 3, 119-28.
MIYAMOTO, T. & AMREIN, H. 2008. Suppression of male courtship by a Drosophila pheromone receptor. Nat Neurosci, 11, 874-6.
MIYAZAKI, T. & ITO, K. 2010. Neural architecture of the primary gustatory center of Drosophila melanogaster visualized with GAL4 and LexA enhancer-trap systems. J Comp Neurol, 518, 4147-81.

MIZUGUCHI, K., PARKER, J. S., BLUNDELL, T. L. & GAY, N. J. 1998. Getting knotted: a model for the structure and activation of Spätzle. Trends Biochem Sci, 23, 239-42.
MOALEM, G. & TRACEY, D. J. 2006. Immune and inflammatory mechanisms in neuropathic pain. Brain Res Rev, 51, 240-64.
MONCRIEFFE, M. C., GROSSMANN, J. G. & GAY, N. J. 2008. Assembly of oligomeric death domain complexes during Toll receptor signaling. J Biol Chem, 283, 33447-54.
MORENO, H., NADAL, M., LEZNIK, E., SUGIMORI, M., LAX, I., SCHLESSINGER, J. & LLINÁS, R. 1998. Nerve growth factor acutely reduces chemical transmission by means of postsynaptic TrkA-like receptors in squid giant synapse. Proc Natl Acad Sci U S A, 95, 14997-5002.
MORISATO, D. & ANDERSON, K. V. 1994. The spätzle gene encodes a component of the extracellular signaling pathway establishing the dorsal-ventral pattern of the Drosophila embryo. Cell, 76, 677-88.
MORIYOSHI, K., RICHARDS, L. J., AKAZAWA, C., O'LEARY, D. D. & NAKANISHI, S. 1996. Labeling neural cells using adenoviral gene transfer of membrane-targeted GFP. Neuron, 16, 255-60.
MOUSSIAN, B. & ROTH, S. 2005. Dorsoventral axis formation in the Drosophila embryo--shaping and transducing a morphogen gradient. Curr Biol, 15, R887-99.
MOWLA, S. J., PAREEK, S., FARHADI, H. F., PETRECCA, K., FAWCETT, J. P., SEIDAH, N. G., MORRIS, S. J., SOSSIN, W. S. & MURPHY, R. A. 1999. Differential sorting of nerve growth factor and brain-derived neurotrophic factor in hippocampal neurons. J Neurosci, 19, 2069-80.
MURO, I., BERRY, D. L., HUH, J. R., CHEN, C. H., HUANG, H., YOO, S. J., GUO, M., BAEHRECKE, E. H. & HAY, B. A. 2006. The Drosophila caspase Ice is important for many apoptotic cell deaths and for spermatid individualization, a nonapoptotic process. Development, 133, 3305-15.
MUSACCHIO, M. & PERRIMON, N. 1996. The Drosophila kekkon genes: novel members of both the leucine-rich repeat and immunoglobulin superfamilies expressed in the CNS. Dev Biol, 178, 63-76.
NAGAPPAN, G., ZAITSEV, E., SENATOROV, V. V., YANG, J., HEMPSTEAD, B. L. & LU, B. 2009. Control of extracellular cleavage of ProBDNF by high frequency neuronal activity. Proc Natl Acad Sci U S A, 106, 1267-72.
NARBONNE-REVEAU, K., CHARROUX, B. & ROYET, J. 2011. Lack of an antibacterial response defect in Drosophila Toll-9 mutant. PLoS One, 6, e17470.
NILSON, L. A. & SCHÜPBACH, T. 1998. Localized requirements for windbeutel and pipe reveal a dorsoventral prepattern within the follicular epithelium of the Drosophila ovary. Cell, 93, 253-62.
NOCKHER, W. A. & RENZ, H. 2006a. Neurotrophins and asthma: novel insight into neuroimmune interaction. J Allergy Clin Immunol, 117, 67-71.
NOCKHER, W. A. & RENZ, H. 2006b. Neurotrophins in allergic diseases: from neuronal growth factors to intercellular signaling molecules. J Allergy Clin Immunol, 117, 583-9.
NOMOTO, H., TAKAIWA, M., MOURI, A. & FURUKAWA, S. 2007. Pro-region of neurotrophins determines the processing efficiency. Biochem Biophys Res Commun, 356, 919-24.
NOMURA, N., MIYAJIMA, N., SAZUKA, T., TANAKA, A., KAWARABAYASI, Y., SATO, S., NAGASE, T., SEKI, N., ISHIKAWA, K. & TABATA, S. 1994. Prediction of the coding sequences of unidentified human genes. I. The coding sequences of 40

new genes (KIAA0001-KIAA0040) deduced by analysis of randomly sampled cDNA clones from human immature myeloid cell line KG-1. DNA Res, 1, 27-35.
NYKJAER, A., LEE, R., TENG, K. K., JANSEN, P., MADSEN, P., NIELSEN, M. S., JACOBSEN, C., KLIEMANNEL, M., SCHWARZ, E., WILLNOW, T. E., HEMPSTEAD, B. L. & PETERSEN, C. M. 2004. Sortilin is essential for proNGF-induced neuronal cell death. Nature, 427, 843-8.
O'MAHONY, A., RABER, J., MONTANO, M., FOEHR, E., HAN, V., LU, S. M., KWON, H., LEFEVOUR, A., CHAKRABORTY-SETT, S. & GREENE, W. C. 2006. NF-kappaB/Rel regulates inhibitory and excitatory neuronal function and synaptic plasticity. Mol Cell Biol, 26, 7283-98.
OBERMEIER, A., HALFTER, H., WIESMÜLLER, K. H., JUNG, G., SCHLESSINGER, J. & ULLRICH, A. 1993. Tyrosine 785 is a major determinant of Trk--substrate interaction. EMBO J, 12, 933-41.
OISHI, I., SUGIYAMA, S., LIU, Z. J., YAMAMURA, H., NISHIDA, Y. & MINAMI, Y. 1997. A novel Drosophila receptor tyrosine kinase expressed specifically in the nervous system. Unique structural features and implication in developmental signaling. J Biol Chem, 272, 11916-23.
OKUN, E., GRIFFIOEN, K., BARAK, B., ROBERTS, N. J., CASTRO, K., PITA, M. A., CHENG, A., MUGHAL, M. R., WAN, R., ASHERY, U. & MATTSON, M. P. 2010a. Toll-like receptor 3 inhibits memory retention and constrains adult hippocampal neurogenesis. Proc Natl Acad Sci U S A, 107, 15625-30.
OKUN, E., GRIFFIOEN, K. J., LATHIA, J. D., TANG, S. C., MATTSON, M. P. & ARUMUGAM, T. V. 2009. Toll-like receptors in neurodegeneration. Brain Res Rev, 59, 278-92.
OKUN, E., GRIFFIOEN, K. J. & MATTSON, M. P. 2011. Toll-like receptor signaling in neural plasticity and disease. Trends Neurosci, 34, 269-81.
OKUN, E., GRIFFIOEN, K. J., SON, T. G., LEE, J. H., ROBERTS, N. J., MUGHAL, M. R., HUTCHISON, E., CHENG, A., ARUMUGAM, T. V., LATHIA, J. D., VAN PRAAG, H. & MATTSON, M. P. 2010b. TLR2 activation inhibits embryonic neural progenitor cell proliferation. J Neurochem, 114, 462-74.
ONO, T., SEKINO-SUZUKI, N., KIKKAWA, Y., YONEKAWA, H. & KAWASHIMA, S. 2003. Alivin 1, a novel neuronal activity-dependent gene, inhibits apoptosis and promotes survival of cerebellar granule neurons. J Neurosci, 23, 5887-96.
OOI, J. Y., YAGI, Y., HU, X. & IP, Y. T. 2002. The Drosophila Toll-9 activates a constitutive antimicrobial defense. EMBO Rep, 3, 82-7.
ORMOND, J., HISLOP, J., ZHAO, Y., WEBB, N., VAILLAINCOURT, F., DYER, J. R., FERRARO, G., BARKER, P., MARTIN, K. C. & SOSSIN, W. S. 2004. ApTrkl, a Trk-like receptor, mediates serotonin- dependent ERK activation and long-term facilitation in Aplysia sensory neurons. Neuron, 44, 715-28.
OSAKI, T. & KAWABATA, S. 2004. Structure and function of coagulogen, a clottable protein in horseshoe crabs. Cell Mol Life Sci, 61, 1257-65.
OTSUNA, H. & ITO, K. 2006. Systematic analysis of the visual projection neurons of Drosophila melanogaster. I. Lobula-specific pathways. J Comp Neurol, 497, 928-58.
PANG, P. T., TENG, H. K., ZAITSEV, E., WOO, N. T., SAKATA, K., ZHEN, S., TENG, K. K., YUNG, W. H., HEMPSTEAD, B. L. & LU, B. 2004. Cleavage of proBDNF by tPA/plasmin is essential for long-term hippocampal plasticity. Science, 306, 487-91.
PARK, J. S., GAMBONI-ROBERTSON, F., HE, Q., SVETKAUSKAITE, D., KIM, J. Y., STRASSHEIM, D., SOHN, J. W., YAMADA, S., MARUYAMA, I., BANERJEE, A.,

ISHIZAKA, A. & ABRAHAM, E. 2006. High mobility group box 1 protein interacts with multiple Toll-like receptors. Am J Physiol Cell Physiol, 290, C917-24.
PARK, J. S., SVETKAUSKAITE, D., HE, Q., KIM, J. Y., STRASSHEIM, D., ISHIZAKA, A. & ABRAHAM, E. 2004. Involvement of toll-like receptors 2 and 4 in cellular activation by high mobility group box 1 protein. J Biol Chem, 279, 7370-7.
PARKER, J. S., MIZUGUCHI, K. & GAY, N. J. 2001. A family of proteins related to Spätzle, the toll receptor ligand, are encoded in the Drosophila genome. Proteins, 45, 71-80.
PATEL, T. D., JACKMAN, A., RICE, F. L., KUCERA, J. & SNIDER, W. D. 2000. Development of sensory neurons in the absence of NGF/TrkA signaling in vivo. Neuron, 25, 345-57.
PATTERSON, S. L., ABEL, T., DEUEL, T. A., MARTIN, K. C., ROSE, J. C. & KANDEL, E. R. 1996. Recombinant BDNF rescues deficits in basal synaptic transmission and hippocampal LTP in BDNF knockout mice. Neuron, 16, 1137-45.
PATTERSON, S. L., GROVER, L. M., SCHWARTZKROIN, P. A. & BOTHWELL, M. 1992. Neurotrophin expression in rat hippocampal slices: a stimulus paradigm inducing LTP in CA1 evokes increases in BDNF and NT-3 mRNAs. Neuron, 9, 1081-8.
PELTIER, D. C., SIMMS, A., FARMER, J. R. & MILLER, D. J. 2010. Human neuronal cells possess functional cytoplasmic and TLR-mediated innate immune pathways influenced by phosphatidylinositol-3 kinase signaling. J Immunol, 184, 7010-21.
PENG, I. F., BERKE, B. A., ZHU, Y., LEE, W. H., CHEN, W. & WU, C. F. 2007. Temperature-dependent developmental plasticity of Drosophila neurons: cell-autonomous roles of membrane excitability, Ca2+ influx, and cAMP signaling. J Neurosci, 27, 12611-22.
PENNACK, J. A. 2008. Functional analysis of DNT1 and TIE in the nervous system of Drosophila. University of Birmingham.
PEREANU, W., YOUNOSSI-HARTENSTEIN, A., LOVICK, J., SPINDLER, S. & HARTENSTEIN, V. 2011. Lineage-based analysis of the development of the central complex of the Drosophila brain. J Comp Neurol, 519, 661-89.
PETERSEN, C. M., NIELSEN, M. S., NYKJAER, A., JACOBSEN, L., TOMMERUP, N., RASMUSSEN, H. H., ROIGAARD, H., GLIEMANN, J., MADSEN, P. & MOESTRUP, S. K. 1997. Molecular identification of a novel candidate sorting receptor purified from human brain by receptor-associated protein affinity chromatography. J Biol Chem, 272, 3599-605.
PINCELLI, C., SEVIGNANI, C., MANFREDINI, R., GRANDE, A., FANTINI, F., BRACCI-LAUDIERO, L., ALOE, L., FERRARI, S., COSSARIZZA, A. & GIANNETTI, A. 1994. Expression and function of nerve growth factor and nerve growth factor receptor on cultured keratinocytes. J Invest Dermatol, 103, 13-8.
PING, Y., WARO, G., LICURSI, A., SMITH, S., VO-BA, D. A. & TSUNODA, S. 2011. Shal/K(v)4 channels are required for maintaining excitability during repetitive firing and normal locomotion in Drosophila. PLoS One, 6, e16043.
POLAK, M., SCHARFMANN, R., SEILHEIMER, B., EISENBARTH, G., DRESSLER, D., VERMA, I. M. & POTTER, H. 1993. Nerve growth factor induces neuron-like differentiation of an insulin-secreting pancreatic beta cell line. Proc Natl Acad Sci U S A, 90, 5781-5.
POLTORAK, A., HE, X., SMIRNOVA, I., LIU, M. Y., VAN HUFFEL, C., DU, X., BIRDWELL, D., ALEJOS, E., SILVA, M., GALANOS, C., FREUDENBERG, M.,

RICCIARDI-CASTAGNOLI, P., LAYTON, B. & BEUTLER, B. 1998. Defective LPS signaling in C3H/HeJ and C57BL/10ScCr mice: mutations in Tlr4 gene. Science, 282, 2085-8.
PROKOP, A., LANDGRAF, M., RUSHTON, E., BROADIE, K. & BATE, M. 1996. Presynaptic development at the Drosophila neuromuscular junction: assembly and localization of presynaptic active zones. Neuron, 17, 617-26.
PROKOP, A. & TECHNAU, G. M. 1991. The origin of postembryonic neuroblasts in the ventral nerve cord of Drosophila melanogaster. Development, 111, 79-88.
PRÉHAUD, C., MÉGRET, F., LAFAGE, M. & LAFON, M. 2005. Virus infection switches TLR-3-positive human neurons to become strong producers of beta interferon. J Virol, 79, 12893-904.
PULIDO, D., CAMPUZANO, S., KODA, T., MODOLELL, J. & BARBACID, M. 1992. Dtrk, a Drosophila gene related to the trk family of neurotrophin receptors, encodes a novel class of neural cell adhesion molecule. EMBO J, 11, 391-404.
QIU, J., XU, J., ZHENG, Y., WEI, Y., ZHU, X., LO, E. H., MOSKOWITZ, M. A. & SIMS, J. R. 2010. High-mobility group box 1 promotes metalloproteinase-9 upregulation through Toll-like receptor 4 after cerebral ischemia. Stroke, 41, 2077-82.
QIU, P., PAN, P. C. & GOVIND, S. 1998. A role for the Drosophila Toll/Cactus pathway in larval hematopoiesis. Development, 125, 1909-20.
QUISTGAARD, E. M., MADSEN, P., GRØFTEHAUGE, M. K., NISSEN, P., PETERSEN, C. M. & THIRUP, S. S. 2009. Ligands bind to Sortilin in the tunnel of a ten-bladed beta-propeller domain. Nat Struct Mol Biol, 16, 96-8.
QURESHI, S. T., LARIVIÈRE, L., LEVEQUE, G., CLERMONT, S., MOORE, K. J., GROS, P. & MALO, D. 1999. Endotoxin-tolerant mice have mutations in Toll-like receptor 4 (Tlr4). J Exp Med, 189, 615-25.
RADEKE, M. J., MISKO, T. P., HSU, C., HERZENBERG, L. A. & SHOOTER, E. M. 1987. Gene transfer and molecular cloning of the rat nerve growth factor receptor. Nature, 325, 593-7.
RATNAPARKHI, G. S., DUONG, H. A. & COUREY, A. J. 2008. Dorsal interacting protein 3 potentiates activation by Drosophila Rel homology domain proteins. Dev Comp Immunol, 32, 1290-300.
RAUVALA, H. & PIHLASKARI, R. 1987. Isolation and some characteristics of an adhesive factor of brain that enhances neurite outgrowth in central neurons. J Biol Chem, 262, 16625-35.
REACH, M., GALINDO, R. L., TOWB, P., ALLEN, J. L., KARIN, M. & WASSERMAN, S. A. 1996. A gradient of cactus protein degradation establishes dorsoventral polarity in the Drosophila embryo. Dev Biol, 180, 353-64.
REICHARDT, L. F. 2006. Neurotrophin-regulated signalling pathways. Philos Trans R Soc Lond B Biol Sci, 361, 1545-64.
RIVEST, S. 2009. Regulation of innate immune responses in the brain. Nat Rev Immunol, 9, 429-39.
ROBERTSON, A. J., CROCE, J., CARBONNEAU, S., VORONINA, E., MIRANDA, E., MCCLAY, D. R. & COFFMAN, J. A. 2006. The genomic underpinnings of apoptosis in Strongylocentrotus purpuratus. Dev Biol, 300, 321-34.
ROBERTSON, H. M., PRESTON, C. R., PHILLIS, R. W., JOHNSON-SCHLITZ, D. M., BENZ, W. K. & ENGELS, W. R. 1988. A stable genomic source of P element transposase in Drosophila melanogaster. Genetics, 118, 461-70.

ROCK, F. L., HARDIMAN, G., TIMANS, J. C., KASTELEIN, R. A. & BAZAN, J. F. 1998. A family of human receptors structurally related to Drosophila Toll. Proc Natl Acad Sci U S A, 95, 588-93.
RODRIGUEZ-VICIANA, P., WARNE, P. H., DHAND, R., VANHAESEBROECK, B., GOUT, I., FRY, M. J., WATERFIELD, M. D. & DOWNWARD, J. 1994. Phosphatidylinositol-3-OH kinase as a direct target of Ras. Nature, 370, 527-32.
ROGERS, M. L., BAILEY, S., MATUSICA, D., NICHOLSON, I., MUYDERMAN, H., PAGADALA, P. C., NEET, K. E., ZOLA, H., MACARDLE, P. & RUSH, R. A. 2010. ProNGF mediates death of Natural Killer cells through activation of the p75NTR-sortilin complex. J Neuroimmunol, 226, 93-103.
ROGULJA-ORTMANN, A., LÜER, K., SEIBERT, J., RICKERT, C. & TECHNAU, G. M. 2007. Programmed cell death in the embryonic central nervous system of Drosophila melanogaster. Development, 134, 105-16.
ROLLS, A., SHECHTER, R., LONDON, A., ZIV, Y., RONEN, A., LEVY, R. & SCHWARTZ, M. 2007. Toll-like receptors modulate adult hippocampal neurogenesis. Nat Cell Biol, 9, 1081-8.
ROSE, D. & CHIBA, A. 1999. A single growth cone is capable of integrating simultaneously presented and functionally distinct molecular cues during target recognition. J Neurosci, 19, 4899-906.
ROSE, D., ZHU, X., KOSE, H., HOANG, B., CHO, J. & CHIBA, A. 1997. Toll, a muscle cell surface molecule, locally inhibits synaptic initiation of the RP3 motoneuron growth cone in Drosophila. Development, 124, 1561-71.
ROSENTHAL, A., GOEDDEL, D. V., NGUYEN, T., LEWIS, M., SHIH, A., LARAMEE, G. R., NIKOLICS, K. & WINSLOW, J. W. 1990. Primary structure and biological activity of a novel human neurotrophic factor. Neuron, 4, 767-73.
ROTH, S., STEIN, D. & NÜSSLEIN-VOLHARD, C. 1989. A gradient of nuclear localization of the dorsal protein determines dorsoventral pattern in the Drosophila embryo. Cell, 59, 1189-202.
ROUSSEL, B. D., MYSIOREK, C., ROUHIAINEN, A., JULLIENNE, A., PARCQ, J., HOMMET, Y., CULOT, M., BEREZOWSKI, V., CECCHELLI, R., RAUVALA, H., VIVIEN, D. & ALI, C. 2011. HMGB-1 promotes fibrinolysis and reduces neurotoxicity mediated by tissue plasminogen activator. J Cell Sci, 124, 2070-6.
ROUX, P. P. & BARKER, P. A. 2002. Neurotrophin signaling through the p75 neurotrophin receptor. Prog Neurobiol, 67, 203-33.
RUIT, K. G., OSBORNE, P. A., SCHMIDT, R. E., JOHNSON, E. M. & SNIDER, W. D. 1990. Nerve growth factor regulates sympathetic ganglion cell morphology and survival in the adult mouse. J Neurosci, 10, 2412-9.
RUSHLOW, C. A., HAN, K., MANLEY, J. L. & LEVINE, M. 1989. The graded distribution of the dorsal morphogen is initiated by selective nuclear transport in Drosophila. Cell, 59, 1165-77.
RUTSCHMANN, S., JUNG, A. C., HETRU, C., REICHHART, J. M., HOFFMANN, J. A. & FERRANDON, D. 2000. The Rel protein DIF mediates the antifungal but not the antibacterial host defense in Drosophila. Immunity, 12, 569-80.
RÖSCH, H., SCHWEIGREITER, R., BONHOEFFER, T., BARDE, Y. A. & KORTE, M. 2005. The neurotrophin receptor p75NTR modulates long-term depression and regulates the expression of AMPA receptor subunits in the hippocampus. Proc Natl Acad Sci U S A, 102, 7362-7.

SALAMA-COHEN, P., ARÉVALO, M. A., MEIER, J., GRANTYN, R. & RODRÍGUEZ-TÉBAR, A. 2005. NGF controls dendrite development in hippocampal neurons by binding to p75NTR and modulating the cellular targets of Notch. Mol Biol Cell, 16, 339-47.

SALEHI, A. H., XANTHOUDAKIS, S. & BARKER, P. A. 2002. NRAGE, a p75 neurotrophin receptor-interacting protein, induces caspase activation and cell death through a JNK-dependent mitochondrial pathway. J Biol Chem, 277, 48043-50.

SALMINEN, A., OJALA, J., KAUPPINEN, A., KAARNIRANTA, K. & SUURONEN, T. 2009. Inflammation in Alzheimer's disease: amyloid-beta oligomers trigger innate immunity defence via pattern recognition receptors. Prog Neurobiol, 87, 181-94.

SALZ, H. K., CLINE, T. W. & SCHEDL, P. 1987. Functional changes associated with structural alterations induced by mobilization of a P element inserted in the Sex-lethal gene of Drosophila. Genetics, 117, 221-31.

SANYAL, S. 2009. Genomic mapping and expression patterns of C380, OK6 and D42 enhancer trap lines in the larval nervous system of Drosophila. Gene Expr Patterns, 9, 371-80.

SARIOLA, H., SAARMA, M., SAINIO, K., ARUMÄE, U., PALGI, J., VAAHTOKARI, A., THESLEFF, I. & KARAVANOV, A. 1991. Dependence of kidney morphogenesis on the expression of nerve growth factor receptor. Science, 254, 571-3.

SCHMID, A., CHIBA, A. & DOE, C. Q. 1999. Clonal analysis of Drosophila embryonic neuroblasts: neural cell types, axon projections and muscle targets. Development, 126, 4653-89.

SCHMIDT, H., RICKERT, C., BOSSING, T., VEF, O., URBAN, J. & TECHNAU, G. M. 1997. The embryonic central nervous system lineages of Drosophila melanogaster. II. Neuroblast lineages derived from the dorsal part of the neuroectoderm. Dev Biol, 189, 186-204.

SCHNEIDER, D. S., HUDSON, K. L., LIN, T. Y. & ANDERSON, K. V. 1991. Dominant and recessive mutations define functional domains of Toll, a transmembrane protein required for dorsal-ventral polarity in the Drosophila embryo. Genes Dev, 5, 797-807.

SCHNEIDER, D. S., JIN, Y., MORISATO, D. & ANDERSON, K. V. 1994. A processed form of the Spätzle protein defines dorsal-ventral polarity in the Drosophila embryo. Development, 120, 1243-50.

SEIDAH, N. G., BENJANNET, S., PAREEK, S., CHRÉTIEN, M. & MURPHY, R. A. 1996a. Cellular processing of the neurotrophin precursors of NT3 and BDNF by the mammalian proprotein convertases. FEBS Lett, 379, 247-50.

SEIDAH, N. G., BENJANNET, S., PAREEK, S., SAVARIA, D., HAMELIN, J., GOULET, B., LALIBERTE, J., LAZURE, C., CHRÉTIEN, M. & MURPHY, R. A. 1996b. Cellular processing of the nerve growth factor precursor by the mammalian pro-protein convertases. Biochem J, 314 (Pt 3), 951-60.

SEIDEL, M. F., HERGUIJUELA, M., FORKERT, R. & OTTEN, U. 2010. Nerve growth factor in rheumatic diseases. Semin Arthritis Rheum, 40, 109-26.

SEPPO, A., MATANI, P., SHARROW, M. & TIEMEYER, M. 2003. Induction of neuron-specific glycosylation by Tollo/Toll-8, a Drosophila Toll-like receptor expressed in non-neural cells. Development, 130, 1439-48.

SERPE, M. & O'CONNOR, M. B. 2006. The metalloprotease tolloid-related and its TGF-beta-like substrate Dawdle regulate Drosophila motoneuron axon guidance. Development, 133, 4969-79.

SHARMA, Y., CHEUNG, U., LARSEN, E. W. & EBERL, D. F. 2002. PPTGAL, a convenient Gal4 P-element vector for testing expression of enhancer fragments in drosophila. Genesis, 34, 115-8.
SHECHTER, R., RONEN, A., ROLLS, A., LONDON, A., BAKALASH, S., YOUNG, M. J. & SCHWARTZ, M. 2008. Toll-like receptor 4 restricts retinal progenitor cell proliferation. J Cell Biol, 183, 393-400.
SHELTON, D. L., SUTHERLAND, J., GRIPP, J., CAMERATO, T., ARMANINI, M. P., PHILLIPS, H. S., CARROLL, K., SPENCER, S. D. & LEVINSON, A. D. 1995. Human trks: molecular cloning, tissue distribution, and expression of extracellular domain immunoadhesins. J Neurosci, 15, 477-91.
SHEN, B., LIU, H., SKOLNIK, E. Y. & MANLEY, J. L. 2001. Physical and functional interactions between Drosophila TRAF2 and Pelle kinase contribute to Dorsal activation. Proc Natl Acad Sci U S A, 98, 8596-601.
SHI, J., BLUNDELL, T. L. & MIZUGUCHI, K. 2001. FUGUE: sequence-structure homology recognition using environment-specific substitution tables and structure-dependent gap penalties. J Mol Biol, 310, 243-57.
SIGRIST, S. J., REIFF, D. F., THIEL, P. R., STEINERT, J. R. & SCHUSTER, C. M. 2003. Experience-dependent strengthening of Drosophila neuromuscular junctions. J Neurosci, 23, 6546-56.
SILOS-SANTIAGO, I., MOLLIVER, D. C., OZAKI, S., SMEYNE, R. J., FAGAN, A. M., BARBACID, M. & SNIDER, W. D. 1995. Non-TrkA-expressing small DRG neurons are lost in TrkA deficient mice. J Neurosci, 15, 5929-42.
SILVER, R., SILVERMAN, A. J., VITKOVIĆ, L. & LEDERHENDLER, I. I. 1996. Mast cells in the brain: evidence and functional significance. Trends Neurosci, 19, 25-31.
SINK, H. & WHITINGTON, P. M. 1991. Early ablation of target muscles modulates the arborisation pattern of an identified embryonic Drosophila motor axon. Development, 113, 701-7.
SLOANE, J. A., BLITZ, D., MARGOLIN, Z. & VARTANIAN, T. 2010. A clear and present danger: endogenous ligands of Toll-like receptors. Neuromolecular Med, 12, 149-63.
SMEYNE, R. J., KLEIN, R., SCHNAPP, A., LONG, L. K., BRYANT, S., LEWIN, A., LIRA, S. A. & BARBACID, M. 1994. Severe sensory and sympathetic neuropathies in mice carrying a disrupted Trk/NGF receptor gene. Nature, 368, 246-9.
SMITH, C. A., FARRAH, T. & GOODWIN, R. G. 1994. The TNF receptor superfamily of cellular and viral proteins: activation, costimulation, and death. Cell, 76, 959-62.
SONG, H. J. & POO, M. M. 1999. Signal transduction underlying growth cone guidance by diffusible factors. Curr Opin Neurobiol, 9, 355-63.
SONG, M. S. & POSSE DE CHAVES, E. I. 2003. Inhibition of rat sympathetic neuron apoptosis by ceramide. Role of p75NTR in ceramide generation. Neuropharmacology, 45, 1130-50.
SOSSIN, W. S. 2006. Tracing the evolution and function of the Trk superfamily of receptor tyrosine kinases. Brain Behav Evol, 68, 145-56.
SPRADLING, A. C., STERN, D. M., KISS, I., ROOTE, J., LAVERTY, T. & RUBIN, G. M. 1995. Gene disruptions using P transposable elements: an integral component of the Drosophila genome project. Proc Natl Acad Sci U S A, 92, 10824-30.
STATHOPOULOS, A. & LEVINE, M. 2002. Dorsal gradient networks in the Drosophila embryo. Dev Biol, 246, 57-67.

STEIN, D., CHO, Y. S., ZHANG, Z. & STEVENS, L. M. 2008. No requirement for localized Nudel protein expression in Drosophila embryonic axis determination. Fly (Austin), 2, 220-8.
STEIN, D., ROTH, S., VOGELSANG, E. & NÜSSLEIN-VOLHARD, C. 1991. The polarity of the dorsoventral axis in the Drosophila embryo is defined by an extracellular signal. Cell, 65, 725-35.
STEPHENS, R. M., LOEB, D. M., COPELAND, T. D., PAWSON, T., GREENE, L. A. & KAPLAN, D. R. 1994. Trk receptors use redundant signal transduction pathways involving SHC and PLC-gamma 1 to mediate NGF responses. Neuron, 12, 691-705.
STEWARD, R. 1989. Relocalization of the dorsal protein from the cytoplasm to the nucleus correlates with its function. Cell, 59, 1179-88.
STRAUSS, R. 2002. The central complex and the genetic dissection of locomotor behaviour. Curr Opin Neurobiol, 12, 633-8.
STRAUSS, R. & HEISENBERG, M. 1993. A higher control center of locomotor behavior in the Drosophila brain. J Neurosci, 13, 1852-61.
STROHMAIER, C., CARTER, B. D., URFER, R., BARDE, Y. A. & DECHANT, G. 1996. A splice variant of the neurotrophin receptor trkB with increased specificity for brain-derived neurotrophic factor. EMBO J, 15, 3332-7.
SUN, H., BRISTOW, B. N., QU, G. & WASSERMAN, S. A. 2002. A heterotrimeric death domain complex in Toll signaling. Proc Natl Acad Sci U S A, 99, 12871-6.
SUN, H., TOWB, P., CHIEM, D. N., FOSTER, B. A. & WASSERMAN, S. A. 2004. Regulated assembly of the Toll signaling complex drives Drosophila dorsoventral patterning. EMBO J, 23, 100-10.
SUN, P. D. & DAVIES, D. R. 1995. The cystine-knot growth-factor superfamily. Annu Rev Biophys Biomol Struct, 24, 269-91.
SUN, Q., SCHINDELHOLZ, B., KNIRR, M., SCHMID, A. & ZINN, K. 2001. Complex genetic interactions among four receptor tyrosine phosphatases regulate axon guidance in Drosophila. Mol Cell Neurosci, 17, 274-91.
SUTCLIFFE, B. 2010. Functional analysis of Drosophila neurotrophins: from neuronal survival to behaviour. University of Birmingham.
SUTCLIFFE, B., FORERO, M. G., ZHU, B., ROBINSON, I. M. & HIDALGO, A. Submitted. Conserved neurotrophin functions at the Drosophila neuromuscular junction. Development.
SUTER, U., HEYMACH, J. V. & SHOOTER, E. M. 1991. Two conserved domains in the NGF propeptide are necessary and sufficient for the biosynthesis of correctly processed and biologically active NGF. EMBO J, 10, 2395-400.
SUZUKI, E., ROSE, D. & CHIBA, A. 2000. The ultrastructural interactions of identified pre- and postsynaptic cells during synaptic target recognition in Drosophila embryos. J Neurobiol, 42, 448-59.
SÁNCHEZ-SORIANO, N. & PROKOP, A. 2005. The influence of pioneer neurons on a growing motor nerve in Drosophila requires the neural cell adhesion molecule homolog FasciclinII. J Neurosci, 25, 78-87.
TAKEDA, K., KAISHO, T. & AKIRA, S. 2003. Toll-like receptors. Annu Rev Immunol, 21, 335-76.
TANAKA, J., HORIIKE, Y., MATSUZAKI, M., MIYAZAKI, T., ELLIS-DAVIES, G. C. & KASAI, H. 2008. Protein synthesis and neurotrophin-dependent structural plasticity of single dendritic spines. Science, 319, 1683-7.

TANG, S. C., ARUMUGAM, T. V., XU, X., CHENG, A., MUGHAL, M. R., JO, D. G., LATHIA, J. D., SILER, D. A., CHIGURUPATI, S., OUYANG, X., MAGNUS, T., CAMANDOLA, S. & MATTSON, M. P. 2007. Pivotal role for neuronal Toll-like receptors in ischemic brain injury and functional deficits. Proc Natl Acad Sci U S A, 104, 13798-803.

TANG, S. C., LATHIA, J. D., SELVARAJ, P. K., JO, D. G., MUGHAL, M. R., CHENG, A., SILER, D. A., MARKESBERY, W. R., ARUMUGAM, T. V. & MATTSON, M. P. 2008. Toll-like receptor-4 mediates neuronal apoptosis induced by amyloid beta-peptide and the membrane lipid peroxidation product 4-hydroxynonenal. Exp Neurol, 213, 114-21.

TANJI, T., HU, X., WEBER, A. N. & IP, Y. T. 2007. Toll and IMD pathways synergistically activate an innate immune response in Drosophila melanogaster. Mol Cell Biol, 27, 4578-88.

TANJI, T., YUN, E. Y. & IP, Y. T. 2010. Heterodimers of NF-kappaB transcription factors DIF and Relish regulate antimicrobial peptide genes in Drosophila. Proc Natl Acad Sci U S A, 107, 14715-20.

TAUSZIG, S., JOUANGUY, E., HOFFMANN, J. A. & IMLER, J. L. 2000. Toll-related receptors and the control of antimicrobial peptide expression in Drosophila. Proc Natl Acad Sci U S A, 97, 10520-5.

TENG, H. K., TENG, K. K., LEE, R., WRIGHT, S., TEVAR, S., ALMEIDA, R. D., KERMANI, P., TORKIN, R., CHEN, Z. Y., LEE, F. S., KRAEMER, R. T., NYKJAER, A. & HEMPSTEAD, B. L. 2005. ProBDNF induces neuronal apoptosis via activation of a receptor complex of p75NTR and sortilin. J Neurosci, 25, 5455-63.

TESSAROLLO, L., TSOULFAS, P., MARTIN-ZANCA, D., GILBERT, D. J., JENKINS, N. A., COPELAND, N. G. & PARADA, L. F. 1993. trkC, a receptor for neurotrophin-3, is widely expressed in the developing nervous system and in non-neuronal tissues. Development, 118, 463-75.

TESSIER-LAVIGNE, M. & GOODMAN, C. S. 1996. The molecular biology of axon guidance. Science, 274, 1123-33.

THOMSON, T. M., RETTIG, W. J., CHESA, P. G., GREEN, S. H., MENA, A. C. & OLD, L. J. 1988. Expression of human nerve growth factor receptor on cells derived from all three germ layers. Exp Cell Res, 174, 533-9.

TISSOT, M. & STOCKER, R. F. 2000. Metamorphosis in drosophila and other insects: the fate of neurons throughout the stages. Prog Neurobiol, 62, 89-111.

TRUMAN, J. W. 1984. Cell death in invertebrate nervous systems. Annu Rev Neurosci, 7, 171-88.

TRUMAN, J. W. 1990. Metamorphosis of the central nervous system of Drosophila. J Neurobiol, 21, 1072-84.

URFER, R., TSOULFAS, P., O'CONNELL, L., SHELTON, D. L., PARADA, L. F. & PRESTA, L. G. 1995. An immunoglobulin-like domain determines the specificity of neurotrophin receptors. EMBO J, 14, 2795-805.

VAILLANT, A. R., MAZZONI, I., TUDAN, C., BOUDREAU, M., KAPLAN, D. R. & MILLER, F. D. 1999. Depolarization and neurotrophins converge on the phosphatidylinositol 3-kinase-Akt pathway to synergistically regulate neuronal survival. J Cell Biol, 146, 955-66.

VALANNE, S., WANG, J. H. & RÄMET, M. 2011. The Drosophila Toll signaling pathway. J Immunol, 186, 649-56.

VAN KESTEREN, R. E., FAINZILBER, M., HAUSER, G., VAN MINNEN, J., VREUGDENHIL, E., SMIT, A. B., IBÁÑEZ, C. F., GERAERTS, W. P. & BULLOCH, A. G. 1998. Early evolutionary origin of the neurotrophin receptor family. EMBO J, 17, 2534-42.

VAN VACTOR, D., SINK, H., FAMBROUGH, D., TSOO, R. & GOODMAN, C. S. 1993. Genes that control neuromuscular specificity in Drosophila. Cell, 73, 1137-53.

VEGA, J. A., GARCÍA-SUÁREZ, O., HANNESTAD, J., PÉREZ-PÉREZ, M. & GERMANÀ, A. 2003. Neurotrophins and the immune system. J Anat, 203, 1-19.

VERMA, I. M., STEVENSON, J. K., SCHWARZ, E. M., VAN ANTWERP, D. & MIYAMOTO, S. 1995. Rel/NF-kappa B/I kappa B family: intimate tales of association and dissociation. Genes Dev, 9, 2723-35.

VETTER, M. L., MARTIN-ZANCA, D., PARADA, L. F., BISHOP, J. M. & KAPLAN, D. R. 1991. Nerve growth factor rapidly stimulates tyrosine phosphorylation of phospholipase C-gamma 1 by a kinase activity associated with the product of the trk protooncogene. Proc Natl Acad Sci U S A, 88, 5650-4.

VOGEL, C., TEICHMANN, S. A. & CHOTHIA, C. 2003. The immunoglobulin superfamily in Drosophila melanogaster and Caenorhabditis elegans and the evolution of complexity. Development, 130, 6317-28.

VON SCHACK, D., CASADEMUNT, E., SCHWEIGREITER, R., MEYER, M., BIBEL, M. & DECHANT, G. 2001. Complete ablation of the neurotrophin receptor p75NTR causes defects both in the nervous and the vascular system. Nat Neurosci, 4, 977-8.

WADACHI, R. & HARGREAVES, K. M. 2006. Trigeminal nociceptors express TLR-4 and CD14: a mechanism for pain due to infection. J Dent Res, 85, 49-53.

WAGH, D. A., RASSE, T. M., ASAN, E., HOFBAUER, A., SCHWENKERT, I., DÜRRBECK, H., BUCHNER, S., DABAUVALLE, M. C., SCHMIDT, M., QIN, G., WICHMANN, C., KITTEL, R., SIGRIST, S. J. & BUCHNER, E. 2006. Bruchpilot, a protein with homology to ELKS/CAST, is required for structural integrity and function of synaptic active zones in Drosophila. Neuron, 49, 833-44.

WAN, H. I., DIANTONIO, A., FETTER, R. D., BERGSTROM, K., STRAUSS, R. & GOODMAN, C. S. 2000. Highwire regulates synaptic growth in Drosophila. Neuron, 26, 313-29.

WANG, J., TAO, Y., REIM, I., GAJEWSKI, K., FRASCH, M. & SCHULZ, R. A. 2005. Expression, regulation, and requirement of the toll transmembrane protein during dorsal vessel formation in Drosophila melanogaster. Mol Cell Biol, 25, 4200-10.

WANG, K. C., KIM, J. A., SIVASANKARAN, R., SEGAL, R. & HE, Z. 2002. P75 interacts with the Nogo receptor as a co-receptor for Nogo, MAG and OMgp. Nature, 420, 74-8.

WEBER, A. N., GANGLOFF, M., MONCRIEFFE, M. C., HYVERT, Y., IMLER, J. L. & GAY, N. J. 2007. Role of the Spatzle Pro-domain in the generation of an active toll receptor ligand. J Biol Chem, 282, 13522-31.

WEBER, A. N., TAUSZIG-DELAMASURE, S., HOFFMANN, J. A., LELIÈVRE, E., GASCAN, H., RAY, K. P., MORSE, M. A., IMLER, J. L. & GAY, N. J. 2003. Binding of the Drosophila cytokine Spätzle to Toll is direct and establishes signaling. Nat Immunol, 4, 794-800.

WEHRMAN, T., HE, X., RAAB, B., DUKIPATTI, A., BLAU, H. & GARCIA, K. C. 2007. Structural and mechanistic insights into nerve growth factor interactions with the TrkA and p75 receptors. Neuron, 53, 25-38.

WELLMANN, H., KALTSCHMIDT, B. & KALTSCHMIDT, C. 2001. Retrograde transport of transcription factor NF-kappa B in living neurons. J Biol Chem, 276, 11821-9.
WHALEN, A. M. & STEWARD, R. 1993. Dissociation of the dorsal-cactus complex and phosphorylation of the dorsal protein correlate with the nuclear localization of dorsal. J Cell Biol, 123, 523-34.
WHITE, K., GRETHER, M. E., ABRAMS, J. M., YOUNG, L., FARRELL, K. & STELLER, H. 1994. Genetic control of programmed cell death in Drosophila. Science, 264, 677-83.
WIENS, G. D. & GLENNEY, G. W. 2011. Origin and evolution of TNF and TNF receptor superfamilies. Dev Comp Immunol.
WIESMANN, C. & DE VOS, A. M. 2001. Nerve growth factor: structure and function. Cell Mol Life Sci, 58, 748-59.
WIESMANN, C., ULTSCH, M. H., BASS, S. H. & DE VOS, A. M. 1999. Crystal structure of nerve growth factor in complex with the ligand-binding domain of the TrkA receptor. Nature, 401, 184-8.
WILLIAMS, M. J., RODRIGUEZ, A., KIMBRELL, D. A. & ELDON, E. D. 1997. The 18-wheeler mutation reveals complex antibacterial gene regulation in Drosophila host defense. EMBO J, 16, 6120-30.
WILSON, C., GOBERDHAN, D. C. & STELLER, H. 1993. Dror, a potential neurotrophic receptor gene, encodes a Drosophila homolog of the vertebrate Ror family of Trk-related receptor tyrosine kinases. Proc Natl Acad Sci U S A, 90, 7109-13.
WILSON, K. H. 2009. The genome sequence of the protostome Daphnia pulex encodes respective orthologues of a neurotrophin, a Trk and a p75NTR: evolution of neurotrophin signaling components and related proteins in the bilateria. BMC Evol Biol, 9, 243.
WINANS, K. A. & HASHIMOTO, C. 1995. Ventralization of the Drosophila embryo by deletion of extracellular leucine-rich repeats in the Toll protein. Mol Biol Cell, 6, 587-96.
WINBERG, M. L., TAMAGNONE, L., BAI, J., COMOGLIO, P. M., MONTELL, D. & GOODMAN, C. S. 2001. The transmembrane protein Off-track associates with Plexins and functions downstream of Semaphorin signaling during axon guidance. Neuron, 32, 53-62.
WOO, N. H., TENG, H. K., SIAO, C. J., CHIARUTTINI, C., PANG, P. T., MILNER, T. A., HEMPSTEAD, B. L. & LU, B. 2005. Activation of p75NTR by proBDNF facilitates hippocampal long-term depression. Nat Neurosci, 8, 1069-77.
XIONG, W. C. & MONTELL, C. 1995. Defective glia induce neuronal apoptosis in the repo visual system of Drosophila. Neuron, 14, 581-90.
XU, B., GOTTSCHALK, W., CHOW, A., WILSON, R. I., SCHNELL, E., ZANG, K., WANG, D., NICOLL, R. A., LU, B. & REICHARDT, L. F. 2000. The role of brain-derived neurotrophic factor receptors in the mature hippocampus: modulation of long-term potentiation through a presynaptic mechanism involving TrkB. J Neurosci, 20, 6888-97.
XU, D., WOODFIELD, S. E., LEE, T. V., FAN, Y., ANTONIO, C. & BERGMANN, A. 2009. Genetic control of programmed cell death (apoptosis) in Drosophila. Fly (Austin), 3, 78-90.
YAAR, M., ELLER, M. S., DIBENEDETTO, P., REENSTRA, W. R., ZHAI, S., MCQUAID, T., ARCHAMBAULT, M. & GILCHREST, B. A. 1994. The trk family of receptors

mediates nerve growth factor and neurotrophin-3 effects in melanocytes. J Clin Invest, 94, 1550-62.
YAGI, Y., NISHIDA, Y. & IP, Y. T. 2010. Functional analysis of Toll-related genes in Drosophila. Dev Growth Differ, 52, 771-83.
YAMADA, M., OHNISHI, H., SANO, S., NAKATANI, A., IKEUCHI, T. & HATANAKA, H. 1997. Insulin receptor substrate (IRS)-1 and IRS-2 are tyrosine-phosphorylated and associated with phosphatidylinositol 3-kinase in response to brain-derived neurotrophic factor in cultured cerebral cortical neurons. J Biol Chem, 272, 30334-9.
YAMASHITA, T. & TOHYAMA, M. 2003. The p75 receptor acts as a displacement factor that releases Rho from Rho-GDI. Nat Neurosci, 6, 461-7.
YAMASHITA, T., TUCKER, K. L. & BARDE, Y. A. 1999. Neurotrophin binding to the p75 receptor modulates Rho activity and axonal outgrowth. Neuron, 24, 585-93.
YANG, H., WANG, H., CZURA, C. J. & TRACEY, K. J. 2005. The cytokine activity of HMGB1. J Leukoc Biol, 78, 1-8.
YANO, H., TORKIN, R., MARTIN, L. A., CHAO, M. V. & TENG, K. K. 2009. Proneurotrophin-3 is a neuronal apoptotic ligand: evidence for retrograde-directed cell killing. J Neurosci, 29, 14790-802.
YEH, E., GUSTAFSON, K. & BOULIANNE, G. L. 1995. Green fluorescent protein as a vital marker and reporter of gene expression in Drosophila. Proc Natl Acad Sci U S A, 92, 7036-40.
YOON, S. O., CASACCIA-BONNEFIL, P., CARTER, B. & CHAO, M. V. 1998. Competitive signaling between TrkA and p75 nerve growth factor receptors determines cell survival. J Neurosci, 18, 3273-81.
YORK, R. D., YAO, H., DILLON, T., ELLIG, C. L., ECKERT, S. P., MCCLESKEY, E. W. & STORK, P. J. 1998. Rap1 mediates sustained MAP kinase activation induced by nerve growth factor. Nature, 392, 622-6.
ZACCARO, M. C., IVANISEVIC, L., PEREZ, P., MEAKIN, S. O. & SARAGOVI, H. U. 2001. p75 Co-receptors regulate ligand-dependent and ligand-independent Trk receptor activation, in part by altering Trk docking subdomains. J Biol Chem, 276, 31023-9.
ZAGREBELSKY, M., HOLZ, A., DECHANT, G., BARDE, Y. A., BONHOEFFER, T. & KORTE, M. 2005. The p75 neurotrophin receptor negatively modulates dendrite complexity and spine density in hippocampal neurons. J Neurosci, 25, 9989-99.
ZHANG, D., YAO, L. & BERND, P. 1996. Expression of neurotrophin trk and p75 receptors in quail embryos undergoing gastrulation and neurulation. Dev Dyn, 205, 150-61.
ZHAO, X., KUJA-PANULA, J., ROUHIAINEN, A., CHEN, Y. C., PANULA, P. & RAUVALA, H. 2011. High mobility group box-1 (HMGB1; amphoterin) is required for zebrafish brain development. J Biol Chem, 286, 23200-13.
ZHONG, Y. & WU, C. F. 2004. Neuronal activity and adenylyl cyclase in environment-dependent plasticity of axonal outgrowth in Drosophila. J Neurosci, 24, 1439-45.
ZHOU, Y., YE, L., WAN, Q., ZHOU, L., WANG, X., LI, J., HU, S., ZHOU, D. & HO, W. 2009. Activation of Toll-like receptors inhibits herpes simplex virus-1 infection of human neuronal cells. J Neurosci Res, 87, 2916-25.
ZHU, B., PENNACK, J. A., MCQUILTON, P., FORERO, M. G., MIZUGUCHI, K., SUTCLIFFE, B., GU, C. J., FENTON, J. C. & HIDALGO, A. 2008. Drosophila neurotrophins reveal a common mechanism for nervous system formation. PLoS Biol, 6, e284.

ZHU, X., SEN, J., STEVENS, L., GOLTZ, J. S. & STEIN, D. 2005. Drosophila pipe protein activity in the ovary and the embryonic salivary gland does not require heparan sulfate glycosaminoglycans. Development, 132, 3813-22.